

**THE RECENT MORPHO-TECTONIC HISTORY
OF THE VAALPUTS RADIOACTIVE WASTE REPOSITORY
AND ENVIRONS**

DION BRANDT

Thesis submitted to the Faculty of Science,
University of the Witwatersrand, in fulfilment of
the requirements for the degree of
DOCTOR OF PHILOSOPHY

Johannesburg, 1998

ABSTRACT

This study deals with a region in the Northern Province, centred around Vaalputs, the National Radioactive Waste Disposal site. The study area constitutes two distinct geomorphological terrains: the western section consists of rugged, mountainous, granitic terrane, with steep cliffs that include weathered and silicified basement; the eastern section consists of the generally featureless, gently undulating Bushmanland Plateau. The latter is characterized by low-amplitude palaeo-dunes which have a north-northeasterly trend. Precambrian crystalline rocks belonging to the Namaqualand Metamorphic Complex and late Palaeozoic (Karoo) rocks form the basement to Cretaceous and Cenozoic deposits in the region. Seismic studies in the Vaalputs area have indicated that there is appreciable seismic activity over a broad region of the northern Cape. In addition, satellite images and aerial photographs have recorded the presence of a network of lineaments in recent cover. The objectives of this study were to obtain a better understanding of the Late-Mesozoic and Cenozoic tectonic history of the region. Geomorphological, sedimentological and geological episodes were identified, described and correlated to the major tectonic events in the area.

During the Late-Cretaceous the Dasdap Formation was deposited as a result of uplift along the marginal escarpment (west coast), in an alluvial fan setting. Crater sediments overlying olivine melilitites and kimberlites were also deposited contemporaneously with the Dasdap Formation. The late Cretaceous saw tropical conditions which caused extensive deep weathering and silicification of the Namaqualand Metamorphic Complex and the Dasdap Formation. This wet period was terminated approximately at the end of the Cretaceous with the onset of aridification. Tectonism largely in the form of reactivated older structures caused differences in the elevation of the palaeo-weathered and silicified surfaces and the initial deepening of a north-northwest oriented graben. Continued deepening of the graben during the Tertiary allowed for the deposition of the fluvial (floodouts) and aeolian Vaalputs sediments. Calcrete horizons preserved in the Vaalputs

sequence of sediments indicate drier interludes and define previous land surfaces during tectonically less active periods or during periods of lower sediment supply. Post-depositional alteration and bioturbation resulted in the generally structureless and massive sediments of the Vaalputs Formation. Overall desiccation throughout the Cenozoic finally gave rise to the aeolian dominated Gordonia Formation and present day micro-environments, consisting predominantly of aeolian deposits, deflation pans, and lag deposits. The source of the Gordonia sediments is primarily the underlying Vaalputs Formation which is in a state of degradation. Surface processes (primarily aeolian) have reworked and modified the surface into longitudinal dunes with a transverse component.

Since the Cretaceous two primary stress fields have given rise to the numerous tectonic products observed in the study area. The study area is affected by two important uplift axes: the Griqualand-Transvaal and the Kamiesberge axes, which were active between the Miocene and the Plio-Pleistocene. On a regional scale the larger and older Pan African age (700 Ma.) faults are predominantly north-northwesterly trending and have been reactivated. At about 60 Ma ago, the minimum principal stress was most probably oriented to the NW causing extensive dip-slip faulting with a northeasterly strike. The stress field, active during most of the Cenozoic, had an ENE oriented minimum principal horizontal stress, and accompanied the development of a fault-bound sedimentary basin, which was filled by the sediments of the Vaalputs Formation. This stress field is probably still active as evidenced by numerous recent structural features.

DECLARATION

I declare that this research represents my own work carried out under the supervision of Prof. T.S. McCarthy, from the Department of Geology, at the University of the Witwatersrand. No part of this research has been submitted, or is being submitted, for a degree at any other university.

Signed at Johannesburg on the 10th day of September 1998

A handwritten signature in black ink, appearing to read 'D Brandt' followed by a stylized flourish.

Dion Brandt

ACKNOWLEDGEMENTS

The Atomic Energy Corporation is thanked for their financial contributions and logistical support of the study, and the University of the Witwatersrand for their financial support during 1996 and 1997. Anglo American Corporation is thanked for the use of their satellite image processing facilities, and in particular, Paul Linton for his time and invaluable information during the remote sensing phase of the project.

A special thanks to all those who accompanied and assisted with my field work at Vaalputs. To Dr. Ingrid Stengel, Dr. John Hancox and Dr. Norman Smith for their valuable guidance and discussions. To Lynda Whitefield and Diana du Toit for their assistance in the drafting of various figures for this thesis. To Michael Butier and Prof. Balt Verhagen of the Schonland Research Laboratory, University of the Witwatersrand, for their assistance in the ^{14}C dating of various calcrete samples.

My extended gratitude to my supervisor Prof. T.S. McCarthy and to Dr M.A.G. Andreoli (of the Atomic Energy Corporation) for their constructive discussions and criticisms, and enthusiastic guidance throughout the research.

A special thanks to my wife, Jane, for patience and support throughout the study period.

CONTENTS

	Page
ABSTRACT	ii
DECLARATION	iv
ACKNOWLEDGEMENTS	v
TABLE OF CONTENTS	vi
LIST OF FIGURES	xi
LIST OF TABLES	xviii
CHAPTER 1 : INTRODUCTION	1
1.1 Location and Geographical Setting of the Study Area	1
1.2 Stratigraphy	5
1.3 Objectives	7
CHAPTER 2 : METHODS USED IN THIS STUDY	9
2.1 Satellite Imagery and Airphoto Interpretation	9
2.2 Field Mapping and Sampling	11
2.3 Sedimentological Studies of Surficial Deposits	12
2.4 Analytical Techniques	14
CHAPTER 3 : PREVIOUS WORK	16
3.1 Geomorphic Evolution of the Northern Province: Models of Landscape Development	16
3.1.1 Models of Passive Rifting	16
3.1.2 Escarpment Evolution	18
3.1.3 Landscape Development of Southern Africa	20
3.1.4 Landscape Evolution of the Study Area	23
3.1.5 Palaeodrainage Evolution	25
3.2 Post-Karoo Sedimentation in the Study Area	26

3.2.1 The Dasdap Formation	26
3.2.2 The Vaalputs Formation	28
3.2.3 The Gordonia Formation	30
3.3 Structure	31
3.4 Climatic History	33
3.4.1 Global Mesozoic and Cenozoic Climate Changes	33
3.4.2 Climatic Record in the Northwestern Cape	34
CHAPTER 4 : REGIONAL GEOLOGY	37
4.1 Proterozoic Basement	37
4.1.1 Stratigraphy of the Supracrustals	37
4.1.2 Intrusions	42
4.1.3 Structure	43
4.2 Permo-Carboniferous Karoo Cover	44
4.3 Late Cretaceous - Early Tertiary Intrusions	48
4.4 The Dasdap Formation	49
4.5 Palaeo-weathered Rocks	51
4.6 The Vaalputs Formation	52
4.7 The Gordonia Formation	53
CHAPTER 5 : THE CRETACEOUS	55
5.1 The Dasdap Formation	55
5.1.1 Field Occurrences	55
5.1.2 Petrology	61
5.1.2.1 Petrographic Descriptions	61
5.1.2.2 Modal Analysis	65
5.1.3 Chemistry	66
5.1.4 Discussion	69
5.2 The Palaeo-Weathered Landsurface	78
5.2.1 Field Occurrences	78

5.2.2 Petrology	81
5.2.3 Chemistry	84
5.2.4 Discussion	94
CHAPTER 6 : THE VAALPUTS FORMATION	102
6.1 Field Occurrences	103
6.2 Facies Identification and Descriptions	104
6.2.1 The White Clay Facies	106
6.2.2 The Pebbly Clay Facies	107
6.2.3 The Gritty Clay Facies	111
6.2.4 Red Sands	114
6.2.5 Calcrete	116
6.3 Chemistry of the Vaalputs Sediments	118
6.3.1 The White Clay Facies	118
6.3.2 The Pebbly Clay and Gritty Clay Facies	119
6.3.3 Red Sands	119
6.4 Chronology	120
6.5 Discussion	123
CHAPTER 7 : THE GORDONIA FORMATION AND PRESENT DAY MICRO-ENVIRONMENTS	134
7.1 Identification of the Micro-environments	135
7.2 Aeolian Deposits	135
7.3 Deflation Pans	153
7.4 Lag Deposits	167
7.5 Bioturbated Deposits	171
7.5.1 Types of Bioturbation	172
7.5.2 Characteristics of Bioturbated Sediments	179
7.5.3 The Effects of Bioturbation on Sediment Dispersal	180
7.6 Chemical Sediments	185

7.6.1 Iron Oxide Cemented Facies - Dorbank	185
7.6.2 Calcrete	190
7.6.3 Silcrete	190
7.7 Grain Size Parameters: a Comparison with the Vaalputs Formation	190
7.8 Chemical Results: a Comparison with the Vaalputs Formation	195
7.9 Discussion	203
CHAPTER 8 : STRUCTURE	209
8.1 Lineament analyses	209
8.2 Structure of the Palaeo-weathered Cretaceous Land Surface	219
8.2.1 Faulting	220
8.2.2 Slickensides	222
8.2.3 Slickenside Analysis	226
8.2.4 Comparative Joint Analysis	232
8.2.4.1 Jointing in the Basement Rocks	232
8.2.4.2 Jointing in the Surficial Sediments	236
8.3 Evidence of Neotectonic Activity	238
8.3.1 Deformation in the Karoo Rocks	239
8.3.2 Reactivation of Older Structures	243
8.3.3 Disturbance of Recent Drainage Patterns	245
8.3.3.1 The Buffels River	245
8.3.3.2 The Dasdap Drainage	248
8.3.4 Seismicity	251
8.4 Discussion	254
CHAPTER 9 : DISCUSSION	261
CHAPTER 10 : CONCLUSIONS	272
REFERENCES	275

APPENDICES

Appendix A:	Major Element Results - The Dasdap Formation	302
Appendix B:	Major Element Results - Palaeo-Weathered Basement	303
Appendix C:	Animal Species Identified at Vaalputs	304
Appendix D:	Sample Preparation of Heavy Mineral Concentrates	305
Appendix E:	Major Element Results - Surficial Sediments and Recently Weathered Basement	306
Appendix F:	Structural Data of Planes Containing Slickensides in the Palaeo-Weathered Basement	307

LIST OF FIGURES

	Page
Figure 1.1	Location of the Vaalputs National Radioactive Waste Disposal Facility and study area. Inset is area of broader investigation and is shown in Figure 1.2.
	1
Figure 1.2	Area of broader investigation showing the main features of the region. Inset shows the area of detailed investigation (see Figure 1.3).
	2
Figure 1.3	Approximate area investigated, showing Vaalputs, the national nuclear waste disposal site. Spot heights are given in metres. Also shown are the approximate positions of the drainage divides in the area.
	4
Figure 2.1	TM-5 LANDSAT image of the study area using bands five (filtered), three, and two (red, green, blue respectively). N is to the top, and the image covers an area of approximately 200 km x 160 km.
	10
Figure 4.1	Typical appearance of the landscape in the western parts of the study area developed on the Namaqualand Metamorphic Complex.
	38
Figure 4.2	Namaqualand-Bushmanland tectonic subdivisions and structures (after Joubert, 1986a).
	39
Figure 4.3	Karoo sediments and dolerite intrusions in the study area (after Andersen, 1992).
	46
Figure 4.4	The Dwyka Group at Boonstevlei showing a typical erratic littered surface.
	47
Figure 4.5	The arenaceous Dasdap sediments, or Kookoppe, on the farm Banke (near Platbakkies).
	50
Figure 4.6	Palaeo-weathered basement on the western part of Vaalputs.
	51
Figure 4.7	The Vaalputs sediments exposed in the intermediate waste disposal trench. The succession of exposed sediments is approximately 8 metres thick.
	52
Figure 4.8	Sand covered area typical of the Gordonia Formation which covers the greater part of the Bushmanland Plateau in the study area. The crest of a low amplitude dune is seen in the background.
	54
Figure 5.1	Dasdap sediment occurrences in the study area with present drainage patterns (modified after Niemand, 1986).
	56
Figure 5.2	Lithofacies assemblage and simplified vertical profiles for the Dasdap Formation sediments.
	57
Figure 5.3	The Dasdap sediments: (a) basal conglomerate lying unconformably on altered basement gneisses; (b) large fragments or boulders of the basement gneiss included in the basal conglomerate; (c) planar cross-bedded sandstone lying directly on an altered gneiss surface; (d) coarse, immature, trough cross-bedded arkosic grits; (e) iron oxide staining in the upper parts of the upper sandstone unit; and (f) basal conglomerate of a new cycle.
	60
Figure 5.4	Thin sections of the Dasdap sediments: (a) very coarse sand/ grit from the basal sediments (Kookoppe) (plane polarized light); (b) trough cross-bedded sandstone (Kookoppe) (plane polarized light); (c) planar-bedded to massive sandstone (Kookoppe) (crossed-polarized light); (d) siltstone (Kookoppe) (plane polarized light); (e) ferruginous sandstone (Burtons Puts) (plane polarized light) and; (f) ferruginized siltstone (Kookoppe) (plane polarized light). Field of view in all cases: 0.9x1.38 mm.
	64

Figure 5.5	Ternary plots of: the basal sediments of the Kookoppe (▲); the overlying finer-grained sediments of the Kookoppe (■); the distal sediments on the farm Burtons Puts (◆); and a distal sediment from Vaalputs (●). (a) Excluding all intergranular material (8 points). (b) Whole sample, assuming all intergranular material is the product of <i>in situ</i> alteration (7 points - excluding the highly silicified and ferruginized siltstone - Sample VP-K1B)	65
Figure 5.6	(a) SiO_2 - Al_2O_3 - Fe_2O_3 , and (b) K_2O - CaO - Na_2O ternary plots for the Dasdap Formation: the basal (proximal) sediments of the Kookoppe (◆); an overlying finer-grained (proximal) sediment from the Kookoppe (▲); distal sediments on the farm Burtons Puts (●), and distal sediments from Rondegat (▲).	67
Figure 5.7	TM-5 LANDSAT image of the surficial feature referred to as the Dasdap alluvial fan by Levin and Raubenheimer (1983), approximately 25 kilometres due south of Vaalputs. The image is approximately 30 kilometres across.	70
Figure 5.8	Map showing actual palaeocurrent directions determined from sedimentary structures, and inferred palaeocurrent directions for the Dasdap sediments.	73
Figure 5.9	Sketch map showing the position of the possible alluvial fans which may have given rise to the Dasdap sediments.	77
Figure 5.10	Palaeo-weathered rocks in the study area.	79
Figure 5.11	The silicified basement occurrences in the study area overlying weathered basement, which passes gradually downward into unaltered basement.	80
Figure 5.12	Photomicrographs of: (a) relatively unaltered basement gneiss (crossed-polarized light; field of view: 1.4x2.1 mm); (b) transition zone from fresh to palaeo-weathered basement (crossed-polarized light; field of view: 0.7x1.1 mm); (c) palaeo-weathered zone (crossed-polarized light; field of view: 1.4x2.1 mm); and (d) silicified basement (plain-polarized light; field of view: 1.4x2.1 mm).	82
Figure 5.13	Percentages of oxides plotted against height from the top of the silicified zone, for: (a) SiO_2 ; (b) TiO_2 ; (c) Al_2O_3 ; (d) Fe_2O_3 ; (e) MnO ; (f) MgO ; (g) CaO ; (h) K_2O ; and (i) Na_2O .	86
Figure 5.14	SiO_2 - TiO_2 - Fe_2O_3 ternary plot for six silicified zone samples and data of Summerfield (1983c), used to distinguish weathering and non-weathering silicites.	89
Figure 5.15	Plot of CIA values for selected palaeo-weathered basement samples versus height.	90
Figure 5.16	Calculated and actual weathering trends of selected profiles in the palaeo-weathered basement occurrences. Pl = plagioclase; Ks = alkali feldspar; Mu = muscovite; Ka = kaolinite. The large solid dot represents average granite of Nesbitt and Young (1984) and the large open dot, on the base line, the calculated proportions of Ca, Na, and K in leachants (derived from granite). The arrow on the lower dashed line shows the calculated initial trends followed by the leachates during the initial weathering stages; the upper dashed line was calculated from observed bulk compositional trends (Nesbitt and Young, 1989). The other trends are palaeo-weathering trends of this study.	92
Figure 6.1	Approximate suboutcrop boundary for the Vaalputs sediments compiled from TM-5 Landsat data and geological maps of Andersen (1992) and Andreoli et al. (1986).	104

Figure 6.2	(a) Location of the two waste disposal trenches at the disposal site (see previous figure). (b) Northwest-southeast section through the Vaalputs sediments and waste disposal trenches. Also indicated are the facies encountered in these trenches. Sediment thicknesses and depths to basement were obtained from Jamieson (1986).	105
Figure 6.3	Generalized stratigraphic column of the Vaalputs Formation.	106
Figure 6.4	Coarse pebble lens in the pebbly clay facies.	108
Figure 6.5	(a) Southern face of the intermediate-level waste disposal trench, showing the sharp contact between the lower pebbly clay facies and the gritty clay facies. (b) Close-up view of the contact showing the abundant root casts at this surface.	109
Figure 6.6	Typical grain size distribution for the pebbly clay facies.	111
Figure 6.7	Gritty clay facies with numerous rhizocretions and evidence of termite activity (note the red sand lull).	112
Figure 6.8	Typical grain size distributions for the gritty clay facies.	113
Figure 6.9	Grain size distributions for the facies boundary horizon and a burrow feature.	116
Figure 6.10	Eastern wall of the low level waste disposal trench showing the development of calcrete at three depths in the pebbly clay facies.	117
Figure 7.1	TM-5 LANDSAT image of the Vaalputs site and surrounding area showing the north-northeasterly oriented dunes in the vicinity of Vaalputs. The image is approximately 40 kilometres across (also note 2 km scale bar).	134
Figure 7.2	Photo taken from a dune crest and slightly obliquely to the dune orientation (022°). This photograph also shows a deflation pan developed in the inter-dunal trough area.	136
Figure 7.3	Windward (west) side of a dune showing the vegetation cover and bioturbation	137
Figure 7.4	The leeward (eastern) side of the dune covered by several grass types and small flowering plants.	138
Figure 7.5	West-east profile of a dune, showing the present surface and the subsurface calcrete horizon.	139
Figure 7.6	West-east dune profile, superimposed on (a) mean grain size (larger ϕ values represent smaller particle sizes), (b) sorting (larger ϕ values represent poorer sorting), and (c) skewness.	140
Figure 7.7	TM-5 LANDSAT image of the Vaalputs site and surrounding area showing the positions of the four traverses used for the northern (a), mid- (b), southern (c), and Santab lineament (d) traverses. The image is approximately 120 kilometres across.	143
Figure 7.8	Aerial photograph of the Santab lineament, looking southwest towards Santab-se-Vloer.	143
Figure 7.9	Sedimentary parameters for the northern traverse.	144
Figure 7.10	Sedimentary parameters for the mid-traverse.	145
Figure 7.11	Sedimentary parameters for the southern traverse.	146
Figure 7.12	Sedimentary parameters for the Santab lineament traverse.	147
Figure 7.13	Stages of dune formation (a), dune stabilization (b), and dune modification (c).	151
Figure 7.14	Typical occurrence of a deflation pan on the eastern side of Vaalputs.	154
Figure 7.15	Section and simplified stratigraphic sketch through a deflation pan floor.	155

Figure 7.16	(a) Immature deflation pan. Note the highly bioturbated and pebble strewn pan floor. (b) Mature deflation pan with well developed lunette and muddy pan floor.	157
Figure 7.17	Plane-tabled sketch map of an immature pan, developing in an interdunal area, on the eastern boundary of Vaalputs.	158
Figure 7.18	Plane-tabled sketch map of a mature deflation pan, developed in an interdunal area, approximately two kilometres to the southeast of the disposal site.	159
Figure 7.19	Plane-tabled sketch map of a mature deflation pan, developed on a resistant, horizontal substrate, approximately two kilometres to the southeast of the Vaalputs airfield.	160
Figure 7.20	North-south and east-west profiles across a typical deflation pan in the study area.	161
Figure 7.21	Proposed stages of interdunal deflation pan development. Sections are west-east, that is, most of the migration would be predominantly in a direction into the page.	166
Figure 7.22	(a) Typical lag deposits on the present land surface. (b) Terrane covered by lag deposit showing typical subrounded pebbles of various compositions. (c) Calcrete lag deposit resulting from calcrete outcrop in the vicinity of the deposit.	168
Figure 7.23	Size frequency histograms for pebble lag deposits: VP-53; VP-54; and VP-62.	170
Figure 7.24	The two common forms of termite mounds observed in the study area.	174
Figure 7.25	Bioturbation in dune deposits consists typically of burrows of small animals. The slightly older material forming the roofs of the burrows is a light brown colour; the red sands surrounding the burrows are more recent aeolian sands.	175
Figure 7.26	(a) Large animal burrows, in more stable areas, that is, where the soil is reasonably consolidated or cemented. (b) Calcrete may form the roof of large burrows. (c) Large areas of extensive bioturbation caused by large animals.	177
Figure 7.27	Mounds destroyed by animals burrowing in search of food.	178
Figure 7.28	Positions of the sites chosen for the heavy mineral study, using the A.E.C geological map of the waste disposal site (compiled by Andreoli et al., 1986).	181
Figure 7.29	The heavy mineral concentrations versus distance for site B: (a) ilmenite, north-south profile; (b) ilmenite, east-west profile; (c) iron-oxide, north-south profile; and (d) iron-oxide, east-west profile.	182
Figure 7.30	Iron oxide cemented facies, with the typical deep red colour and calcrete lined fractures.	187
Figure 7.31	Plot of mean grain size versus standard deviation (sorting) for the Vaalputs and Gordonla sediments. Fields for the typical range of Vaalputs (vertically hashed) and the Gordonla (horizontally hashed) Formations are superimposed on the data. Dune and river sand fields are after Friedman (1961).	192
Figure 7.32	Plot of skewness versus standard deviation (sorting) for the Vaalputs and Gordonla sediments. Fields for the typical range of Vaalputs (vertically hashed) and the Gordonla (horizontally hashed) Formations are superimposed on the data. Fields exclude the highly variable pebbly deposits.	193
Figure 7.33	Plot of mean grain size versus skewness for the Vaalputs and Gordonla sediments. Fields for the typical range of Vaalputs (vertically hashed) and the Gordonla (horizontally hashed) Formations are superimposed on the data. Fields exclude pebbly deposits.	194

Figure 7.34	Plots of SiO_2 versus (a) TiO_2 , (b) Al_2O_3 , (c) Fe_2O_3 , (d) MnO , (e) MgO , (f) CaO , (g) Na_2O , and (h) K_2O for the Gordonia and Vaalputs sediments, and selected sample suites from weathered surface basement deposits, Dwyka, and the Dasdap sediments.	200
Figure 7.35	Fe_2O_3 - MgO - Al_2O_3 ternary plot of the Vaalputs sediments and selected samples from the weathered surface basement, the white clay facies, surficial deposits of the Gordonia Formation, and Dwyka clay.	202
Figure 7.36	Stages in the development of the Gordonia Formation and surficial micro-environments.	207
Figure 8.1	Structural lineaments in the Vaalputs area derived from TM-5 Landsat data (various combinations). Gr=Garing fault; Gs=Gasab fault; R=Riembrek fault; S= Santab fault; St=Stofkloof fault; V=Vaalputs fault; B=Bok-puts fault and GTA=Griqualand-Transvaal Axis of uplift.	210
Figure 8.2	Rose diagram showing strike of all lineaments, as determined from data presented in Figure 8.1. All data are expressed as percentages of total lineament length.	211
Figure 8.3	Lineaments of Vaalputs superimposed on elevation contours of the base of the Vaalputs Formation. Basement rock contours were determined by Jamieson (1986). Section X-X' is described below (see Figure 8.5).	213
Figure 8.4	Topographic west-east cross section of Vaalputs, indicating the vertical displacements of palaeo-weathered and silicified basement occurrences.	215
Figure 8.5	West-east cross section of the eastern part of Vaalputs. The section is approximately 500 metres to the north of the disposal site, the position of which is shown in Figure 8.3. Solid lines represent primary (prominent) lineaments, whereas dashed lines are secondary lineaments.	216
Figure 8.6	Lineament map for the Dasdap area, obtained using SPOT panchromatic imagery. Also shown are the present land surface contours and the Dasdap drainage.	217
Figure 8.7	Rose diagram showing strike of all lineaments for the Dasdap area, as determined from data presented in Figure 8.6. All data are expressed as a percentage of total lineament length.	218
Figure 8.8	Map of the western portion of Vaalputs, that is, to the west of the Springbok road, showing the occurrences of altered basement and the observed lineaments (for section A-F see Figure 8.10). Lower case letters represent areas where detailed slickenside analyses were carried out, and are referred to in Section 8.2.2.	219
Figure 8.9	Staggered northeast trending cross section (the position of which is shown in Figure 8.9). Solid lines = primary faults; dashed lines = probable/secondary faults.	221
Figure 8.10	Typical well preserved slickensided surface in the prominent palaeo-weathered basement occurrences.	222
Figure 8.11	Stereo-net plot of all poles to the measured planes containing slickensides in the palaeo-weathered basement.	224
Figure 8.12	Rose diagram of all strike orientations of planes containing slickensides in the palaeo-weathered basement.	225
Figure 8.13	Rose diagram of all strike orientations of planes in the palaeo-weathered basement occurrences which are believed to be associated with tectonism (n=29).	226

Figure 8.14	Orientations of selected surfaces of proposed tectonic origin. For localities see Figure 8.8.	227
Figure 8.15	(a) Slip movement directions on movement planes for all proposed tectonically derived fractures in the palaeo-weathered basement occurrences on the western part of Vaalputs; (b) selected data of (a), which conforms to the case $C=1/1.1$ of Aleksandrowski (1985) [shown in (c)].	231
Figure 8.16	Orientation data summarized in rose diagrams for joints in the: (a) unaltered basement; (b) palaeo-weathered basement; and (c) silicified basement. All rose diagrams have class intervals of five degrees.	235
Figure 8.17	Typical calcrete-filled joint in the upper section of the surficial sediments (southwest wall of the low level waste disposal trench).	237
Figure 8.18	Orientation of joints present in the low and medium level waste disposal trenches ($n=21$).	238
Figure 8.19	(a) East-west section showing folding in the Karoo sediments in proximity to a vertical dolerite dyke (mostly replaced by calcrete). The hammer is positioned in the centre of the dyke. (b) East-west section, 20 metres to the east of (a).	240
Figure 8.20	Northeast oriented faulting in the Dwyka rocks in the area of the Krom River, approximately 80 kilometres southeast of Vaalputs.	242
Figure 8.21	Santab-se-Vloer with the higher western margin in the distance which defines the western Santab fault.	242
Figure 8.22	Surface expression of the eastern Santab fault, trending 160° .	243
Figure 8.23	Fault breccia in a shear zone adjacent to the Stofkloof fault.	244
Figure 8.24	Part of aerial photograph (number 1652, job number 588) showing the effects of possible fault reactivation along the Buffels River in the area around Rooifontein. Scale of photograph is 1:35 000, N to the top, and flow direction is from the east to the west. Fault f-f coincides with the road.	246
Figure 8.25	Photograph taken from the eastern side of the north-northeast trending lineament at Rooifontein, showing the accumulation of sediments in the foreground, that is, on the eastern side of the lineament (f-f).	247
Figure 8.26	Southwest-northeast profile of the present Dasdap drainage. Letters refer to detailed sections in the following figure.	249
Figure 8.27	Detailed sections of the Dasdap drainage (see previous figure for positions): (a) 5-6 km section; (b) 7.1-7.7 km section; (c) 8.2-9.0 km section; (d) 12.6-13.4 km section. Dashed lines indicate approximate average slopes for various sections of the profiles.	249
Figure 8.28	Epicentres of seismic events recorded by the A.E.C. in the northwestern Cape.	251
Figure 8.29	Recorded events (56 in total) for the period January to September 1996. Circles are directly proportional to the magnitude (ranging between 0.6 and 4.4). Also plotted are the primary lineaments of the region. Dashed line indicates the approximate position of the Great Escarpment and K refers to the area investigated in the vicinity of the Krom River.	253
Figure 8.30	Regional strain ellipses associated with the deformational phases responsible for the observed structures in the Vaalputs region at about 60 Ma (a), and during most of the Cenozoic (b).	256

Figure 9.1	Proposed depositional environment for the Dasdap Formation.	263
Figure 9.2	Simplified cross-section of the Vaalputs region during: (a) the Cretaceous weathering phase; and (b) the initial modification of the Cretaceous surface.	265

LIST OF TABLES

	Page
Table 1.1 Lithostratigraphy of the Vaalputs region, modified after Andreoli et al. (1987). Double lines represent unconformities.	6
Table 3.1 Post-Gondwanaland development of the southern African landscape, according to Partridge and Maud (1987).	22
Table 4.1 Lithostratigraphic subdivisions of rock suites intrusive into the Namaqualand Metamorphic Complex as applicable to the study area (after SACS, 1980; Joubert, 1986a; and Ashwal, 1997).	42
Table 4.2 Structural events of Precambrian age for Namaqualand (modified after Clifford et al., 1975; Allsopp et al., 1979; Joubert, 1986a; and Andersen, 1992).	44
Table 5.1 CIA values of the Dasedap sediments and mean values for the palaeo-weathered basement vaalputs.	69
Table 5.2 Normative chemical compositions for the major minerals of the basement, and the silicified and weathered zones.	94
Table 5.3 Petrographic and chemical criteria used for distinguishing weathering and non-weathering profile silcretes (Summerfield, 1983a).	96
Table 6.1 Range of sedimentary parameters obtained for five samples of the pebbly clay facies.	110
Table 6.2 Range of sedimentary parameters obtained for three samples of the gritty clay facies.	114
Table 6.3 Range of sedimentary parameters for the red sands and the two facies in which they occur.	115
Table 6.4 Sample localities, and ¹⁴ C age data for the calcrete samples.	121
Table 7.1 Average sedimentary parameters for the constituents of a deflated area or pan.	162
Table 7.2 Sedimentary parameters for two surface (VP-53 and VP-54) and one 80-centimetre-depth* (VP-62) lag deposit.	169
Table 7.3 Results of element-normalised, semi-quantitative S.E.M. results for ilmenite grains. All data are given in weight percent.	184
Table 7.4 Range of sedimentary parameters for the iron oxide rich sandstone (Dorbank), and the Gordonia Formation (aeolian sediments only).	188
Table 8.1 Characteristics of two slickenside types (based on proposed origins) present on fracture surfaces in the palaeo-weathered and silicified basement occurrences.	223
Table 8.2 Average, and range of joint densities obtained for the unaltered basement, and the palaeo-weathered and silicified basement.	234

CHAPTER 1: INTRODUCTION

1.1 Location and Geographical Setting of the Study Area

The study area covers a region in the Northern Province, centred around Vaalputs, the national radioactive waste disposal site (Figure 1.1). Vaalputs is situated approximately 90 kilometres to the southeast of Springbok, and the study area lies between 29°50' and 30°30' south, and 18°10' and 18°50' east. The study area comprises the eastern part of Namaqualand and the western part of Bushmanland, situated at an elevation of about 1000 metres above sea level. This area affords a window into the geomorphic, sedimentologic and tectonic development of the Bushmanland Plateau extending back to the mid- to upper-Cretaceous. Although the entire region around Vaalputs was investigated (Figure 1.2 shows the area of broader investigation), most of the detailed work was carried out on the property of Vaalputs and its environs (Figure 1.3).

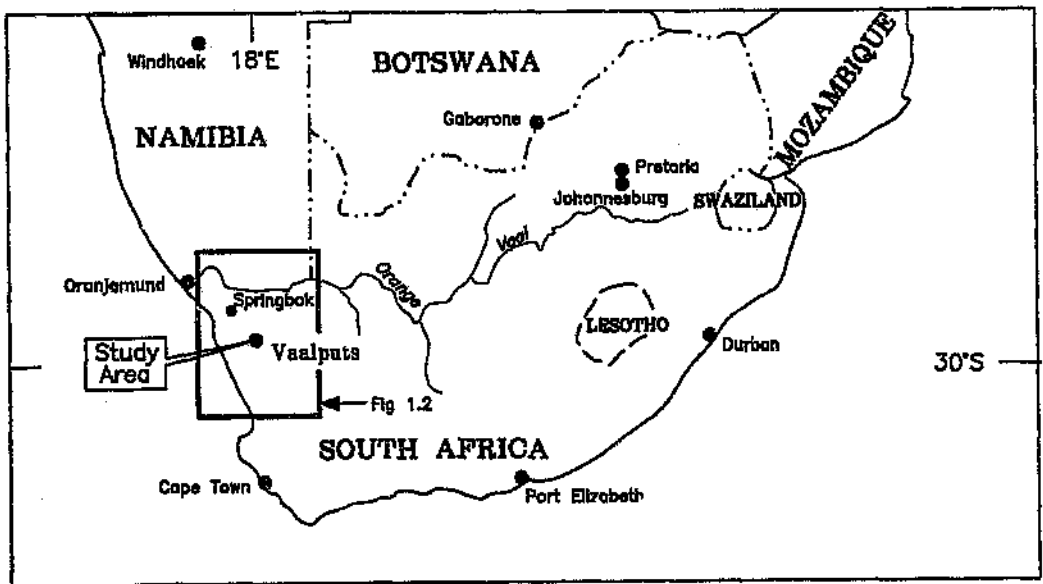


Figure 1.1 Location of the Vaalputs National Radioactive Waste Disposal Facility and study area. Inset is area of broader investigation and is shown in Figure 1.2.

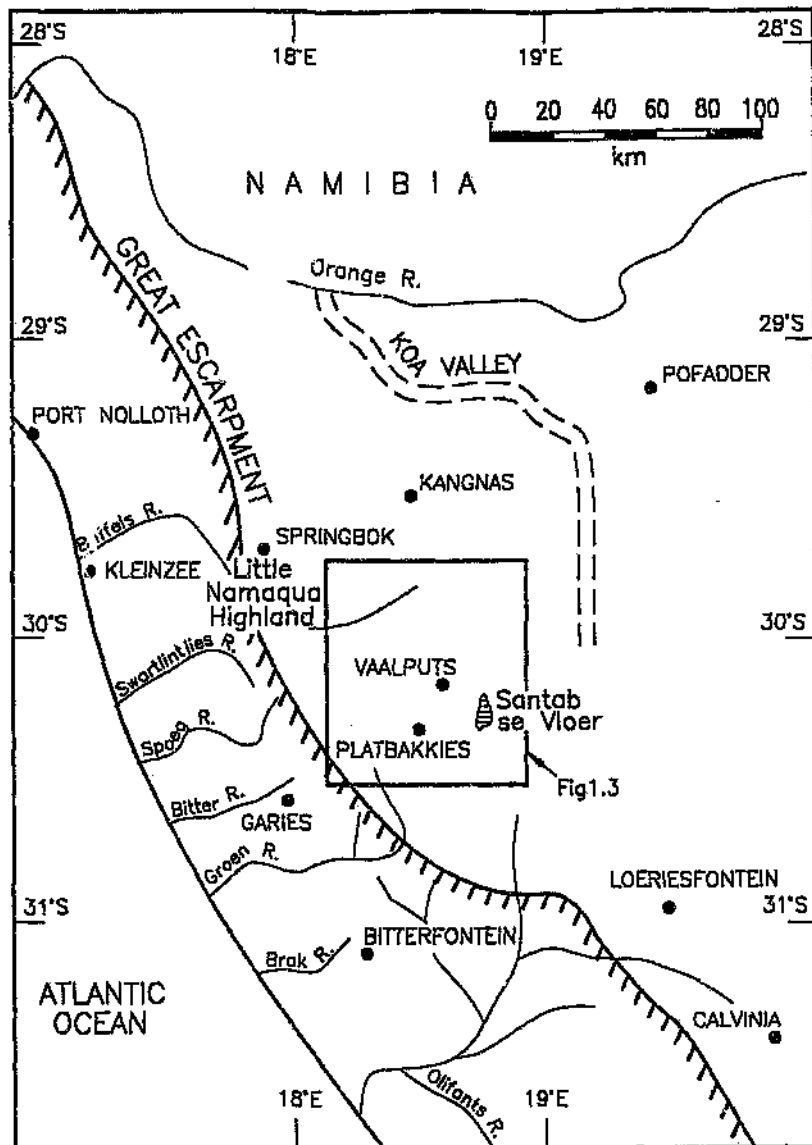


Figure 1.2 Area of broader investigation showing the main features of the region. Inset shows the area of detailed investigation (see Figure 1.3).

The study area may be separated into two distinct geomorphological terrains, which are separated by a major N-S watershed (Figure 1.3). This watershed is defined approximately by the main Springbok-Platbakkies road. The western section consists of rugged mountainous granitic terrain, with steep cliffs of altered and silicified basement. The basement gneiss outcrops typically form tors and bornhardts. In this

area, sandy pediments, with more gentle slopes form the valley floors. The eastern section consists of the generally featureless, and gently undulating Bushmanland Plateau. The slightly undulating eastern portion is characterized by low-amplitude palaeo-dunes which have a north-northeasterly trend.

The higher lying rugged terrane in the west includes the Little Namaqua Highland (Figure 1.2) at an elevation of approximately 1200 metres in the study area (and which may reach elevations of 1700 metres further to the west), which is heavily dissected by drainage. The drainage on the more rugged western side is largely controlled by geological structure and follows deeply incised fracture defined lineaments. The lower inland surface, at an elevation of 1000 - 1100 metres, has been variously named the Bushmanland Plateau (Mabbutt, 1955) and the African surface (King and King, 1959; Partridge and Maud, 1987). The drainage on the eastern lower lying area follows the interdunal areas or troughs of palaeo-dunes, and frequently ends in a depression or deflation pan. The largest pan in the study area is Santab-se-Vloer (Figure 1.3). The eastern end of the "dune field" is terminated by a low scarp of calcretized Dwyka tillite at Santab-se-Vloer. Slightly further to the east, basement rock outcrops become fairly prominent, but in the central part of the "dune field" no outcrop is present.

The main watershed in the area which divides the Bushmanland Plateau and Namaqualand, separates the drainage basins of the Olifants, Buffels and the (inactive) Koa Rivers (Figure 1.2). The drainage basins of the Buffels River occupy the west, the Olifants River the south and southwest, and the Koa River the northeast (Levin, 1988). The drainage divide of the Koa and Buffels Rivers is defined by the marginal scarp, which trends approximately north-south. The southern Olifants drainage is, however, more complex, with a tributary system of this river developed west of the marginal escarpment and which closely resembles the Buffels River (McCarthy et al., 1985). The Olifants River catchment also encompasses the southeastern portion of the study area, which lies on the Bushmanland Plateau (Figure 1.3). The watershed separating the Koa and Olifants Rivers is poorly defined due to the gentle land surface on which it has formed.

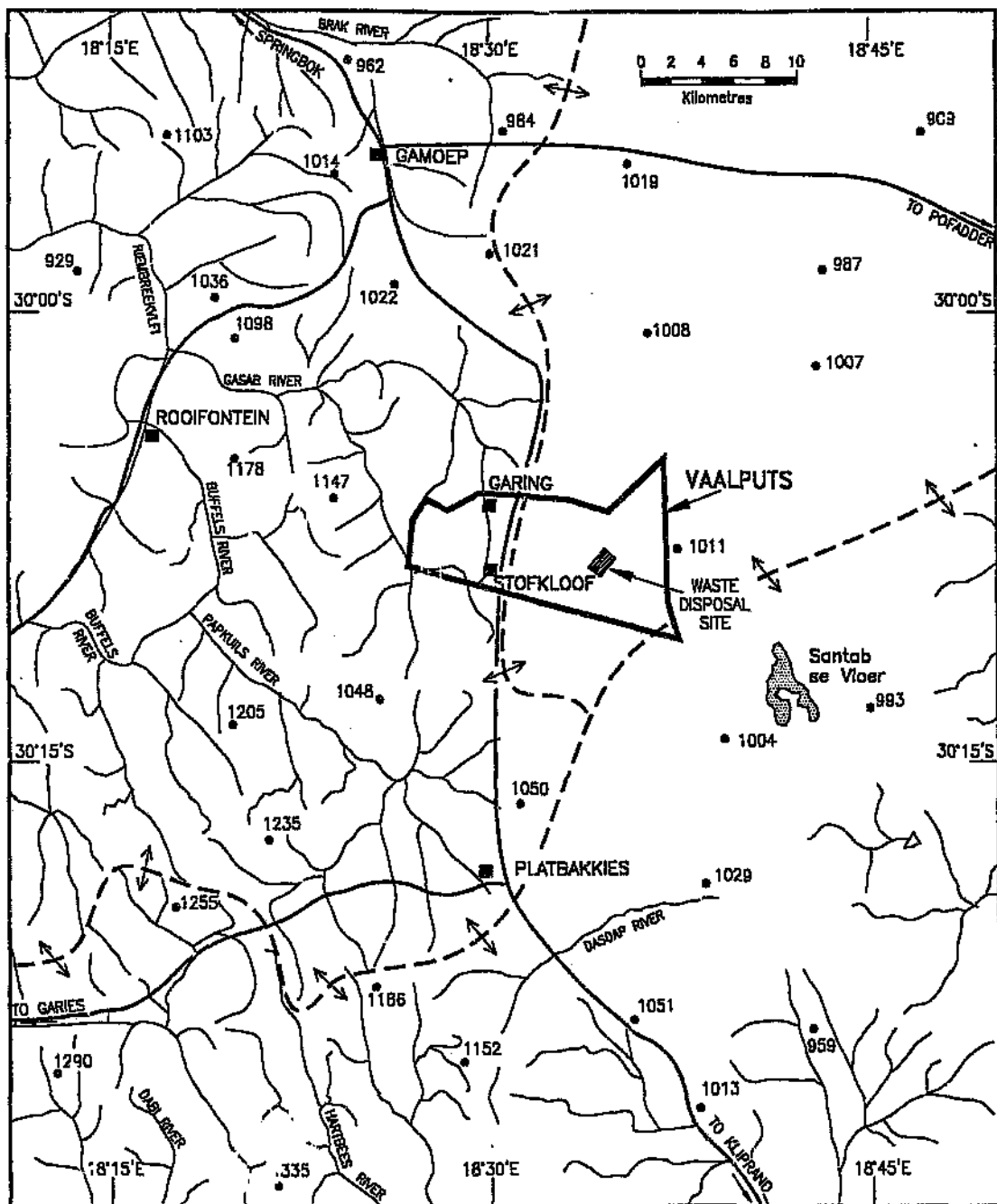


Figure 1.3 Approximate area investigated, showing Vaalputs, the national nuclear waste disposal site. Spot heights are given in metres. Also shown are the approximate positions of the drainage divides in the area.

The climate of this area is characterised by anticyclonic conditions throughout the year (Brynard, 1988). Day-night temperatures varying between 7°C and 36°C for summer, and between -1°C and 22°C for winter, may be experienced. The western part of the Bushmanland Plateau falls in the rain shadow of the mountain land to the west during the winter rainfall period, and in summer the interior winds lack moisture, generally resulting in low summer rainfall. The area, therefore, lies in the transitional zone between summer and winter rainfall regions, and has an average precipitation of 74 millimetres per annum (Redding and Hudson, 1983). However, sporadic flashfloods with more than 100 millimetres recorded per individual storm, occur occasionally. Flashfloods of this nature have been noted to totally submerge the surface (particularly in flatter areas) and cause severe erosion. Vegetation is sparse on both the sand covered plateau in the eastern, and on the rocky outcrops in the western parts of the area.

According to the Weather Bureau, strong winds (the strongest are northerly), have been known to gust up to 36.6 m.s⁻¹ (for the period 1952-1973) and a gust of 54.4 m.s⁻¹ can be expected every 100 years in the Upington area. In the Vaalputs area in particular, the predominant wind direction is south-southwest (17%) with average wind speeds of 3 to 8 m.s⁻¹ (Hambleton-Jones, 1986). Winds of up to 11 m.s⁻¹ are also experienced in this sector, but only 1% of the time. Northeast (14%) and northwest (1%) winds are experienced for a total of 28% of the year and wind speeds rarely exceed 8 m.s⁻¹. Also, according to Hambleton-Jones (1986), the frequency of calms (<1 m.s⁻¹) is 2%, suggesting that the wind blows virtually all year round in this region. Sand and dust storms are common phenomena in the region, in particular those resulting from the dry easterly berg winds during the winter months. Wind direction, duration, and average velocity data indicate a resultant direction from west to east. This resultant direction has implications for sediment transport in the area (Vaalputs and Gordonia Formations).

1.2 **Stratigraphy**

The detailed geology and stratigraphic relationships of the Vaalputs region were determined by Andreoli et al. (1987) and Ashwal et al. (1997). The presently accepted

stratigraphy for the region, is summarized in Table 1.1, but will be dealt with in more detail later. The results of this study suggest that some minor changes to this stratigraphic sequence should be made.

Table 1.1 Lithostratigraphy of the Vaalputs region, modified after Andreoli et al. (1987). Double lines represent unconformities.

Sequence Group/sub-group Suite	Formation/ Granite type	Lithology	Age (Ma)	Origin
	Gordonia	Red sand	2-20	Aeolian
	Vaalputs (Red Clay)	Calcrete and silcrete nodules Brown, grey and white sandy to gritty clay with intercalated pebble bands	0-35 20-35	Chemical precipitate Alluvial fan and fluvial sheetwash
	White Clay	Grey-white sandy to gritty clay and weathered basement Siliceous sandstone	20-35	In-situ weathering of basement rocks
	Dasdap	Conglomerate Immature cross-bedded arkosic grits	20-38	Alluvial fan
		Olivine-mellilitite Kimberlite	35-67	Intrusions
Karoo Supergroup		Dolerite Tillite	180 ~295	Intrusions Glacial
		Pegmatites		Syn- to late-tectonic intrusions
Vaalputs Suite		Diorite, norite Hyperstheneite, anderbite Quartzolite, nelsonite	~10-5	Late-tectonic basic intrusions into the Garies Group
Kliprand Charnockite Suite		Charnockite		
Syntectonic Granite Suite	Leucogranite Vaalputa Stofkloof	Various granitoids	~1050	Syn- to late-tectonic granitic intrusions into the Garies Group
Hoogoor Suite		Undifferentiated quartzo-feldspathic (pink) gneisses		
Little Namaqualand Suite	Nababeep	Augen gneiss		Granitic intrusions
Okiep Group (Garies Subgroup)		Quartzo-feldspathic gneiss Granulite (undifferentiated)	1040- 1150	Metamorphism of ancient arkosic-peilitic gneisses, basin intrusions

Precambrian crystalline metamorphic and intrusive rocks belonging to the Namaqualand Metamorphic Complex form the basement to the late Palaeozoic (Karoo) rocks. These are both overlain by Tertiary (Dasdap/Vaalputs) deposits (e.g., Brynard,

1988). Younger surficial deposits cover most of the Bushmanland Plateau, and overly the clayey deposits of the Vaalputs Formation, and the gravels and sands of the Dasdap Formation (Andreoli et al., 1987). The younger deposits have tentatively been correlated with the Gordonia Formation (SACS, 1980), and are referred to as such in this study. Isolated outcrops of calcrete, consisting of nodular calcrete, with occasional silcrete, occur at Vaalputs. Depressions and valleys in the area to the west of the main water-shed and in the escarpment are commonly infilled by deposits of alluvium, which are slightly ferruginized in places. These deposits are also believed to be of recent age.

1.3 Objectives

Seismic data of the Council for Geosciences, and recent seismic studies carried out by the Department of Earth and Environmental Technology (E.E.T) staff of the Atomic Energy Corporation (A.E.C) in the Vaalputs area and environs have indicated that there is appreciable seismic activity over a broad region of the northern Cape. In addition, satellite images and aerial photographs have recorded the presence of a network of lineaments in recent cover. It was, therefore, proposed that a detailed study be made of the Mesozoic and Cenozoic tectonic history of this area. The study aimed at better understanding passive rift continental margin evolution and the intraplate seismicity associated with such a margin. Also, the geomorphology of the area has previously only been examined on a reconnaissance basis, and a variety of discrete events have been recognized. However, the geomorphological, sedimentological and geologic episodes needed to be placed in a more thoroughly constrained time frame. The main sedimentological/geomorphological events concerned are:

- i) the Dasdap Formation;
- ii) palaeo-weathering/palaeosol formation;
- iii) the Vaalputs Formation;
- iv) the Gordonia Formation/recent sedimentation; and
- v) the present-day surface processes.

The environmental significance (sedimentology) and palaeo-climate of each of these episodes was investigated, as this may provide insight into long-term climatic change

and hence repository performance. In addition, certain of these geomorphic episodes may be directly correlatable to major tectonic events in the area, which could provide valuable tectonic information. The response of the landscape development to tectonic processes plays an important role in controlling the infilling of sedimentary basins (e.g. Summerfield, 1991b). The primary objectives of this investigation were, therefore, aimed at understanding the Cenozoic neotectonic structural history of the rocks; the geomorphological and sedimentological conditions under which the surficial sediments were deposited; and to place the major geomorphological and geological episodes into a well constrained, relative time frame.

CHAPTER 2: METHODS USED IN THIS STUDY

2.1 Satellite Imagery and Airphoto Interpretation

Satellite images and aerial photographs, together with existing data were used to produce a comprehensive lineament map of the area, and to identify and to produce distribution maps of the geomorphological features and sedimentary deposits. TM-5 LANDSAT and SPOT data were acquired from the Satellite Applications Centre, Hartbeeshoek. The data were processed by the writer using computer facilities at Anglo American Corporation's Head Office, Johannesburg, and at the University of the Witwatersrand. The Map and Image Processing System (MIPS) software was employed for image processing.

The processing of the TM-5 LANDSAT data used a number of combinations of the seven available bands. The area covered by the quarter scene (TM path 176, row 81, quadrant B) used for this study is bounded by latitudes 29°35' and 30°25' S, and longitudes 18°10' and 19°15' E. Combinations including a high pass filter on band five (infra-red) and principal components of bands one through four were analyzed and interpreted for lineament identification. The various combinations used were found mostly by trial and error methods (also pers. com. to P. Linton of the Anglo American Corporation). In addition to the structure observed using these combinations, data obtained from other combinations using primarily bands three, five and seven, and the principal components of bands one through four, were included in the final compilation of a lineament map for Vaalputs and the Vaalputs environs.

A hard copy of the false colour composite combination using band five (filtered), band three, and band two, assigned the colours red, green and blue respectively, was produced. Figure 2.1 shows this image and some of the localities frequently referred to in this work. Various geomorphological features and sedimentary deposits were also identified using primarily this combination. The 5(filtered)-3-2 combination of bands (Figure 2.1) was particularly useful for the mapping of various lithological units, such as the altered basement occurrences and Dwyka outcrops.

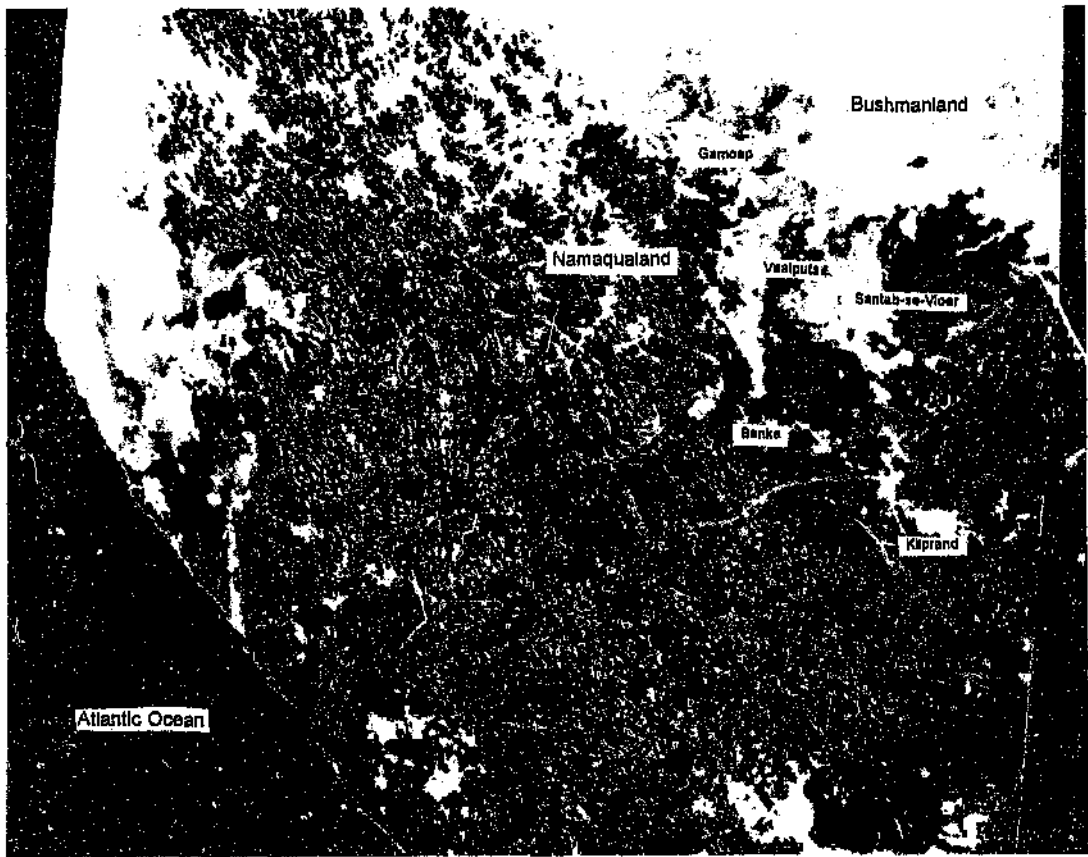


Figure 2.1 TM-5 LANDSAT image of the study area using bands five (filtered), three, and two (red, green, blue respectively). N is to the top, and the image covers an area of approximately 200 km x 160 km

In addition to LANDSAT data, SPOT panchromatic remote sensing data of the study area were processed using the Map and Image Processing System (MIPS) software. The data were filtered and sun-shaded to facilitate lineament identification. These satellite images provided a synoptic view of the structural features, geomorphology and geology of the region, and thus created a context for more detailed, ground-based studies.

2.2 Field Mapping and Sampling

This phase of the project involved fault mapping and the collection of detailed structural data, including slickenside measurements. Field mapping and ground studies of large and small scale structures were aided by airphoto interpretations. These studies were carried out on basement exposures, and in particular on palaeo-weathering profiles on the western side of Vaalputs. A detailed comparative joint analysis of the unaltered basement with that of the overlying palaeo-weathered basement was carried out to determine the effects of jointing on these occurrences, and the degree to which joint orientations may correlate with the orientations of larger structures.

A suite of basement rocks and their overlying palaeosols were sampled from the outcrops on the western side of Vaalputs to compare the palaeo-weathering profile with more recent weathering profiles. This study made use of mineralogical, geochemical, and petrological techniques. Other weathered basement materials (Namaqualand Metamorphic Complex gneisses and Dwyka Group) were collected from various localities in the Vaalputs region to enable geochemical comparison with the Vaalputs and Gordonia sediments. This was undertaken to determine the provenance of the surficial sediments preserved in the area. Samples of the lithified Dardap Formation, which forms part of the basement to the surficial sediments was sampled for a geochemical and petrological analysis.

A detailed sedimentological study of the surficial deposits of the region was undertaken to determine the depositional history and origin of the various deposits. These included the Vaalputs, and Gordonia Formations. In addition a study was made of present day processes taking place in localized environments or micro-environments, on the Gordonia Formation deposits, as an aid to interpreting the older Vaalputs deposits. Samples of the Vaalputs and Gordonia Formations, as well as recent deposits were collected from the waste disposal trenches, percussion boreholes and from the surface. Samples were chosen to best represent the various facies, and the micro-environments encountered at surface. Grain size and geochemical and petrological analyses were undertaken on these samples.

Several calcrete samples were collected from various horizons exposed in the waste disposal trenches, as well as from surface outcrop at Vaalputs. The primary aim of the calcrete sampling was for ^{14}C dating, in an attempt to obtain approximate or at least minimum ages for the various horizons, which could allow for a better chronological understanding of the geomorphological and tectonic events responsible for the surficial deposits of the area.

2.3 Sedimentological Studies of Surficial Deposits

Trench exposures, made for the disposal of radioactive waste, were mapped and sampled. Several drill-cores were studied and sampled, particularly for the lower Vaalputs sediments which were not exposed in the waste disposal trenches. Surface deposits and micro-environments were identified, investigated and sampled. Each micro-environment was carefully analyzed in terms of spatial occurrence, physical characteristics (including section profiles for the aeolian dunes and deflation pans), and appearance. Topographic profiles were obtained using a Kern level and staff, at an interval spacing of 10 metres and 5 metres for the dunes and deflation pans respectively. Shallow trenching was carried out in the various surficial deposits to obtain 3-dimensional information in these areas. In addition, a sand size analysis was carried out to determine the size distribution of material in relation to processes and provenance. This investigation included the following:

- i) A detailed particle size distribution of representative material in each of the recognised micro-environments. Several samples were collected from each micro-environment to determine grain-size distributions within each environment. In addition to determining the processes responsible for each micro-environment, the sedimentary parameters could be compared to possible sediment sources.
- ii) Collection of surface samples along four long east-west traverses across the Vaalputs area to determine regional grain size variations. Also included was a traverse, on a northerly extension of, and perpendicular to, the Santab lineament, which forms the eastern limit of the Vaalputs basin. Samples were collected at depths of

approximately 5 centimetres, along three, approximately 20 kilometre long, east-west traverses at 1 kilometre spacings, and along a six kilometre long, east-west, traverse across the northerly extension of the Santab lineament.

A heavy mineral study over known ultramafic (kimberlitic) intrusions which underlie the surficial sediments, was carried out. This was done to determine the possible surface expression of these intrusions, in the form of heavy mineral concentrates. Ilmenite is a diagnostic mineral of kimberlite-related and other mafic intrusions and, therefore, concentrations of this mineral in the sediments overlying such intrusions could be used as an indicator of bioturbation.

Samples collected were sieved in the field to obtain the $1\phi-0\phi$ (0.5mm-1mm) size fraction, as this fraction is larger than that expected to be of aeolian origin. Primary concentrates were obtained from 100 grams of this size fraction which was "jigged" for three minutes in a portable mechanical jig. Parameters such as water level in the jig and time of operation were standardized to ensure reproducibility. A motor driven vibrating mechanism concentrated the heavy minerals in the central part of the sieve which was placed in the water. The heavy mineral concentrates obtained in the field were further concentrated in the laboratory using bromoform.

The heavy mineral concentrate contained primarily ilmenites, various iron oxides and garnets. As some of the iron oxide grains have a similar appearance to ilmenite, unambiguous identification of ilmenite is difficult. In an attempt to resolve this problem polished sections were prepared of selected samples and analyzed using the Scanning Electron Microscope (S.E.M.), EDAX system at the Electron Microscope Unit, University of the Witwatersrand. Two grains of ilmenite (one of definite kimberlitic origin - supplied by Prof. R.G. Cawthorn, and one from a mafic pipe outcrop from the farm Kalkdraai, approximately 20 kilometres to the south of Vaalputs) were used for comparative purposes. This allowed for ilmenite to be distinguished from other iron oxide grains by their composition.

2.4 Analytical Techniques

Grain size analysis

Standard sand size analyses using the mechanical sieving methods were performed on the unconsolidated sediment samples. Samples were reduced in size to approximately 100 grams using a mechanical sample splitter. For coarse pebbly deposits, samples ranging in size from 850 to 1350 grams were used to accommodate the larger pebble fractions, as a normal 100 gram sample would not allow for representative grain size data. Grain sizes were determined for the coarse pebble fractions by individually measuring the diameters of several hundred pebbles.

The samples were sieved for approximately 10 minutes using a sieve size interval of 0.5 phi. The sieving method employed was that of Friedman and Johnson (1982). The fractions retained on each sieve were recorded and size distribution data for each sample were graphically presented in the form of frequency histograms and cumulative frequency curves. Statistical measures (mean, standard deviation/sorting, and skewness) of the frequency distributions were determined graphically using the cumulative-frequency curves (see Folk, 1974).

Petrographic procedures

Modal and textural analyses were undertaken on selected grain-mounts and thin sections of surface materials for the various micro-environments, as well as from the sediments of the Vaalputs and Dasdap Formations. The Vaalputs Formation samples were all collected from drillcores or from the exposures offered by the waste disposal trenches. Point counts were made using a Swift Point Counter (Model E) to determine relative proportions of quartz, feldspar and rock fragments. For the modal analyses 200 to 300 points per thin section were counted. Graphs represented by Galehouse (1971) showing probable error at 95 % confidence level plotted against points counted for various mineral percentages, indicate that this number represents an optimum investment of time. No distinction was drawn between plagioclase and K-feldspar. Lithic fragments included polycrystalline quartz (sedimentary and metasedimentary), cemented, and undifferentiated rock fragments. The modal percentages of the lithic

fragments may be slightly underestimated due to the difficulty in recognising decomposed granitic gneiss grains in certain more clay-rich sediments.

Chemical and mineralogical analyses

Chemical and mineralogical analyses were carried out using the X-ray fluorescence and X-ray diffraction techniques in the Geology Department, University of the Witwatersrand. Samples were crushed and milled to a fine powder. Approximately 2 grams of powder were weighed into a silica crucible and heated to 1000°C for six hours. The sample was reweighed to calculate the loss on ignition (LOI). Approximately 0.28 grams of baked powder was mixed with NaNO₃ and Spectroflux 105 (lithium tetraborate, lithium carbonate and lanthanum oxide). This mixture was melted to make fusion discs after the method of Norrish and Hutton (1969).

Samples were analyzed for major and minor element oxides on a Phillips PW 1400 X-ray fluorescence spectrometer. The results are tabulated in Appendix E. Total iron contents are expressed as Fe₂O₃. Analytical precision (2σ) for the major elements are: Fe₂O₃: 0.01%; TiO₂: 0.01%; MnO: 0.01%; K₂O: 0.01%; P₂O₅: 0.01%; SiO₂: 0.1%; MgO: 0.1%; Na₂O: 0.1%; Al₂O₃: 0.1%; CaO: 0.01%. These statistics represent the total analytical uncertainty in the procedure, including sample preparation.

X-ray diffraction was used to determine the mineralogy of the clay fractions of selected samples throughout the study area. The clay fraction was mounted on a plastic tile and analyzed using a Phillips PW 1830 diffractometer with a Geiger detector and graphite monochromator, employing Cu radiation. The instrument settings were: kV = 40 and mA = 20. Minerals were determined using standard identification tables.

SEM work was carried out on heavy mineral concentrates of surficial deposits from selected sites at Vaalputs as described previously (Section 2.4). Finally ¹⁴C dating techniques were carried out on selected calcrete samples by the Schonland Research Centre, University of the Witwatersrand.

CHAPTER 3: PREVIOUS WORK

3.1 Geomorphic Evolution of the Northern Province: Models of Landscape Development

The morphology of the southern African landscape has been studied since the beginning of the century (e.g. Suess, 1904; Penck, 1908). As the present study involved the understanding of various aspects of landscape development, from the time of the break up of Gondwanaland, and the effects this would have on passive continental margins (escarpment development), and the repercussions on their marginal hinterland areas such as that in which Vaalputs is situated, a brief review of previous work on passive rifting models is given.

3.1.1 Models of Passive Rifting

The development of the "Great Escarpment" (western part of the study area), which forms an integral part in the evolution of the Tertiary drainage systems (de Wit, 1993), has been debated for some time. The Great Escarpment, which trends roughly parallel to the coast at distances of between 50 and 300 kilometres in southern Africa, separates the elevated interior from the coastal margin. Suess (1904) identified the Great Escarpment as a denudational feature, unrelated to faulting. Along the southern and southeastern sub-continent, the escarpment has been suggested (Partridge and Maud, 1987) to be the result of major updoming, which preceded the rifting and continental separation (142 Ma ago). The northern Mozambique Basin was formed between 142 and 133 Ma, while the earliest separation along the west coast has been dated to 127 Ma (Dingle et al., 1983). According to Dingle et al. (1983) the development of the African continental margin was paralleled by a shift in sedimentary depocentres from mid-continental cratonic areas to the actively developing marginal zones. Uplift along the continental margin has long been recognised by others, e.g. Dixey (1955a); Maud (1961); De Swart and Bennet (1974); and Dingle et al. (1983).

Martin (1953) and Dixey (1955b), however, believe that the Great Escarpment may be

a much older feature, and have argued for the existence of a pre-Karoo escarpment which was not very far from the present escarpment. Visser (1981; 1985) supports this by placing the western edge of his Carboniferous Cargonian Highland close to the present escarpment. De Wit, (1988) believes that the western escarpment is closely associated with an exhumed pre-escarpment.

The past few decades have seen the introduction of various models of passive rifting. These include models of pure shear (e.g. McKenzie, 1978), simple shear (e.g. Wernicke, 1981; 1985), hybrid - pure and simple shear (e.g. Coward, 1986), and compound - passive extension and secondary convection (e.g. Keen, 1985). Summerfield (1988) suggests that the major incentive for the introduction of these models has been the inability of existing lithospheric extension models to account for the obvious morphological features of passive margins, especially their often significant marginal upwarps. Rowley and Sahagian (1986) suggest a non-uniform, continuous stretching within a polygonal region bounded by symmetrical, outward-sloping boundaries within the mantle as a modification to these models. They believe that crustal uplift results from asthenospheric upwelling beneath the regions in which the geometry produces a thinning of the lithosphere below the crust.

Dunbar and Sawyer (1988) highlighted the tendency for rifts to follow orogenic belts and to avoid cratonic regions. They also point out that different kinds of local weakness in the lithosphere may influence the mode of rift development. They argue that, where failure is associated with weakness located in the crust, rifting will result in a graben formation with shoulder uplift (with little or no volcanism). By contrast they predict that a mantle weakness failure will generate an initial lithospheric doming and extensive volcanism with graben formation occurring only at a later stage. Both these models correspond in their effects to the conventional contrast between passive and active rifting but, according to Dunbar and Sawyer (1988), both rifting styles may occur in response to regional tensional stresses within the lithosphere.

Nyblade and Robinson (1994) refer to the elevated eastern and southern parts of Africa as the African Superswell, which is characterized by anomalously elevated topography,

exceeding global mean values by more than 1000 metres in places. Partridge et al. (1995b) suggest that although the early movements or episodes of uplift contributed to the amplitude of the African Superswell, they were superimposed upon a landscape that was already at a high elevation. Nyblade and Robinson (1994) argue that the generation of the Great Escarpment implies the existence of the Superswell prior to, or contemporaneously to continental rifting; large scale uplift being inhibited by the existence of extensive sedimentary sequences on the continental shelf and slope. In contrast Partridge and Maud (1987) prefer the Great Escarpment as primarily a product of the high pre-rifting elevation of Africa, which occupied a central position within the Gondwanaland mosaic.

3.1.2 Escarpment Evolution

Ollier (1985b) interpreted the escarpments of southwest Africa to be genetically related to continental rifting and that they have retreated inland from the rift hinge zone since continental breakup when baselevels dropped considerably and/or the margins of the continents were uplifted. Kooi and Beaumont (1994) investigated the factors that control escarpment evolution and retreat using a quantitative surface process model, which supports the interpretation of Ollier (1985b). Gilchrist et al. (1994) also proposed a conceptual model of landscape evolution and employed a numerical surface process model to explore the controls on landscape development in the context of escarpment development. Their model calculates isostatic response by averaging denudational unloading and sedimentary loading for various time steps since the time of rifting. In a similar study Tucker and Slingerland (1994) presented model results suggesting that bedrock channel steepening and lateral retreat are viable mechanisms for large-scale, long-term escarpment retreat. Their results couple escarpment retreat and isostatic uplift, which in turn provides a mechanism for impeding divide migration.

Lambeck and Stephenson (1985) have argued, along with Summerfield (1985) and Thomas and Summerfield (1987), that although scarp retreat lowers the landscape overall, flexural isostasy in response to denudational unloading can promote net uplift on relatively uneroded plateau areas in the vicinity of retreating escarpments. Gilchrist

and Summerfield (1990) also pro. used a model of isostatic response to contrasting denudation rates on either side of the rift shoulder during passive continental rifting. Their model predicts a flexural bulge up to 600 metres in amplitude which migrated inland from the coast over a period of 100 million years since rifting. They predict that the amplitude and wavelength of the marginal uplift will vary as a function of both the height of the escarpment and the flexural properties of the underlying lithosphere. In support of their model they recalculated sedimentation rates off the west coast of southern Africa, based on the work of Rust and Summerfield (1990), which suggests that sedimentation rates increased through the Cretaceous and peaked in the Palaeocene and Eocene. Dingle et al. (1983) and Partridge and Maud (1987) report records of a decline in sedimentation rates through the Cretaceous, which became more pronounced following climatic deterioration at the end of the Cretaceous. Based on these findings Partridge et al. (1995b) suggest that the results of Rust and Summerfield are in error due to sparse borehole data and imperfect calibration of seismic reflectors. Ten Brink and Stern (1992) considered uplift to have occurred early after rifting in response to both thermal and isostatic influences. Partridge et al. (1995b), however, showed that their conclusions were not supported by geomorphic and other evidence, and that nowhere within the offshore marine sequences could pulses of Cenozoic sedimentation, and consequent loading of the continental shelf, have occurred on a scale to cause so large an isostatic response.

According to Summerfield (1991b) isostasy is critical in accounting for the topography of mature passive margins and that neither thermal nor mechanical effects associated with rifting can adequately explain the persistence of upwarps for > 100 Ma after rifting and their location > 100 kilometres from the zone marking the boundary between rifted and non-rifted lithosphere. Rust and Summerfield (1990) used sediment accumulation rates and Brown et al. (1990) used apatite fission track dating to determine the denudational history of the western margin of southern Africa. Also, rather than generating a discontinuous response (Gunn, 1949) to progressive escarpment retreat from a newly formed passive margin, the flexural isostatic model (e.g. Summerfield, 1991b) predicts the gradual development of a marginal upwarp inland of the escarpment.

3.1.3 Landscape Development of Southern Africa

The morphology of the southern African landscape is, to a great extent, controlled by the underlying geology, that is, both structure and lithology. Most of southern Africa is characterised by a mature landscape, which contains several erosion surfaces, separated by prominent scarps (de Wit, 1993). King (1951) interpreted these surfaces as successive periods of erosion produced by pediplanation, in which back-wearing is predominant. King (1949) argued that the co-existence of different aged land surfaces is possible only if landscape evolution proceeds under a process of pediplanation, through backwearing. The various surfaces he claimed were best dated in relation to the time of termination of the relevant erosion cycle by the process of uplift. These surfaces King (1951) classified as: the Gondwana surface (Jurassic); the African surface (mid-Cretaceous); the post-African surface I (Miocene); and the post-African surface II (late Tertiary). Wellington (1955) questioned the widespread preservation of a Gondwanaland surface (Jurassic) as recognized by King (1951), and considered the existence of such a relic landscape highly unlikely as these elevated areas were considered to have been continuous up to the present. King (1949) also subdivided the Quaternary into three phases, each of which, he suggests, was initiated by tectonic movement.

In contrast to pediplanation, a model of peneplanation or down-wearing during landscape development was first proposed by Davis (1899). Later Dixey (1942, 1955a) supported this model and also recognised a late Jurassic peneplain. Dixey (1955a) identified a first major erosion cycle which lasted from the early Cretaceous to the mid-Miocene, with most of the planation occurring in the Cretaceous and early-Tertiary. During this latter period large areas of the Karoo cover were stripped, resulting in the exposure of the pre-Karoo surface (Dixey, 1942). Mabbutt (1955) interpreted the Little Namaqua Highland as an exhumed pre-Karoo feature. De Wit (1988), as already mentioned, also argued that the Namaqualand sector of the Great Escarpment is an exhumed pre-Karoo feature, rather than an erosional feature, as believed by most workers. However, Partridge (1994) argues that this interpretation seems unlikely for a number of reasons: (i) no outliers of Karoo rocks are preserved within the escarpment

zone or between the foot of the escarpment and the Atlantic coast (older sedimentary rocks of the Nama Supergroup are, however, commonly preserved as outliers in these areas); (ii) silcrete caps overlying deep weathering mantles of the African erosion surface (Cretaceous) are fairly extensively preserved above and below the escarpment, which if Karoo rocks had ever covered, had clearly been removed by erosion prior to the late Cretaceous; and (iii) the form of the scarp front is compatible with subaerial erosion of the present drainage net and with the structure of the Namaqualand Metamorphic Belt, that is, there is no obvious evidence of superimposition or discordant drainage with the existing structure, as would be expected if the drainage were inherited from other cover rocks.

Dixey (1955a) also recognised three end-Tertiary erosion cycles (late Pliocene, Plio-Pleistocene and Pleistocene). The distribution of Karoo and Cretaceous sediments, and the disposition of major erosion surfaces are manifestations of repeated continental uplifts (Dixey, 1955b). Beetz (1933), identified a sub-escarpment surface in Angola which is warped beneath upper Cretaceous marine sediments, and extrapolated this surface to Namibia and South Africa. This surface was noted to be associated with leaching and silicification.

King (1955) proposed a correlation of land-surfaces with tectonic events, following earlier work of Gunn (1949), and suggested that monoclinial uplift could be explained in terms of a model of isostatic compensation, which linked onshore erosion and offshore sedimentation to the mechanical properties of the lithosphere and mantle. This model, after being abandoned for approximately three decades was reconsidered as a possible explanation for uplift along passive continental margins, and in particular within the coastal hinterland of Africa (e.g. Ollier, 1985a; 1985b; Summerfield, 1985).

Partridge and Maud (1987) provided a comprehensive report of the post-Gondwanaland development of the southern African landscape and a valuable reassessment of L.C. King's scheme of landscape evolution (and its derivatives). In this re-interpretation of the geomorphic history of southern Africa, they link both terrestrial and marine evidence. Their results are summarized in Table 3.1.

Table 3.1 Post-Gondwanaland development of the southern African landscape, according to Partridge and Maud (1987).

Event	Age
Break up of Gondwanaland and initiation of Great Escarpment	Late Jurassic/Early Cretaceous (\approx 142 Ma BP)
African cycle of erosion with minor tectonic interludes	Late Jurassic/Early Cretaceous to end of Early Miocene (\approx 25 Ma BP)
Moderate uplift of 150-300 m (150 m in the study area)	End of Early Miocene (\approx 18 Ma BP)
Post-African I cycle of erosion	Early mid-Miocene to Late Pliocene (\approx 2.5 Ma BP)
Major uplift of up to 900 m on the east coast (100 m in the study area)	Late Pliocene (\approx 2.5 Ma BP)
Post-African II cycle of erosion	Late Pliocene to Holocene

According to Partridge and Maud (1987) the initiation of an erosion cycle is dependent on the creation of a new set of base levels, which may be achieved by tectonic movement or may equally easily be caused by a fall in sea level, especially in coastal areas. They, therefore, suggest that the global eustatic fluctuations during the Cenozoic, first documented by Vail et al. (1977), offer an alternative origin for onshore erosion cycles. Siesser and Dingle (1981) and Hendey (1981) produced similar eustatic curves for southern Africa, and Hendey (1983) suggested that eustatic fluctuations are solely responsible for the sequence of land surfaces and benches characterizing the coastal hinterland of southern Africa. Hendey (1983) entirely discounted the influence of tectonic factors. Dingle and Hendey (1984) developed this concept further and linked river capture and changes in the palaeo-drainage on the Bushmanland Plateau, above the Great Escarpment, to changes in sea level.

According to Summerfield (1985) discrepancies exist between landscape chronology

proposed by King (1962; 1972) and more recent stratigraphic evidence from continental margins. The complex response of passive continental margins to base level changes resulting from varying coastal geometry and style of tectonic adjustment was emphasised (Summerfield, 1985). Summerfield concluded that a relative fall in sea level will not always initiate a landscape cycle, but, more likely, is to be of local significance, and that no satisfactory mechanism had been proposed which would produce the uplift necessary to initiate landscape cycles of widespread significance.

According to Summerfield (1988) the results obtained by Partridge and Maud (1987), which indicates a major phase of rapid uplift some 100 Ma or so after rifting (see Table 3.1), significantly constrains the range of applicable tectonic models. Summerfield believes that such episodic uplift combined with its preferential location inland of, but parallel to, the present continental margin suggests an isostatic rather than a thermal model for passive margin development. Summerfield (1988), however, does not agree with their view that the major Late Pliocene uplift is a delayed isostatic response to the major erosion of the African cycle, given the abundant data from regions affected by glacio-isostasy which demonstrates the rapidity of the isostatic response of the lithosphere to changes in load.

Ollier and Marker (1985) examined the physiography of the Great Escarpment of southern Africa and interpreted the escarpment as separating two surfaces only. The higher "palaeoplain" averages about 1500 metres in elevation and represents a modified dicyclic land surface dating back to before the breakup of Gondwanaland and the lower surface or coastal plain. They identified several periods of uplift around the continental margins, with the western interior lagging behind to form the Kalahari Basin. Ollier and Marker (1985) also interpreted the uplift to be approximately symmetrical around southern Africa.

3.1.4 Landscape Evolution of the Study Area

Partridge and Maud (1987) regard the deep weathering and kaolinization of the basement granites and gneisses (also referred to as palaeo-weathered basement, and

occurring in the "Little Namaqua Highlands" in the study area - shown in Figure 1.2) as part of the composite planation cycle of the African surface, which, by the late Cretaceous, reduced the sub-continent to a vast undulating plain. They further recognised this surface both below and above the Great Escarpment. It has been suggested (McCarthy et al., 1985) that the Little Namaqua Highland surface is at least Cretaceous in age as indicated by dinosaur remains (*Kangnasaurus coetzeei*) recorded at Kangnas (Figure 1.2), north of Gamoep, in sediments lying in a wide, shallow valley of the Highland surface (Haughton, 1915; Mabbutt, 1955). According to McCarthy et al. (1985), the area now comprising the western Bushmanland Plateau, on which Vaalputs is situated, consisted of a western highland bordered on the east by an extensive, gently undulating plain. A humid climate over a long morphodynamically stable period resulted in kaolinization of the surface. During this period they suggest that the upper Orange-Vaal system flowed to the south of this area, and the lower Orange flowed along the present Orange valley. A possible increase in precipitation along with uplift gave rise to the extensive alluvial fan system, now partly preserved as the Dasdap Fan (McCarthy et al., 1985). They also associated igneous activity with the tectonic instability responsible for the uplift. This uplift they suggest, may have initiated the events which led to the capture of the Orange-Vaal system by the Koa River in the Miocene.

The plateau to the east of the "Little Namaqua Highlands", known as the "Bushmanland" erosion surface (900-1200 metres in elevation) is equated with the African surface (Mabutt, 1955), and marks the onset of the aridity at the end of the Cretaceous. A pre-Pliocene age for the incision into the kaolinized plateau is suggested (McCarthy et al., 1985) by the reported occurrence of an early Pliocene horse (*Notohipparion namaquense*) found some 55 kilometres east of Springbok (Haughton, 1932). According to McCarthy et al. (1985), extensive dune fields were produced when sands liberated in the western highlands were blown eastwards. This caused the choking of the Koa River and the ultimate cessation of flow. Cessation of flow has also been attributed to the influence of tectonic warping (Du Toit, 1933), which has been shown to influence drainage elsewhere on the sub-continent (Mayer, 1973; Stratten, 1979; McCarthy, 1983). It was possible that during this arid period calcrete formation

took place (McCarthy et al., 1985). The final stage of landscape formation they have interpreted as the degradation, which is still in progress, of the dune field associated with a diminishing sand supply, and caused by the breakthrough of the Buffels and Olifants River systems into the inland plateau.

3.1.5 Palaeodrainage Evolution

An account of previous geomorphological work would be incomplete without reference to the changing views on its palaeodrainage. The present and most widely accepted views are that a major early Cretaceous river system (the "Karoo River" according to de Wit) drained the central interior of southern Africa, and via the present, lower Olifants River drained into the Atlantic Ocean (Dingle and Hendey, 1984; Partridge and Maud, 1987; de Wit, 1993). De Wit (1993) identified the "Kalahari River", of Cretaceous age, having its head waters within the area of the Kalahari Basin and draining to the Atlantic Ocean via the lower course of the Orange River. Capture of the Karoo by the Kalahari River, through the Koa Valley, in the Miocene was suggested by Dingle and Hendey (1984), McCarthy et al. (1985), and Partridge and Maud (1987). De Wit (1993) prefers an independent source from the headwaters of the Orange/Vaal system for the Karoo drainage. This he bases on studies of heavy mineral assemblages of the Koa drainage, and claims that the diamonds of the Koa Valley were probably eroded when gravel remnants of the ancient Karoo River were tapped by headwaters of the Koa drainage.

De Wit (1993) believes that two periods of Tertiary fluvial activity (the Miocene Koa Valley and the Pliocene Sak River and Carnarvon Leegte) suggest markedly humid periods, which diverge from the pattern of increasing desiccation during the Tertiary. Partridge (1994) suggested, using fauna and flora fossil evidence, that conditions at those particular times were considerably more humid than exist in the area today, but finds the erosional surfaces difficult to explain solely in terms of ephemeral climatic shifts. Partridge (op. cit.) would rather account for these observations by large-scale tectonic movements, which elevated the south-eastern hinterland of the subcontinent, and which increased the gradients of the westward flowing drainages. Local tectonic movements, of the ENE - WSW trending Griqualand - Transvaal axis of upwarping (50

metres), in the northern part of the study area was noted by Partridge (1994). This upwarping has caused the long profile of the Koa channel to slope away in both directions since the occupation of the Koa river in this valley in the mid-Miocene. Partridge and Maud (1987) also noted abundant evidence of late (probably Pliocene) movements along this axis further to the northeast. These movements, they suggest led to the capture of the Vaal River and the Dry Harts River by the lower Harts River, and the steepening of the right bank tributaries of the lower Vaal River. They further suggest that the Koa River ceased to flow due to these movements, rather than desiccation during the late Miocene.

3.2 Post Karoo Sedimentation in the Study Area

3.2.1 The Dasdap Formation

In 1911 Rogers noted an area of rock, which he refers to as "silcrete type" rocks, on the Bushmanland Plateau, occurring from the farm Banke in the south to Vaalputs in the north. Levin and Raubenheimer (1983) reported the presence of an extensive alluvial fan, on the farms Banke, Burtons Puts, and Platbakkies, which they noted on a LANDSAT image of the Bushmanland Plateau (see Figure 2.1). Several outcrops of sedimentary rocks (referred to as the Dasdap Formation), on the farms Banke (No. 409) and Burtons Puts (No. 408), were described in some detail for the first time by Levin et al. (1986), during the regional investigation of a part of Bushmanland. The distribution of these deposits was first shown on Reuning's (1930) map and form part of the deposits referred to by him as "deposits of prae-surface quartzite age". The investigations by Levin et al. (1986) were part of a larger study by the A.E.C. to determine the suitability for locating a low and intermediate level radioactive waste repository site in the area. They interpreted these sediments to have been deposited under the high energy conditions prevailing in the proximal part of an alluvial fan. The presence of Dwyka clasts in the Dasdap sediments and the absence of Dwyka outcrop in this region, they propose, suggests a time of deposition during the final stages of Dwyka erosion. McCarthy et al. (1985), however, found in a geomorphic analysis of the area, that the conglomeratic horizons were of an oligomictic nature, comprised

predominantly of blue-grey vein quartz pebbles, and suggested a provenance area in which Dwyka tillite was absent. In the initial studies of Levin et al. (1986), it was observed that the Dasdap sediments were silicified. This they believed, originated from the release of silica as a result of kaolinization of the basement gneissic rocks; however, they placed the deposition period for the Dasdap sediments after the main Cretaceous weathering event, which affected the basement occurrences on the western parts of Vaalputs. According to McCarthy et al. (1985) the rapid accumulation of sediment (Dasdap Formation) during the Oligocene was triggered by uplift and a possible increase in precipitation.

Brynard (1988) provided geochemical and petrological descriptions of the Dasdap Formation. In his petrogenic interpretation he states that the highly silicic nature of these rocks probably accounts for their preservation and suggests that the major weathering process involving kaolinization and silicification probably took place prior to the deposition of the sediments. This suggestion he based on the fact that silicified clasts of sandstone occur in what appeared to be an unsilicified matrix of the sandstones and grits. Brynard (1988), however, mentions an alternate explanation, involving a process of selective silicification which affected only certain horizons of the sedimentary succession. Brynard (1988) also noticed that the Dasdap sediments were subjected to severe leaching, and which probably occurred in a similar environment to that of the palaeo-weathered basement rocks of the region.

Local disturbance of the Dasdap sediments associated with the presence of ultramafic plugs was first referred to by Rogers (1911), and was subsequently investigated by Reuning (1930; 1932). McCarthy et al. (1985) also noticed that the dips of the surficial sandstone are disturbed for a considerable distance from pipes. These features can be seen in the present Dasdap drainage to the east of the Gamoep-Vanrhynsdorp road, on the farm Burtons Puts (8km southeast of Platbakkies - Figure 1.3). McCarthy et al. (1985), using field relationships, suggested that the Dasdap sediments were deposited pene-contemporaneously with pipe emplacement. Levin et al. (1986) also noted evidence of ultramafic igneous activity, which they suggest was associated with the accumulation of the Dasdap sediments.

3.2.2 The Vaalputs Formation

Levin et al. (1986) proposed a model for the deposition of the sediments in the Vaalputs basin based on a study of boreholes and outcrops of sedimentary rocks to the south of Vaalputs. They suggested that the similarity between clasts obtained from drilling at the Vaalputs site and those found in the Dasdap conglomerates at Banke and Burtons Puts, near Platbakkies (see Figure 1.3 and 2.1) indicate that the sequences appeared to be genetically linked. They also noted on an edge enhanced infrared LANDSAT image what appeared to be a fan-shaped extension to the north of the Dasdap formation. This they also used to support their contention that the two Formations are genetically linked. The initiation of the Vaalputs sedimentation was suggested by Levin et al. (1986) to have occurred during the Oligocene uplift, when a palaeotributary of the Koa River flowing northeast from the Dasdap area across Vaalputs, cut into the kaolinized surface, leaving a channel partly filled with alluvium consisting of basement, Dasdap sediments and transported kaolin. Thus, they proposed that the Vaalputs sediments constitute the northern distal extension of an alluvial fan that originated to the southwest of Vaalputs. Levin et al. (1986) attribute the regrading of the Dasdap fan and subsequent redeposition of the material on to the "Vaalputs fan", to climatic conditions changing from pluvial to more arid conditions. This they support with fossil evidence from the Koa Valley, some 50 kilometres northwest of Vaalputs, suggesting that the regrading was well advanced by the late Tertiary and was followed by the encroachment of dune sands.

White clay

Levin et al. (1986) interpreted the underlying and lowermost "white clay" sediments of the Vaalputs Formation as equivalent to the Dasdap Formation, that is, largely reworked Dasdap sediments. Brynard (1988) suggests an *in situ* weathering of the basement rocks under arid conditions for the formation of the "white clay", rather than a process of smectitisation of an existing predominantly kaolinitic succession as proposed by Levin et al. (1986). They require that the "white clay" in which kaolinite would have predominated, had subsequently been partially converted into smectite clay. Relations between clay minerals are not understood well enough to infer a reaction relationship

between minerals, or whether multiphase assemblages are stable (Velde, 1985). According to Brynard (1988) there is little supporting evidence for the hypothesis of clay conversion and he concludes that the hypothesis of *in situ* weathering is the only explanation of the petrogenesis of the "white clay" as the chemical and morphological features of the Dasdap Formation and the "white clay" unit are too different. A hiatus before the onset of the sedimentation of the overlying "red sands" in the Vaalputs basin was proposed by Brynard (1988).

"Red clay"

Andersen et al. (1983) suggested that the material constituting the "red clay" (the bulk of the sediments) of the Vaalputs Formation which overlies the white clay represents the distal portion of an alluvial fan which originated southwest of Vaalputs. According to Brynard (1988) the presence of iron-oxide nodules and blue quartz clasts supports the idea that the red clay sediments represent partially reworked Dasdap Formation rocks. The absence of iron-oxide nodules in the underlying "white clay", however, Brynard (1988) suggests, indicates a different origin for this unit.

Calcrete

Calcrete is a common surface feature in the study area and several calcrete horizons are preserved in the sediments of the Vaalputs Formation. Netterberg (1969) found that the maximum depth of calcrete formation, for a rainfall of less than 254 millimetres is 1.27 metres and calcrete virtually never occurs in areas receiving rainfall in excess of 550 millimetres (Vaalputs receives less than 100 millimetres on average - see Section 1.1). Netterberg also found that the permeability of soils plays an important role in the depth of formation, with more permeable soils allowing for deeper calcrete formation. Calcrete may form on steep slopes and vegetation may influence calcrete formation by precipitation of carbonate by transpiration or solution of carbonate through the action of acids and the carbon dioxide released by roots (Netterberg, 1969).

Brynard (1988) suggests that the calcretes in the Vaalputs Formation (or "red clay") are of a non-pedogenic origin, that is, ascending ground water, which necessitates that the ground water table at the time of formation must have been at a much higher level than

at present. He suggests that the nodules observed at various levels in the surficial formations indicate that the ground water table may have descended gradually in time, but periodically remained constant to allow the formation of a thin calcrete layer. This interpretation is also derived from the assumption that the Vaalputs Formation represents the distal portion of an alluvial fan, and calcium being a highly mobile element would have been largely lost from the parent material during transportation to the site of deposition. Brynard (1988) did, however, note that this process does not fully account for, or explain the multiple layers of calcrete.

3.2.3 The Gordonia Formation

The sand cover of the Bushmanland Plateau overlies remnants of the Vaalputs and Dasdap Formations. The gentle topography of these deposits, was described by Levin et al. (1986), as hummocky longitudinal dunes oriented in a northeasterly direction. Desiccation in the late Miocene (*circa* 10 Ma) (Siesser, 1980), according to McCarthy et al. (1985), produced extensive dune fields, as sand, liberated in the western highland from the gneissic country rocks, was blown eastwards. The small pans and other deflation surfaces on the dunes, they suggest, all point to an aeolian setting in an advanced state of degradation.

According to Brynard (1988) the red sand is of an aeolian origin, and the source of the material could be any basement rocks in the region or further afield. Later, dune degradation gave rise to the present-day topography (Brynard, 1988). The occurrence of durban (an iron cemented subsurface horizon) in these deposits, and which is believed to be a consequence of a reasonably stable land surface, has been reported by several workers, including Van der Merwe (1940), Klintworth (1948), and Ellis and Schloms (1978 and 1982).

3.3 Structure

Conventional interpretation of seismicity near the southern African continental margin, according to Hartnady (1990), invoke an isostatically generated differential stress due to erosional unloading and depositional loading across the continent-ocean boundary. In contrast Cloetingh and Kooi (1992) suggested that plate dynamics cause continually changing states of stress in the lithosphere and they ascribe vertical motions and accelerations in tectonic subsidence in the late Cenozoic record to increased levels of compressional stress in the plates. They also believe that sediments in rifted basins around the Atlantic indicate an intensive global compressional tectonic phase associated with the reorganization of plates in the late Cenozoic. Zobak et al. (1989) reported that in several crustal plates the maximum horizontal stress orientation is sub-parallel to the direction of absolute plate motion, thus suggesting that the dominant stress distribution in the plate interior is indicated by the forces driving the plates. Versfelt and Rosendahl (1989) suggest that relationships between regional tensional stresses and pre-rift structures and rift location become less clear as the scale of investigation decreases because much more detailed data on rift architecture and stress fields are required for them to be identified at the small scale.

Prior to the 1980s, no detailed mapping had been carried out in the region of Vaalputs (Andersen, 1992). Studies of a more regional nature were conducted by Joubert (1971), whose map shows numerous north-northwest trending faults in the Vaalputs region. More recently Joubert (1986a; 1986b) suggested that Namaqualand can be regarded as a model for Proterozoic accretion. Andersen et al. (1983) recognised an east-west trending shear zone to the north of Vaalputs, known as the Kamiesbees Shear Zone, as well as the flat-lying nature of the fabric in syntectonic granitoids. They also produced a regional map of the Vaalputs region, which was used for the compilation of a more detailed geological map of Vaalputs (Andreoli et al., 1987). Andersen (1992), using aeromagnetic data, confirmed that the prominent direction of faulting in the Vaalputs region is north-northwest, and that this faulting first occurred during the Pan African event at ± 700 Ma, and has been rejuvenated several times since then. Andersen (1992) also noticed that these faults displace the Dwyka tillite at Santab-se-

Vloer as well as the Cenozoic Vaalputs sediments. He noted that one of these faults displaces the Platbakkies Shear Zone in a direction which is downthrown to the west. The Garing fault, which shows a prominent aeromagnetic lineament was shown by magnetic modelling and confirmed by drilling to be vertical and at least 100 metres wide (Andersen, 1992). Andreoli et al. (1987; 1996) recognised slicken shed jasper in the products of the Cretaceous weathering event, on the western part of Vaalputs. These slickensides Andreoli et al. (1987) attributed to Post-Cretaceous fault reactivation for the Garing fault. Andreoli et al. (1996) and Andersen (1992) also inferred Cenozoic, post-Tertiary reactivation for this fault as it was seen on aerial photographs to cross-cut the sediments of the Vaalputs basin.

According to Levin et al. (1986), the onset of the deposition of the Dasdap alluvial fan began in Late Cretaceous to Early Tertiary times, with the uplift of the Kamiesberg highlands to the southwest of the Bushmanland Plateau. This rejuvenation was suggested by Andersen (1992) to have taken place along the prominent north-south and north-northwest trending Pan-African faults that cut the area, resulting in "the extensive alluvial fan system extending from the western edge of the plateau, northwards through Vaalputs".

Carrington and Kensley (1969) and Tankard (1976) showed that Pleistocene raised beaches on the Namaqualand coast to the west of Garies occur at higher levels than elsewhere along the west coast. An extension of the Griqualand-Transvaal axis was found to coincide with the raised beaches, and it was suggested that their elevation may be related to recent uplift along that axis. These observations are in agreement with those of Du Toit (1933), who suggested a Pleistocene upwarping, which may still be active at present. Moore (1979) suggested that periods of continental uplift may bear a temporal relationship to variations in spreading rates at the northern mid-Atlantic ridge, and that epeirogenesis and volcanic activity on the sub-continent (including the intrusions in the basement of the study area around Garies and Gamoep) are genetically related to such processes.

3.4 Climatic History

3.4.1 Global Mesozoic and Cenozoic Climate Changes

Evidence indicates that past global climatic conditions have been characterized by short severe cold periods (glaciations), interspersed with long warm intervals with temperatures exceeding those of today (Frakes, 1979). The evolution of Cenozoic land forms and sedimentary formations are dynamically related to climatic events and climatic changes. Oxygen isotope determinations on planktonic and benthic foraminifera from deep sea cores allowed considerable advances in the reconstruction of the climatic history of the late Mesozoic and Cenozoic (Frakes, 1986). These studies showed that the long warming trend of the Mesozoic ended in the Cretaceous. Vail and Hardebol (1979) showed that sea level changes broadly paralleled the evolution of Mesozoic and Cenozoic climates, and decreased from a maximum highstand in the late Cretaceous. Hallam (1985) equated the late Cretaceous climate with that of today. Barron et al. (1981) suggested that the high northern and southern Cretaceous latitudes may have had cooler temperatures, possibly favouring limited glacial conditions during the late Cretaceous. Frakes (1979), using terrestrial floras and marine macro- and micro-fossil evidence, interpreted the Cretaceous mean annual temperatures as 10 to 15°C higher than at present, with tropical to subtropical conditions prevailing to latitudes at least 45° either side of the equator.

According to Savin (1977) and Crowley (1983) worldwide decreases in bottom and surface ocean water temperatures are evident between the early Cretaceous and the Eocene, and that this cooling trend continued throughout the Cenozoic. In Neogene times the general trend was towards the spread of aridity, accompanied by the restriction of forests, the extinction of numerous floral types, and the expansion of woodlands, savannas and grasslands (Axelrod and Raven, 1978). Glaciation at high latitudes commenced in the Eocene/Oligocene culminating in mid-latitude glaciation phases, interspersed with warmer phases during the Pleistocene (Frakes, 1986).

According to Lindesay (1990), factors which caused global and regional climatic shifts,

include Antarctic glaciation, changes in horizontal and vertical ocean circulation patterns, and alterations in the chemical composition of the atmosphere. The former two are linked and both are associated with plate tectonic events that caused changes in the palaeo-geography (Lindesay, 1990). Partridge et al. (1995a,b) believe that evidence from the Southern Hemisphere, points to a number of tectonic and volcanogenic interludes during the Neogene that are likely to have exerted a significant influence on regional and perhaps global climate patterns. Ruddiman and Kutzbach (1989) have shown that Cenozoic uplift is a potential cause and regional modifier of global climatic change. Collisions, rifting, and changes in pattern of plate boundaries may provide several tectonic mechanisms to influence regional and global climates (Partridge et al., 1995a,b). Partridge et al. (1995a,b) linked sea level falls with decreases in spreading rates, as a drop in spreading rates leads to a decrease in the volume of spreading ridges, causing an increase in the volume of the ocean basins, and hence a drop in sea level. Engebretson et al. (1992) estimated a drop in spreading rates from 3.5 km³/yr to less than 2.5 km³/yr, between 50 Ma and the present. These figures gave an estimated 200 metre sea level fall. The above factors, Partridge et al. (1995a,b) suggest, could have indirectly affected Cenozoic climates through changes in the albedo which would be affected by the ratio of land to ocean.

Berner (1994) found that reduced CO₂ emission along the oceanic ridges could have contributed to the Cenozoic cooling from 50 Ma to the present. An increase in the distribution of elevation with respect to surface area, that is, a net increase in hypsometry, may be one of the most striking changes that took place within some continents during the Cenozoic (Partridge et al., 1995a,b). This uplift relative to the geoid is as distinct as that caused by a fall in sea level.

3.4.2 Climatic Record in the Northwestern Cape

According to Partridge (1985) the earliest deposits with dateable fossils in the Gamoeep district of Namaqualand occupy the uppermost deposits of melilitite diatremes which have been radiometrically dated between 71 and 64 Ma. Fossils and pollen in sediments at Arnot (or Banke), considered to be of end Cretaceous to Palaeocene age,

are indicative of a drier subtropical forest community than is characteristic of the latter part of the Cretaceous. This indicates the beginning of a trend towards cooler and drier climates during the early Tertiary.

According to Tankard and Rogers (1978) desiccation has progressively increased in southern Africa since the late Eocene, following the eradication of temperate rain forests in Namaqualand. Several humid pulses, associated with sea level rises have been noted for the Middle Miocene and Plio-Pleistocene (e.g. Hendey, 1978). These observations are largely based on studies of terrestrial deposits, including those of the Langebaanweg area, and continental shelf deposits. Aridification, particularly to the north of the Orange River was the response to a stable anticyclonic circulation caused by a new oceanic temperature regime (Partridge, 1985).

Dingle and Hendey (1984) concluded that rainfall and runoff in the southern African interior, during the late Palaeogene, was much lower than today. These results were based on the interpretation of various coastal exit points of the Orange River and its sediment discharge. Semi-arid conditions continued in the south Namib coastal zone and increased during the rest of the Pliocene. Vertebrate fossils recovered from Elizabeth Bay and Arris Drift along the Namibian coast, suggest a warm, mesic, woodland environment for the early to mid-Tertiary (e.g. Hendey, 1978). Early mid-Miocene fossils discovered in extensive alluvial deposits at Bosluispan, to the northeast of Vaalputs support this interpretation (Partridge, 1985).

The climate before and during deposition of the Vaalputs Formation was considered by McCarthy et al. (1984) and Brynard (1988) to have been humid, allowing for the deep kaolinization of the bedrock. According to Siesser (1980), desiccation was probably initiated by the onset of cold water upwelling along the coast in the late Miocene (ca 10 Ma). Late Tertiary deposits preserved as middle-Miocene fluvial sediments along the Orange/Vaal, Koa, and Namib Rivers, and at Langebaan have been interpreted (de Wit, 1993) as a wet phase. De Wit (1993) uses the presence of isolated phosphogenic deposits along the Namaqualand coast to support this interpretation. During the Pliocene, equatorward movement of the westerlies and growth of the polar ice-caps

focused atmospheric subsidence in the present subtropical high pressure belt resulting in aridity (Muller et al., 1990). Conditions along the west coast became cooler and drier. According to Muller et al. (1990) the east-west climate gradient, much as in modern times, was established in the Pliocene (4 Ma) and in the late Pliocene (3 - 1.8 Ma) aridification increased and average temperatures dropped. A wet phase occurring during the Pliocene was recognised by de Wit (1993), by the occurrence of terraces along the major river systems and at Langebaanweg, which he correlates with transgressions along the coast (90 and 50 metre complex). According to Lamb (1972) the Quaternary is characterized by the occurrence of ice ages resulting in generally colder and drier conditions over most of Africa. The interglacial conditions resembled the present-day climate (van Zinderen Bakker, 1982). According to Muller et al. (1990) southern Africa experienced no glacial conditions during the Quaternary.

Stratigraphic and sedimentological investigations (Partridge and Dalbey, 1986) of deposits in the central Karoo provide evidence of palaeoclimatic changes since the mid-Pleistocene. Preserved pan deposits include alluvial gravels and sands which Partridge and Dalbey (1986) interpret as a response to changes in discharge and meander geometry, indicating increased run-off and wetter climates. According to Deacon and Lancaster (1988) evidence of high lake levels and pans in the Bushmanland indicates a period (30 000 - 14 000 BP) of wetter climates.

Beaumont (1986), using changes in archaeological visibility in Bushmanland and Griqualand West, suggest that favourable habitats existed for the late Stone Age hunter-gatherers during the late-Pleistocene and Holocene. This pattern is, however, in contrast to that indicated for Southern Africa as a whole (eg. Deacon and Thackeray, 1984).

CHAPTER 4: REGIONAL GEOLOGY

The study area is entirely underlain by granitic gneisses of the Namaqualand Metamorphic Complex which are well exposed in the western and southwestern parts, in the area of the Kamiesberge. In the central part of the study area the Namaqualand Metamorphic Complex lies under a cover of unconsolidated pebbly clays, sandy clays, calcrete and aeolian sands, which reach thicknesses of up to 30 metres. Alluvial sediments are found as outcrop to the south of Vaalputs in what is known as the Dasdap Formation. The presence of lithified alluvial deposits in this area and the apparent fan shape of these sediments has led previous workers to interpret this entire sequence of sediments as an alluvial fan deposit. The eastern part of the study area is mainly underlain by tillites of the Dwyka Group, which forms the western margin of the Karoo Supergroup. A more detailed description, and distribution of the above mentioned lithologies is given in this chapter.

4.1 Proterozoic Basement

4.1.1 Stratigraphy of the Supracrustals

The Proterozoic rocks which form the "basement" in the study area consist of polyphase deformed and metamorphosed sediments and volcanics, forming vast expanses of gneisses and granites (Tankard et al., 1982), and are referred to as the Namaqualand Metamorphic Complex. Figure 4.1 shows the typical landscape formed by these gneisses in the study area. This complex has been correlated with the Natal Metamorphic Province (Joubert, 1986a). The Namaqualand Metamorphic Complex extends northwards into Namibia, to the east of Luderitz, and is faulted against the Kaapvaal Craton in the east (De Wit, 1993). Although the details of the various rock units of the Namaqualand Metamorphic Complex are beyond the scope of this study, these rocks control the composition and tectonic styles of the overlying sediments, and are, therefore, briefly discussed. They also control the orientation of recent drainage patterns, and hence influence the geomorphology of the region.



Figure 4.1 Typical appearance of the landscape in the western parts of the study area developed on the Namaqualand Metamorphic Complex.

The thick, older meta-sediments and meta-volcanics are grouped together as a pre-tectonic rock unit (Haughton, 1969). This unit has been subjected to intense deformation, metamorphism and intrusions, and was deposited between 1350 and 2000 Ma (SACS, 1980). Intrusions of various compositions (predominantly granites and gneisses) comprise the syntectonic rock units of 1100 to 1900 Ma age (Joubert, 1986a). According to Joubert (1971) the Namaqualand Metamorphic Complex attained high grade metamorphism during the Namaqua metamorphic event. The lithologies in the West Coast Belt were overprinted by early Pan-African thrusting and fabric development at about 700 Ma (Allsop et al., 1979), resulting in retrograde metamorphism and the development of lower amphibolite facies at the coast (Moore and Reid, 1989). The main divisions in the Namaqualand Metamorphic Complex, according to Kröner and Blignault (1976) are the Kheis, Gordonia and Bushmanland Subprovinces, and the West Coast Belt (Figure 4.2). The Namaqualand Metamorphic Complex can be subdivided into a series of domains and subprovinces, which are separated from one another by crustal-scale shear zones (Joubert, 1986a). The study area falls within the Bushmanland Subprovince and is, therefore, dealt with in greater detail than the other subprovinces.

Gordonia Subprovince

The western boundary of the Gordonia Subprovince is defined by the Pofadder Shear Zone (Figure 4.2) which is one of the major north-west trending shear zones imprinting this subprovince (Stowe, 1983). Joubert (1986a) proposed right lateral displacement, of at least 85 kilometres, as well as extensive vertical displacement. The main movement along this shear is believed to have taken place at about 1000-1300 Ma (Moore, 1981), and it has been suggested (e.g. De Wit, 1993) that this structural weakness may have undergone some readjustment in Karoo and post-Karoo times.

Bushmanland Subprovince

The Bushmanland Subprovince (Figure 4.2), located to the east of the West Coast Belt, to the west of the Pofadder Shear Zone, and to the south of the Orange River, is divided into the Okiep and Bushmanland Groups, which according to Joubert (1986a) have common lithologies. According to De Wit (1993) the gross structural trend in the Bushmanland Subprovince is east-west, and on entering the Gordonia Subprovince swings north-east, due to the dextral movement along the Pofadder Shear Zone. Joubert (1986a) noted approximate north-south trending shear zones at the base of the escarpment, in the western part of the Bushmanland Subprovince. These shears are due to Pan-African deformation, which also dominates the West Coast Belt. The Bushmanland Subprovince can be further subdivided into terrains separated by large scale strike-slip shear zones (Joubert, 1974; 1986a). The Putsberg Shear Zone (Buffels River) subdivides the Bushmanland Subprovince into the Okiep Terrane, in the north, and the Garies Terrane, in the south. The Garies Shear Zone forms the southern boundary of the Garies Terrane. In the study area, these rocks form the basement on which Karoo and Cenozoic sediments were deposited. The Garies Terrane consists of gneisses of both sedimentary and intrusive origin which have undergone several phases of tectonism, and have been metamorphosed to granulite facies (Albat, 1984).

The basement to the supracrustal rocks of the Bushmanland Subprovince is known as the Achab Gneiss (Watkeys, 1986), and consists of a variety of rock types. Praekelt and

Colliston (1988) recognised a discontinuity, consisting of an intermittently developed conglomerate, between the Bushmanland Subprovince and the underlying gneisses, in the Aggeneys area. The supracrustal rocks of the Bushmanland Subprovince were divided by Joubert (1986b) into four groups: the Aggeneys Sequence (distinctive orthoquartzite or aluminous schist, or gneiss association), the Southern Group (feldspathic quartzites and metapelites), grey biotite gneiss, and metapelites. The Aggeneys Sequence is equivalent to the Bushmanland Group of Colliston et al. (1989).

The area focused on in this study consists mainly of biotite gneisses and quartzo-feldspathic gneisses of the Garies Subgroup (Andersen, 1992) of the Okiep Group. In general rocks of granitic bulk composition containing relic granitic textures are the most common rock types in the study area (Brynard, 1988). On his map, Andersen (1992) also differentiated magnetite quartzites, iron formations and calc-silicate rocks. Andersen (1992) and Andreoli et al. (1986) give detailed accounts and descriptions of the various rock types encountered at Vaalputs and in the surrounding region. Charnockitic rocks, defined as metamorphic or magmatic rocks of granitic bulk composition containing orthopyroxene and perthite, and typically of a dark grey-green to black colour are well developed in the study area.

Richtersveld Subprovince

The Richtersveld Subprovince (Figure 4.2), separated from the Gordonia Subprovince in the north by the Pofadder Lineament and the Tantalite Valley Line, and from the Bushmanland Subprovince in the south by the Wortel Line, was recognised by Joubert (1986a) to be between 2000 and 1730 Ma.

West Coast Belt

The West Coast Belt (Figure 4.2) is dominated by the Pan-African deformation which gave rise to an approximate north-south set of shear zones (Joubert, 1986a). These structures control the geomorphology of the Great Escarpment and many coastal rivers. A set of north-northwest trending fractures and shear zones, associated with monoclinial folding,

are suggested to be the result of the final phase of deformation (Joubert, 1986a). According to Joubert (1986a) this final phase of uplift exposed the high grade rocks of Namaqualand and Bushmanland.

Coarse grained alkali feldspar-quartz-muscovite pegmatites were noted in the Vaalputs area (Andersen, 1992); the best of which are developed on the farm Riembreek where they form a prominent outcrop 500 metres wide and more than 5 kilometres in length. Quartz veins were also noted in the outcrop on the western parts of Vaalputs

4.1.2 Intrusions

According to Andersen (1992) in the vicinity of Vaalputs the supracrustals have been intruded by granites of the Spektakel Suite which have caused extensive migmatization and anatexis. Intrusions into the Namaqualand Metamorphic Complex are listed in Table 4.1.

Table 4.1 Lithostratigraphic subdivisions of rock suites intrusive into the Namaqualand Metamorphic Complex as applicable to the study area (after SACS, 1980; Joubert, 1986a; and Ashwal, 1997).

Suite	Age	Rock Type
Koperberg	1070	diorite, norite, hypersthénite
Spektakel	1170	granite
Keimoes		grey gneiss, charnockitic granulite
Hoogoor		quartzo-feldspathic pink gneiss
Little Namaqualand	1200	augen gneiss
Gladkop	1800	biotite gneiss
Voolstdrift		peridotite, diorite, granite

Andreoli et al. (1986) and Andersen (1992) recognised several intrusive granitic units within the Namaqua province in the Vaalputs area. These include the Little Namaqualand Suite, the Hoogoor Suite, and the syntectonic granite-gneiss Suite (Riembreek granite gneiss, Stofkloof granite gneiss, and the Vaalputs granite gneiss), which range in age from approximately 1800 Ma to 1070 Ma (SACS, 1980). The presence of several younger intrusions in the Vaalputs area, as indicated by an early magnetic survey conducted by the Geological Survey of South Africa, and followed up by drilling, by the Okiep Copper Company on the farm Norabees, consist of noritic rocks similar to those of the Koperberg Suite mined in Springbok (Andreoli et al., 1986; 1994; Andreoli pers. comm.). In the Vaalputs area, the Koperberg Suite typically includes hypersthene, norite, nelsonite (hypabyssal rocks comprised chiefly of ilmenite, magnetite and apatite), quartzolite (plutonic rock with more than 90% quartz), enderbite (plagioclase rich charnokite) and anorthosite (Andreoli et al., 1986; 1994). Several intrusive bodies of the Koperberg Suite were mapped by Andreoli et al. (1986) at Vaalputs.

4.1.3 Structure

The general regional structural trend of the Bushmanland Subprovince gneisses (Figure 4.2) is east-west. In the Pofadder area it is northeast as a result of dextral movement along the Pofadder Lineament, and in the west the general trend is south-southeast, believed to be a result of large scale crustal movement along the north-northeast trending Pan-African shears (Joubert, 1986a). Andersen (1992) recognised four structural events of Precambrian age in Namaqualand. His results (also modified after Clifford et al., 1975. Allsopp et al., 1979; and Joubert, 1986a) are summarized in Table 4.2.

Table 4.2 Structural events of Precambrian age for Namaqualand (modified after Clifford et al., 1975; Allsopp et al., 1979; Joubert, 1986a; and Andersen, 1992).

Phase of Deformation	Age (Ma)	Structural Event	Associated Intrusions
	ca. 700 Pan African	Dextral shearing in western Namaqualand (N-S, NNW, NNE).	
D4		Monoclinial folding	
Late D3	ca. 1000	Dextral wrenching Flexural slip folding Shearing	Pegmatites
D3	1070±20	Steep structures	Koperberg Suite
Early D3	ca. 1170	E-W open folding Thrusting	Spektakel Suite
D2	1213±22	Recumbent folding and regional metamorphism	Little Namaqualand Suite
D1	ca. 1850	Isoclinal folding in supracrustal rocks	

The dominant fracture trend in the study area is north-northwest, and according to Andersen (1992) most outcrops show some signs of sympathetic fracturing. Joubert (1986a) has assigned a Pan African age (700 Ma) to this faulting. In the western portion of the study area the faults are clearly visible, particularly on aerial photographs and satellite images. On the eastern, sand covered portion of the study area, lineaments are less obvious and require more advanced remote sensing techniques and geophysical methods to define.

4.2 Permo-Carboniferous Karoo Cover

Only the Permo-Carboniferous Dwyka Group and the Permian Eccra Group occur in the Western Cape, which are intruded by Early to Late Jurassic dolerite sills and dykes (De Wit, 1993). In the study area the Karoo Supergroup rests unconformably on the

Namaqualand Metamorphic Complex, and may be overlain in places by younger sediments of the Vaalputs and Gordonia Formations. The lower Permo-Carboniferous Dwyka Group tillites are the dominant Karoo Supergroup lithology in the area, the distribution patterns of which are shown in Figure 4.3. These occurrences were determined using TM-5 LANDSAT imagery, and the inferred extent of this sequence (Figure 4.3) underlying the more recent sediments, was determined from drillcore data (after Andersen, 1992). Drillcores at Vaalputs have shown the existence of Dwyka in the form of several small pockets underlying the Vaalputs Formation. Thicknesses of the Dwyka occurrences vary from zero at the western limits to several metres on the eastern margin of the study area. Several Karoo dolerite outcrops have been mapped (Andersen, 1992) in the Vaalputs area (Figure 4.3) and to the northwest of Santab-se-Vloer.

The pre-Karoo topography, is presently being exhumed along the north-western margin of the Karoo Basin and isolated basement highs, surrounded by almost horizontally bedded Karoo sediments are evident (De Wit, 1993). Dwyka Group tillite facies is found in the lower parts of the irregular terrain and younger Karoo shales lap onto the basement highs (De Wit, 1993). According to Du Toit (1909) the pre-Karoo valleys on the Namaqualand Metamorphic Complex formed part of the drainage systems which supplied sediments from the basement to the basins of the Nama Group and Cape Supergroup. Visser (1985) described major north-south trending (parallel to major structural trends) pre-Karoo valleys in the north-western Cape which were exploited by glaciers of the Permo-Carboniferous ice-sheet. Halbich (1962) suggested that little adjustment, if any, took place after glaciation, and according to De Wit (1993) the local geomorphology and drainage pattern is represented by the exhumed pre-Karoo topography. Partridge (1994), in contrast, prefers an erosional origin for the observed landscape, for a number of reasons, the details of which have been discussed in Section 3.1

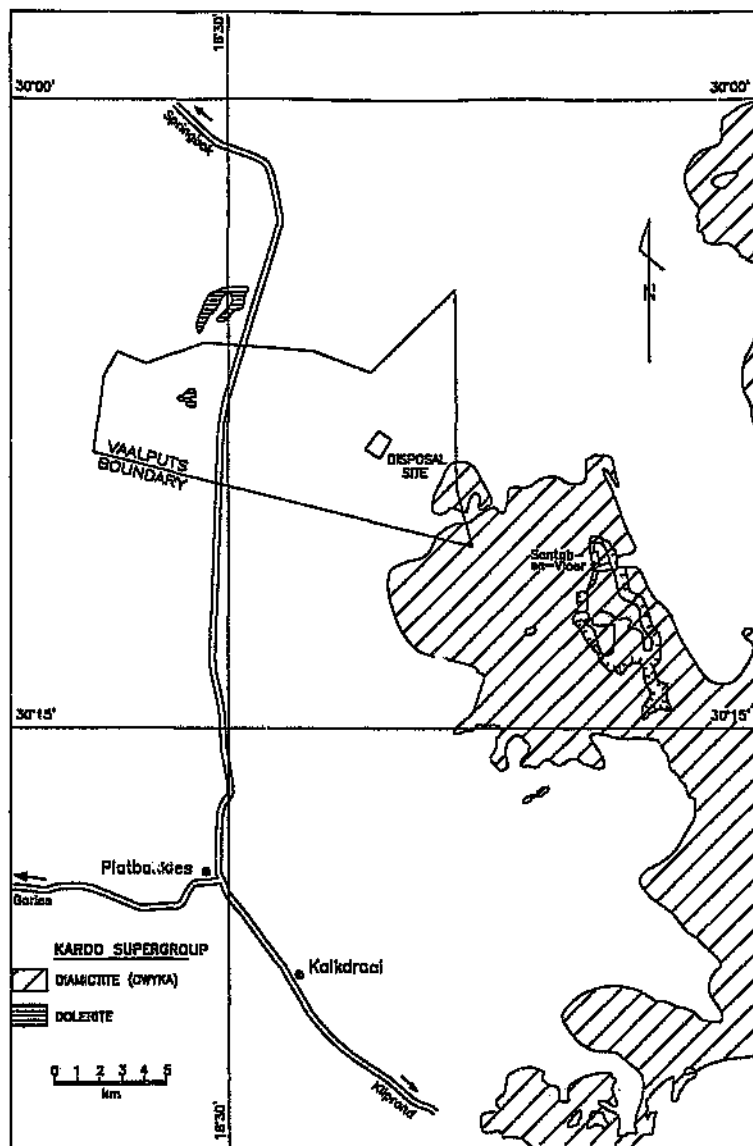


Figure 4.3 Karoo sediments and dolerite intrusions in the study area (after Andersen, 1992).

The Dwyka Group, at the base of the Karoo Supergroup, as described by Visser (1985) is comprised of massive clast rich arenaceous and clast poor, argillaceous diamictite, bedded diamictite, massive carbonate rich diamictite, basement-derived breccia, dropstone argillite and fine to coarse grained sandstone. The area north of Kliprand belongs to the

Namaqua Basin where the Dwyka Group has a total thickness of 130 metres (Andreoli et al, 1987), and the entire eastern portion of the study area is overlain by the Dwyka Group. Generally the Dwyka Group is poorly exposed, with some of the better exposures occurring at Santab-se-Vloer and further to the south-southeast (20-30 kilometres) at Boonstevlei. Characteristically weathered Dwyka tillite surfaces are littered with erratic pebbles and boulders (one millimetre to several decimetres in diameter) (Figure 4.4). The clasts are usually well-rounded, smooth and comprise a wide range of lithologies, including stromatolitic dolomite (Namaqualand West Supergroup), amygdoloidal lava (Ventersdorp Supergroup), banded ironstone, quartzite, and jasper (Strydom, 1979; Visser, 1985). The ice flow in west Namaqualand was generally from the north (Stratten, 1968), and was derived essentially from the Kalahari and the Warmbad basins (Visser, 1988).

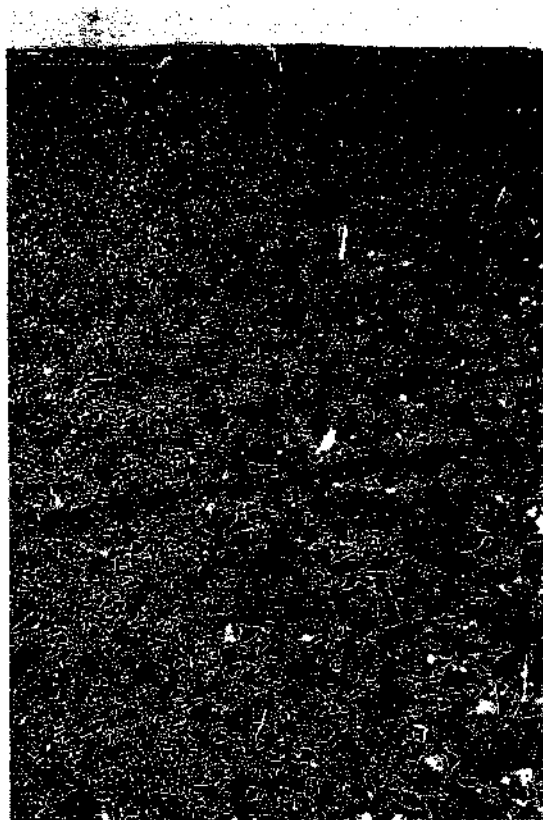


Figure 4.4 The Dwyka Group at Boonstevlei showing a typical erratic littered surface.

According to Andersen (1992) the prominent Dwyka lithology in the area of Santab-se-Vloer (approximate western margin of the Karoo rocks in the study area) is a brownish sandstone (he also noted some indurated shale in the southern parts), where a desert pavement is formed of basement derived debris and carbonate nodules. The distribution of the Dwyka Group and the shape of Santab-se-Vloer (also noted by Andersen, 1992) is controlled by a set of north-northwest trending fractures. Andersen (1992) considers these fractures as faults of Pan African age, which were reactivated during Karoo times and probably also during the Tertiary.

Dwyka float in two areas on Bok-Puts (the farm to the south of Vaalputs) indicates that the Dwyka Group extended further west than its present western boundary, and also that several outliers of the Dwyka most probably occur beneath the more recent sediments (the Vaalputs and Gordonias Formations) in the western parts of the study area. Near the farm Platbakkies, approximately 20 kilometres to the south of Vaalputs, some Dwyka remnants are preserved at the base of north-south trending valleys (Reuning, 1930; Visser, 1981).

As the Koa valley in the eastern portion of the study area is floored by basement gneisses, it appears that the Bushmanland surface to the west of the Koa valley lies close to the pre-Dwyka erosion surface. Evidence of a more rugged or undulating pre-Dwyka surface may be seen on the farm Norabees, to the east of Vaalputs, where large areas of bevelled basement are exposed in a depression near the farm house. The Dwyka in this area occurs as isolated outliers.

4.3 Late Cretaceous - Early Tertiary Intrusions

Late Cretaceous sediments are preserved in the Namaqua Mobile Belt (northwestern Cape) in several kimberlite-type craters (De Wit, 1993). According to De Wit (1993) these intrusions are generally younger than the Early to Middle Cretaceous Kaapvaal Craton intrusions. Late Cretaceous dinosaur remains (*Kangnasaurus Coetzeei*) were found in the sediments in the Kangnas Valley (Rogers, 1915), and the sediments were

interpreted by De Wit et al. (1992) as an olivine melilitite crater infill. According to Moore and Verwoerd (1985) the sediment filled maars, in the northern part of Bushmanland, occurring above diatremes of kimberlites, olivine melilitites and olivine nephelinites are all related to a period of alkaline activity, which occurred during the Late Cretaceous to Early Tertiary. A Late Cretaceous age for these crater deposits has also been inferred by Scholtz (1985) and Smith (1986) using macro- and micro-palaeontology.

In addition to the above mentioned intrusions, poorly exposed Phanerozoic, melilitite plugs, typically occurring as strewn boulders or mounds have been delineated by magnetic methods (Joubert, 1971; Moore and Verwoerd, 1985). Rogers (1911) and Reuning (1931) described other Phanerozoic sediment-filled kimberlite and related pipes in the area between Gamoep and Platbakkies. The argillaceous and arenaceous diatreme infill material was considered by Levin et al. (1986) to be contemporaneous with the Dasdap Formation. Scholtz (*op. cit.* in Moore and Verwoerd, 1985) gives a palynological interpreted age of the sediments as Palaeocene (54-64 Ma). The necks of several pipes are well preserved on the farms Bok-Puts and Riembreek, and consist of breccia fragments (country granite gneisses), which vary in size from 10 centimetres to more than a metre. Andersen (1992) noted that many of these pipes appear to fall on or close to older northeasterly trending faults, which he suggests may have played a direct role in the location of the pipes. A more detailed account of the late Cretaceous/Tertiary intrusions in the area, and the implications of their ages, is given in Chapter 5

4.4 The Dasdap Formation

The type locality of the arenaceous Dasdap sediments (also referred to as the "Kookoppe"; Figure 4.5) is found on the farm Banke approximately 30 kilometres to the south of Vaalputs. These north-south striking hills were first described in detail in the regional study of Bushmanland during the investigation as to the suitability of the radioactive waste repository site (Andersen, 1983). The Kookoppe are approximately 2.5 kilometres long and form flat topped hills (approximately 15 metres high), which have a very similar morphology

to the flat topped, palaeo-weathered basement occurrences on Vaalputs. The Dasdap sediments vary in thickness from one metre in the south to over four metres in the north (Niemand, 1986) and are found capping, or on the upper parts of these hills. The basal Dasdap sediments lie unconformably on the Namaqualand Metamorphic Complex, which is well exposed in the steep sided faces of the Kookoppe, and which follows an undulating plane on what was once the granitic depositional surface. The underlying basement and the sediments are generally highly weathered, and are only preserved by a more silicified Dasdap Formation cap rock.



Figure 4.5 The arenaceous Dasdap sediments, or Kookoppe, on the farm Banke (near Platbakkies).

The Dasdap Formation sediments which outcrop on the farm Banke consist of a basal conglomerate, overlain by conglomerate and sandstone which grades into trough cross-bedded grits and massive sandstone intercalated with siltstone. Percussion boreholes drilled at farms to the south of Vaalputs, that is, at the farms Banke, Platbakkies, and Bok Puts, as well as on Vaalputs, penetrated up to 35 metres of a gritty silicified sandstone resembling the Dasdap Formation (Brynard, 1988).

Several occurrences of the Dasdap sediments are also found to the east of the Kookoppe along the present Dasdap drainage, and generally form higher ground than the surrounding country side. Although only parts of the Dasdap stratigraphy have been preserved in the eastern outcrops, it is evident that the sediments become progressively finer grained towards the east. A more detailed account of these sediments is given in Chapter 5.

4.5 Palaeo-weathered Rocks

The remnants of Cretaceous (Partridge and Maud, 1987; Andersen, 1992) weathering form distinct geomorphological features in the study area (Figure 4.6). These features occur on the western parts of Vaalputs and extend southwards to the Dasdap sediments on the farm Banke. These more resistant outliers consist of palaeo-weathered (and silicified) basement rock overlying unaltered basement, and according to Joubert (1971) represent relics of what he interpreted as the Bushmanland Plateau. These palaeo-weathered rocks were found to extend to considerable depths below the Kalahari sands and the Vaalputs Formation (Andersen, 1992).

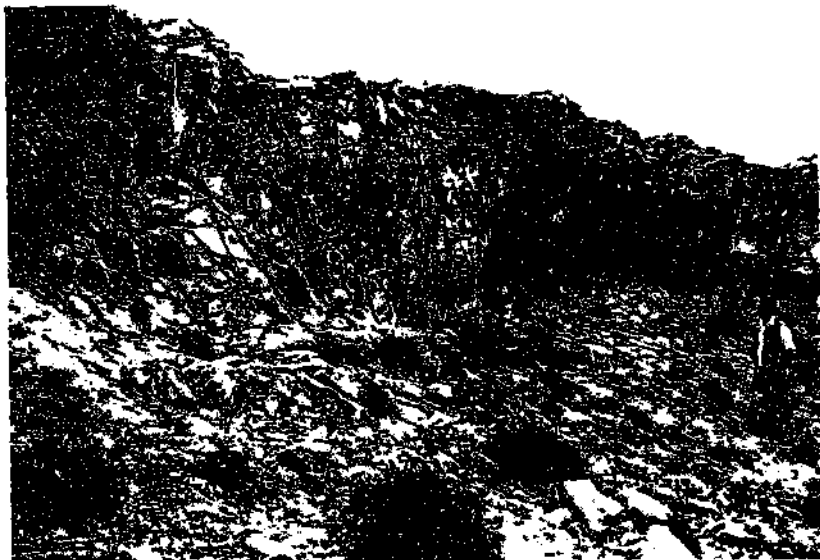


Figure 4.6 Palaeo-weathered basement on the western part of Vaalputs.

Evidence of post-Mesozoic tectonism is obvious in the palaeo-weathered and silicified basement rocks in the western parts of the study area, inferring that several faults identified in this area remained active well into the Tertiary. The palaeo-weathered rocks of the region are discussed in more detail in Chapter 5 and the structure of these occurrences is dealt with in Chapter 8.

4.6 The Vaalputs Formation

Extensive drilling at Vaalputs revealed a "channel-like depression" cut into the basal sediments (Dasdap sediment correlatives) and which is filled with "red gritty to sandy clay" (Brynard, 1988). These sediments are referred to as the Vaalputs Formation and are best exposed in the waste disposal trenches at Vaalputs (Figure 4.7). Where the basal sediments are absent, the Vaalputs sediments lie directly on the weathered basement. The Vaalputs sediments consist of alluvial and aeolian derived sediments, as well as evaporites and duricrusts.

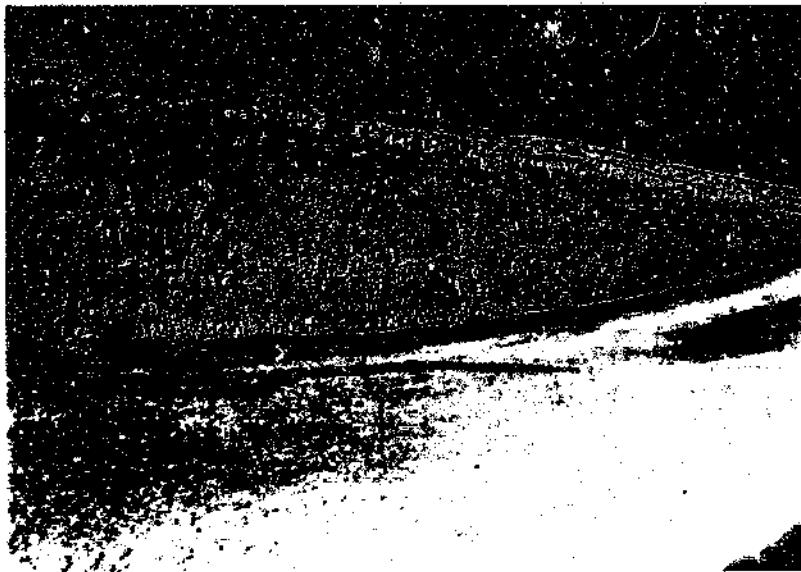


Figure 4.7 The Vaalputs sediments exposed in the intermediate waste disposal trench. The succession of exposed sediments is approximately 8 metres thick.

Brynard (1988) recognised three cycles of deposition, each of which was truncated by a period of calcretization. Concentrations of blue quartz pebbles, as well as iron-oxide nodules and several other clast types form lenses or discontinuous layers in the Vaalputs sediments. These clasts are also scattered throughout the rest of the succession. Brynard (1988) interpreted the Vaalputs Formation as the accumulations of reworked sediments of the Dasdap alluvial fan by surface processes and bioturbation. These sediments are discussed in more detail in Chapter 6.

4.7 The Gordonia Formation

Younger surficial deposits referred to as the Gordonia Formation, cover most of the Bushmanland Plateau and overly the Karoo Supergroup and the Vaalputs and Dasdap Formations. In the study area these sediments commonly consist of a thin veneer of sand between 0.5 and 2 metres in thickness (Brynard, 1988), in the form of hummocky, northeasterly orientated, longitudinal dunes. The presence of small pans and deflation surfaces on these dunes, as well as the coarse average grain size, and low relief of the dunes, were interpreted by McCarthy et al. (1985) to represent an advanced state of degradation. Figure 4.8 shows this generally featureless, sand covered land surface.

Various types of sand, distinguished primarily on colour include a red sand typically found on dune forms and a light brown sand which occurs mainly on flatter and generally more degraded areas. Isolated outcrops of calcrete outcrop as a result of deflation. The eastern limit of the dune field is terminated by a low scarp of Dwyka rocks, with basement outcrops becoming more prominent further to the east. Several lineaments can be followed from the outcrop area in the west through the Vaalputs Basin in the east, which is filled with much younger unconsolidated sediments, suggesting that these faults have undergone post-Tertiary rejuvenation. A detailed account of these sediments is given in Chapter 6 and the structure of the basin is dealt with in Chapter 8.



Figure 4.8 Sand covered area typical of the Gordonia Formation which covers the greater part of the Bushmanland Plateau in the study area. The crest of a low amplitude dune is seen in the background.

CHAPTER 5: THE CRETACEOUS

The Cretaceous to Late-Cretaceous record in the study area consists of the Dasdap sediments, and palaeo-weathered basement, and is believed to be significant in the understanding of the geomorphic, sedimentologic and tectonic history of the region. It should be noted that the age for the Dasdap sediments, as suggested by previous workers (see Table 1.1), is somewhat different to that exhibited by the results of this study. This chapter deals with these two Cretaceous occurrences in detail and attempts to determine the conditions responsible for their formation. The reasons for the proposed older age of the Dasdap Formation is also discussed in this chapter.

5.1 The Dasdap Formation

5.1.1 Field Occurrences

Outcrops of various sedimentary lithologies, including conglomerate and sandstone, and referred to as the Dasdap Formation, have been mapped by several workers, e.g. Levin et al. (1986). The Dasdap sediments (Figure 5.1) are exposed on the farm Banke at outcrops referred to as the "Kookoppe" (see Figure 4.5), as well as along the present Dasdap drainage on the farm Burtons Puts (portion Kalkdraai). The thicknesses of these preserved sediments as noted in the Kookoppe outcrops may be up to eight metres, but are generally less than three metres. According to Brynard (1988) percussion boreholes drilled on farms to the south of Vaalputs penetrated up to 35 metres of material resembling the Dasdap Formation. The isolated outliers (in the western parts/Kookoppe - Figure 5.1) and inliers (eastern parts of landsurface covered by Gordonia) lie unconformably on the Namaqualand Metamorphic Complex. The following section deals with the various lithofacies identified in the Dasdap sediments. Figure 5.2 gives a simplified schematic lithofacies assemblage and vertical profile for the Dasdap sediments. All lithofacies codes used in this work are from the classification system of Miall (1977; 1978).

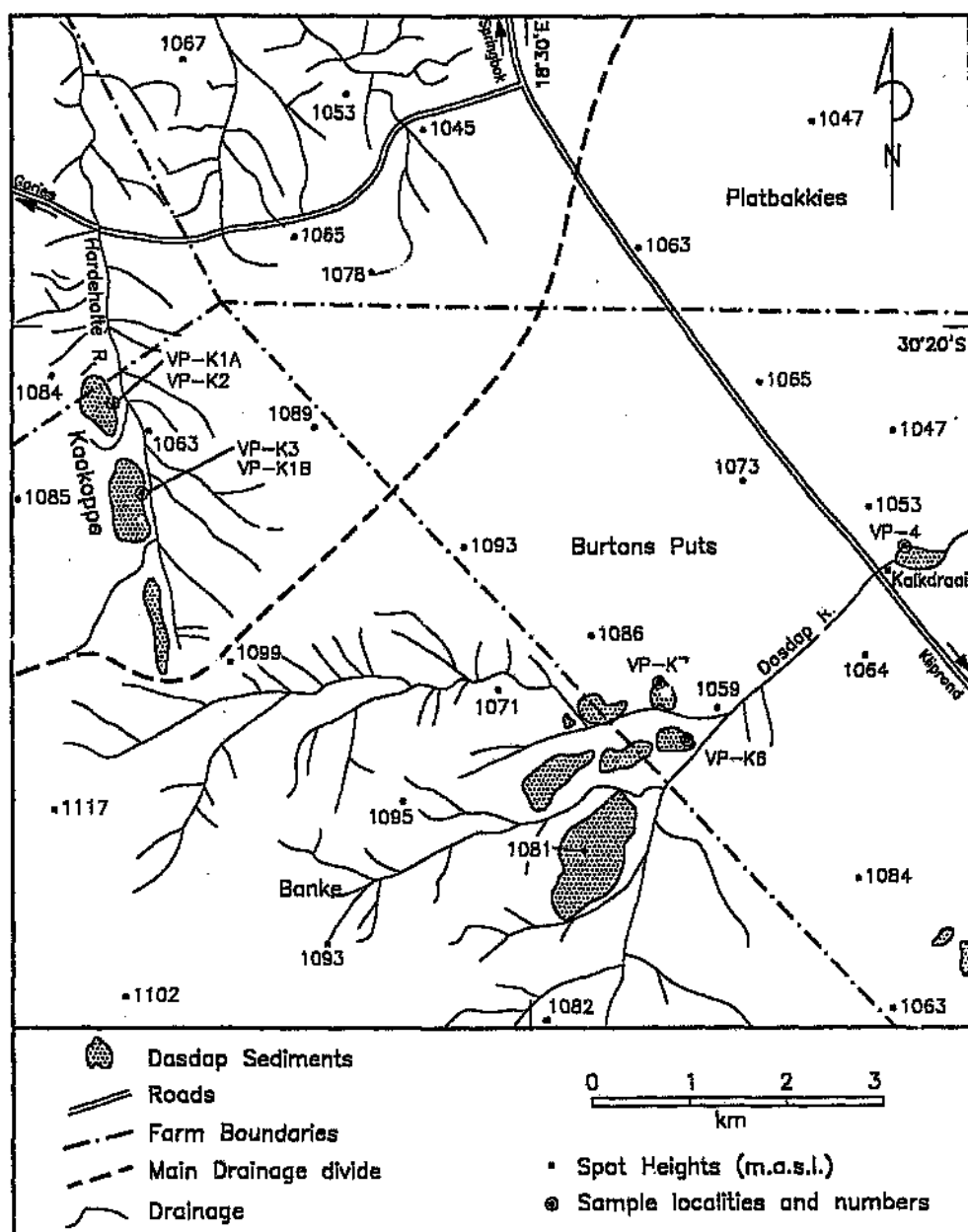


Figure 5.1 Dasdap sediment occurrences in the study area with present drainage patterns (modified after Niemand, 1966).

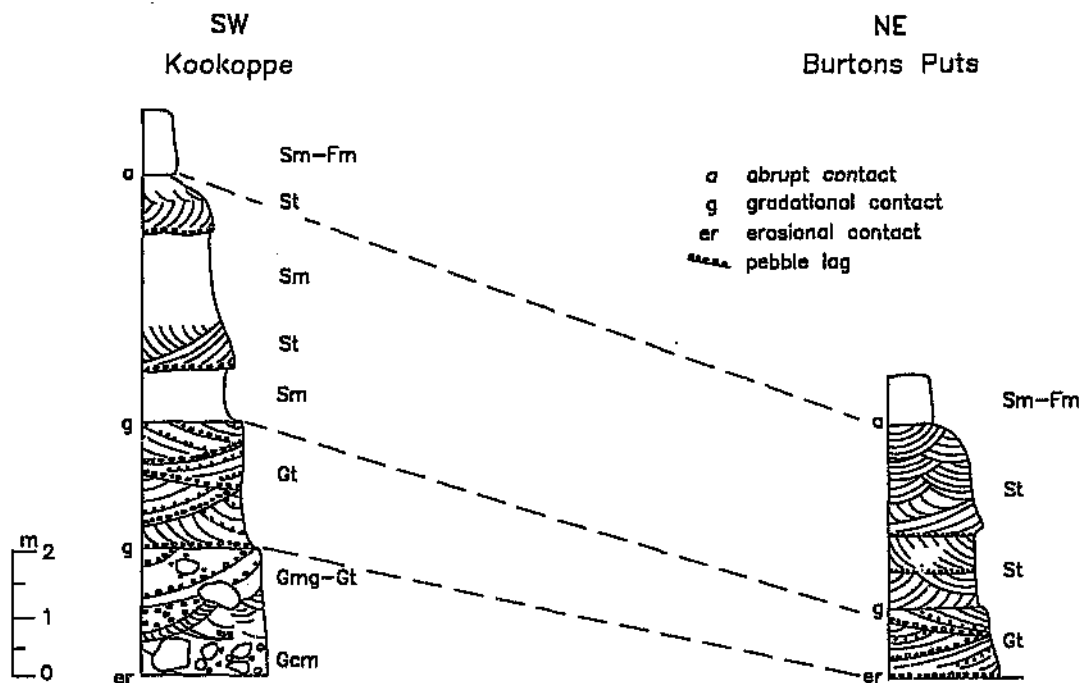


Figure 5.2 Lithofacies assemblage and simplified vertical profiles for the Dasdap Formation sediments.

The basal conglomerate (Gmg-Gcm-Gt)

The exposures at the Kookoppe (Figure 5.1) exhibit a basal conglomerate lying unconformably on weathered basement gneisses, and are typically greater than one metre in thickness (Figures 5.2 and 5.3a). The basal contact is erosional on a gently undulating basement topography. The basement was observed, in places, to be fairly deeply scoured, with steep sided channels (1 to 2 metres deep). Narrower channels exhibit an overlapping relationship. The channels often contain large, non-oriented blocks of the basement gneiss (Figure 5.3b), which may be more than 1 metre in diameter, and which were probably deposited as cut-bank erosion and collapsed blocks (Le Roux, 1986). Numerous enlarged fractures and joints in the basement gneisses contain rounded fragments of basement material and coarse basal deposits of the Dasdap sediments. The basal conglomerate (polymict or more commonly oligomict) is poorly sorted, with clasts ranging from a few millimetres (grit) to greater than 15 centimetres (cobbles and boulders) in diameter:

generally the clast size is of the order of two to four centimetres and may be either clast, or matrix supported. The clasts are typically sub-rounded, but may be quite angular, suggesting that these deposits are proximal. Several pebbles were noted to be extraformational in nature (e.g. jasper, quartzite, sandstone) suggesting a possible Dwyka origin. The two most common pebble types are blue-grey quartz (sometimes forming an oligomictic conglomerate) and basement gneiss. The blue-grey quartz pebbles were derived locally from quartz veins, which have been observed to be quite common in the metamorphosed basement gneiss outcrops of the region. The size of the boulders in Figure 5.3b shows evidence of the energy which was associated with these lowermost sediments. Boulders of a gneissic composition were noted to be weathered to various degrees. The matrix of the conglomerate consists of poorly sorted, finer, predominantly quartz grits and sands cemented by silica.

The lower conglomeratic sandstones and grits (Gt)

The basal conglomerate grades upwards into conglomeratic sandstones and trough cross-bedded grits (Figure 5.3). This facies type, when well developed, may contain several alternating layers of conglomerate and sandstone, and may exceed two metres in thickness. The repeated conglomerate layers (usually less than 20 millimetres thick) are well sorted and contain clasts approximately 8 millimetres in diameter. The upper contact is gradational (Figure 5.3), and grades into massive sandstone intercalated with silicified siltstone (Levin et al., 1986). According to Niemand (1986) sandstone layers in these lower sediments are usually less than 150 millimetres thick.

The basal conglomerate was not observed at outcrops on the farm Burtons Puts (Figure 5.1), where a pebbly sandstone lies directly on a weathered gneissic surface (Figure 5.3c). Conglomeratic lenses were noted in the coarse trough (and occasionally planar) cross-bedded sandstones. Le Roux (1986) noted the preservation of anti-dunes which he interprets as having formed in rapid very shallow flow with little reworking by slower currents. Upward fining trends, as observed within cycles at the Kookoppe, were also noted in these more distal sandstones. Coarser, less mature, trough cross-bedded arkosic grits (Figure 5.3d) are locally developed at the outcrops on Burtons Puts.

The upper sandstone (Sm-St-Fm)

This uppermost sediment may be silicified, particularly at the Kookoppe, resulting in flat-

topped mesas (see Figure 4.5). This sandstone unit appears to be the most extensively developed Dasdap sediment as it comprises a large fraction of the Kookoppe and the outcrops on the farm Kalkdraai to the southeast of the Kookoppe (Figure 5.1). This unit fines upwards, usually from a coarse sand to a fine sand or silt, through a vertical thickness of several metres. It has been noted to be coarser grained and thicker (up to 4 metres) in the northern outcrops (Niemand, 1986). The sandstones are typically massive, but occasionally exhibit some trough and planar cross-bedding. Silicified and ferruginized parts are generally massive. These sediments are commonly stained by iron oxide in their upper parts (Figure 5.3e), which typically coincides with the present land surface. Subsequent ferruginization, in the form of nodules, was noted by Levin et al. (1986). Iron oxide colours these sediments with various shades of yellow, red and brown. Niemand (1986) suggested an unconformable relationship between the silicified sandstone and the ferruginized sandstone, which he bases on observations of an inconsistent oligomict, well sorted conglomerate at the base of the ferruginized sandstone.

Le Roux (1986) noted large, well-defined lenses of pure kaolinitic clay which he interprets as "a kaolin mud moved in suspension as a dense cloud or slurry, settling out in scour pools left behind by the passing flood waters". It should be noted that some of the clay lens contacts with the adjacent grits and sandstones are gradational. Angular quartz grains may be preserved or even locally concentrated in these lenses. However, more typically, these microcrystalline lenses exhibit no preservation of grains or sedimentary structures. These clayey occurrences may have a reddish colour (Figure 5.3e) which Le Roux (1986) attributed to oxidation and subaerial exposure shortly after deposition, and suggested that this material is similar to "decomposed feldspar porphyroblasts" which he noted at the same locality in the underlying gneiss. The typical conchoidal fracturing and hardness is suggestive of silicification. It should be noted that the surrounding or adjacent sediments contain a very high proportion of kaolinitic matrix (also noted by Le Roux).

Several cycles of upward fining sedimentation were observed in these upper sediments (Figure 5.2). Figure 5.3f shows the base of a new cycle, with a well developed conglomerate at the base, on a scour surface. Levin et al. (1986) reported randomly distributed small and large pebbles in these sediments which include "clay balls". This they suggest is the weathered basement which formed part of the source material of these sediments.

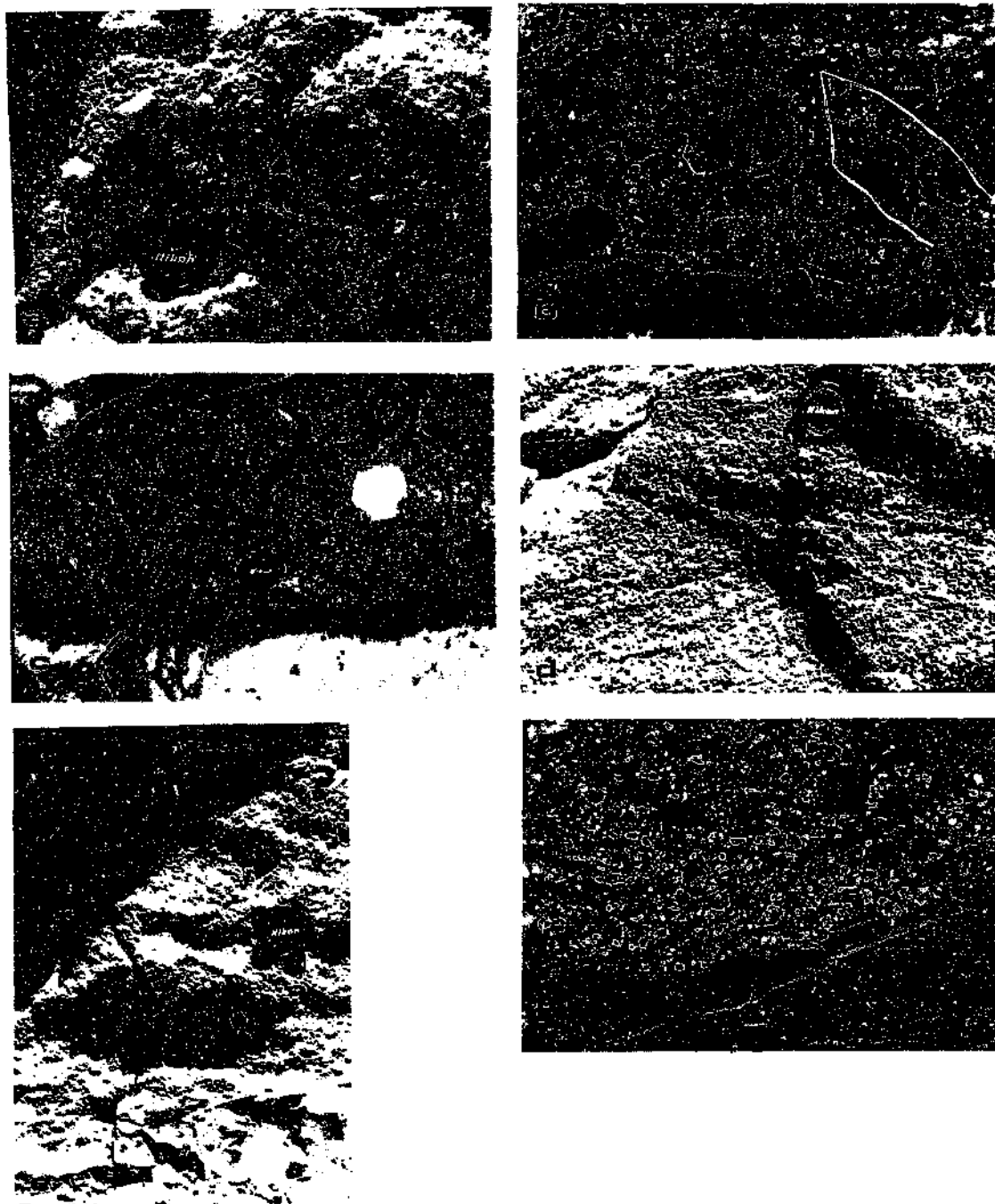


Figure 5.3 The Dasdap sediments (a) basal conglomerate lying unconformably on altered basement gneisses; (b) large fragments or boulders of the basement gneiss included in the basal conglomerate; (c) planar cross-bedded sandstone lying directly on an altered gneiss surface; (d) coarse, immature, trough cross-bedded arkosic grits; (e) iron oxide staining in the upper parts of the upper sandstone unit; and (f) basal conglomerate of a new cycle

5.1.2 Petrology

The Dasdap sediments have been described by previous workers (e.g. Levin et al., 1986 and Brynard, 1988), but no detailed petrographical description of these sediments has been given previously. Thus, for completeness, a petrographic description for each of the sedimentary units described above, excluding the large-clast conglomeratic basal sediments, is given below. Modal and textural analyses were undertaken on seven representative thin sections of the various sediments described in the preceding section.

5.1.2.1 Petrographic Descriptions

Basal sandstones

The basal sandstone samples analyzed (sample numbers VP-K1A and VP-K2: Figure 5.1), from the Kookoppe outcrops are comprised predominantly of very angular to subangular quartz fragments and minor oxides. The grains are often embayed, and set in a clay matrix (Figure 5.4a). Sample VP-K2 is less altered: plagioclase and potassium feldspar grains are either partly preserved or their original outline and texture is clearly evident. Sample VP-K1A is composed of approximately 40% clay and Sample VP-K2 of approximately 35% due to, what appears to be predominantly, the *in situ* alteration of feldspar grains. In crossed-polarized light (Sample VP-K2 in particular) some less altered feldspar grains are multiple-twinned plagioclase whereas others are microcline, showing typical cross-hatch twinning. In these samples kaolinite is the major clay mineral with subordinate illite and smectite. The feldspars are typically brownish in plane-polarized light owing to alteration. In crossed polarized light the microcrystalline clay matrix appears isotropic. Sample VP-K2 has been replaced by calcite in places (see relatively high CaO weight percent in the following section). Sample VP-K1A (Figure 5.4a) lacks the coarser pebbly fraction and is rather classified as a very coarse sand to grit. Some detrital iron-oxide (magnetite and ilmenite) grains are present (Sample VP-K1). Secondary disseminated iron-oxide, and grains coated by iron-oxide, most probably in the form of hematite are also present. Both samples are mineralogically and texturally immature sediments (due to their high clay and feldspar content, high particle angularity and poor sorting), consisting predominantly of

basement derived mineral or rock fragments.

Trough cross-bedded sandstone

In thin section this moderately to well-sorted, very coarse sandstone from the lower conglomeratic sediments (Figure 5.4b, Sample number VP-K6), contains angular to rounded quartz grains set in an iron-rich quartz cement. This once fairly porous sediment has been cemented by what appears to be predominantly rim cement (cement enclosing the entire grain and having the same crystallographic axis as the grain) and some blocky cement (cement nucleating in the interstitial areas, usually on finer clay particles of the matrix, and in no preferred crystallographic orientation). Many grain margins have embayments which are filled by a cement (the cement and matrix material constitutes 28% of the sample). This more distal sample (VP-K6) from the outcrops on the farm Burtons Puts contains only minor feldspar (and clay).

Planar-bedded to massive sandstone

This moderately-sorted medium sandstone (Sample number VP-K3, Figure 5.4c), from the Kookoppe outcrops, shows a wide range of grain shapes, consisting almost entirely of quartz, and ranging from rounded to very angular. Some detrital, well-rounded, smaller ilmenite and magnetite grains are also present. Angularity of the quartz grains may be attributed to corrosion, and results from the numerous grain margin embayments. The monocrystalline quartz grains exhibit a typical fractured pattern, along which further corrosion has taken place. This sediment shows evidence of being highly porous prior to cementation or silicification (the cement constitutes 16% of the sample). Iron staining of the cement has resulted in a brownish coloration.

Siltstone

This clay-rich sediment (Sample number VP-4, Figure 5.4d), from the farm Burtons Puts, exhibits fine to very fine, highly corroded, quartz grains set in a fine clay matrix (72% clay content). Some detrital and well rounded ilmenite and magnetite grains are also dispersed throughout the matrix. The quartz grains are rounded to very angular: the embayed shape being controlled mainly by corrosion of the rims. The matrix appears to be the result of the *in situ* breakdown of feldspar grains, although due to alteration the original grain outlines

are no longer evident.

A similar sample (Sample number VP-5) from outcrop on the southern portion of Vaalputs was analyzed. This slightly coarser-grained sediment also contains highly corroded quartz grains set in a cemented and clayey matrix. The matrix in this sample is more silicified than sample VP-4 (Figure 5.4d), with the cement constituting 43%, and clay constituting 15% of the inter-granular material. The resemblance of these sediments suggests that they were probably deposited under similar conditions.

Ferruginous sandstone

This moderately to well sorted, coarse to very coarse sandstone (Sample number VP-K7, Figure 5.4e) from the outcrops on the farm Burtons Puts, is very similar to the trough cross-bedded sandstone (Sample VP-K6, Figure 5.4b), containing very angular to rounded quartz grains cemented by iron-oxide. In this sample (VP-K7) the cement appears to be almost entirely composed of iron-oxide, that is, no evidence of quartz cement was noted. The iron-oxide cement constitutes 36% of this sample and is opaque in both plane- and crossed-polarized light. The quartz grain margins, as in other samples (e.g. Sample VP-K6, Figure 5.4b), are embayed from corrosion.

Ferruginized siltstone

This clay-rich sediment (Sample number VP-K1B, Figure 5.4f) from the Kookoppe, is reddish in handspecimen due to the high iron oxide content. This lithology was previously described as an alluvial clay deposit (e.g. Le Roux, 1986). In thin section the matrix shows clear evidence of highly altered, medium-grained, fairly well-rounded relics of feldspar grains. The quartz grains, which are scattered throughout the matrix are also medium grained, with corroded grain margins. In addition to the high iron content, some silicification in the altered matrix is also evident. The silicified clayey matrix forms the bulk (81%) of this sample.

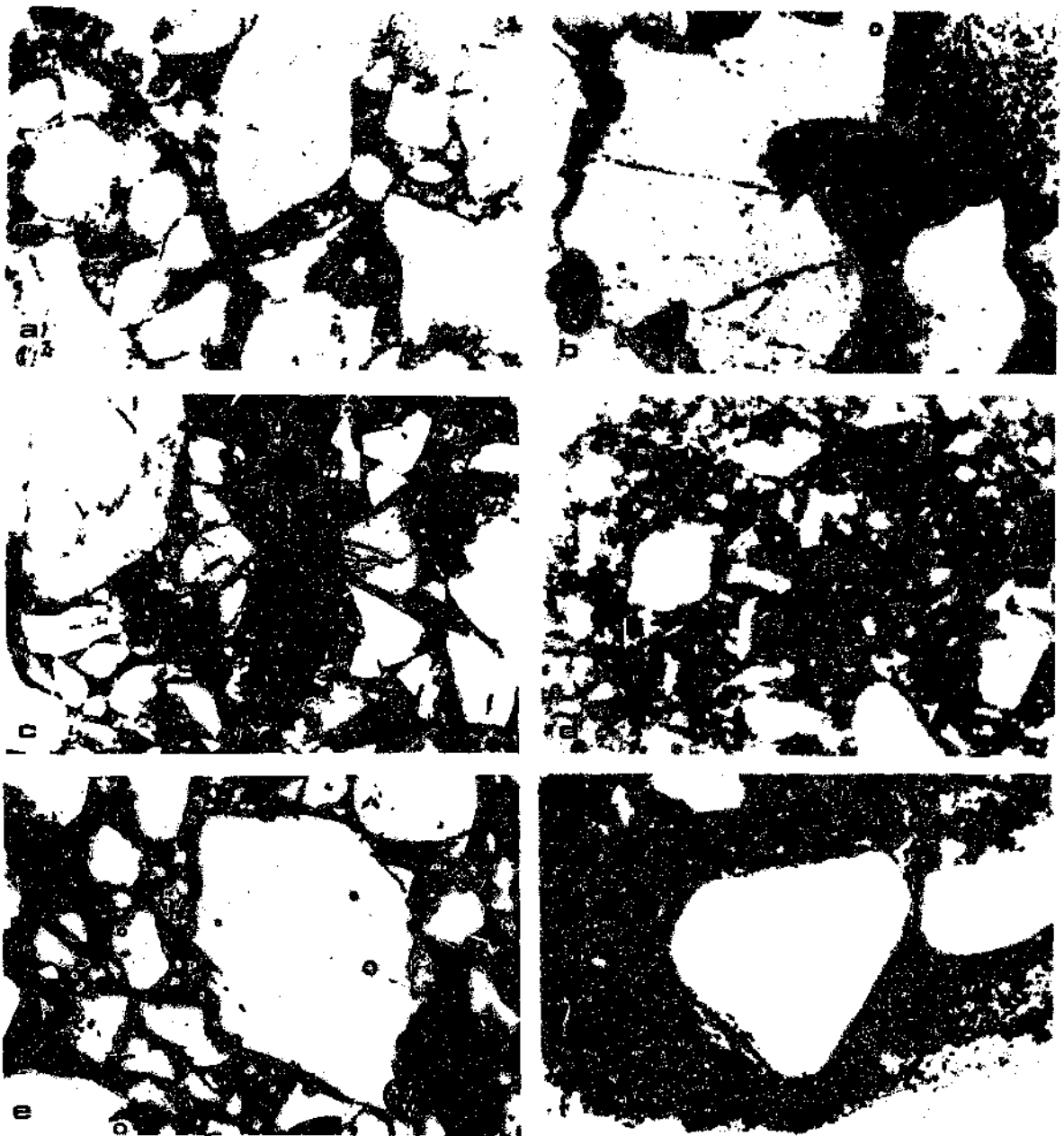


Figure 5.4 Thin sections of the Dasycrinid sediments. (a) very coarse sand/ grit from the basal sediments (Kookkoppe) (plane polarized light). (b) trough cross-bedded sandstone (Kookkoppe) (plane polarized light). (c) planar-bedded to massive sandstone (Kookkoppe) (crossed-polarized light). (d) siltstone (Kookkoppe) (plane polarized light). (e) ferruginous sandstone (Burtons Puts) (plane polarized light) and (f) ferruginized siltstone (Kookkoppe) (plane polarized light). Field of view in all cases: 0.9 x 1.35 mm.

5.1.2.2 Modal Analysis

The modal analysis generally revealed either a very high clay matrix content, a high cement content, or a combination of matrix and cement, for all the analyzed samples. The modal percentages (Quartz-Feldspar-Rock Fragments) for the analyzed samples are represented on ternary plots in Figures 5.5a and 5.5b. Figure 5.5a excludes the matrix or cement and Figure 5.5b assumes that all the matrix or cement was originally derived from the *in situ* weathering of feldspar or remobilization and cementation of quartz.

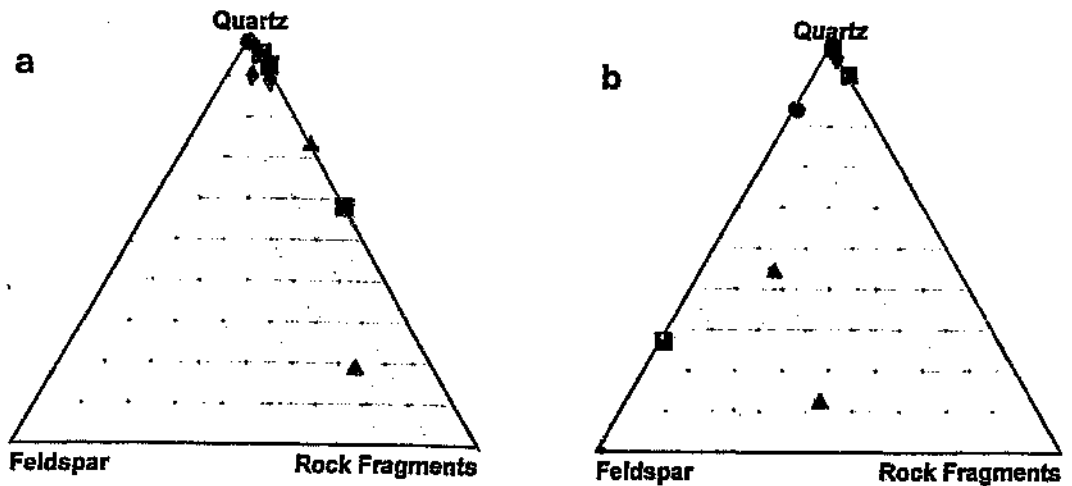


Figure 5.5 Ternary plots of: the basal sediments of the Kookoppe (▲); the overlying finer-grained sediments of the Kookoppe (■); the distal sediments on the farm Burtons Puts (◆); and a distal sediment from Vaalputs (●). (a) Excluding all intergranular material (8 points). (b) Whole sample, assuming all intergranular material is the product of *in situ* alteration (7 points - excluding the highly silicified and ferruginized siltstone - Sample VP-K1B).

The two plots (Figures 5.5a and 5.5b) are similar in that all samples with the exception of three (two basal, proximal samples, and one finer grained, less mature, proximal sediment, all from the Kookoppe) contain high concentrations of quartz grains (Figure 5.5a) or remobilized quartz, now in the form of cement (Figure 5.5b). The three exceptions (Figures

5.5a and 5.5b) are immature sediments containing very high percentages of altered basement rock fragments which are feldspar rich. The shift of these three points towards a higher feldspar content in Figure 5.5b is due to the inclusion of clay as feldspar.

Law et al. (1990) developed a classification system for Witwatersrand quartzites, whereby altered lithologies, primarily "arenites" be distinguished from "wackes" in terms of cross-stratification, sorting, and amount of matrix material. Their classification scheme differs from those of other workers in that it allows for the post-depositional alteration (mineralogical and textural) of the original detrital assemblage and arrives at the genetic precursors for altered sediments. The types and abundances of secondary minerals thus reflect post-depositional processes and primary detrital components reflect pre- and syn-depositional processes. This classification system was found to be useful for the clay rich Dasdap samples described above, which would have otherwise mostly been classified as "wackes". However, using the classification of Law et al. (1990), and the observations that most of the facies encountered from the Dasdap showed some form of stratification/ cross-stratification and were moderately to well sorted, confirmed that the nomenclature used in the previous section is accurate. The classification system also confirmed that intense *in situ* alteration of most of the Dasdap sediments has taken place, resulting in the high clay matrix content.

5.1.3 Chemistry

The chemical compositions of five representative samples from the Dasdap sediments, from the Kookoppe outcrops and the outcrops on the farm Borens Puts were determined. In addition, two analyses determined by Brynard (1988) of Dasdap sediments on the farm Rondegat, to the south of Vaalputs (shown in Figure 5.8) were used for the more northerly Dasdap occurrences. The major elements were believed to be more useful than trace elements in comparing the various sediment types of the Dasdap Formation. Two ternary plots ($\text{SiO}_2\text{-Al}_2\text{O}_3\text{-Fe}_2\text{O}_3$ and $\text{K}_2\text{O-CaO-Na}_2\text{O}$) were used to represent the major chemical constituents of the seven analyses. In addition, the chemical index of alteration for these sediments was determined and used for a comparison to other palaeo-weathered basement occurrences in the region. The chemical results are tabulated in Appendix A.

SiO₂-Al₂O₃-Fe₂O₃ ternary plot

This ternary plot (Figure 5.6a) shows the similarity of the various sediments of the Dasdap Formation. Two exceptions to the typical 70 to 90 SiO₂ weight percentages (Appendix A), which are not shown in Figure 5.6a are the basal sediment (VP-K2) which has been partly replaced by calcite, and the altered sandstone sample from the farm Rondegat (Sample RGT 4), which is slightly enriched in Al₂O₃. The small variations observed in Figure 5.6a are believed to be primarily due to small differences in iron and clay (feldspar) content. The silicified sandstone (RGT 4) from the farm Rondegat, which is fairly high in aluminium, Brynard (1988) attributed to the altered (kaolinized) nature of this sediment.

K₂O-CaO-Na₂O ternary plot

Four samples plot (Figure 5.6b) very near 100% CaO, primarily because the Na₂O and the K₂O values are zero or very low (Appendix A). The immature basal sediment has higher values for sodium and potassium, most probably due to the higher feldspar content typically found in these proximal sediments. The two Rondegat sediments (Figure 5.6b) contain slightly higher proportions of sodium, which may be due to the percussion drilling method of sample collection, that is, contamination by other sediments and/or the basement may have affected these values.

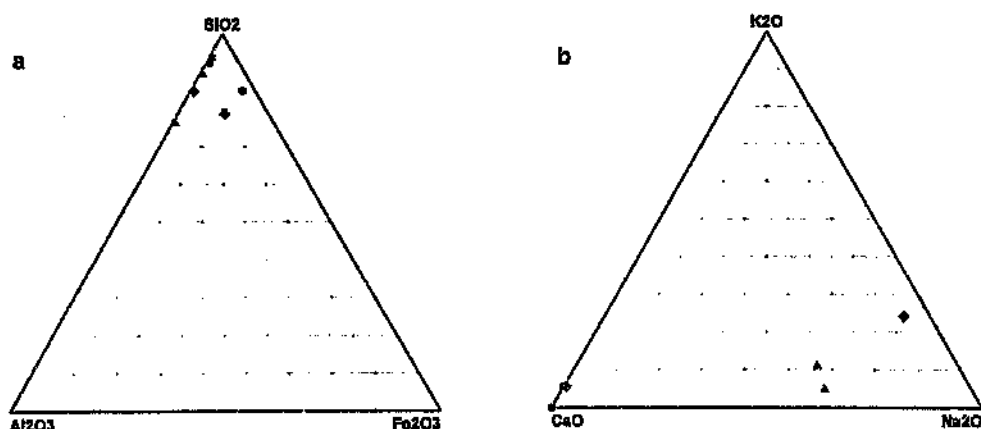


Figure 5.6 (a) SiO₂-Al₂O₃-Fe₂O₃, and (b) K₂O-CaO-Na₂O ternary plots for the Dasdap Formation: the basal (proximal) sediments of the Kookoppe (♦); an overlying finer-grained (proximal) sediment from the Kookoppe (*); distal sediments on the farm Burtons Puts (●), and distal sediments from Rondegat (▲).

Chemical Index of Alteration (CIA)

Plagioclase is the most abundant mineral in the exposed, non-weathered, continental crust (Nesbitt and Young, 1984) and is among the more rapidly weathered silicates (e.g. Garrels and MacKenzie, 1967; Grant, 1963). Petrographic and XRD studies (Wahlstrom, 1948; Lovering, 1959; Meunier and Velde, 1976; Markovics, 1977; Nesbitt, 1979; Nesbitt et al., 1980) indicate that, during weathering, large amounts of kandites (kaolinite-group minerals) are ultimately produced at the expense of plagioclase. Illites are also formed during the weathering of granitic rocks (Brock, 1943; Wahlstrom, 1948; Sand and Bates, 1953; Grant, 1963; Nesbitt et al., 1980) and mass balance considerations (source of K), coupled with the antipathic relationship between the K-feldspar content and the amount of illite produced *in situ*, require the illite to be derived from weathering of K-feldspar (Nesbitt and Young, 1989). Calcium, sodium and potassium are generally removed from the feldspars by solution so that the proportion of alumina to alkalis typically increases in the weathering product (Nesbitt and Young, 1982).

According to Nesbitt and Young (1982) a good measure of the degree of weathering can be obtained by the calculation of the CIA using molecular proportions:

$$\text{CIA} = [\text{Al}_2\text{O}_3 / (\text{Al}_2\text{O}_3 + \text{CaO} + \text{Na}_2\text{O} + \text{K}_2\text{O})] \times 100;$$

whereby the resultant value is a measure of the proportion of Al_2O_3 versus the labile oxides in the analyzed sample. They give values ranging between 45 and 55 for granitoids, idealized muscovite gives a value of 75 and illite ranges between 75 and 85 as do montmorillonites and beidelites. Kaolinite and chlorite would show higher values, very close to 100. Table 5.1 lists the CIA values of the Dasdap sediments, the mean of these values, as well as, range and mean values for the palaeo-weathered basement on Vaalputs.

Table 5.1 CIA values of the Dasdap sediments and mean values for the palaeo-weathered basement on Vaalputs.

Dasdap Formation:		Namaqualand Metamorphic Complex:	
Sample Number	CIA value	CIA value	
VP-K1A	86.9		
VP-K2	12.0		
VP-K3	98.7		
VP-K6	97.2		
VP-K7	94.5		
RGT 4	93.0		
RGT 5	92.5	Range of CIA values	58.1-67.6
Mean	70.2	Mean (n=18)	63.0

From the values presented above it is evident that although the mean values are similar the typical CIA value for the Dasdap sediments is much higher than that of the palaeo-weathered basement at Vaalputs, which is presumably a consequence of the abundance of kaolinite in these sediments. The arenaceous samples (with the exception of VP-K2 which has been calcified - see Appendix A) generally have higher CIA values, indicating that detrital feldspars have largely been converted to kaolinite.

5.1.4 Discussion

Levin and Raubenheimer (1983) reported the presence of an extensive alluvial fan noted on a LANDSAT image, in the area of the Dasdap sediments. A combination of satellite imagery and field observations were used to support their interpretation of the existence of an alluvial fan in this area. The surficial feature which Levin and Raubenheimer (1983) refer to as the Dasdap alluvial fan and with which they associated the Dasdap sediments

is shown in Figure 5.7. Levin et al. (1986) interpreted the Vaalputs sediments as an alluvial fan resulting from the regrading of the Dasdap Fan, to the south, and the subsequent redeposition of the material, to the north, into the Vaalputs Fan.

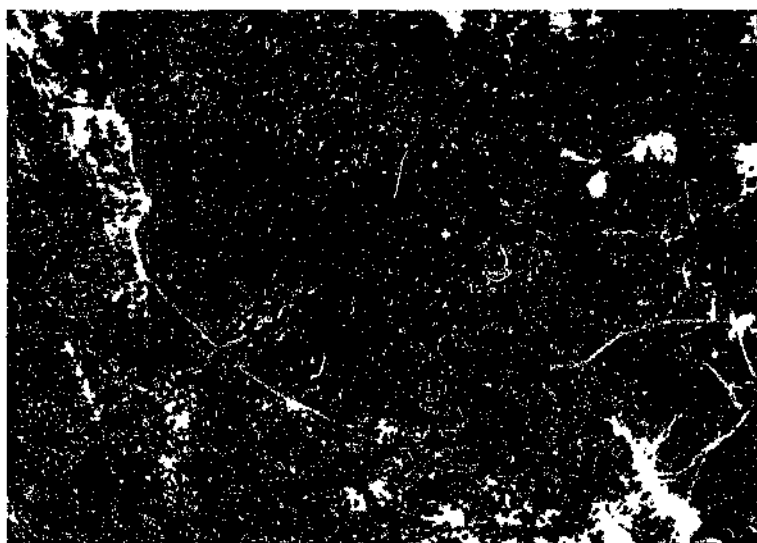


Figure 5.7 TM-5 LANDSAT image of the surficial feature referred to as the Dasdap alluvial fan by Levin and Raubenheimer (1983), approximately 25 kilometres due south of Vaalputs. The image is approximately 30 kilometres across.

A re-examination of these sediments suggests that the Dasdap Formation, which is comprised of alluvial sediments, is generally unrelated to the macro-features previously observed on satellite images and interpreted as an alluvial fan. Thus, the feature observed on the image (Figure 5.7), and denoted by aeolian dunes is, therefore, not believed to be an alluvial fan. The following sections deal with new evidence, supporting alternative views for the origin and distribution of these sediments.

Palaeo-weathering of the Dasdap sediments

Brynard (1988) noticed remnant gneissic rock textures in the basal succession of these sediments, in which the feldspars are completely altered to clays, and occur as "fan-like

books". Also, remnant myrmekitic textures were noted with only the intergrowths of quartz occurring as worm-like rods, remaining in the matrix. Also, portions of these sediments have been completely silicified. Niemand (1986) noted evidence for more than one period of silicification in the form of older silicified pebbles preserved in the sediments, as well as that preserved on the present land surface in the form of the silicified cap rocks of the Kookoppe. Brynard (1988) suggested that a major period of weathering involving kaolinization and silicification probably took place prior to the deposition of the sediments, due to the presence of silicified clasts of sandstone in what he interpreted as non-silicified matrix. An alternative explanation of post depositional alteration would require a process of selective silicification which would have affected only certain sedimentary horizons, and which he states, seems unlikely. Brynard (1988) and McCarthy et al. (1984) concluded that the Dasdap Formation has experienced extensive kaolinization and silicification, suggesting that deposition predates the kaolinization and silicification of the basement rocks.

The chemical analyses of this study are in agreement with extensive weathering, which has resulted in the breakdown of feldspars to clay minerals (kaolinite, and minor smectite and illite) and silicification which has caused both the corrosion and cementation of grains. The low Ca (with the exception of one sample) and alkali values are a consequence of the almost complete breakdown of feldspar to clay. The high CIA values are a direct consequence of the abundant clay mineral, kaolinite. The Dasdap sediments exhibit much higher CIA values than any other palaeo-weathered basement outcrop in the region, which may be attributed to a fairly highly weathered source, as well as, subsequent *in situ* weathering. However, the fact that these arenaceous sediments have high CIA values indicates *in situ* weathering.

The angularity (due to embayments) of grains and the overall appearance of these sediments is suggestive of predominantly *in situ* palaeo-weathering, rather than suspension settling of clay particles in what was suggested by Le Roux (1986) as a high-energy-type deposit. However, Le Roux (1986) did suggest that silica may have been

released into the sediments during kaolinization of the basement gneisses. The kaolin clay lenses may represent channel switching and deposition of a feldspar rich or partly weathered sediment (the source material for these sediments are the basement gneisses), which would weather (*in situ*) to an almost pure clay. Petrographic evidence of this study shows conclusive evidence that these sediments were affected by post depositional kaolinization and silicification.

Palaeocurrent Directions

The Dasdap sediments become progressively finer-grained and thinner towards the east and south, where they lack the basal conglomeratic sediments (Figure 5.2), suggesting a general palaeocurrent direction to the southeast. Levin et al. (1986) reported consistent palaeocurrent directions towards the southwest, which they observed, trended subparallel to structural trends in the basement. On the farm Burtons Puts, they noted a wider range of palaeocurrent directions which they suggested were the result of a fan-shaped distributary system.

Le Roux (1986) carried out a comprehensive palaeocurrent study with a total of 169 readings, trough cross laminations constituting 94% of the readings. The Kookoppe outcrops display a very consistent palaeocurrent direction to the southeast, with a vector mean azimuth of 154° and evidence for a very straight (standard deviation: 28°; sinuosity value: 1.04) dispersal system. To the southeast, on Burtons Puts, a wider range of palaeocurrent directions was obtained with a south-southwesterly trend (mean azimuth: 191°; standard deviation: 38°; sinuosity: 1.07). These values also suggest a fairly straight dispersal system. Palaeocurrent data of this study confirmed a direction towards the south and southeast for the proximal Kookoppe sediments in the west, and a wide range (south-southwest to east-northeast) in the more distal eastern outcrops. Figure 5.8 summarises these results, and other inferred palaeocurrent directions.

The southeast palaeocurrent trend in the Kookoppe outcrops matches the strike of lineaments in the region. Le Roux (1986) proposed a possible reversal of the north-

northwest trending Hardeholte River (shown in Figure 5.1), which follows the topography of the "fan scour surface" in the vicinity of the Kookoppe outcrops. Le Roux (1986) suggests that debris carried along this main channel fanned out to the south (observed in outcrops on Burton's Puts), where sediment thickness is less and conglomeratic deposits are uncommon. No obvious evidence of structural control was noted for these outcrops.

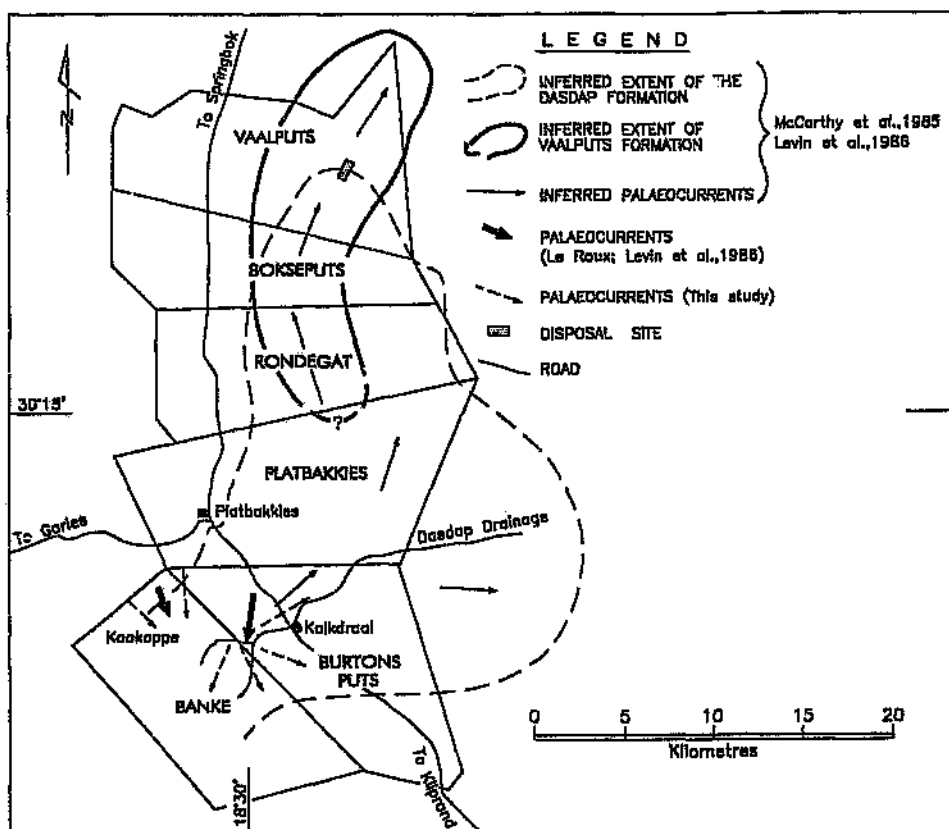


Figure 5.8 Map showing actual palaeocurrent directions determined from sedimentary structures, and inferred palaeocurrent directions for the Dasdap sediments.

All the Dasdap sediments, that is, the Kookoppe and the outcrops on the farm Kalkdraai, occur at a similar topographic elevation (the southeastern Kalkdraai outcrops are no more than 20 metres lower than the Kookoppe), suggesting that both sediment suites belong to the same depositional episode, and that in this particular region tectonism has not

displaced these sediments vertically by more than a few tens of metres.

Percussion drilling on the farm Platbakkies (Figure 5.1) revealed 35 metres of "gritty silicified sandstones". Levin et al. (1986) presumed that these sandstones belong to the Dasdap Formation. In addition, 20 metres of "yellowish to white sandstones" in the southeast corner of the farm Bok se Puts, and which outcrop on Vaalputs (generally covered by *Gordonia* sediments), suggests that the Dasdap sediments may extend as far north as the southern portion of Vaalputs. Petrographic and chemical results of this study also suggest that the Dasdap sediments occur to the north of the well exposed outcrops in the area around the present Dasdap drainage.

Age of the Dasdap Formation

Andersen (1992) suggested that ultramafic igneous activity preceded and possibly accompanied the uplift associated with the deposition of the Dasdap sediments. This suggestion is based on the observation that sediments having a similar appearance to those of the Dasdap Formation, fill breccia vents on Vaalputs and the neighbouring farm Riembreek. The Vaalputs melilitite pipe, on which these observations are based is described in detail by Andersen and Muller (1984). All these sediments appear to be weathered in a similar way to those of the Dasdap sediments on the farm Burtons Puts and at the Kookoppe.

From descriptions given by Reuning (1932) of the Arnot pipe at Banke, it appears as though certain pipes in this area, which are believed to be the source of ilmenite present in the Dasdap sediments, have suffered almost no erosion, and still contain most of their original crater fill sediments (McCarthy et al., 1985). McCarthy et al. (1985), therefore, suggest that the Dasdap sediments were deposited pene-contemporaneously with pipe emplacement.

Haughton (1930) suggested an early Tertiary age for fossil frogs found in the Banke crater fill material. Estes (1977) proposed an Eocene to Oligocene age for these deposits. This age, however, relies heavily on the work of Kröner (1973) who reported ages of 35 to 37 Ma (K/Ar method) for other melilitite occurrences to the north and south of the area in

question. According to Scholtz (1985) the fossil assemblage in the Arnot pipe at Banke suggests proximity to the Cretaceous-Tertiary (60-70 Ma) boundary, with a high possibility of at least a pre-Eocene age. Five zircon dates from pipes in the Arnot area yield a tightly grouped age, within a 7 Ma time span, around the Cretaceous-Tertiary boundary (Cornelissen and Verwoerd, 1975; Moore, 1979).

Other workers (eg. Coetzee et al., 1983) have obtained somewhat similar ages (late Cretaceous to early Tertiary), using palynological data and floral assemblages found at Banke in the crater fill material. These ages relate well to radiometric geochronological work, using zircon uranium-lead, in which ages of 64 Ma, 67 Ma, and 69 Ma were obtained for the Camp, Platbakkies and Rieimbreek pipes respectively (Dr. J. Bristow, pers. comm. to TSM: McCarthy et al., 1985). McCarthy et al. (1985) assigned an age of 70 Ma (late-Cretaceous) to the Banke and Boschjeslaagte pipes. All the above results suggest that two or more episodes of pipe emplacement are preserved in this area. McCarthy et al. (1985) use these data for the argument that the palaeo-weathered and silicified surfaces already existed at the end of the Cretaceous, rather than Tertiary, as suggested by Mabbutt (1955).

From the numerous ages of intrusions associated with the Dasdap sediments and related deposits it would appear that the age of these deposits cannot be determined accurately. They do, however, appear to be of a Cretaceous rather than an Oligocene age as suggested by previous workers (e.g. Andreoli et al., 1987). The *in situ* weathering of these sediments is also strongly suggestive of deposition prior to a major weathering and silicification episode such as that which occurred during the Late-Cretaceous (Partridge and Maud, 1987).

Depositional environment

Previous workers have interpreted what is primarily an aeolian dune field (shown in Figure 5.7), in the Dasdap area, as an alluvial fan, due to the alluvial nature of the Dasdap sediments, which are of relatively small aerial extent, and the apparent alluvial-fan-shape noted on the satellite image. Le Roux (1986) suggested that this alluvial fan feature may be derived from erosion of the Dasdap Formation, but may be the *in situ* weathering products of the underlying Dasdap sediments. No obvious morphological form, such as the

semi-conical shape, restricted radial length, plano-convex-profile, and comparatively high values of radial slope (Blair and McPherson, 1994) for the Dasdap sediments is recognizable. Therefore, the interpretation of these sediments in this study is based solely on sediment types (facies) and their associations. The results of this study show that although Dasdap-type sediments may occur as far north as Vaalputs, they should not be delineated by the apparent alluvial fan shaped features noted on satellite imagery, which shows predominantly surficial aeolian sediments of the Gouda Formation.

According to Le Roux (1986) the presence of "fairly thick scour pool suspension clays and sieve deposits suggests abrupt slow-downs in current velocity". This he interprets as channel abandonment on alluvial fans. For the more distal sediments which includes the silicified sandstone outcrops on the southern portion of Vaalputs, it is proposed that sheet flows covering much wider areas resulted in large sheets of sand which were deposited in upper flow regimes. The upward fining noted in the sequence of sediments may be attributed to channel abandonment or to lateral accretion, whereas the abrupt upward coarsening may be due to the reactivation of a channel after a period of temporary channel abandonment or tectonic reactivation (uplift of the source area).

Areas of higher elevation to the north and to the west of these sediment accumulations provided the required gradients for the development of high energy deposits. It is thus envisaged that the watershed at the time of deposition was further to the north and west. The rivers inland of the present divide have not incised to the same degree as those on the coastal side as they have an elevated, local base level. These deposits may well have been related to an episode of uplift in the northern hinterland or escarpment area. The Dwyka was probably locally developed in the provenance area, due to the presence of well rounded Dwyka erratics in the basal sediments, suggesting that the Dwyka occurred further to the west, than is indicated by the present western margin of the Dwyka. The area flanking the eastern and southern margin of this highland became the site of rapid accumulation of sediment in a fluvial-alluvial fan system. McCarthy et al. (1985) suggested a possible increase in precipitation, coinciding with uplift, for the accumulation of these sediments. The Dasdap sediments are, therefore, believed to have been deposited in a series of high energy episodes, as indicated by the large pebble basal conglomerate,

including basement material, high energy bed-forms (lunate dunes, antidunes and upper planar lamination), and the multiple unconformities with coarse sediment or conglomerate bases. Blair and McPherson (1994), on the basis of an extensive study of modern alluvial fans concluded that fans may be readily distinguished from other sedimentary environments including gravel-bed rivers. These distinctions are reflected and determined by the morphology, hydraulic, sedimentary processes, and resultant facies and facies assemblages of alluvial fans. Sediments of the Dasdap Formation are all suggestive of alluvial fan deposits and Figure 5.9 shows a proposed alluvial fan sediment pattern which may have given rise to the observed Dasdap sediments during this period.

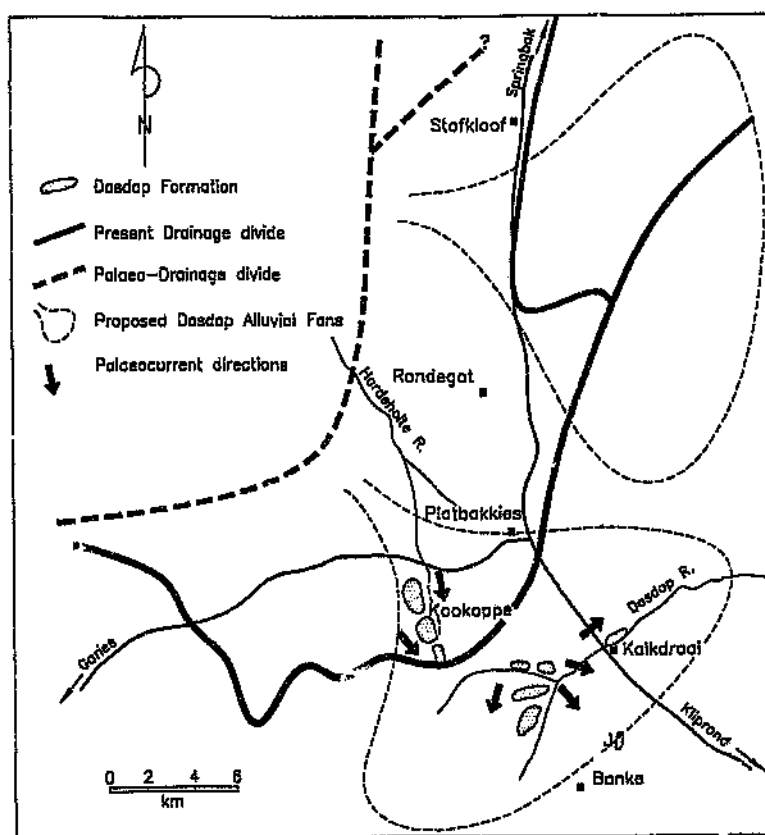


Figure 5.9 Sketch map showing the position of the possible alluvial fans which may have given rise to the Dasdap sediments.

5.2 The Palaeo-Weathered Landsurface

Palaeo-weathering has effected large areas of the basement lithologies in the study area. The palaeo-weathered occurrences of the region generally consist of weathered rock overlain by a silicified cap-rock. Partridge and Maud (1987) refer to this surface as the "silcrete-capped African surface" and have assigned it a Cretaceous age. These palaeo-weathered products form an integral part of the study as the palaeo-weathering episode has affected sediments such as the Dasdap Formation, and presumably provided some of the source material for younger surficial sediments.

5.2.1 Field Occurrences

The extent of the palaeo-weathered basement occurrences, as determined from satellite imagery and confirmed by ground studies, is shown in Figure 5.10. A more detailed map of the palaeo-weathered rocks on the Vaalputs property is shown in Figure 8.8. Figure 5.11 shows the typical appearance of the palaeo-weathered profile, with the resistant silicified cap-rock overlying the palaeo-weathered basement. The silicified horizons range from 1 to 3 metres in thickness and have a well-developed joint system (also seen in the underlying palaeo-weathered zone), which is predominantly vertical with less sub-horizontal elements, producing a columnar appearance. The silicified zones typically display a sub-conchoidal fracture.

The less resistant palaeo-weathered zone underlying the cap-rocks averages 2 to 3 metres in thickness, but may attain thicknesses of 5 metres or may be totally absent. The transition from the relatively unaltered to the palaeo-weathered basement, as well as the contact with the overlying silicified zone, may undulate by a metre or two, but is generally horizontal at most outcrops. The lower contact (unaltered basement to palaeo-weathered basement) is usually gradational over one to two metres, whereas the upper contact (palaeo-weathered basement to silicified basement) is less gradational usually over less than half a metre.

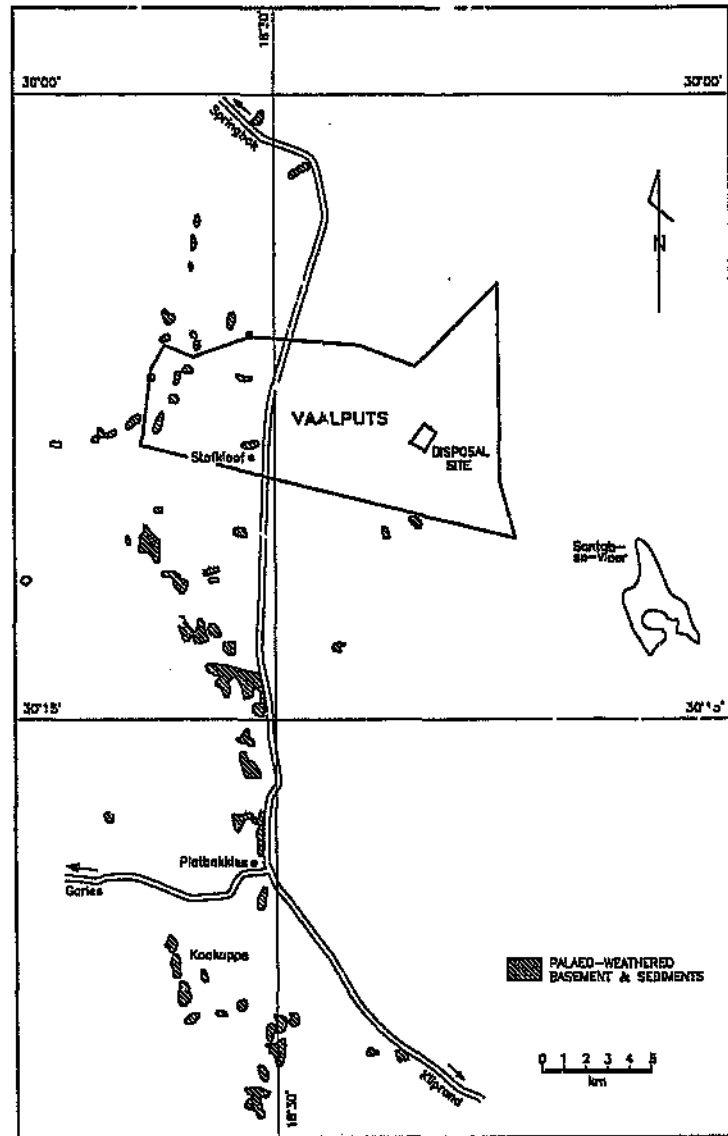


Figure 5.10 Palaeo-weathered rocks in the study area.

More modern differential weathering within these rocks appears to occur primarily along joints. Joints and other fractures in the rock form a typical meshwork of channels which have allowed the subsequent movement of water and dissolved ions. These recent

processes have given rise to the development of numerous caves and hollows in the steep-sided faces offered by these outcrops. Moreover, iron impregnation along the joints has resulted in a different resistance of the joint surfaces with respect to the interjoint blocks, and erosion has resulted in a boxwork type appearance, with joints being more prominent. Although the joints appear to have been an early feature, the concentration of iron along the joints appears to be a more recent weathering phenomenon. Mass movement on the slopes of these basement occurrences has resulted in many slip scars and rockfalls which contain massive blocks of the weathered and silicified basement. This material would ultimately be transferred from interfluvies and from valley-side slopes, towards lower levels in the landscape (often fault lines) and eventually into drainage channels.



Figure 5.11 The silicified basement occurrences in the study area overlying weathered basement, which passes gradually downward into unaltered basement.

On the eastern portion of Vaalputs where the Vaalputs and Gordonia sediments are extensively developed, a white clay facies, possibly associated with the same episode of palaeo-weathering has been encountered in boreholes and road cuttings, such as that on

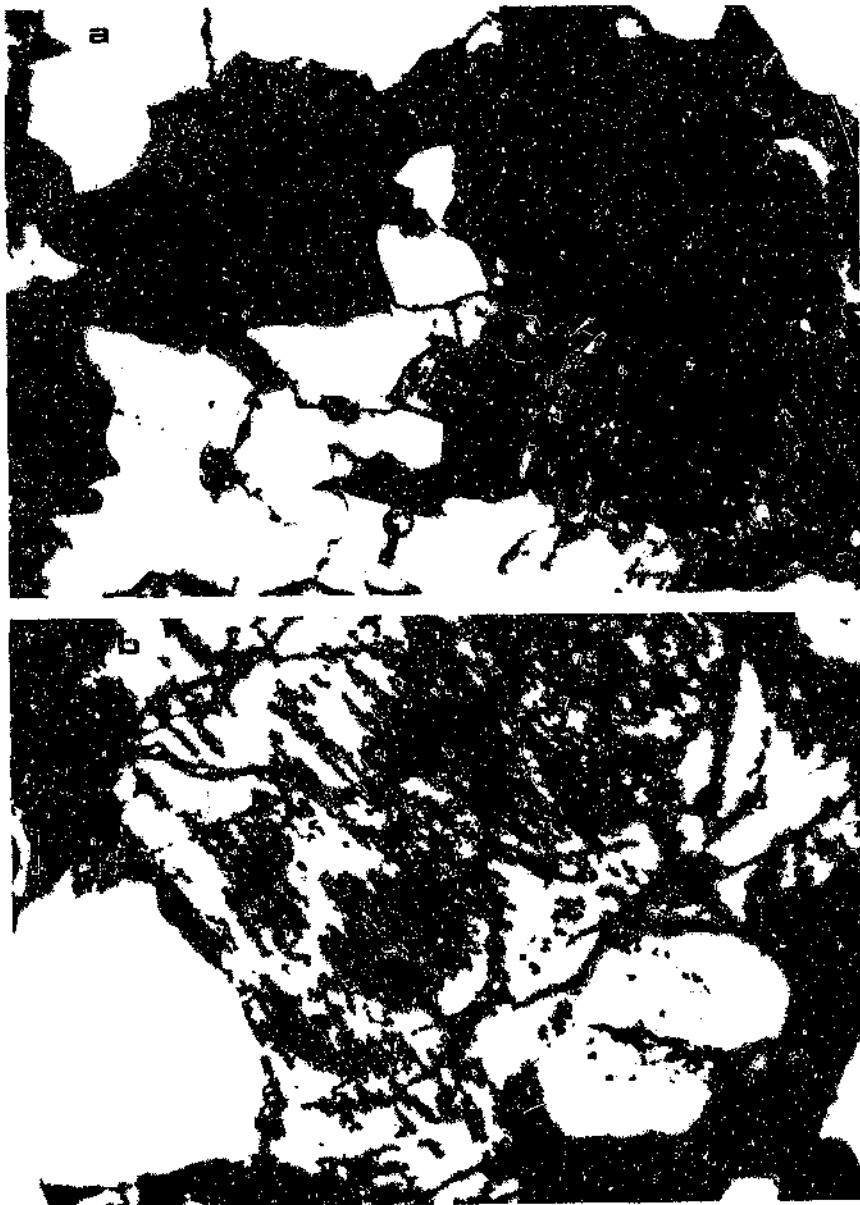
the "Norabees access road" on the southern boundary of Vaalputs. Examination of the boreholes (McCarthy et al., 1985) has suggested that some regrading of this surface occurred prior to the deposition of the overlying or upper Vaalputs sediments. This, according to Levin and Raubenheimer (1983), is further supported by the observation that unaltered basement outcrops to the north of Garing, while palaeo-weathered basement occurs to the south. The scarp forming the western margin of the Santab valley (Santabse-Vloer: Figure 5.10) has been suggested (McCarthy et al., 1985) to represent the eastern limit of this surface, although similar occurrences have been observed approximately 35 kilometres to the east of Vaalputs at the "Tafelkoppe".

5.2.2 Petrology

Thin sections were prepared from samples of each of the zones (unaltered, palaeo-weathered, and silicified basement) from two profiles. The micromorphology of these samples reflects both the original material characteristics and the effects of the subsequent diagenesis (Smale, 1973; Summerfield, 1978; Summerfield, 1983c; Summerfield and Whalley, 1980; Watts, 1978; Whalley, 1978). Mineralogically the sections appear fairly similar, with the palaeo-weathered zone containing slightly more clay than the silicified zone (which exhibits iron stained silica cement). XRD analysis on the silicified and palaeo-weathered zone samples revealed the presence of illite, kaolinite and some smectite. The exact proportions of these clays were not determined due to the difficulty in obtaining reasonable quantitative values from XRD data, and due to the variability of clay compositions from one sample site to the next.

Figures 5.12a-d are photomicrographs of the various zones. Figure 5.12a is of the relatively unaltered basement gneiss (some alteration of the feldspars may be observed). The grain boundaries show few embayments and no secondary silicification is present in this sample. Figures 5.12b and c show sections of the transition zone (unaltered to weathered basement) and the palaeo-weathered basement, respectively. Figure 5.12b clearly shows the feldspar in the initial stages of weathering and Figure 5.12c shows almost completely altered feldspar surrounding quartz grains. The quartz grain boundaries, in this zone (Figure 5.12c), are partly embayed due to dissolution. Remobilization

and cementation of silica is strongly evident in the silicified zone (Figure 5.12d) where the matrix is composed predominantly of iron-stained cryptocrystalline silica or microquartz, appearing opaque in thin section, and in which the quartz grain boundaries are strongly embayed. The palaeo-weathered zone (Figure 5.12c) contains the greatest percentage of altered feldspars in comparison to the basement and silicified zones, which makes this zone more susceptible to modern weathering and erosion. It should be noted that modern weathering is confined to the surface of the outcrops whereas the palaeo-weathering was more extensive, penetrating and affecting large volumes of the basement rock.



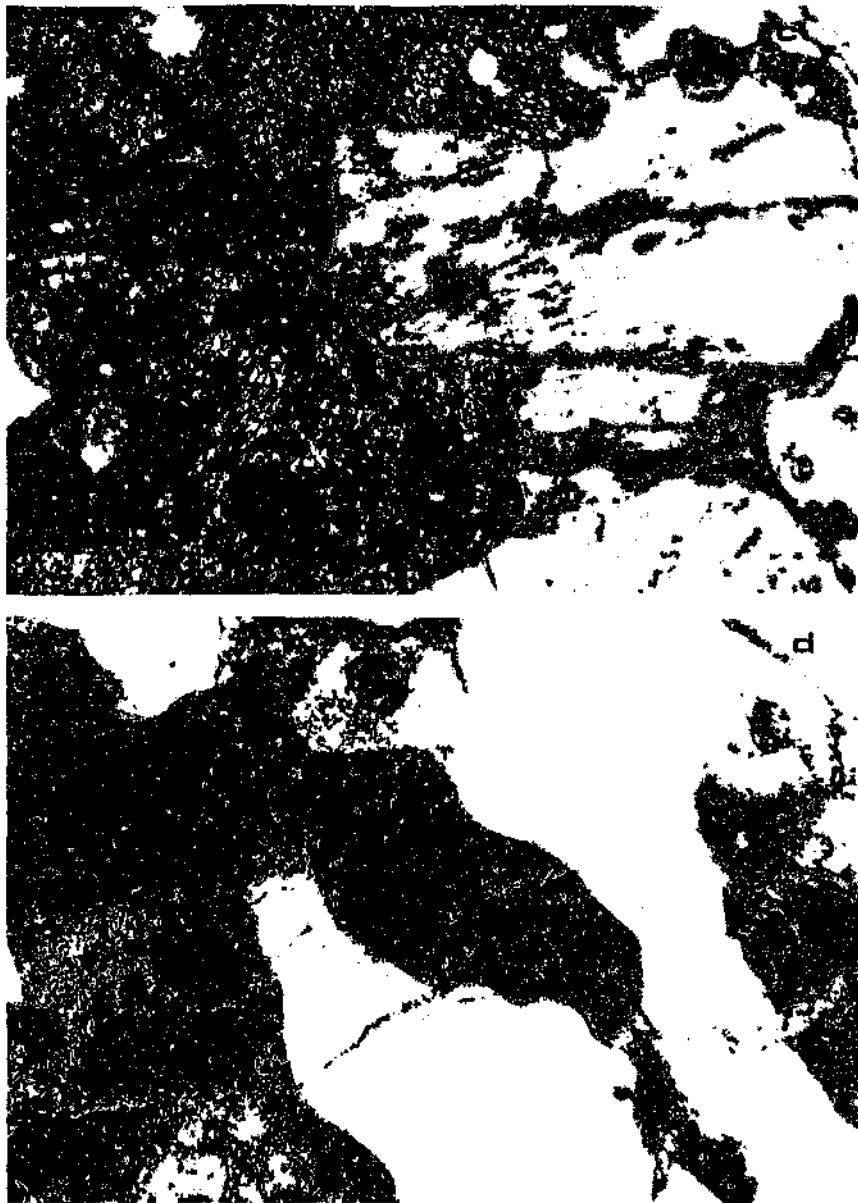


Figure 5.12 Photomicrographs of: (a) relatively unaltered basement gneiss (crossed-polarized light; field of view: 1.4x2.1 mm); (b) transition zone from fresh to palaeo-weathered basement (crossed-polarized light; field of view: 0.7x1.1 mm); (c) palaeo-weathered zone (crossed-polarized light; field of view: 1.4x2.1 mm); and (d) silicified basement (plain-polarized light; field of view 1.4x2.1 mm).

5.2.3 Chemistry

Nine samples were collected at approximately one metre vertical intervals at two profiles (three samples from each zone) to determine changes throughout the prominent palaeo-weathered basement occurrences in the study area. These data could then also be compared to modern weathering profiles of known origins and climatic settings. The results of these chemical analyses are tabulated in Appendix B. Percentages of selected oxides were plotted against height from the top of the silicified zone, that is, from the tops of the prominent mesas (Figures 5.13a-h).

SiO₂

With the exception of one point (Profile 2, 5 metres depth) Figure 5.13a shows that the silicified zone generally contains a greater percentage of silica (particularly at approximately one metre from the top) than the underlying palaeo-weathered zone, but similar amounts to the unaltered basement. It appears, therefore, that only a small increase in silica with respect to the underlying palaeo-weathered rock was sufficient to preserve these flat-topped features. Although externally derived silica may have been introduced into the weathering mantle, estimates of absolute element gains and losses during the formation of silcrete and the palaeo-weathered basement indicate that sufficient silica could have been mobilised by the decomposition of the thickness of bedrock represented by the existing profiles.

TiO₂

From Figure 5.13b it is obvious that all the titanium values, with the exception of one (Profile 2, 4 metres depth), have fairly similar values. The mobilization of titanium in the formation of the silicified zone does not appear to have been a major process.

Al₂O₃

No major changes in the aluminium concentrations are obvious in Figure 5.13c. The

mobility of aluminium in most silcrete forming environments prevents its conventional use as a reference element to assess absolute gains and losses of other elements during the silicification process (Summerfield, 1983c).

Fe₂O₃

The increase in concentration of iron near the base of the palaeo-weathered zone suggests that iron has been leached from the overlying rocks into the lower part of the profile (Figure 5.13d). In the one case (Profile 1) there is also a slight increase in concentration of Fe at the base of the silicified zone.

MnO

A similar pattern to that observed for iron may be seen for manganese in one of the profiles (Profile 2, Figure 5.13e). This is attributed to leaching from the overlying rocks which are depleted in manganese. The other profile (Profile 1) has not been affected by leaching to the same extent as Profile 2, and shows relatively constant values throughout the profile.

MgO

Magnesium in Profile 1 shows an overall increase from the basement to the top of the palaeo-weathered zone (Figure 5.13f), after which it decreases with height to the top of the profile. Profile 2 shows no distinct pattern below the silicified zone, but, also decreases in MgO with height after the silicified zone contact. Therefore, with the exception of a slight increase towards the top of the palaeo-weathered zone and a decrease through the silicified zone no major changes are obvious for this oxide.

CaO

Calcium, with the exception of one point (top of Profile 2), shows an overall decrease with height (Figure 5.13g), suggesting that calcium was leached from the entire weathered profile and perhaps partly deposited at the contact between the basement and palaeo-weathered zone. Due to the presence of illite in the palaeo-weathered and silicified zones, calcium may have, rather, been removed from the plagioclase, during the formation of illite.

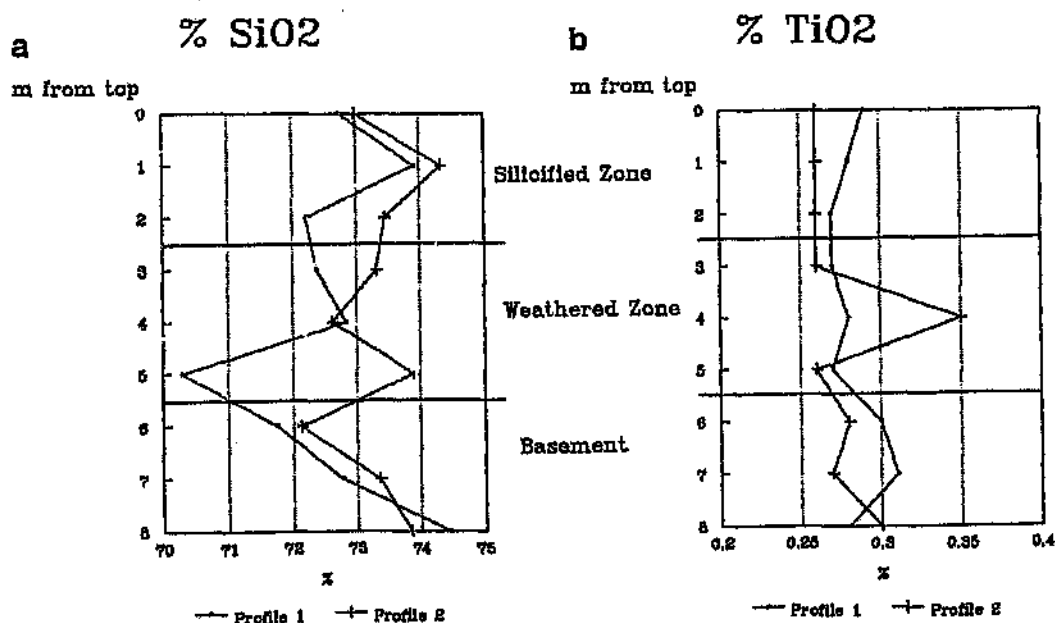
Profile 1 shows relatively low values throughout, suggesting that the original unaltered basement had a low calcium content to begin with. The slight increase at the top of Profile 1 may be the result of a secondary surface deposit, such as calcrete concentrations in joints and other fractures.

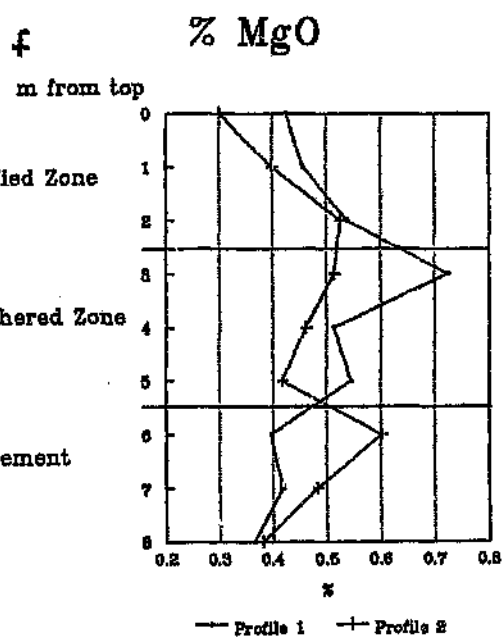
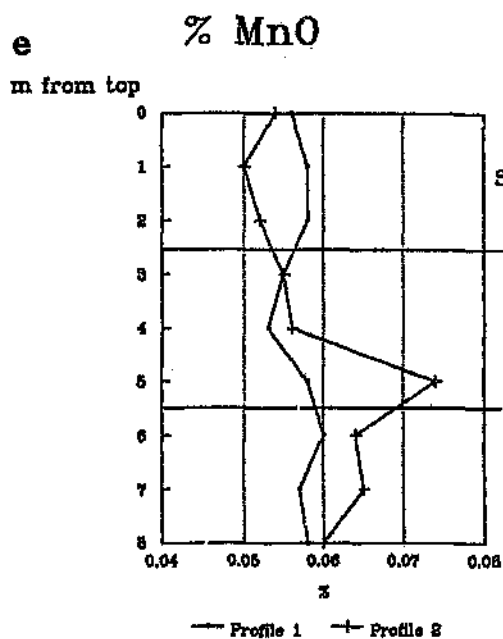
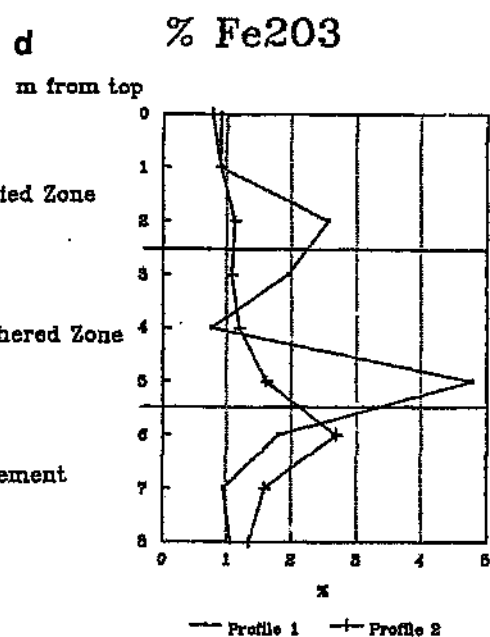
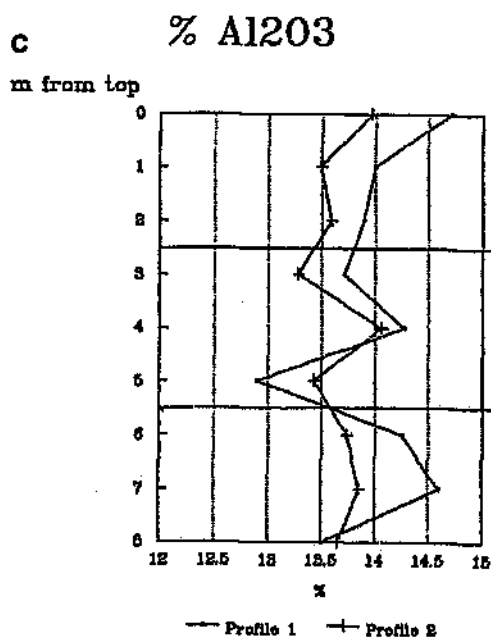
K_2O

Potassium is slightly enriched between 4 and 6 metres depth (Figure 5.13h). This depth corresponds approximately with the base of the palaeo-weathered zone, and is probably due to the presence of illite (some kaolinite and smectite were also found to be present using XRD analysis), or the removal of potassium in the overlying part of the palaeo-weathering profile. However, potassium is most probably concentrated in the lower parts due to the conversion of feldspar to illite.

Na_2O

Sodium (Figure 5.13i), generally decreases with height. Profile 2 shows a particularly sharp change and decrease in sodium concentration at the approximate basement - palaeo-weathered zone boundary, suggesting that sodium was most probably removed from the feldspars by solution during the palaeo-weathering process.





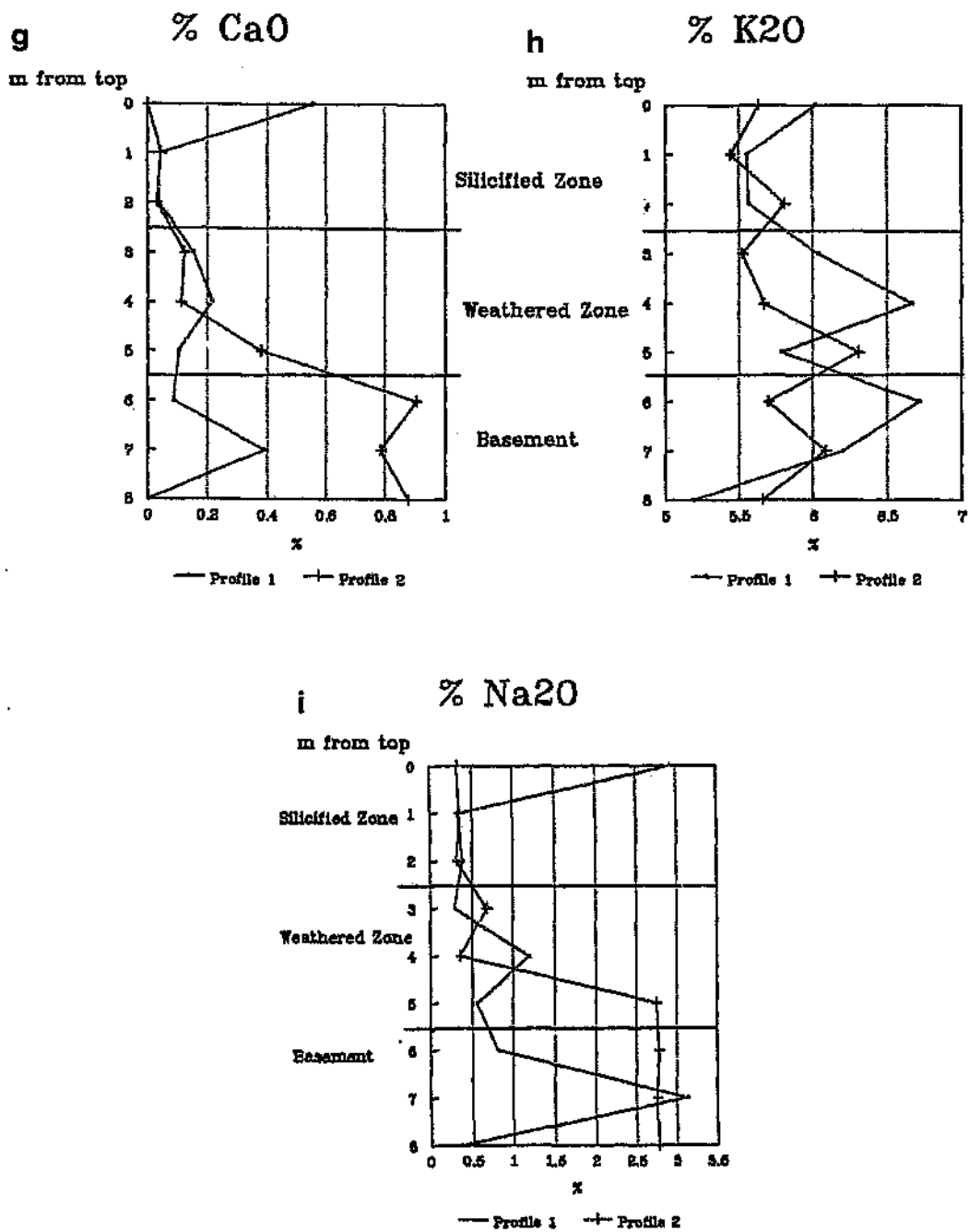


Figure 5.13 Percentages of oxides plotted against height from the top of the silicified zone, for: (a) SiO_2 ; (b) TiO_2 ; (c) Al_2O_3 ; (d) Fe_2O_3 ; (e) MnO ; (f) MgO (g) CaO ; (h) K_2O ; and (i) Na_2O .

SiO₂ - TiO₂ - Fe₂O₃ ternary plot (the silicified zone)

Summerfield differentiated weathering profile and non-weathering profile types on the basis of titanium (anatase) content using major element bulk chemical analyses. The former types are titanium-rich (TiO₂ > 1.0%) and have a composition similar to the global mean, whereas the latter types are, by comparison, titanium poor (TiO₂ < 0.2%).

Data for the six silicified zone samples were plotted on the ternary plot of Summerfield (1983c) which he uses to distinguish silcretes formed in association with weathering profiles and those that are not (Figure 5.14). Four of the six data points fall into or close to the field of non-weathering profile silcretes, however, two points, with low TiO₂ and SiO₂ < 98% lie outside both of the fields. These results show that the silicified rocks of the study area could not be classified using this method. According to Summerfield (1983c) titanium abundances appear to be related to host material chemistry in addition to the environment during the silcrete genesis, that is, the host material chemistry of the studied rocks may be the reason for these nonconformal results.

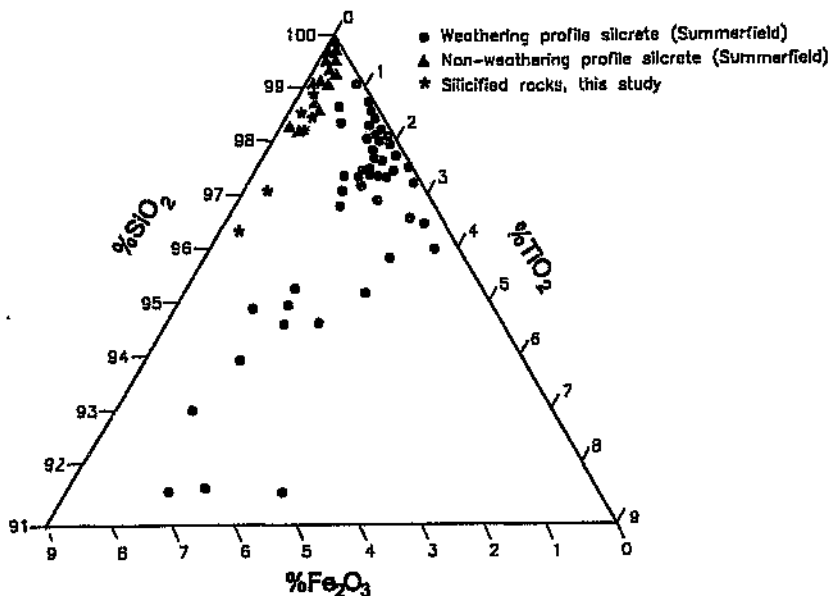


Figure 5.14 SiO₂ - TiO₂ - Fe₂O₃ ternary plot for six silicified zone samples and data of Summerfield (1983c), used to distinguish weathering and non-weathering silcretes.

Chemical Index of Alteration (CIA)

The CIA values, as described in Section 5.1.3, are used here to confirm the extent of alteration, as indicated by the gross morphology and the petrographic results, for the palaeo-weathered and silicified basement occurrences. Figure 5.15 shows the CIA values for the samples from the three zones for the two selected profiles.

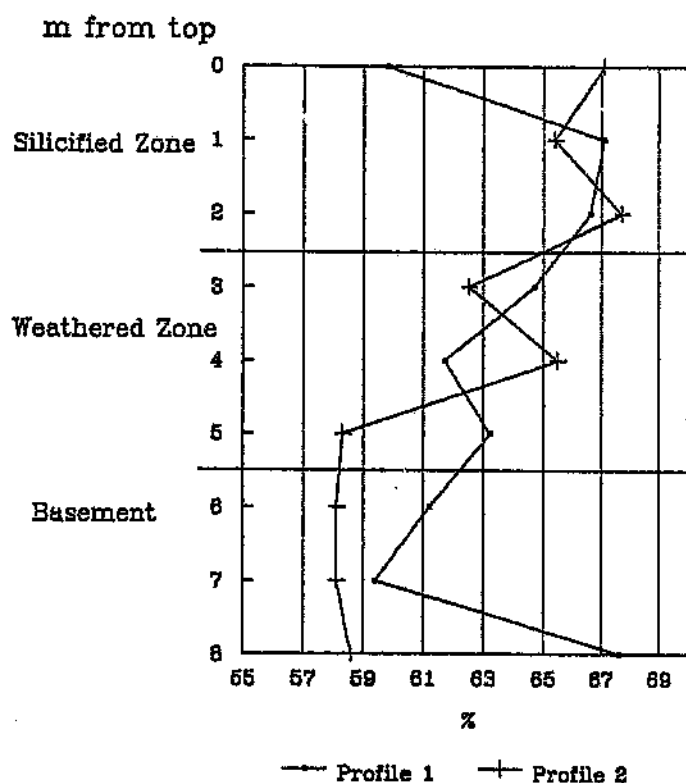


Figure 5.15 Plot of CIA values for selected palaeo-weathered basement samples versus height.

Figure 5.15 shows an obvious trend (except for two values in Profile 1: top and bottom) from lower values in the relatively fresh basement to progressively higher values in the

silicified zone. These values also show that the alteration is fairly subtle with increasing height from the basement, and that even the basement is altered to some degree, with values for the granitoids plotting a little higher than the typical 45 - 55% range for granitoids (Nesbitt and Young, 1982).

The CIA values for the palaeo-weathered basement underlying the Vaalputs Formation, obtained from drillcores, generally yield slightly higher CIA values (ranging between 71.0 and 86.2%) than the exposed palaeo-weathered basement. Typical values for the suboutcrop is about 72% suggesting that the palaeo-weathered basement occurrences on the western part of Vaalputs and those from below the Vaalputs sediments have experienced similar degrees of weathering.

Al₂O₃ - CaO+Na₂O - K₂O ternary plot

Nesbitt and Young (1984) predicted weathering trends for a variety of igneous rocks using kinetic data for feldspar dissolution. The bulk composition of a average granite (large solid dot) and the calculated composition of the weathering solution (open dot) removed from non-weathered granite during the initial stages of weathering (Nesbitt and Young, 1984) are plotted in Figure 5.16. Mass balance restrictions require that the compositional trend of the weathered residues plot on a line emanating from the fresh rock, and directed away from the solution composition. The arrow on the mid-section of this line illustrates the predicted residual weathering trend for average granite. Once the trend approaches the Al₂O₃-K₂O line, it is redirected toward the Al₂O₃ apex; apparently, incongruent dissolution of the potassic phases releases K to solution in preference to Al resulting in a trend toward the Al₂O₃ apex (Nesbitt and Young, 1989). Granite was plotted as it was found to have a similar bulk chemical composition to the basement granitoids encountered at Vaalputs. Bulk compositions of samples taken from two palaeo-weathering profiles (Profiles 1 and 2), as well as three samples of the palaeo-weathered basement underlying the Vaalputs Formation, are also plotted on Figure 5.16.

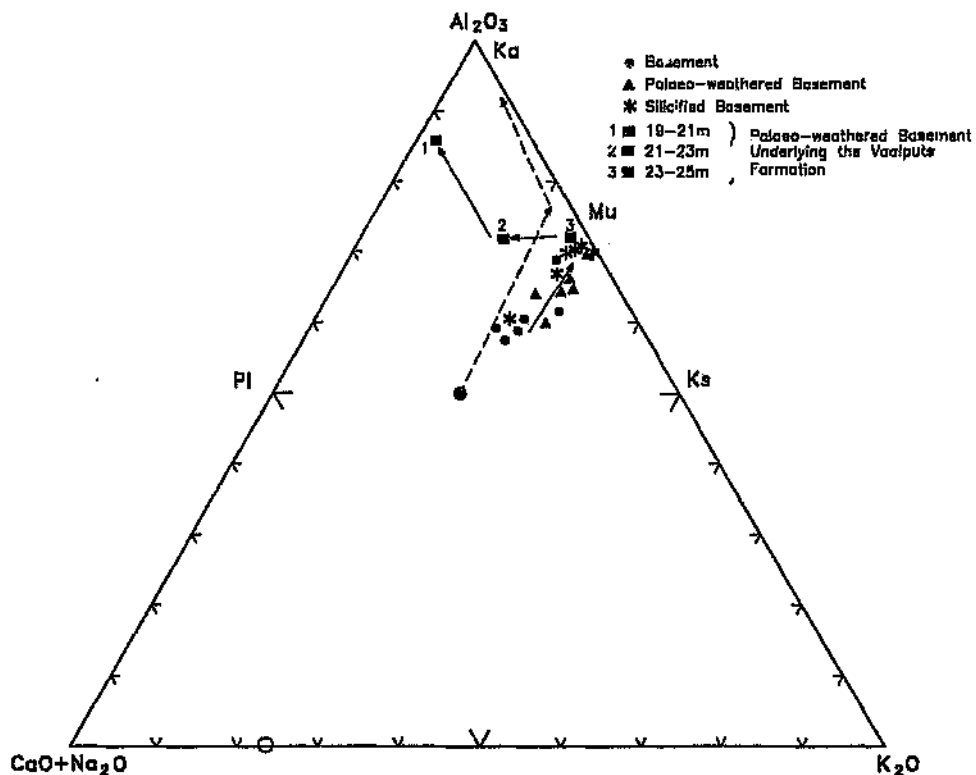


Figure 5.16 Calculated and actual weathering trends of selected profiles in the palaeo-weathered basement occurrences. Pl = plagioclase; Ks = alkali feldspar; Mu = muscovite; Ka = kaolinite. The large solid dot represents average granite of Nesbitt and Young (1984) and the large open dot, on the base line, the calculated proportions of Ca, Na, and K in leachates (derived from granite). The arrow on the lower dashed line shows the calculated initial trends followed by the leachates during the initial weathering stages; the upper dashed line was calculated from observed bulk compositional trends (Nesbitt and Young, 1989). The other trends are palaeo-weathering trends of this study.

The trends for the basement occurrences (western outcrops) mirror the trends of granite as determined by Nesbitt and Young (1989). The small differences may be attributed to heterogeneity in the original composition of the Vaalputs basement rocks. The samples used in this study have also not undergone the same degree of weathering as that of the

predicted trend (Figure 5.16). The suboutcrop palaeo-weathered samples (underlying the Vaalputs sediments) give a somewhat different result. The two lower most (and least weathered) samples have similar compositions to that expected for granite except that the trend in this case, reflects a decrease in K_2O a little before that of the predicted trend (Figure 5.16). This is most probably due to the higher than expected CaO values in these samples (see Appendix B).

Lovering (1959) showed that the Mazaruni Granite of British Guiana, located in a very high rainfall region shows that calcium and sodium are extracted from the granite in preference to potassium. The weathering trend of fresh granite, calculated from kinetic data (Nesbitt and Young, 1984) conforms closely to the observed bulk composition trend of the Mazaruni Granite, as does the initial part of the trend for this study. According to Nesbitt and Young (1989) the trends obtained can be used as templates against which the chemical history of ancient profiles can be read. Singer (1980) and Nesbitt and Young (1984) discuss the effects of climate on weathering profiles and suggest that the extent of weathering is determined primarily by the amounts of acids introduced into the profile by rainfall derived solutions. The Mazaruni weathering profile trend, which shows a similar trend to the initial part of the weathering profile trends obtained for this study, formed under tropical conditions where rainfall is 250-375 cm/year. However, Nesbitt and Young (1989) conclude that climate does not have a significant effect on weathering trends within the compositional space represented by Figure 5.16, and that these trends are rather primarily controlled by the bulk compositions of the parent rocks.

Normative chemical calculations, using the data in Appendix B, indicate that kaolinite is the predominant clay mineral and that even the "unaltered basement" contains a significant proportion of clay (Table 5.2). These results also suggest that most of the kaolinite is derived from Na-feldspar, and that only a small increase in silica has given rise to the resistant caprock of these landforms.

Table 5.2 Normative chemical compositions for the major minerals of the basement, and the silicified and weathered zones.

	Quartz (%)	K-feldspar (%)	Na-feldspar (%)	Kaolinite (%)
Silicified Zone	38.1	32.5	13.6	12.4
Weathered Zone	35.2	33.7	13.8	13.4
Basement	31.3	33.5	26.3	6.3

5.2.4 Discussion

Silcrete is an indurated product of surficial and near surface silicification, formed by the cementation and/or replacement of bedrock, weathering products, unconsolidated sediments, soil or other materials, and produced by low temperature physical and chemical processes (Goudie, 1973; Grant and Aitchison, 1970; Lamplugh, 1902, 1907; Summerfield, 1978). The various forms of secondary silica include opal, cryptocrystalline quartz or well-crystallised quartz (Milnes and Thiry, 1992). According to Nash et al. (1994) the prerequisites for the formation of silcrete are: a source of silica; the availability of moisture to act as a transporting agent; and a mechanism to cause precipitation

Ollier (1991) noted two environments: one where silica is made available by solution and another where it is precipitated. Wopfner (1978) envisaged two types of silcretes: quartz-microquartz silcretes associated with kaolinized profiles which form in acid groundwater environments in areas of subdued relief with poor drainage; and opal silcretes which form under alkaline hypersaline conditions associated with shorelines of palaeo-lakes. Twidale and Milnes (1983) postulated acid weathering conditions near the margins of basins, where clay minerals are degraded and produce silica-enriched solutions, and which are considered to move laterally as soil water or groundwater to sites in lower reaches of the basin where conditions are appropriate for silica precipitation. According to Milnes and Thiry (1992) supergene conditions are usually implied, particularly processes above the phreatic zone or in environments associated with soil formation. According to Summerfield (1983c), as silcretes may grade into some other duricrust type, it cannot be precisely characterized by its bulk chemical composition, although a minimum content of 85 weight percent SiO_2 provides an arbitrary lower limit. The "silcretes" of the study area do not meet

this requirement and are only slightly enriched in silica with respect to the original host rock. They are therefore referred to as silicified rocks rather than silcretes.

There is little published information on profile variation in the chemical composition of silcretes and weathering deposits, and, analyses from a number of profiles in southern Africa indicate no simple systematic variation in element abundance within silcrete horizons (Summerfield, 1978). In addition, the silcrete mineralogy reflects the host material characteristics and the effects of chemical breakdown and dissolution, as well as the conditions under which the authigenic mineral component was formed. Although silcretes are undoubtedly of palaeo-environmental significance, the conditions under which they have formed is controversial. Shaw and Nash (1997), demonstrated, in a study of recent silcretes in the distal reaches of the Okavango delta fan, Botswana, that it is difficult, if not impossible to specify the precise chemical environments of silcrete formation, and that several processes may work together during silcrete formation.

Petrographical results

Summerfield (1981) recognised two silcrete types: that which occurs primarily as a caprock on flat-topped erosion remnants and those forming horizons within weathering profiles. Using southern African silcretes Summerfield (1983a) differentiated these two silcrete types (non-weathering profile and weathering profile silcrete) by their distinctive petrographic and geochemical characteristics (Table 5.3). Although the silicified zones of the study area are not true silcretes, the criteria used by Summerfield (1983a) for distinguishing non-weathering and weathering silcretes was found to be applicable, to some degree, to the Cretaceous weathered basement occurrences of the Vaalputs region. Based purely on field observations the "silcrete" in the study area appears to be of the latter type, due to the presence of a weathered unit overlain by a thick silicified cap-rock.

The silicified zone displays an F-fabric, which is the most common type of fabric in silcretes (Summerfield, 1983c). According to Summerfield (1983c) F-fabric silcretes may be formed by displacement or partial replacement of skeletal grains or by silicification of an existing F-fabric host material. "Silcretes" of the Vaalputs region display characteristics of replacement of a pre-existing F-fabric host material and dissolution of skeletal quartz grains

resulting in embayments at the grain margins. Summerfield (1979) also suggests that most of the dissolution, if not all, must pre-date silicification. Summerfield noted that embayed skeletal grains in southern Africa silcretes usually seem to have been inherited from host materials, such as weathering deposits, in which there is abundant evidence of quartz grain dissolution.

Table 5.3 Petrographic and chemical criteria used for distinguishing weathering and non-weathering profile silcretes (Summerfield, 1983a).

	Non-weathering profile silcrete	Weathering profile silcrete
<i>Host materials</i>	large variety	single (variety of bedrock)
<i>Common fabric types</i>	F-(floating) fabric	F-(floating) fabric M-(matrix) fabric
<i>Other fabrics</i>	GS-(grain supported) fabric M-(matrix) fabric	-
<i>Silica matrix type</i>	mega-quartz, chalcedony, micro-quartz and crypto-crystalline silica	crystalline quartz and crypto-crystalline silica
<i>Titanium content</i>	Ti-poor	Ti-rich and composition similar to the global mean
<i>Diagnostic petrographic characteristics</i>	Chalcedony vugh fills	authigenic glaeboles and colloform features

According to Summerfield (1983c) a clay matrix tends to favour the formation of opaline and cryptocrystalline silica or microquartz rather than chalcedony which tends to replace carbonates. Thin sections of the silicified zone, and to a lesser extent the palaeo-weathered zone, exhibited significant cryptocrystalline silica as the intergranular material. Also, the matrix has a turbid appearance, which was noted by Summerfield (1983c) to be present in the matrix of silcretes, in the form of sesquioxides.

Based on the petrological observations, the silicified cap-rocks of the Vaalputs region may be classified as *weathering profile silcretes*, that is, they are formed in a single host material, they have a F-fabric, their matrix is of a crypto-crystalline silica type and they are

authigenic in nature (Table 5.3).

According to Büdel (1982) the formation of silcrete at depth under humid conditions and decomposition ("grus development") is the most widespread form of humid-tropical chemical decomposition, in which the dark components and feldspars in crystalline rock are altered into various grades of clay minerals, while the quartz grains remain preserved. During this type of alteration the joint systems and other structures in the rock may be preserved. Bremer (1967) suggests that the development of silcrete or silicified basement requires a humid (fully tropical) climate in areas of "very flat relief with little epeirogenic activity and constant climate".

Chemical results

Chemically silcretes are comparatively simple materials, and should be highly siliceous ($> 95\% \text{ SiO}_2$), with only aluminium, iron and titanium present in significant amounts (Summerfield, 1983c). This is not the case of the silicified zone in the study area, as they are only slightly silicified and as mentioned before, are not true silcretes. According to Summerfield (1983a), evidence for prevailing pH conditions during formation of weathering profile silcretes is provided by the apparent behaviour of titanium. Absolute enrichment of TiO_2 with respect to bedrock in both silcrete and the associated weathered material is indicated by absolute elemental gain-loss calculations (Summerfield, 1983b). Below a pH of approximately 3.75 titanium becomes significantly mobile in weathering environments (Baes and Mesmer, 1976). Between a pH of 2 and 4.7-6.7 titanium hydroxyl complexes tend to be absorbed onto quartz because over this pH range silica and titanium surfaces have opposite charges (Watts, 1977). This suggests that weathering profile silcrete development occurred in an environment in which the pH was approximately 4. Summerfield (1983a) observed the replacement of weathering profile clays (predominantly kaolinite and illite), using petrographic and geochemical techniques. However, Summerfield (1986) argues that on their own, such relationships, which show only relative changes in element concentrations, do not indicate whether titanium has been mobilised and concentrated in association with silcrete formation or whether the relative concentration increase is attributed to the removal of other components. Summerfield suggests that the southern African weathering profile silcretes show evidence that their

high titanium concentrations have resulted from absolute accumulation of titanium in association with silcrete formation. One line of evidence is the expected volume reduction during bedrock weathering and silcrete development that would be required to explain the high concentrations of titanium if this had been achieved by the removal of other components (Summerfield, 1986). In the examined exposures there is no evidence, in the form of bedrock structures, for isovolumetric weathering and silcrete formation (Summerfield, 1983b; 1984). In addition, as the rocks of this study are not true silcretes, but merely silicified, the diagnostic features observed by Summerfield may not be as obvious as was expected.

Summerfield's (1983a) proposed two models for silcrete formation involving predominantly vertical movements of silica: *per ascensum* mechanisms of capillary rise and evaporation of a silica saturated solution, at or near the surface and associated with groundwater and water-table fluctuations; and the *per descensum* mechanism or downward percolation of silica-charged waters. A problem with the *per ascensum* model is accounting for relatively thick (more than a few centimetres) silcrete horizons. The *per descensum* or downward percolation models provide a more viable explanation for the thick silicified occurrences observed at Vaalputs. The silicified horizons most probably formed below surface within the pallid zone of the lateritic profile. Weathering towards the top of the profile released silica which was leached downwards and then precipitated. The downward percolation of silica released through bedrock weathering and clay mineral authigenesis, together with water-table fluctuations, according to Summerfield (1983a), appears to be the most likely mechanism for the formation of silcretes associated with weathering profiles in southern Africa. This Summerfield attributes to the occurrence of silcrete horizons within kaolinitic/illitic clay weathering profiles. The small increase in silica observed in the palaeo-weathered profiles, suggests that pHs were low and that silica was concentrated in this region during a wetter period. The existence of horizontal silicified horizons within the weathering profiles suggests some water-table control over pH fluctuations and silica precipitation. Although limited seasonal water-table movements may have occurred, a prolonged dry season, as suggested by Frankel and Kent (1938), Smale (1973) and others as a prerequisite for a capillary rise mechanism of silcrete formation is not considered likely. This Summerfield (1983a) attributes to the fact that many silcretes in the Cape

coastal zone are found at considerable depths in the weathering profiles and are only thin surface crusts, rather than the typical silcrete thicknesses observed. Thick silcrete could not form in this way as initial silica precipitation at the surface would inhibit further capillary rise to the surface. The observations of the palaeo-weathered occurrences are suggestive of alteration probably close to a phreatic surface which corresponded at the time to the active weathering front.

The major element chemistry of this study, with the exception of TiO_2 , shows typical characteristics of a weathering profile, for example, the removal of Na, K and Ca from the upper parts of the weathering profile and a marked concentration of these oxides in the lower parts of the profile; the Chemical Index of Alteration for both profiles are typical of a weathering profile formed in humid conditions; the Al_2O_3 -CaO+Na₂O-K₂O ternary plot of the studied profiles conform reasonably well with predicted weathering trends of Nesbitt and Young (1984), as well as with trends of recent profiles formed under humid conditions. Normative chemical calculations of this study indicate that the predominant clay mineral in the palaeo-weathered basement occurrences is kaolinite and that only subtle changes in the mineralogy (as indicated in Table 5.2) have resulted in these landforms.

CIA values suggest that the palaeo-weathered basement at the base of the Vaalputs sediments are in a more advanced state of alteration, and probably formed contemporaneously with the palaeo-weathered basement on the western parts of Vaalputs. Subsequent weathering of the basement may have also resulted from ground water accumulation at the base of the Vaalputs sediments. Ground water is commonly bound by bedrock below basin sediments (Toth, 1962). Clay particles eluviated from the overlying Vaalputs sediments may accumulate at the base of the Vaalputs sediments which would also give rise to an increased concentration of weathering products in these palaeo-weathered basement occurrences.

Morphology of the palaeo-weathered landsurface

According to Twidale et al. (1970) and Grandin and Thiry (1983) silcretes have important associations with palaeosurfaces and must require very stable geomorphic and geologic conditions to achieve the extent of silicification and the observed relationship with

palaeosurfaces. Silcrete (duricrusts in general) formed by fluvial processes can involve deposition within channels or valleys, deposition from sheetfloods, and/or lateral seepage of groundwater and throughflow water (Goudie, 1983). According to Nash et al. (1994), valleys, like pans, are a potentially important site for the development of duricrusts as water tables are generally elevated in the vicinity of depressions. As noted by Nash et al. (1994), in a study on the Kalahari valley streams, a lack of consistent stratigraphy through a region (as observed in the study area, where the palaeo-weathered basement is restricted to certain areas) may suggest that the duricrusts develop as a direct result of processes related to the presence of a valley (or depression). Movements of water towards the valley over long time periods may also alter pre-existing duricrusts or other host material. In addition the development of any linear depression would influence flowpaths of groundwater and throughflow. The linear distribution of the studied duricrusts (Figure 5.10) is suggestive of a palaeo-drainage pattern, however, Partridge and Maud (1987) showed that this surface was extensive over southern Africa. The linear distribution of these features is, therefore, more likely a consequence of subsequent tectonism in the region.

Thomas (1974) in an etch-surface model for tropical landscape development reports that areas of metamorphic rocks such as biotite schists and amphibolites commonly carry a thick duricrust which protects the underlying clays from erosion. Thomas (1974) noted that duricrusts generally form areas of higher relief and may rise above more 'resistant' rocks such as granite or acid gneiss. According to Wayland (1947) the onset of denudation or the stripping process may be induced by tectonism. This is believed to have been responsible for the incised areas of the study area, which correlate well with faults and lineaments of the region, as will be discussed later. An additional process believed to be responsible for the observed landforms is that of removal of material by solution from the underlying pallid zone (Trendall, 1962). This process not only forms a major component of mineral loss in rocks, but also a major part of the total denudation. Evidence of this process is seen in the form of caves in the palaeo-weathered zone, that directly underlies the more resistant silicified basement.

Summerfield (1983c) noted that in South Africa columnar jointing appears to be associated with weathering profiles and that these may develop in response to the desiccation of a

hydrated siliceous matrix formed during initial silicification, though post-formational weathering may also be significant. The parallel slope retreat observed on these palaeo-weathered occurrences is controlled by the rate of undercutting and weathering of the silicified cap-rock. Where the silicified cappings are finally removed, the underlying weathered material suffers more rapid erosion. This indicates the important preservative role that silicified rocks may play where they overlie less resistant materials, in this case the palaeo-weathered basement. These silicified surfaces would therefore remain in the landscape for very long periods, initially forming non-dissected surfaces and subsequently as silicified cap-rock residuals lying at higher elevations than younger land surfaces.

Age of the palaeo-weathered occurrences

The dating of phases of weathering and silcrete formation, even approximately, poses difficulties (Summerfield, 1983a) and therefore direct dating of the palaeo-weathered basement occurrences was not possible. The host material provides a maximum age, while the overlying sediments may give guidance on the minimum age. For the case at Vaalputs it can safely be assumed that alteration pre-dates the sediments of the overlying Vaalputs Formation. As the palaeo-weathering has affected the Dasedap sediments, the age of this weathering episode post-dates the Dasedap sediments which appear to have a maximum age of 60-70 Ma (e.g. Scholtz, 1985). Also, Partridge and Maud (1987) have confidently associated this alteration with the late-Cretaceous to early Tertiary. Callen (1983) concentrated on stratigraphic relationships and also concluded that silcrete formation was essentially an end-Cretaceous phenomenon. This together with the ages of the Dasedap sediments constrains the age of these altered occurrences to this period.

CHAPTER 6: THE VAALPUTS FORMATION

The Vaalputs Formation is preserved in a depression or the "Vaalputs Basin" on the inland side of the marginal scarp, in what has been referred to (e.g. Levin et al., 1986) as a channel like depression, cut into the sediments of the Dasdap Formation and gneisses of the Namaqualand Metamorphic Complex. Depressions on the inland side of the marginal scarp appear to be a fairly common feature of the Great Escarpment of Southwestern Africa. The five topographic profiles of Gilchrist et al. (1994) of the southwestern margin of southern Africa all exhibit this feature. It appears that only in some cases where these depressions (gralans) are well developed (and erosion and deposition is taking place) may sediments be deposited and preserved, such as in the case of the Vaalputs Formation.

Levin et al. (1986) suggested that during a period of Oligocene uplift, a palaeotributary of the Koa River, flowing to the northeast from the Dasdap area (approximately 30 kilometres south of Vaalputs) across Vaalputs, cut into the kaolinized surface, leaving a channel partly filled with alluvium (basement, Dasdap sediments, and transported kaolin). This, together with the regrading of the Dasdap sediments during the Miocene, they propose, led to the accumulation of the Vaalputs sediments. The Vaalputs sediments have been referred to by Brynard (1988) as "red clay" and classified as a "gritty to sandy clay to sandy clay-loam" using the textural classification of Hillel (1971). The previous workers suggested that pebble accumulations in the Vaalputs Formation are the result of the reworking of the Dasdap fan sediments by surface processes, including fluvial action and bioturbation.

Levin et al. (1986) noted that where the Dasdap Formation is absent the "red sandy gritty clay" lies directly on the kaolinized bedrock. Levin et al. (1986) also recognised three cycles of deposition, each followed by calcretization or silcretization. The lowermost grey sediments with large calcrete or silcrete nodules they interpreted as having formed under humid conditions, while the overlying brown sediments, with small calcrete nodules at the top, they suggest, points to increased aridification. The sediments are overlain by what they refer to as the present day calcrete layer underlying the less consolidated sediments

of the Gordonia Formation.

The Vaalputs sediments were investigated in this study to determine the sedimentary processes and tectonic controls responsible for their accumulation. In addition it was believed that a detailed analysis of the Vaalputs sediments would allow for a better understanding of the origin and characteristics of the overlying Gordonia Formation.

6.1 Field Occurrences

The exact extent of the Vaalputs Formation is unknown as it is covered by the overlying aeolian sands of the Gordonia Formation. The suggested, approximate limit of suboutcrop, for these sediments is, however, shown in Figure 6.1 (as determined from TM-5 Landsat imagery and field observations). The aerial extent is somewhat different to that suggested by other workers (e.g. Andreoli et al., 1987 and McCarthy et al., 1985) who interpret the Vaalputs Formation as an alluvial fan with a source area to the south of Vaalputs. The Vaalputs sediments appear to be more extensive than was previously thought to be the case, extending further south, and may include areas previously identified as belonging only to the Dasdap Formation. The Vaalputs sediments are a lot thinner (few metres) and less developed in the southern parts of the study area. The Vaalputs Formation sediments do not outcrop. However, exposures of the sediments were available for study in trenches excavated for the disposal of low and intermediate level radioactive waste. Figure 6.2a shows the location and orientation of the two waste disposal trenches in which most of the study of the Vaalputs Formation was carried out. Figure 6.2b is a northwest - southeast section through the site, showing the portion of the Vaalputs sediments analyzed in this study. Numerous percussion drill cores of the sediments are available, but, the nature of these is such that they do not allow for the recognition of sedimentary structures or contact relationships. They usually only supply lithological and some stratigraphical information. Consequently, the faces offered by the two waste disposal trenches were primarily used for this study.

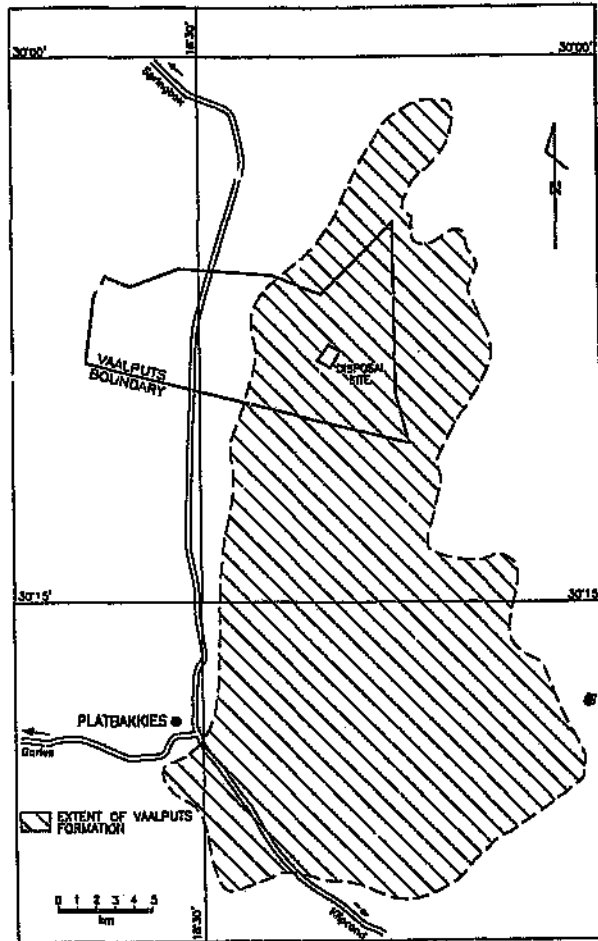


Figure 6.1 Approximate suboutcrop boundary for the Vaalputs sediments compiled from TM-5 Landsat data and geological maps of Andersen (1992) and Andreoli et al. (1986).

6.2 Facies Identification and Descriptions

The Vaalputs sediments are comprised of several facies, each of which exhibits distinctive characteristics. The facies identified at Vaalputs (from drill cores and trench sections) are: the lower white clay facies, the pebbly clay facies, the gritty clay facies, and several interspersed red sand and calcrete horizons. Due to the lack of palaeontological data, and often palaeocurrent directions and sedimentary structure, lithology was the most important feature in defining the facies types of the Vaalputs sediments.

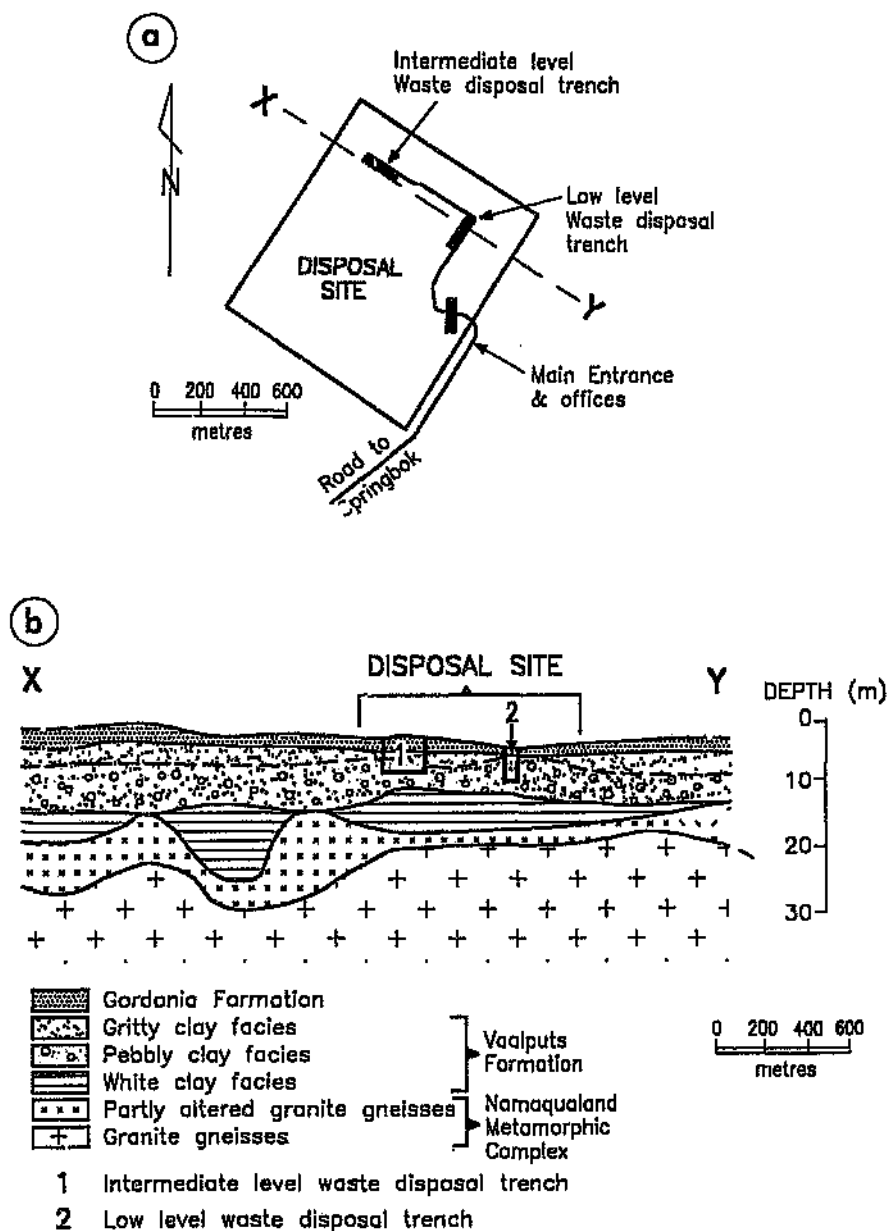


Figure 6.2 (a) Location of the two waste disposal trenches at the disposal site (see previous figure). (b) Northwest-southeast section through the Vaalputs sediments and waste disposal trenches. Also indicated are the facies encountered in these trenches. Sediment thicknesses and depths to basement were obtained from Jamieson (1986).

The main facies types believed to constitute the Vaalputs Formation are described below. A simplified, typical stratigraphic column (Figure 6.3) showing these facies was obtained from exposures of the intermediate-level waste disposal trench (Figure 6.2) and drill-core data.

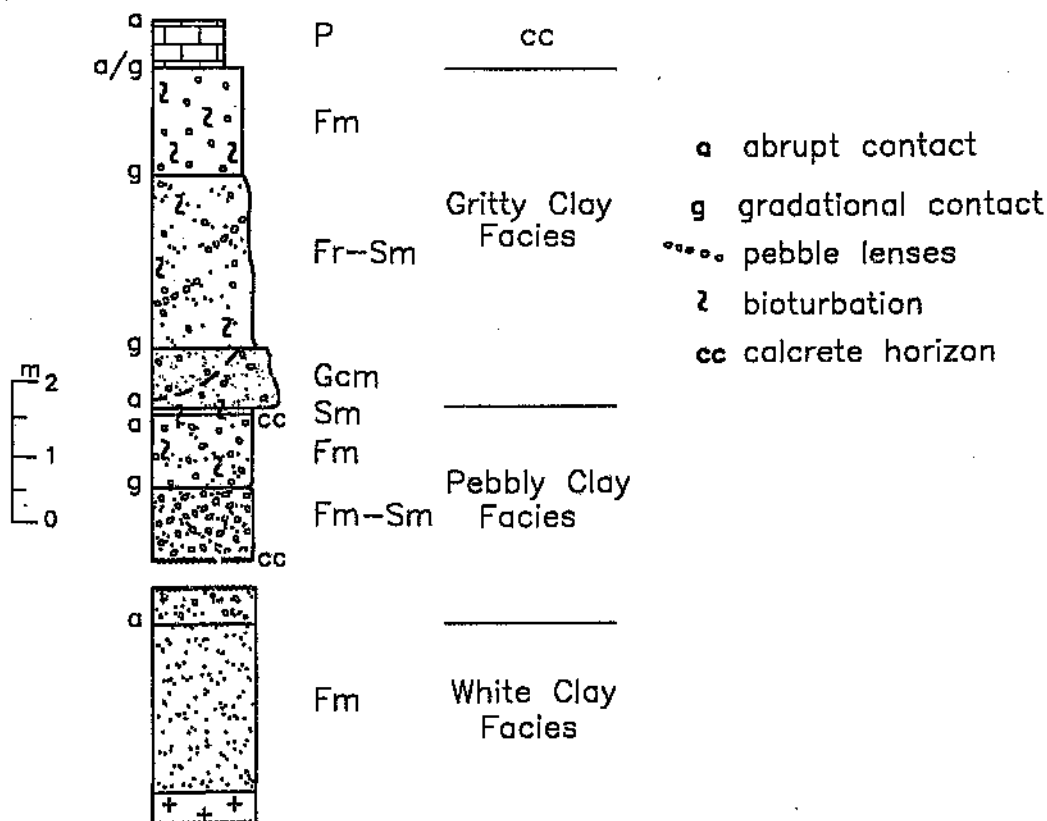


Figure 6.3 Generalized stratigraphic column of the Vaalputs Formation.

6.2.1 The White Clay Facies

Description

This lowermost, massive facies is laterally extensive and overlies the basement (Figure 6.2). It is typically 5 metres in thickness, but was noted to be as thick as 15 metres or absent in places (Jamieson, 1986). The lower contact, with the underlying weathered

granite gneisses is gradational, through depths exceeding 10 metres. The upper contact (Figure 6.3) is fairly sharp, with minor mixing observed at this contact. It is not seen in section in the waste disposal trenches, but has been described from drillcores by Levin (1988). This white clay was noted to vary in composition from a gritty to sandy clay-loam, to a silty-loam, using the textural classification of Hillel (1971).

Petrology and mineralogy

The main constituents of this weathered product, in order of abundance, are: smectite; similar abundances of kaolinite and illite (Brynard, 1988), quartz and minor amounts of oxides (ilmenite predominantly). The quartz grains, comprising 10% or more of the clay-rich samples are generally angular to very angular, vary from very fine-grained to coarse-grained and tend to be comprised predominantly of a brown smoky quartz.

6.2.2 The Pebbly Clay Facies

Description

This predominantly massive, yellow-brown, clay dominated facies contains coarse to medium sand, with scattered pebbles and lenses of pebbly-gritty sediments, and is generally greater than 4 metres in thickness. According to estimates taken from Jamieson (1986) this unit may be as thick as 10 metres. The pebbly lenses are usually about 2 metres in length and 30 centimetres thick, and contain a large range of pebble sizes (coarse grit to pebbles up to 3 centimetres in diameter) which are sub-angular to sub-rounded in a matrix of sand, silt and clay (similar to the host sediments) (Figure 6.4). The pebbles are comprised of blue quartz, iron-oxide nodules, sandstone and jasper, in descending order of abundance. No obvious bedding planes were noted in these lenses, although the lenses themselves define a crude bedding. It must be emphasized that this facies is poorly sorted and that even the pebbly lenses are matrix supported, with the matrix consisting of sand and clay.

The lower contact of this facies, with the underlying white clay facies, is not exposed in the

trenches. The upper contact, with the overlying gritty clay facies, is sharp (Figure 6.5a). This contact, which is only exposed in the intermediate-level trench has an approximate dip of 10° to the east. Abundant calcretized root casts or rhizocretions which have been filled by iron-oxide rich sands, and disseminated calcrete define this contact, suggesting it represents a palaeo-surface (Figure 6.5b). The term rhizocretion describes the pedodiagenetic accumulations of mineral matter around roots, usually accompanied by cementation, and may occur during life or after death of plant roots (Klappa, 1991). A more detailed account of these features is given in Section 6.2.5.

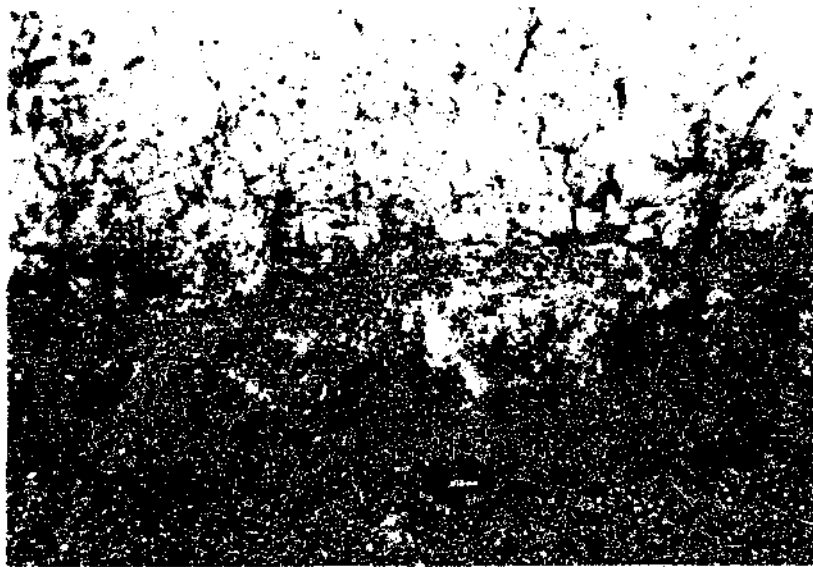


Figure 6.4 Coarse pebble lens in the pebbly clay facies.

No palaeocurrent direction measurements were possible due to the generally massive nature of these sediments. Two approximately 30 centimetre thick calcrete horizons occur in this facies, the positions of which are shown in Figure 6.3: a lower fairly continuous nodular calcrete horizon, and an upper discontinuous and disseminated calcrete horizon, containing rhizocretions and which marks the upper contact.

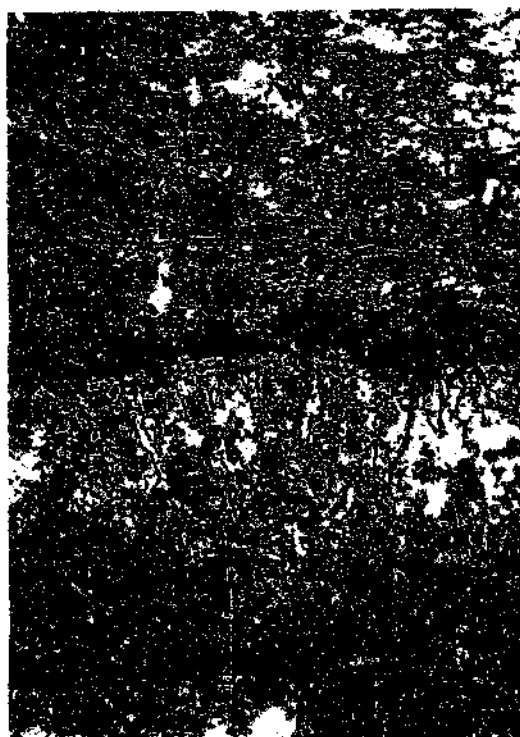


Figure 6.5 (a) Southern face of the intermediate-level waste disposal trench, showing the sharp contact between the lower pebbly clay facies and the gritty clay facies. (b) Close-up view of the contact showing the abundant root casts at this surface.

Petrology and mineralogy

This facies is comprised predominantly of fine-grained to coarse quartz fragments set in a silt to clay matrix (usually more than 10% of the sample; values as high as 75% but typically 30% were reported by Brynard, 1988). The clays consist predominantly of illite and kaolinite with subordinate smectite. Other clast types include feldspar (mostly altered; relic grains often difficult to recognise), rock fragments (usually iron oxide cemented) and minor amounts of biotite and oxides (magnetite and ilmenite). The grains in this facies range from rounded to subangular. The clasts are typically coated with an iron oxide. The high Fe content (see also section on chemistry) accounts for the yellow-brown colour of this sediment.

Grain size parameters

Grain size parameters are summarized in Table 6.1 below. A typical histogram for the grain size distribution of these sediments (excluding pebbly horizons) is shown in Figure 6.6. The coarse mean grain size, the poor sorting and the near symmetrical skewness values in Table 6.1 are clearly depicted in Figure 6.6, which is indicative of a sediment containing a large range of grain sizes. These values are also all in keeping with the observations described in the section above.

Table 6.1 Range of sedimentary parameters obtained for five samples of the pebbly clay facies.

Mean Grain Size (ϕ)	Standard Deviation (Sorting)	Skowness
0.98 - 1.29	1.32 - 1.53	-0.06 - 0.09

Sample No. VP-T2/1

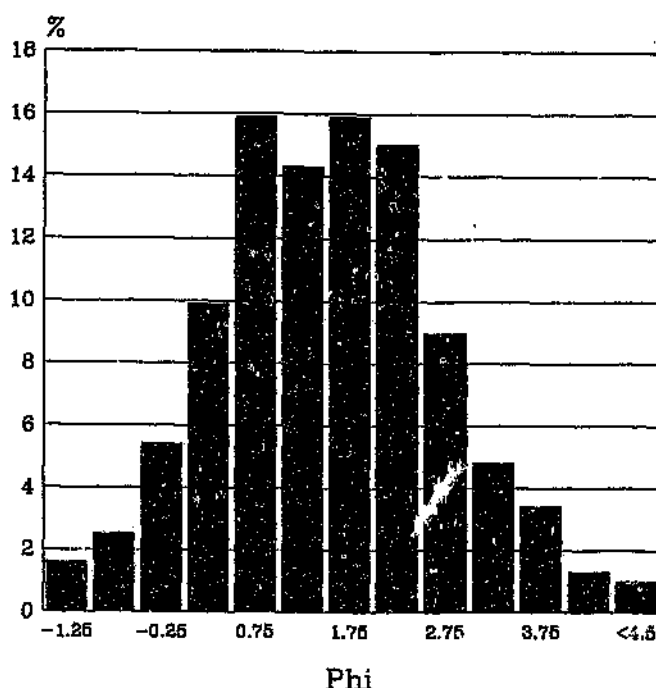


Figure 6.6 Typical grain size distribution for the pebbly clay facies.

6.2.3 The Gritty Clay Facies

Description

This olive-green to brown unit is typically 3 to 4 metres, but may be more than 6 metres, in thickness (Figure 6.3). The upper contact, with a calcrete horizon, may be either sharp or gradational, and is approximately horizontal. "Bio-activity" was observed throughout this facies, and includes calcretized rhizomes and termite nests (Figure 6.7). Also, commonly found throughout this unit are circular burrow-like features, up to two to three centimetres in diameter, filled by fine to medium red sand. These features are presumably younger than the host sediments. Fractures, infilled (partly or entirely) with calcrete, and extending several metres from the upper contact of this unit are common. As in the underlying pebbly

clay facies the clays consist predominantly of illite and kaolinite, with subordinate smectite (Brynard, 1988). Pebbly and gritty, poorly sorted lenses, typically 5 metres long and 0.5 metres thick, are found in this clay-rich facies. It should be noted that they are generally not as common as in the underlying pebbly clay facies. Pebbles in these lenses may be up to 5 centimetres in diameter, and consist mostly of blue and white quartz, with some altered basement gneiss and what appears to be Dwyka lithologies (altered mafic igneous and metamorphic rocks, granite gneisses and quartzite). Some iron oxide nodules and minor fresh feldspar fragments were noted. The main differences between this facies and the underlying facies are: colour; fewer pebble lenses; distinct recent bioturbation; and a slightly higher clay content.



Figure 6.7 Gritty clay facies with numerous rhizocretions and evidence of termite activity (note the red sand infill).

Petrology and mineralogy

In thin section this sediment consists of angular to subrounded clasts, consisting of a wide range of particle sizes (fine to coarse sands), and set in a fine-grained clay matrix constituting more than 10% of the sample. The clasts are comprised predominantly of quartz. Other clast types are: feldspar (highly altered), rock fragments (generally iron oxide cemented), and minor amounts of biotite and iron oxides (magnetite and ilmenite).

Grain size parameters

Grain size distributions of two samples for this facies (one from the low-level and the other from the intermediate-level waste disposal trench) are shown as histograms in Figure 6.8. The two samples exhibit similar grain size distributions. The sample from the intermediate-level trench, however, contains a greater fine fraction, resulting in a shift to the right (negatively skewed). The two histograms are also believed to represent the possible range of variability of the sediments within the facies. The range of values obtained for this facies are tabulated in Table 6.2.

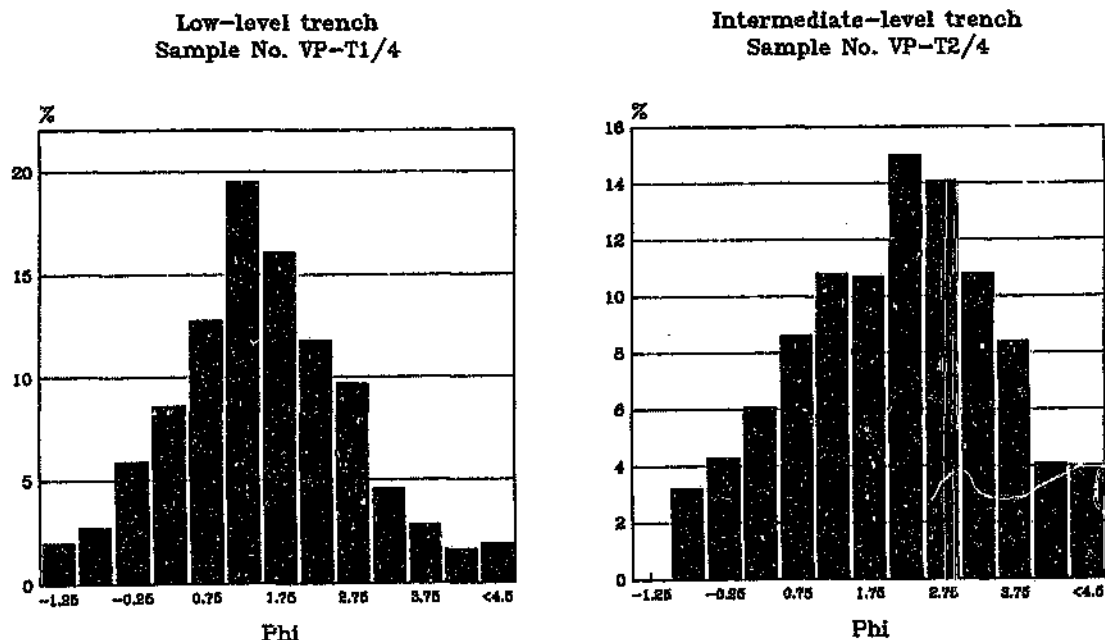


Figure 6.8 Typical grain size distributions for the gritty clay facies.

Table 6.2 Range of sedimentary parameters obtained for three samples of the gritty clay facies.

Mean Grain Size (ϕ)	Standard Deviation (Sorting)	Skewness
0.93 - 1.92	1.30 - 1.52	-0.06 - 0.05

6.2.4 Red Sands

Description

Red sands were found to be locally developed at various positions in the stratigraphy of the Vaalputs sediments. They occur as horizons or infillings of cavities related to bioturbation within the two previously described facies. As previously discussed, horizons of red sands, such as that overlying the pebbly clay facies, occur on what must have been a palaeo-landsurface. These iron rich sandy horizons are no more than 30 to 40 centimetres thick (Figure 6.5b). A less extensively developed, but similar horizon, was noted at the top of the gritty clay facies. Both the lower, and the upper contact, with the calcrete layer in this case, are sharp. Red sands were also noted in burrows and termitite nests (Figure 6.7). These sands, although similar in appearance and character to the horizons overlying the two previously described facies appear to be derived from the surface sediments by "bio-tunnel" infilling. Sedimentary structures are lacking in this generally homogeneous facies.

Petrology and mineralogy

This facies, which displays a typical red colour consists predominantly of iron-oxide coated quartz grains, set in a fine-grained clay matrix (constituting as much as 18%, but typically around 10 to 12%). The grains consist of a coarse sand to grit and may be rounded to sub-

angular. Few rock fragments and minor altered feldspar grains were also noted.

Grain size parameters

Grain size parameters for these sands are summarized in Table 6.3. Also included in this table, for comparison, are the values for the two host facies, that is, the pebbly clay facies and the gritty clay facies. Grain size distributions of two samples (one from the facies boundary horizon and one from a burrow feature) are shown as histograms in Figure 6.9. The two histograms exhibit similar grain size distributions to their host sediments (c.f. Figure 6.6 and 6.8) and, thus, have similar sedimentary parameters (Table 6.3), except that they are slightly better sorted, slightly more fine-skewed, and have slightly larger mean grain sizes (0.87ϕ to 0.93ϕ). A surface dune sand in the vicinity of the trenches gave a similar mean grain size of 0.91ϕ , suggesting that these burrows were filled with sediment from the surface. The slightly larger mean grain sizes, compared to the host sediments, appear to be related to a slightly lower clay content.

Table 6.3 Range of sedimentary parameters for the red sands and the two facies in which they occur.

	Mean Grain Size (ϕ)	Standard Deviation (Sorting)	Skewness
Red sands (n=4)	0.87 - 0.93	1.27 - 1.44	0.09 - 0.10
Gritty clay facies (n=3)	0.93 - 1.92	1.30 - 1.52	-0.06 - 0.05
Pebbly clay facies (n=5)	0.98 - 1.29	1.32 - 1.53	-0.06 - 0.09

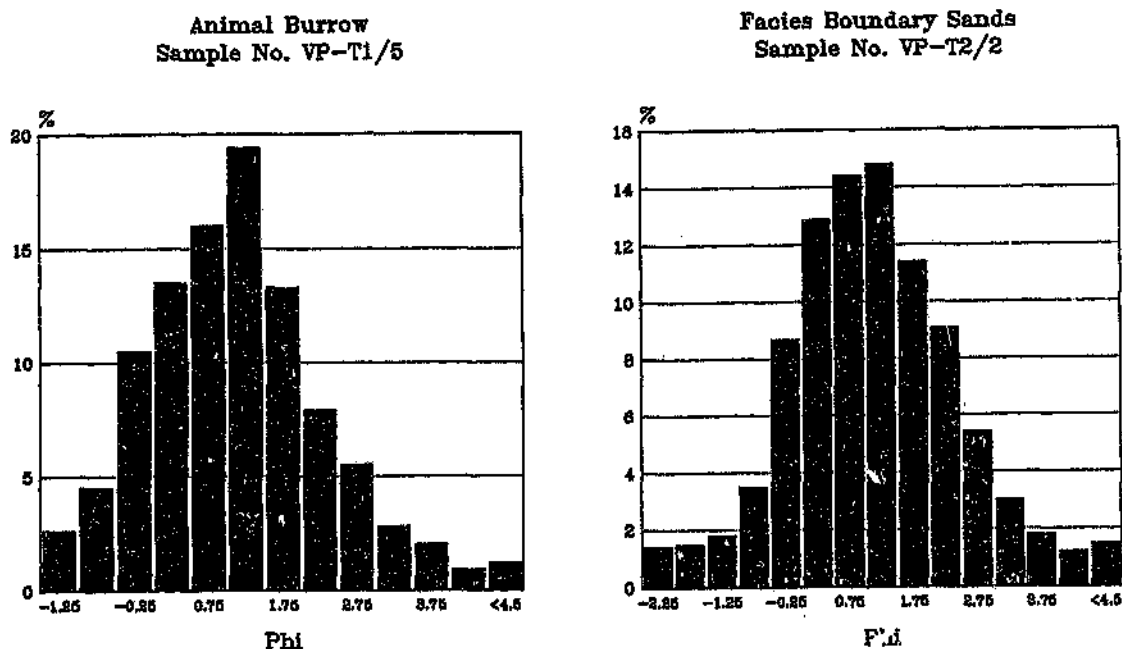


Figure 6.9 Grain size distributions for the facies boundary horizon and a burrow feature.

6.2.5 Calcrete

According to Netterberg (1969), calcrete by definition comprises any material formed by the cementation and/or partial or complete replacement of a pre-existing soil by predominantly CaCO_3 . Any calcified soil containing greater than 50% total carbonate (calcite plus dolomite) is referred to as calcrete rather than a calcified product. Calcrete results from the cementation and displacive and replacive introduction of calcium carbonate into soil profiles, bedrock and sediments (Wright and Tucker, 1991). This will occur in areas where vadose and shallow phreatic groundwaters become saturated with respect to calcium carbonate: a prominent feature in climatic zones where a season moisture deficit occurs, allowing calcium carbonate to accumulate (Goudie, 1973; 1983).

Description

Three calcrete horizons were recognised in the waste disposal trenches which expose the upper 8 metres of the Vaalputs Formation. These calcrete horizons are shown in Figure 6.10. The lowermost horizon (situated approximately in the middle of the pebbly clay facies) is typically nodular or disseminated and has an undulating morphology, possibly reflecting a palaeo-land surface. The middle horizon is more disseminated and stringy and occurs in the upper parts of the pebbly clay facies. The uppermost horizon, which is a well developed, massive and horizontally bedded calcrete horizon occurs either at the top of the gritty clay facies (where developed) or at the top of the pebbly clay facies (Figure 6.10).



Figure 6.10 Eastern wall of the low level waste disposal trench showing the development of calcrete at three depths in the pebbly clay facies.

The lowermost, nodular calcrete is typically coated in iron-oxide. Iron oxide occurs interlayered with the concentric layers making up the nodules as well as on the outer surface. All the calcretes were found to contain numerous angular sand grains, with a large range of sizes, and which are typical characteristics of the host sediments. As most of the nodules contain relatively little of the original matrix, displacive growth (Wright and Tucker,

1991) seems the most likely mechanism. The uppermost calcrete horizon is the "cleanest" (least sand grains and impurities), and best developed. Quartz is the most common mineral constituting the detrital grains, with sub-ordinate feldspar, magnetite and ilmenite.

Abundant rhizcretions were observed at various depths, and are fairly common along the upper pebbly clay facies contact (described earlier in Section 6.3). This form of calcrete may well be non-pedogenic in origin, whereby carbonate is precipitated due to transpiration by plants. These forms of rhizoliths are typically circular in cross section and cylindrical in shape, with lengths varying from a few centimetres to several tens of centimetres. Downward bifurcations with decreasing diameters were noted on these generally vertical features.

Occasionally isolated or scattered gypsum crystals were observed a few tens of centimetres below the various calcrete horizons. According to Wright and Tucker (1991) gypsum is more soluble than calcite, allowing it to be moved to lower depths in the profile and, therefore, gypsic horizons typically underlie calcic ones.

6.3 Chemistry of the Vaalputs Sediments

The chemistry of the various constituents, excluding the carbonate rich calcrete horizons, were determined for the Vaalputs Formation. The individual chemical analyses are presented in Appendix E, and a general description of the chemistry of each of the facies is given below.

6.3.1 The White-clay Facies

The chemical results for this facies are highly variable due to the inhomogeneous nature of the underlying basement from which this facies is derived. Samples with low silica

contents may be related to noritic basement, whereas those with higher values are related to granitic gneisses. Titanium is generally fairly low in this facies with values ranging from approximately 0.2 to 0.6%. Al_2O_3 is also highly variable and may exceed 20%, presumably due to the varying stages of alteration and high clay fraction. This facies is generally depleted in iron and magnesium with respect to the overlying sediments, with typical values around 2% and 0.02% respectively. MgO and CaO concentrations are relatively low (<1% and <3% respectively). The sodium and potassium concentrations (<1.5% and 0 to 6% respectively) are typical for the weathered state of this facies, that is, the sodium has passed into solution during weathering and the potassium concentrations are probably due to the presence of illite.

6.3.2 The Pebbly Clay and Gritty Clay Facies

These two facies are dealt with together as they were found to have very similar chemical signatures. These facies typically have SiO_2 values around 55 to 60%, with Al_2O_3 as high as 20%. Iron concentrations are fairly high (approximately 6%), primarily due to the abundance of iron oxide which coats grains and occurs as detrital ilmenite and magnetite grains. Manganese is generally low (0.08%) but higher than the weathered country rock (0.02-0.06%). MgO concentrations (2-3%) may be attributed to local concentrations in calcretized sands and clay, or to the presence of smectite clay. Overall, CaO concentrations are low (<1%). The sodium and potassium (approximately 1.5% and 3% respectively) may be attributed partly to feldspar, and illite which forms a significant component of these sediments.

6.3.3 Red Sands

This facies appears very similar (and is genetically related) to the surface sediments and, therefore, have a similar chemistry. These sediments are slightly higher in silica

(approximately 65%) and slightly lower in Al_2O_3 (approximately 12%), than their host sediments, due to the dominance of quartz sand. The red sands have similar Fe_2O_3 and MnO concentrations (approximately 5% and 0.08% respectively) to the host sediments for similar reasons: iron oxide coated grains and detrital ilmenite and magnetite grains are common. Manganese may occur with iron oxides and hydroxides. MgO and CaO concentrations are similar to the host sediments and may also be attributed to localized calcite development or to the presence of smectite clay (MgO). Sodium and potassium have slightly higher and lower concentrations respectively, compared to the host sediments. This may be due to the less altered nature of the red sands which have a little more fresh feldspar and less clay.

6.4 Chronology

Limited chronological information is available for the lithologies overlying the basement gneisses of the Namaqualand Metamorphic Complex and, therefore, six calcrete samples were collected from various depths and localities in the Vaalputs Formation for ^{14}C dating. Bulk samples were analyzed as the identification and separation of specific phases was not possible. Samples were processed at the Schonland Research Centre, University of the Witwatersrand. This method of dating was not expected to give precise ages as calcrete typically forms over a period of time by depositional episodes of carbonate, which when sampled, provides a mean age (e.g. Vogel, 1982). The sample localities, and the ^{14}C age data for the six samples are given in Table 6.4. As the data typically gives average ages, the calcrete in all cases must have been in existence since at least that date.

Table 0.4 Sample localities, and ^{14}C age data for the calcrete samples

Sample No.	% Modern Carbon	Age (yrs)	Sample Locality and Calcrete Type
VP-68	4.5 ± 0.8	$25\,635 \pm 1\,353$	Intermediate level waste disposal trench: 1.5 m depth, uppermost Vaalputs Fm. Gritty clay facies massive horizontally bedded calcrete
VP-67	0.4 ± 0.8	$> 50\,000$	Intermediate level waste disposal trench: 4 m depth, lower to mid-Vaalputs Fm. Pebbly clay facies disseminated, stringy calcrete
VP-66	0.2 ± 0.8	$> 50\,000$	Intermediate level waste disposal trench: 7 m depth, lower Vaalputs Fm. Pebbly clay facies disseminated, nodular calcrete
VP-69	1.2 ± 0.8	$36\,562 \pm 4\,222$	Low level waste disposal trench: 7 m depth, mid-Vaalputs Fm. Gritty clay facies undulating, massive calcrete
VP-T1/8	10.0 ± 0.4	$19\,040 \pm 324$	Low level waste disposal trench: 7 m depth, mid-Vaalputs Fm. Gritty clay facies undulating, massive calcrete
VP-C2	8.0 ± 0.5	$20\,880 \pm 501$	Surface, northern Vaalputs boundary 1 m depth, underlying Dorbank and aeolian sands massive/ nodular calcrete

The ages of the calcrete are compatible with the depths or positions of the various calcretes, in that calcrete obtained from the lowermost calcrete horizon have the lowest percentage of modern carbon, and give ages in excess of 50 000 years. The uppermost

sample from the intermediate level waste disposal trench (Sample VP-68) and the surface sample (Sample VP-C2) have similar ages around 25 000 and 20 000 years respectively, suggesting that these calcretes are the most recently deposited. Sample VP-69 gives an age of approximately 36 000 years, which conforms well with the position of the sample site, that is, stratigraphically it lies between Samples VP-67 and VP-66 (> 50 000 years), and the uppermost calcrete layer (Sample VP-68) of the Vaalputs Formation (25 000 years).

Sample VP-T1/8 is the only sample with an age that does not correlate well with the other ages. This sample was taken from the same calcrete horizon as Sample VP-69. Fractures observed in the Vaalputs sediments may be responsible for this, as percolating water has been noted to line the fractures with calcrete, which could presumably infiltrate further down and affect deeper calcrete horizons. Generally the high clay content of these sediments is believed to have provided a reasonable seal from this kind of mixing, however, the results of this study show that the deposits are undoubtedly older than 50 000 years as predicted by previous workers (eg. Levin et al., 1986) and that ground water containing more recent carbon has infiltrated these sediments. The uppermost or surface calcrete underlying the ferruginized and aeolian deposits appears to be younger, but, the younger ages may also be a consequence of the later introduction of modern carbon.

Calcretes of the study area, with which de Wit (1993) has associated calcretized Miocene terraces, such as at Paarde Kolk and Nels Kop, which post-date the incision of the northward draining rivers of the Bushmanland during the Miocene, and which pre-date the younger gravels at Brandvlei and Van Wyksvlei, have been assigned an age between the late-Miocene and the late-Pliocene. Other workers (e.g. Levin et al., 1986) have assigned similar ages to these deposits of 2 - 20 Ma. According to de Wit (1993) it is unlikely that the calcrete, which extensively covers the Bushmanland plateau, developed prior to the early Pliocene. This de Wit largely bases on the presence of early Pliocene horse remains, below thin calcrete 65 kilometres east of Springbok (Haughton, 1932). Partridge and Maud (1987) have also equated the area covered by the Bushmanland calcrete to the post-

African I surface (early mid-Miocene to late-Pliocene). The Vaalputs sediments, therefore, may well be of an early to mid-Cenozoic (Oligocene - Pliocene) age as suggested by previous workers. This age is compatible with structural and sedimentological observations of this study and is in agreement with the above ^{14}C age results. As the Vaalputs sediments are subject to bioturbation they cannot be dated using thermoluminescence and, furthermore, they contain no original organic material for radiocarbon dating. As a consequence, little new information regarding the age of these sediments could be obtained.

6.5 Discussion

The somewhat unusual characteristics of the Vaalputs sediments, believed to be the key in diagnosing their origin, are discussed, after which a depositional environment for the various facies is proposed.

Sediment characteristics

The overall poor sorting, large mean grain size and overall variability of parameters indicate modification and *in situ* weathering of the original sediments. The high clay content and remnant angular quartz grains of the white clay facies is indicative of *in situ* weathering, rather than an alluvial product as suggested by previous workers. Brynard (1988) noticed that SiO_2 generally decreases upwards in a smooth trend (partially or wholly) in the transition from fresh through weathered basement into the overlying white clay, supporting the view that the white clay represents *in situ* weathering of the basement rock. Remnant feldspar grains and a high clay content in the overlying pebbly clay and gritty clay facies are also indicative of *in situ* weathering.

The clay content of the Vaalputs sediments may well be a reflection of a number of conditions that existed in this region, during both the weathering of the parent or basement rocks and later in the accumulation and modification of the sediments. Watson (1992) noted that in many arid environments, silt and clay-sized materials are formed during

weathering. However, according to Pye (1987) the active accumulation of aeolian dust occurs mainly where rainfall is sufficient to support dust-trapping vegetation. The aluminous precursors of the clay minerals of this study include K-feldspar, plagioclase, biotite and muscovite, all of which are abundant in the source rocks. Although various clays are found throughout the Vaalputs sediments, smectite is the dominant clay in the white clay facies, whereas illite is more common in the overlying sediments.

According to Watson (1992) gibbsite and kaolinite are the products of more advanced feldspar weathering and are rare except where ancient weathering profiles are developed. Kaolinite is more abundant in wetter (Sieffermann and Millot, 1969; Singer, 1966), older (Briner and Jackson, 1970), or low pH environments (Swindale, 1966). According to Singer (1989) illite is generally stable under arid conditions and may occur as an authigenic mineral formed from smectite by the addition of potassium derived from atmospheric inputs. Brynard (1988) noted that the occurrence of clay minerals in the Vaalputs sediments are generally in accordance with the results of a clay mineral survey of soils in arid to semi-arid regions in South Africa (van der Merwe and Heystek, 1955). They found that illite, smectite, and mixed-layer clays are the main clay minerals, and kaolinite was found to be fairly scarce.

The kaolinite in the Vaalputs sediments is, therefore, presumably an indication of humid conditions such as those proposed for the palaeo-weathered basement rocks. Illite and smectite, typical clay minerals of poorly leached arid soils (Krauskopf, 1967) may be indicative of more arid or semi-arid environments. Brynard (1988) attributed the abundance of smectite in the Vaalputs sediments to the alteration of feldspars in the basement rocks and sediments in an alkaline environment. Brynard (1988) found the pH of the white clay to be 7.3 - 7.8 when compared to the overlying more alkaline sediments of 8.5 pH and also suggested that the kaolinite clay has been partially converted to the smectitic clay of the Vaalputs sediments in a closed basin. Clay minerals are presumably still forming as ion-exchange reactions are important after the initial weathering. Additional effects are those of micro-organisms, and the role of organic material in the weathering process and

redistribution of elements (by the oxidation of organic carbon, iron, manganese and sulphur): evidence of root, and extensive termite activity, is exhibited in the waste disposal trenches.

The various clays are associated with different climates throughout the depositional history of the Vaalputs Formation, with kaolinite forming predominantly during the earlier wetter periods and, illite and smectite forming later during drier periods. The clays have subsequently undergone various forms of alteration and have been redistributed by bioturbation. Vine (1987) observed thorough mixing of clay and iron-oxide to great depths in the aeolian "acid sands" (ferrallitic soils over loose sandy sediment) of the Sahara in Nigeria. Grove (1951) reported thicknesses for these sediments of 12 to 18 metres, which are comparable to thicknesses of the clay rich Vaalputs sediments.

The Dwyka rocks in the area may be a major contributor of CaO and MgO to the sediments and calcrete layers observed in the Vaalputs sediments as the Dwyka is believed to be the only significant source of MgO in the area. Major differences in chemistry suggest that the Dsdap sediments have contributed slightly, if at all, to the Vaalputs Formation. A comparative chemical analysis of all the sediment suites is dealt with in more detail in Chapter 7.

Interpretation

Results of this study do not support the views of previous worker, e.g. Levin et al. (1986) who propose that the sediments of the Vaalputs Formation constitute the northern extension of an alluvial fan originating south-west of Vaalputs, and that the white clay is derived largely from the reworking of the Dsdap Formation. Using the data of this study a reinterpretation of the depositional environments for each of the facies of the Vaalputs Formation is given.

i) White clay facies

The clay percentage or content of the lower white clay (kaolinite and smectite) facies

contains significantly more clay (as much as twice that of the overlying sediments - Brynard, 1988), suggesting a somewhat different origin for this clay rich horizon. Considering the nature of these sediments it is proposed that they are predominantly the result of *in situ* weathering (and minor reworking/mixing) of what was already weathered basement. The chemical and morphological features of the Dasdağ Formation (as also noted by Levin, 1988) and the white clay unit are too different to reconcile and no other hypothesis can be offered to explain the petrogenesis of this unit. The high angularity of the quartz grains is indicative of very little, if any, transport for this material.

ii) Pebbly clay and gritty clay facies

The pebbly lenses scattered throughout these deposits are indicative of high energy fluvial events, such as ephemeral flood deposits. The clasts of the pebbly lenses have the composition for a local source area, that is, the clasts consist predominantly of high grade metamorphic blue quartz. The blue quartz pebbles, due to their hardness, are likely to survive transportation (and weathering) over greater distances than other lithologies, and hence their abundance. The roundness and sphericity of the pebbles indicates that these sediments have been transported over a reasonable distance, presumably from as far as the western marginal scarp.

Overall the sediments are fine grained, containing sands, silt and clay. The high clay content and relic feldspar grains observed in thin section are suggestive of intense *in situ* weathering, which would further contribute to the extremely poorly sorted nature of these sediments. The yellow-brown colour of the lower pebbly clay facies is attributed to the iron content and phases present. According to Loeper (1988) the pedogenic formation of iron oxides is extremely slow in well-drained calcareous soils (these facies contains abundant calcrete), as the rates of dissolution of Fe(II)-containing primary or secondary soil minerals in equilibrium with CaCO_3 are slow, although some calcareous soils are known to contain appreciable iron oxide. Also, the iron oxide contents are reflected in the soil colour, with soils from arid and semi-arid climatic regions characterized by low chromas. Hematite, due to its pigmenting properties dominates the colour of the system in which it is present

(Loepert, 1988). According to Loepert (1988), it is not likely that large amounts of iron oxide would be formed by the pedogenic weathering of secondary minerals in a calcareous environment (calcite controls the pH within the range of approximately 7.5 to 8.5), and therefore, attributes the occurrence of both iron oxide and CaCO_3 within a soil to the translocation of the iron oxide or the CaCO_3 , or both, from outside sources.

The greyer (olive) colour of the gritty clay facies is attributed to slightly different post depositional conditions, and degrees of weathering and soil-forming process, to that of the underlying pebbly clay facies. According to Schwertmann (1988) the grey colour of soils may indicate the removal of iron oxides by microbial reduction. Also, as for the underlying facies the pedogenic formation of iron oxides is extremely slow in well-drained calcareous soils (Loepert, 1988). The reasons for the distinct colour changes, with respect to the underlying facies appears to be primarily due to differences in chemical compositions due to variations in iron content (average relative abundance of Fe_2O_3 : 4.8% versus 5.6% for the pebbly clay facies) and calcrete (average relative abundance of CaO : 0.4% versus 0.5%; and MgO : 2.2% versus 2.6%).

The source area was presumably altered to some extent and from the chemistry, some weathered Dwyka appears to have contributed to the Vaalputs sediments from the area to the east. A driving mechanism for the deposition would have been the high scarps, on both the western and to a lesser extent the eastern sides of these deposits, created by uplift of the escarpment to the west, or basinal development by some other mechanism (see Chapter 8 on structure) on the inland side of the marginal scarp. The upper sharp contact of the lower pebbly clay facies is suggestive of a hiatus during which some erosion may have taken place, and during which vegetation appears to have been more dominant in what was perhaps a slightly wetter period. This statement is based on the occurrence of numerous rhizocretions on the upper contact of the pebbly clay facies. The upper contact of the gritty clay facies, with the calcrete horizon, is again suggestive of a hiatus during which period further and perhaps the final stage of aridification took place.

Sedimentary structures which would usually assist in the interpretation of the environment of deposition are nonexistent. These may have partly been destroyed by soil forming and mixing (bioturbation) processes. Taylor and Goldring (1993) devised a Bioturbation Index (BI) where each grade is described in terms of sharpness of the primary sedimentary fabric, burrow abundance and amount of burrow overlap. This they related to the percentage bioturbation values of Reineck (1963). The Vaalputs sediments may be categorized as grades 4, 5 and 6 which correspond to percent bioturbated values of 61-90, 91-99, and 100 percent respectively (pg 142, Taylor and Goldring, 1993). Intense to complete levels of bioturbation (grades 5 and 6) were commonly noted in the Vaalputs sediments.

In many arid to semi-arid regions of the world, channels flow onto low lying plains, with few tributary contributions and with diminishing downvalley flows (Tooth, 1998). Channels remain well defined for much of their length but capacities eventually decline to a point at which an increasing proportion of the larger floods reaching the distal parts are diverted overbank. Tooth (1998) reported such occurrences in Australia where channelised flow and bedload transport of sands and gravels largely cease, and where large floods continue across typical broad, low-gradient surfaces. Tooth (1998) also reported light vegetation (trees, shrubs and grasses) which are typically surrounded by aeolian sandplains, older alluvial surfaces or low relief hills. Reasons, which are not mutually exclusive, for a diminishing flow include: an over-supply of sediment relative to the transport capacity; declining gradients, aeolian, structural or hydrologic obstructions to flow, resulting in the complete disappearance of channelized flow. This common phenomenon, referred to as "flood outs" in Australia has been described in various other geomorphological works (e.g. Rodier, 1985; Ori, 1989).

A "terminal floodout" as defined by Tooth (1998) is "a site where channelized flow ceases and spills across adjacent alluvial surfaces and ultimately dissipates". It is proposed that the pebbly and gritty clay facies of this study are the result of a similar semi-arid depositional environment in which ephemeral streams, which generally remained dry for

much of the year, dominated the surface. These occurrences can be largely related to Cenozoic climate changes. Increasing desiccation resulted in the retraction of formerly better developed drainage systems, which presumably existed during the time of formation of the lower white clay facies. Floodcut development in the studied area may well have been initiated by a structural barrier, the details of which are discussed in Chapter 8. Unchanneled sheetflows of limited depth and velocity, as described by Tooth (1998) were probably the primary form of sediment transport over what were relatively low slopes. It is likely that several floodouts, particular in the distal reaches (floodplains), converged giving rise to deposition of yellowish red silts and sands (also described by Tooth, 1998 for Australian flood out deposits). Coarser pebbly deposits of well rounded quartz are interpreted as channel bedload deposits. These may be found in the distal portions of floodouts as a result of greater-than-normal flooding or due to channel switching in the more proximal parts. Poorly sorted, gritty or gravelly sands are also typical for distal deposits. Such deposits may be further modified by bioturbation during long periods of no flow.

"Alluvial fans" are commonly applied to a broad spectrum of fluvial geomorphic features that deposit sediment in a fan-shaped form (relatively low-gradient types, braided, distributary and meandering fluvial types) [e.g. Schumm, 1977; Mial, 1978; Adamson et al., 1987; Gohain and Parkash, 1990; Stanistreet and McCarthy, 1993]. However, floodouts, which in the distal reaches are difficult to classify, possessing features common to both floodplains and alluvial plains, differ in the proximal and medial reaches of the drainage systems. In the proximal reaches they are characterised by floodplain formation, by virtue of axial lengths, hydrology, sedimentary processes and the predominantly fine-grained deposits (Tooth, 1998). In particular the geomorphic setting in low-gradient plains, the often large aerial extent and the relatively fine-grained deposits typical of floodouts differentiates them from alluvial fans. Gradients during the deposition of the Vaalputs Formation were probably around 1 in 1000 (based on depth of basin and half-basin-width) which corresponds well with the range of gradients of 1 in 1600 to 1 in 700 reported for floodouts in Australia (Tooth, 1998). Other characteristics differing from those of alluvial fans include:

the lack of extensive distributary channels in terminal fan systems and the often lack of a fan-shaped form.

Fluvial-aeolian interactions in the distal reaches of arid environment drainage systems have been referred to by a number of authors (e.g. Langford, 1989; Nanson et al., 1995), but these reactions are usually very subtle (Tooth, 1998) and are characterized by thin layers of alluvial silts and clays deposited over aeolian sands following flood events. Due to the slow rates of aggradation (and bioturbation during periods of no flow), sedimentary structures are rarely preserved. Changes in the vertical section of the Vaalputs sediments, where subtle changes in grain sizes and colour were noted, may be due to fluvial-aeolian interactions. The bioturbated nature of the Vaalputs sediments makes positive identification of such processes virtually impossible.

iii) Red Sands

As described in the preceding sections, the sand size parameters of these sediments are very similar to their host sediments (and to the overlying Gordonia Formation: described later in Section 7.7), and are typically found in sections of animal burrows or nests. This suggests that they may well have been derived from the aeolian surface deposits. Where they occur as poorly defined horizontal layers within the pebbly clay or gritty clay facies, or infill rhizocretions, they may represent aeolian interactions (as described in the previous section) in what was probably a semi-arid fluvial dominated environment.

iv) Calcrete horizons

A number of soil forming factors, such as climate, parent material, topography, biological activity, and time, were probably involved in the formation of the calcrete. The mechanisms of formation of calcrete which have been proposed by various authors are diverse. Calcrete accumulation according to Watson (1992) is a result of ineffective leaching because of low rainfall and sometimes high evaporation rates. Calcretes have been observed in some polar situations, but are most characteristic of warm areas with limited precipitation (Summerfield, 1983a).

Two possibilities may have given rise to the calcretes observed in the Vaalputs sediments. The downward concentration (*per descensum*) of carbonate, is derived from dust, rainfall and vegetation litter. Aeolian dust is considered to be the major source of ions for calcrete formation (Goudie, 1973; Reeves, 1976). The host soil creates illuvial calcrete in the lower soil horizons as a petrocalcic soil horizon (Goudie, 1983). The *per ascensum* hypothesis requires the downward moving soil waters to penetrate to a certain depth and return towards the surface or near surface zone of the soil by capillary action, bringing with them dissolved carbonate which is deposited as a result of effects such as precipitation.

As the pedogenic process of calcrete formation generally assumes the presence of pre-existing carbonate in the soil, the assumption that the Vaalputs Formation represents the distal portion of the Dasdap alluvial fan, as proposed by others (e.g. Levin et al., 1986) cannot account for the extensive development of calcrete in the Vaalputs sediments (Brynard, 1988). As calcium is a highly mobile element, it would have been largely lost from the parent material during transportation to its site of deposition, and the remaining calcium minerals, Brynard (1988) considers insufficient to account for the high calcium content in the calcrete and other calcareous layers observed in the present profile of the Vaalputs Formation. Brynard (1988), however, does suggest that non-pedogenic calcification due to ascending ground water could account for these calcretes, but would have required a much higher ground water table level than at the present time.

Although Netterberg (1969) recognised that many calcretes are of a complex nature, involving both mechanisms of formation, he believes that most South African, and other calcretes are of a pedogenic origin. The calcretes at Vaalputs, and in particular, the upper calcrete horizon, are believed to be predominantly of the pedogenic type. The distance from the present water table to the upper calcrete layer is too great to account for their formation by non-pedogenic processes. If the water table was higher than the present level during the deposition of the Vaalputs sediments, the calcrete, particularly the lower horizons may have been the result of non-pedogenic processes. The multiple layers of calcrete, however, are more easily interpreted using pedogenic calcrete formation at

different stages of the deposition of the Vaalputs sediments.

An additional processes has been noted and which is believed to have given rise to carbonate deposits in the Vaalputs sediments, particularly along the boundary of the pebbly clay and gritty clay facies: non-pedogenic processes giving rise to the rhizcretions and more nodular forms. Although relatively little detailed work has been carried out on the mechanisms of carbonate precipitation (Wright and Tucker, 1991), some authors (eg. Salomons and Mook, 1986) stress the evapotranspiration and degassing as the main mechanisms of precipitation. According to Cerling (1984) evapotranspiration is the major process in semi-arid calcretes and is probably a major cause of rhizcretion formation. The relatively low partial pressure of CO_2 in arid and semi-arid soils is a contributory factor leading to carbonate precipitation (Marion et al., 1985). Several mechanisms for rhizcretions have been reported such as those of Johnson (1967) who stated that "root sheaths" may form in one of five ways, depending on: "(i) the presence of organic acids exuded by living plant roots; (ii) symbiotic relations between roots and certain soil bacteria; (iii) symbiotic relations between roots and certain soil fungi; (iv) the presence of some blue-green algae which have calcium carbonate precipitating bacteria housed in their slime sheaths; and (v) calcium exclusion properties of some plants which promote the precipitation of calcium carbonate outside the root". Calvet et al. (1975) suggested that rhizcretions formed by: progressive root penetration, resulting in the closer packing of sand grains around the roots; the formation of a calcareous envelope as a result of activity of micro-organisms, the effect of organic acids and evapotranspiration; and centripetal filling of chalky material following death and decay of the root. Klappa (1991) noted the coincidence of sites of calcification, which correspond to naturally occurring calcium-rich layers within plant tissue, suggesting that a substrate or template control governs the form of preservation in petrified samples. On the other hand, the formation of tubules and rhizcretions involves dissolution of mineral components within the rhizosphere and reprecipitation of some or all the dissolved minerals around the root and/or introduction of calcium carbonate-rich solutions from elsewhere. These processes may take place on a living root (Kindle, 1925) or during decay (Klappa, 1991). Thus, although a number of

mechanism of root-related calcium carbonate precipitation have been proposed, roots are undoubtedly fundamental contributors to pedogenic processes and resulting products of calcretization.

In general the calcrete horizons in the Vaalputs sediments are suggestive of drier interludes and most probably define previous land surfaces. That is, some, if not all of these calcrete horizons probably represent surface stabilization stages during less tectonically active periods or during periods of lower water and sediment supply.

CHAPTER 7: THE GORDONIA FORMATION AND PRESENT DAY MICRO-ENVIRONMENTS

Vaalputs is located in an extensive dune field dominated by low amplitude longitudinal dunes. The dunes are orientated in a north-northeasterly direction, and form part of the uppermost sediments in the region referred to as the Gordonia Formation. Figure 7.1 shows the extent of these deposits, which are easily recognisable by their dark brown (false) colour and typical dune field pattern in the TM-5 LANDSAT image. These sediments overlie the remnants of the Vaalputs and Dasdap Formations, and transgress the small scarp on the western side of the Santab Valley in the west (McCarthy et al., 1985). Small deflation pans may be found in the interdunal areas. Other deflated areas may be seen on the dune slopes, or may be developed on older horizontal and more stable surfaces such as basement, older sediments, or calcrete surfaces. The various geomorphological settings on the present land surface form a complex mosaic and are referred to as micro-environments.

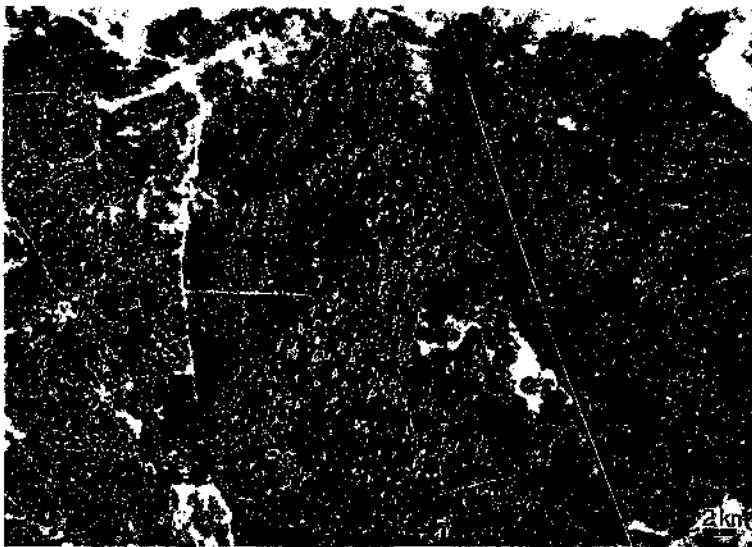


Figure 7.1 TM-5 LANDSAT image of the Vaalputs site and surrounding area showing the north-northeasterly oriented dunes in the vicinity of Vaalputs. The image is approximately 40 kilometres across (also note 2 km scale bar).

Both the Gordonia Formation and the present day surface environments, and the processes which gave rise to these deposits may be associated with the underlying Vaalputs Formation. A detailed study of these younger sediments and the current processes could provide information to past environments. In addition a detailed analysis of these sediments would provide a significant contribution to the understanding of the geomorphic, sedimentologic and tectonic history of the region. This chapter deals with the processes and the environments responsible for these deposits.

7.1 Identification of the Micro-environments

Four separate micro-environments characterising the present-day land surface were recognised and investigated. Each of the environments is believed to be the result of a dominant processes or combination of processes. The four micro-environments recognised are:

- i) aeolian deposits;
- ii) deflation pans;
- iii) lag deposits; and
- iv) bioturbated deposits.

It should be noted that, although a combination of the above micro-environments may occur together, for example, an aeolian dune may be highly bioturbated, each of the environments will be dealt with separately. The present land surface, in general, is believed to be fairly stable but in a state of slow degradation.

7.2 Aeolian Deposits

Occurrence of dune forms

Dune forms dominate most parts of the study area where covered by surficial deposits (Figure 7.1), in particular the eastern side of Vaalputs and extending south to the area around Platbakkies and the present Dasdap drainage. Mobile, or recently mobile, aeolian

deposits are best developed on the eastern half of the Vaalputs property, on older, stable dune forms. Isolated occurrences were observed further to the west, but generally not to the west of the main Springbok - Platbakkies road. Other faint, linear features, identified over parts of the study area, using Landsat imagery, may reflect older reworking of the cover sands by aeolian and fluvial agencies during arid episodes. The fluvial interludes, however, have not succeeded in overprinting the dominant aeolian textural fingerprint visible on the TM-5 Landsat image (Figure 7.1). An area situated approximately two kilometres to the east-southeast of the disposal site was investigated as the dune forms in this area (Figure 7.2.) appeared to be reasonably well preserved. These low amplitude dunes have an approximate north-northeasterly orientation (022°).



Figure 7.2 Photo taken from a dune crest and slightly obliquely to the dune orientation (022°). This photograph also shows a deflation pan developed in the inter-dunal trough area.

Appearance and vegetation

The dune surface sands are generally fairly coarse, red sands. Although the dunes are elongated in a north-northeasterly direction, transverse profile (see next section) clearly

indicates a westerly wind component. Vegetation on the windward (west) side of the dunes consists of small (10-50 cm high) hardy scrub, with no grasses. Bioturbation is prominent on this side. Figure 7.3 shows the typical appearance of the windward side of a dune, looking towards the dune crest. The windward side of the dunes appears to be fairly stable at the present time, or in a state of slight degradation. The vegetation on the dune crests consists of sparse bushes, some grasses and several short flowering plants. The dune crests form a transition zone for vegetation and shows obvious changes from the windward to the leeward sides of the dunes, which are covered by several types of grasses, and often patches of flowering plants (season dependant) (Figure 7.4). Some bioturbation was found on the leeward side of the dunes, but it is less common than on the windward side. The surface sands on the dunes have been stabilized to some extent by the various types of vegetation; however, it has been shown in other studies, e.g. (Ash and Wasson, 1983) that sand may be moved on the dune crests, even with up to 35% of the ground surface colonised by plants.



Figure 7.3 Windward (west) side of a dune showing the vegetation cover and bioturbation.



Figure 7.4 The leeward (eastern) side of the dune covered by several grass types and small flowering plants.

Dune profiles and sand thicknesses

An orthogonal profile (trending approximately 110°), to the dune crest (trend: 022°), was obtained for one of the dunes investigated (Figure 7.5). The profile shows a typical cross section of a dune, which is representative of the dunes in this region: amplitude 5.4 metres and wavelength approximately 550 metres. Although these dunes are longitudinal (see TM-5 Landsat image - Figure 7.1), they are asymmetrical, with steeper, leeward slopes towards the east.

No sedimentary structures were observed in cut-sections on the windward or leeward sides of the dunes. Thomas (1988) reported no internal bedding structures and sedimentary

characteristics (and high silt and clay contents), in certain southern African dunes, which he attributes to post depositional pedogenic weathering of the sands. In all cut-sections a hard calcrete horizon was encountered and found to occur at various depth along the profile. Thicknesses of unconsolidated sand, overlying the calcrete could, therefore, be obtained using conventional trenching and auguring methods. The location of the calcrete layer beneath the sand is shown in Figure 7.5). It should be noted that the subsurface calcrete horizon approximately mirrors the present surface (Figure 7.5). This dune surface-calcrete relationship was noted at another two sites where the dune forms are well preserved (also noted by McCarthy et al., 1985). This subsurface calcrete may take on various forms, including nodular, planar laminar, and disseminated calcrete. Calcareous sands commonly grade downwards into a purer, harder, and often impenetrable nodular or horizontally laminated calcrete. The calcrete horizons appear to be largely continuous over the entire dune field. Areas of predominantly ferruginized and slightly calcretized sands were noted where well developed calcrete was absent.

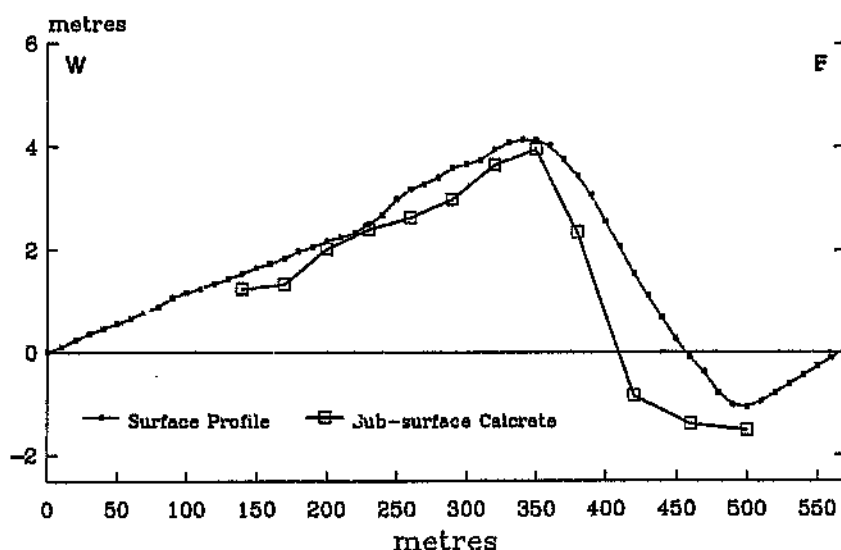
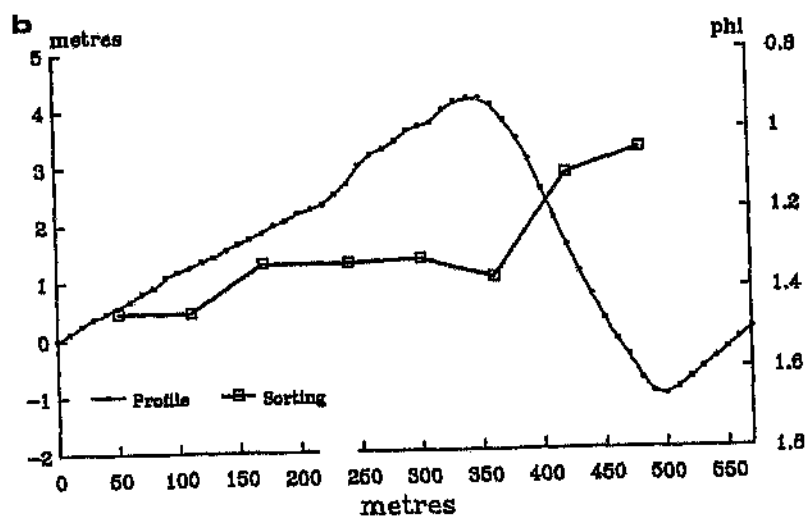
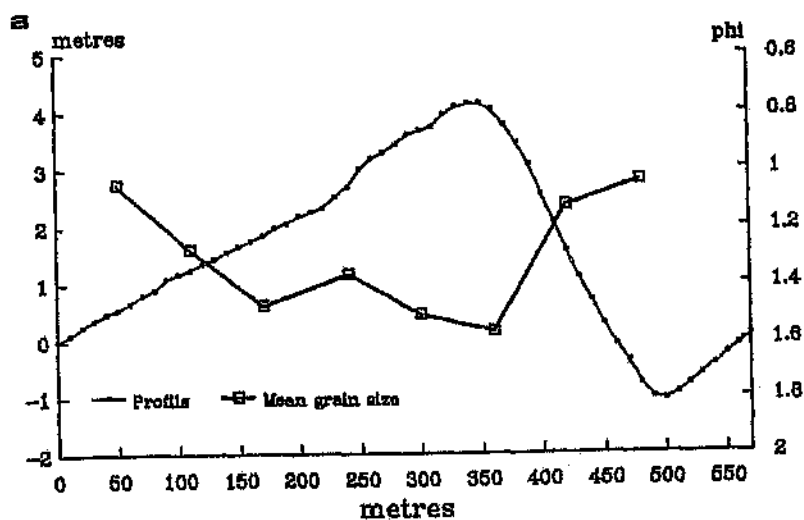


Figure 7.5 West-east profile of a dune, showing the present surface and the subsurface calcrete horizon.

Grain size analysis

Surface samples were collected along the same profile shown on Figure 7.5, at approximately 60 metre spacings. The profile, shown in Figures 7.6a, 7.6b and 7.6c, has superimposed on it, mean grain size variations, sorting and skewness, respectively.



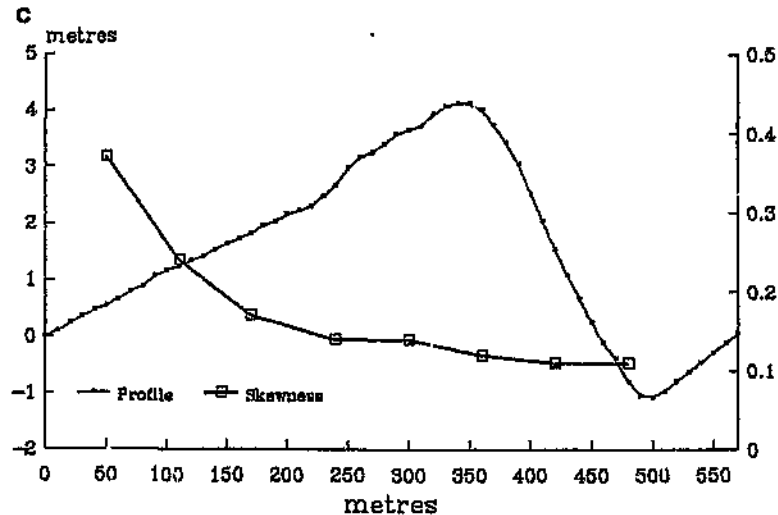


Figure 7.6 West-east dune profile, superimposed on (a) mean grain size (larger ϕ values represent smaller particle sizes), (b) sorting (larger ϕ values represent poorer sorting), and (c) skewness.

Mean grain sizes: (Figure 7.6a) shows that the dune crest has a finer mean grain size, which increases downslope in the leeward and windward directions. All the mean grain size values obtained for this dune range between 1ϕ (0.5 mm) and 1.6ϕ (0.33 mm) which are very similar to those values obtained by McCarthy et al. (1985), for the "red dunes". The average particle size obtained by them was 1.3ϕ (0.41 mm), which they noted is somewhat larger than those recorded for aeolian sands in the Kalahari and Namib Desert, which range from 2.44ϕ (0.18 mm) to 1.99ϕ (0.25 mm) (Lancaster, 1981).

Standard deviation (sorting): (Figure 7.6b) samples of the entire profile are poorly sorted (1.00 - 2.00ϕ). Sorting, however, improves gradually (larger numbers indicate poorer sorting) towards the dune crest and a little more on the leeward slope where the thicker deposits are typically found.

Skewness: Figure 7.6c shows the skewness variations for the profile samples, which vary from strongly fine (positive)-skewed to fine-skewed from the west to the east along the profile.

Petrology and mineralogy

The red sands of the Gordon Formation are mainly comprised of quartz grains, coated by iron-oxide: the colour variation observed in these sediments is believed to be the result of varying iron-contents. A host of heavy minerals similar to those in the basement rocks occur in these sands. Brynard (1988) documented the presence of several clays, including illite, smectite and kaolinite. The sands are generally poorly sorted and contain 4.5% silt to clay sized particles (almost opaque in crossed-polarised light). The grains are subrounded to angular, with low to high sphericity, and are predominantly monocrystalline quartz grains, with a smaller percentage of rock fragments (usually iron oxide cemented quartz grains), highly altered relic feldspar, and oxides (magnetite and ilmenite). The altered feldspar grains are usually red in colour, probably due to iron staining during alteration. A modal analysis for this deposit gave the following fractions: quartz: 64%; highly altered feldspar: 4%; and rock fragments (predominantly iron oxide cemented quartz): 32%.

Regional east-west traverse results

Mean grain size, sorting and skewness were determined for surface samples, taken at one kilometre spacings, along three separate traverses shown in Figure 7.7. This was carried out to determine regional variations in grain size across the dune field. Changes in the sedimentary parameters of the surface sediments, with distance from the basement in the west (a possible source for these sediments) could potentially contribute to the understanding of the source for the surface sediments of this region, as prevailing winds are generally from the west (e.g. Hambleton-Jones, 1986). The sites chosen (Traverses a, b, and c: Figure 7.7) were selected in an attempt to sample the entire field.

In addition, a short traverse (Traverse d: Figure 7.7) extending across the northern part of the Santab lineament was sampled. This was carried out to investigate the obvious colour changes of the sediments on either side of the lineament (Figure 7.8).

The results of a particle size analysis along these traverses (mean grain sizes, sorting, and skewness) are shown in Figures 7.9, 7.10, 7.11 and 7.12, for the northern, mid-, southern, and Santab lineament traverses. Also shown on these figures is an indication of the environment at the sample site. These include areas of higher lying ground and referred to as palaeo-dunes, areas of lower lying ground or interdunal areas which may be in a

state of degradation, and areas which appear to be comprised predominantly of recently mobile sands. A brief description of these results is given below.

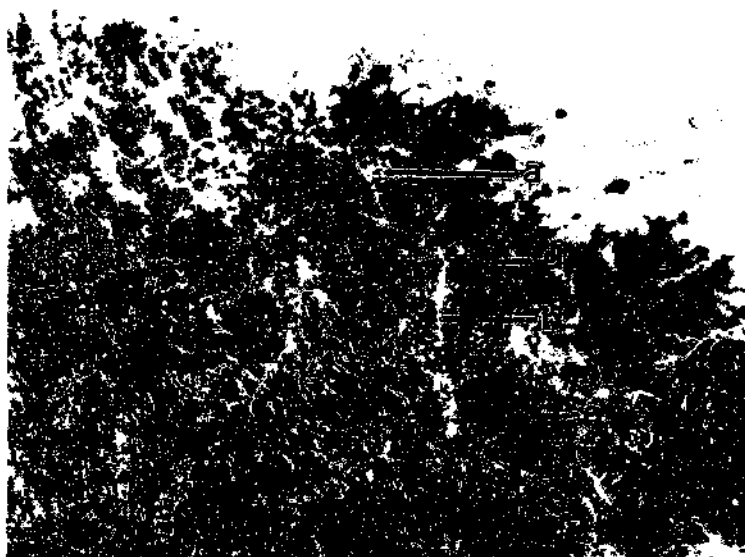


Figure 7.7 TM-5 LANDSAT image of the Vaalputs site and surrounding area showing the positions of the four traverses used for the northern (a), mid- (b), southern (c), and Santab lineament (d) traverses. The image is approximately 120 kilometres across.



Figure 7.8 Aerial photograph of the Santab lineament, looking southwest towards Santab-se-Vloer.

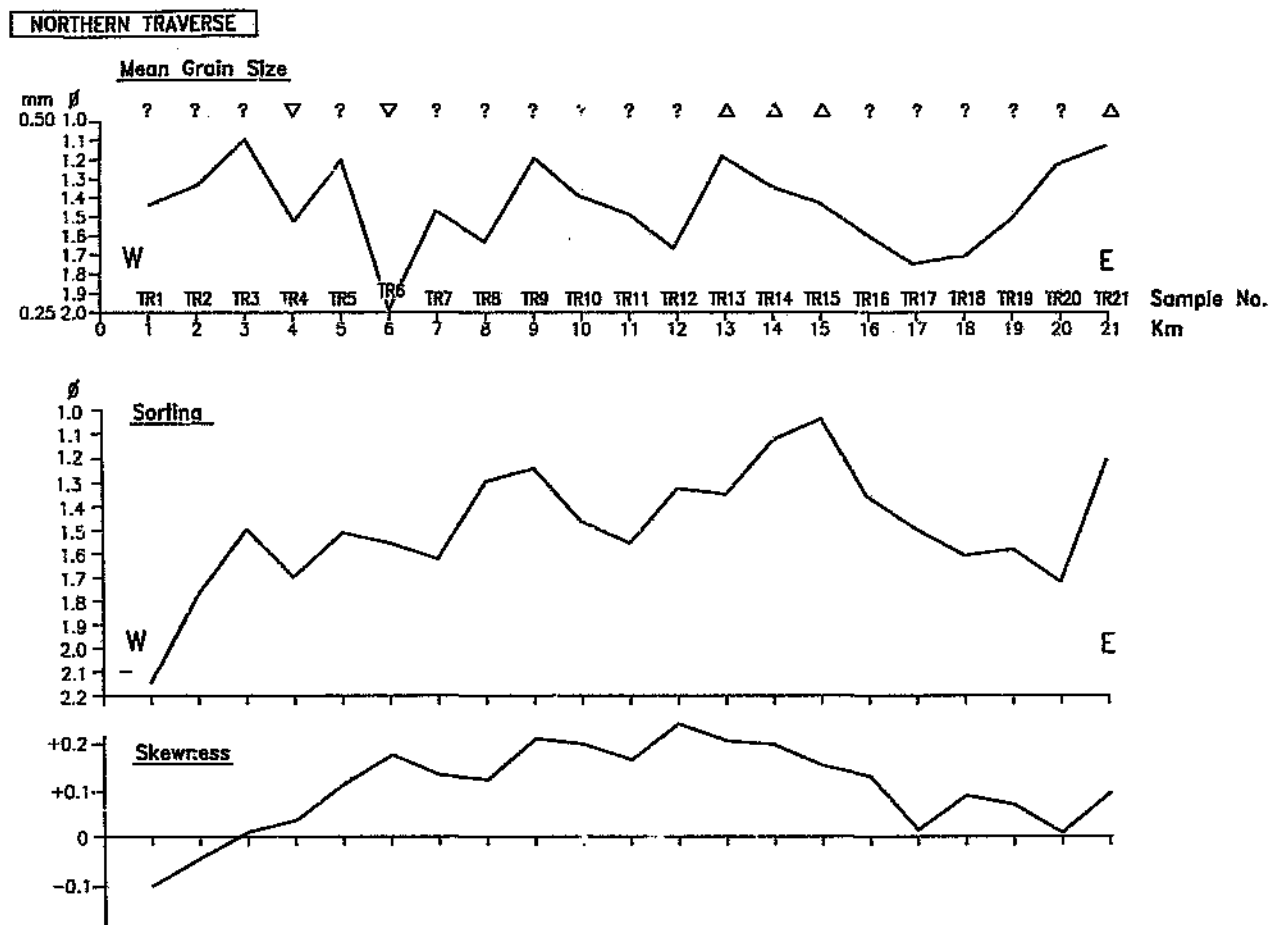


Figure 7.9 Sedimentary parameters for the northern traverse.

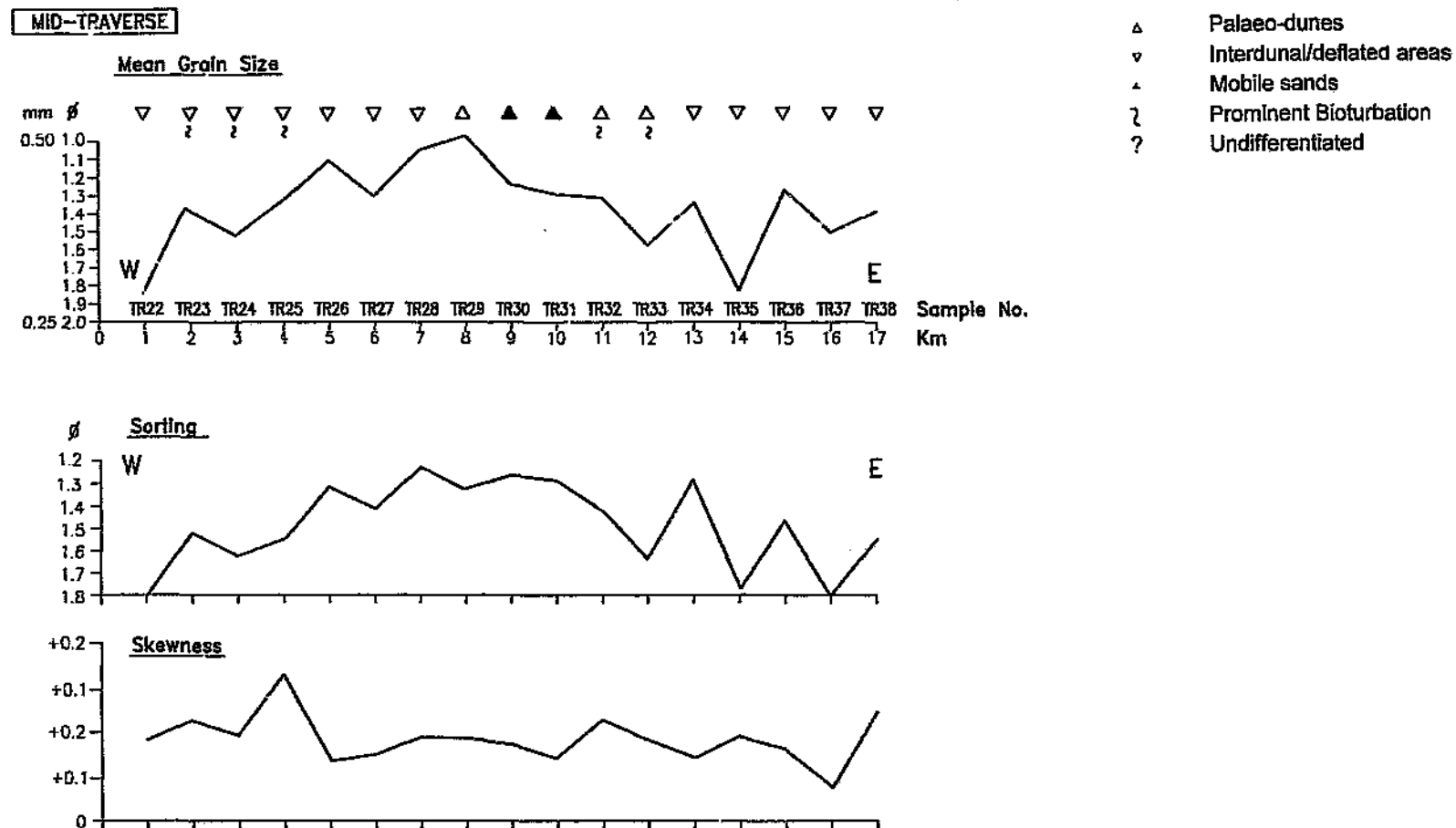
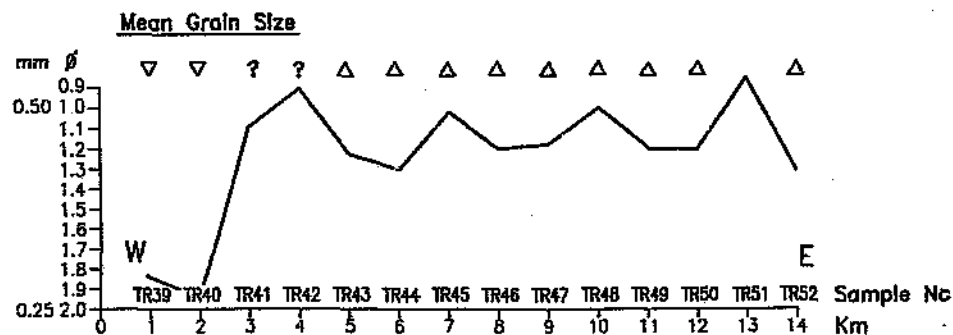


Figure 7.10 Sedimentary parameters for the mid-traverse.

SOUTHERN TRAVERSE



- Δ Palaeo-dunes
- ∇ Interdunal/deflated areas
- \triangle Mobile sands
- $\}$ Prominent Bioturbation
- $?$ Undifferentiated

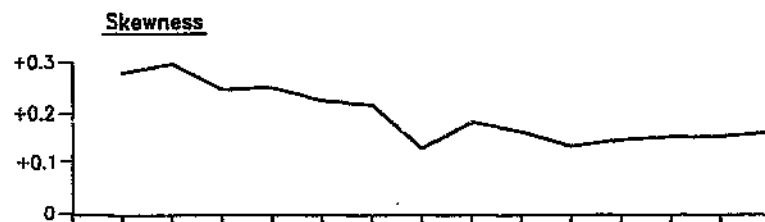
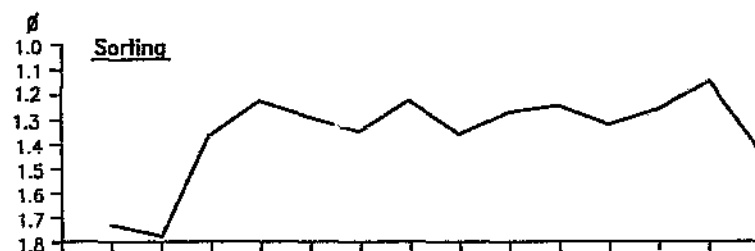


Figure 7.11 Sedimentary parameters for the southern traverse.

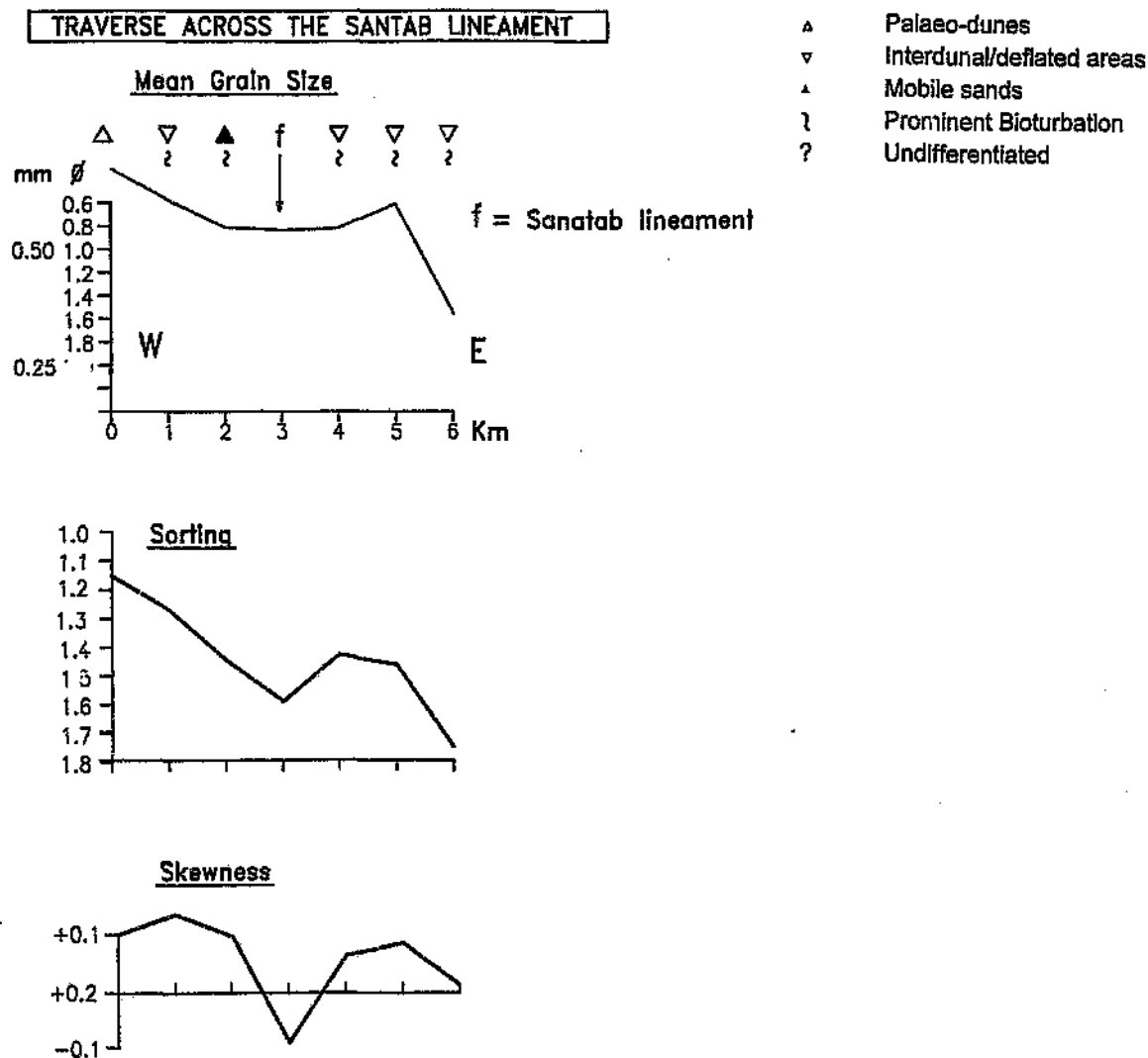


Figure 7.12 Sedimentary parameters for the Santab lineament traverse.

Mean grain size

From the above figures it is evident that the range of mean grain sizes of samples collected from areas identified as aeolian dunes ranged from 0.8 to 1.6 ϕ . Interdunal areas are much more variable in sediment type than aeolian dunes and generally contain a higher percentage of clay as well as a coarser fraction, and hence have a greater range of mean grain sizes: from 0.8 to 2 ϕ . The range of grain size values is similar to the range of values obtained for the individual micro-environment studies (e.g. aeolian deposits gave a range of 1 to 1.6 ϕ).

Mean grain sizes for samples collected on a traverse perpendicular to the Santab lineament (Figure 7.12) all lie within the range determined for the above mentioned three traverses, and no noticeable systematic changes in this parameter are seen across the lineament. Even field observations did not show any distinct differences in size characteristics and colour, although quite evident from the air (Figure 7.8). The western side of the lineament is characterized by red, and what appear to be more mobile dune sands, whereas the eastern side is browner in colour, typical of more stable areas. Basement (predominantly Karoo Supergroup rocks in this area) was found to be at very shallow depths, and exposed in places on the eastern side of the lineament, whereas the surface sediment appears to be mobile, or deposited more recently, on the western side of the lineament.

An important observation of these results is that there are no obvious changes in grain sizes across the traverses, and that the range of grain sizes in a single dune is approximately the same as that over the entire area. The implications of these results are discussed later in this section.

Sorting

The sorting graphs (Figures 7.9, 7.10, 7.11 and 7.12) show a similar pattern to the mean grain size graphs, except for a portion of the sorting graph in the "northern-traverse" plot. This profile, using Landsat imagery (Figure 7.7) was identified to be cross-cut by drainage (particularly in the vicinity of Sample numbers TR6 - TR15). Besides this exception, the sorting for all the traverses generally improves with a corresponding increase in mean grain size. The range of values for sorting, as determined from the three graphs (northern, mid- and southern traverses) for dune dominated areas is: 1 to 1.65 ϕ . For interdunal and lower lying (deflated) areas the range for sorting is again much higher due to the variability of the sediments encountered in such environments: 1 to 2.1 ϕ .

For the Santab lineament traverse (Figure 7.12) sorting is also generally better in the aeolian dominated areas with poorer sorting observed on the eastern side of the lineament.

Skewness

The skewness graphs for the northern, mid- and southern traverses (Figures 7.9, 7.10,

7.11 and 7.12) exhibit positive (fine skewed) values for 50 of the 52 sampled sites. Generally skewness is fairly consistent fluctuating around approximately 0.2 - 0.3 for most of the samples. The southern profile shows a gradual decrease over the first half of the profile, and is fairly consistent over the second half which consists only of aeolian dunes. The range of skewness values for aeolian dune micro-environments as determined from all three profiles ranges from 0.09 to 0.37. Interdunal areas, in this case, have a similar range, that is, 0.05 to 0.33.

The skewness graph for the traverse across the Santab lineament (Figure 7.12) show similar skewness values on both sides of the lineament.

Discussion

As indicated by aerial photographs and satellite images (e.g. Figure 7.1), the present, or surface deposits of the Bushmanland Plateau, which overly the Vaalputs and Dasdap Formations, are primarily the result of aeolian processes during arid conditions. Besler (1983) conducted a study of 393 sand samples from the Namib sand sea, the Kalahari, the Rub'-al-Khali, and the western and eastern Sahara, and developed a response diagram to distinguish between sand particles that exhibit aeolian mobility in response to the present wind regime. All the samples of this study fall within the range of what Besler refers to as stable aeolian deposits, suggesting that the dunes encountered in the study area are all in a stable state, or in a state of degradation. It should also be noted that Besler (1983) reported ϕ values of around 1.0 and of up to 1.2, for mean grain sizes and sorting respectively, for stable aeolian deposits, under similar conditions to those experienced at Vaalputs. These values are very similar to those obtained for this study (c.f. Figure 7.6).

Schlegel et al. (1989) reported regional grain size and heavy mineral studies over selected parts of the southern Kalahari sand cover and concluded that dune crest sands could be readily distinguished by their fineness (and better sorting) in comparison with what they termed "mixed sands". The latter they found to be predominantly fluvatile in nature, with some aeolian sands. Schlegel et al. (1989) obtained a range of mean grain sizes for the dune crest sands and the "mixed sands" of 1.61-2.77 ϕ (mean: 2.11 ϕ) and 1.26-2.76 ϕ (mean: 2.16 ϕ), respectively. This distinction is clearly visible in Figure 7.6a which shows finer mean grain sizes for the dune crest samples. Mean grain sizes for this study are generally larger than those of Schlegel et al. (1989) with

dune crest sands of the Vaalputs area falling into the range of 1.25-1.60 ϕ .

The thicker sands on the leeward side of the dunes appear to reflect greater sand accumulation and are also the least bioturbated part of the dune. As the dune troughs define drainage paths and the dune crests are generally in a state of degradation, they cannot readily be distinguished by sorting, as those of Schlegel et al. (1989) in the southern Kalahari.

According to Leeder (1982) wind-blown deposits generally show positive skewness because of the low tendency of wind in moving coarse particles which are usually left behind in the form of a lag deposit. The results of the skewness essentially reflect those of the mean grain size and sorting, and which is believed to be a consequence of greater deflation or degradation on the windward side of the dune. In addition, Lancaster (1981) noted the lack of systematic grain size distributions across the profile of active dunes in southern Africa, which he attributes to post depositional pedogenic weathering, and which may well effect the grain size distribution of this study.

Dune stabilization and modification

The dune deposits of the study area have been modified by degradation and erosion, as well as some localised aggradation. The lack of sedimentary structures noted in cut-sections (windward and leeward sides) is believed to be primarily due to the extensive bioturbation observed in the study area. As previously mentioned the atypical low amplitude of the dunes are suggestive of some degradation or lowering. Small pans have developed in the dune streets, and locally on the dunes themselves. Thomas (1988) reported the occurrence of very similar 5 metre high dunes in the Kalahari, which he strongly believes to be regraded stabilized features, principally under the effect of sheetwash (Flint and Bond, 1968).

The partly degraded dunes appear to be stabilized to a large extent by a subsurface calcrete layer. Several well preserved dunes were investigated, the shapes of which were all found to be associated with such a sub-surface layer. In certain cases the calcrete approximately defines what appears to be the original aeolian dune surface, as the calcrete layer has a more enhanced shape or typical dune morphology (Figure 7.13a). That is, the calcrete appears to have formed after deposition of the dune at a fairly shallow depth below the dune surface (Figure 7.13b). Calcrete formation

presumably resulted in the stabilization of the dune form during a period of little or no aeolian deposition. Continued and downward precipitation of calcrete, as well as degradation are believed to have given rise to the landforms of the present day, with some localised aggradation taking place on the leeward sides of the dunes resulting in an increased thickness of sand on this side (Figure 7.13c). The thickness of sand on the windward side is generally reduced, often exposing the calcrete horizon.

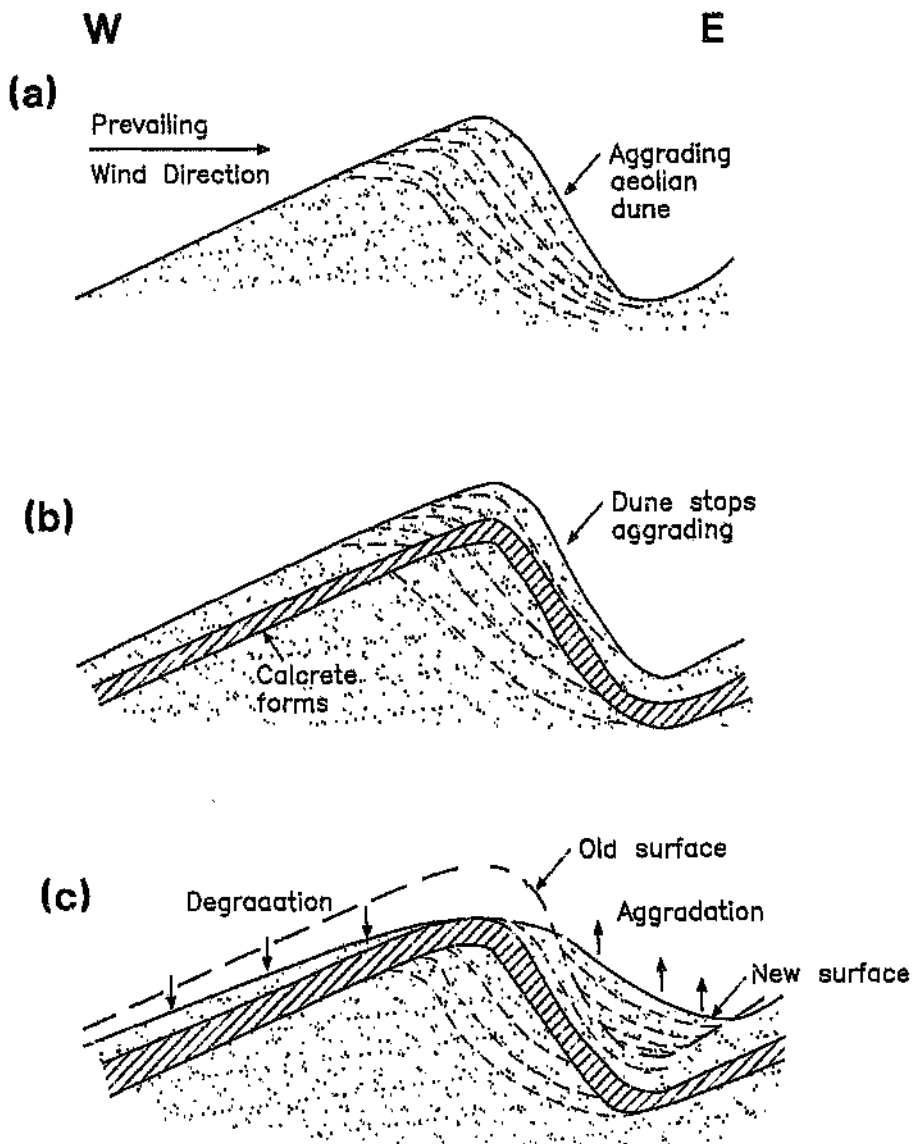


Figure 7.13 Stages of dune formation (a), dune stabilization (b), and dune modification (c).

The present state of the dunes, that is, low amplitude features (due to degradation) with generally more degradation on the windward side and accumulation of sediment on the leeward side, and mixed by bioturbation processes, would result in small lateral variations (mean grain size and sorting) of a massive clay rich, but overall coarse sediment. The stabilizing mechanism for these dune forms is the calcrete horizon which appears as an undulating calcrete layer in section and which migrates downwards with continued overall degradation.

Discussion of the traverse results

Most of the sedimentary parameters obtained for this study are similar to those obtained for the study of the micro-environments, that is, the ranges for the various sedimentary parameters observed along the traverses are similar to those of an individual dune.

The prevailing wind is from the southwest, and hence a decrease in grain size might be expected in a northeasterly direction. A sand source in the southwest, as suggested by McCarthy et al. (1985) would have accentuated such a decrease in grain size. The three long traverses, however, show no decrease in mean grain size from the western marginal scarp. Instead, the mean grain sizes vary with local micro-environment.

Although no obvious changes in mean grain sizes were noted across the Santab lineament and the fact that the basement in this area was found to be at very shallow depths, and exposed in places on the eastern side of the lineament suggests that the dune deposits have accumulated on what appears to be the downthrown side of a north-northwest trending fault. Also, the less consolidated sediments on the western side of the lineament appear to be younger, suggesting that faulting or fault reactivation may have taken place in the recent past along this lineament (discussed in Chapter 8).

The "mirror-relationship" of sorting to mean grain size for the aeolian deposits is attributed to the sorting abilities of aeolian processes, particularly the removal of fines. All the sorting values correspond well with the range of values obtained for an

individual dune. The better sorting observed on the western side of the Santab lineament is again most probably due to the sorting abilities of aeolian processes.

According to Friedman (1961) positive skewness is normal for aeolian sands. Skewness, as seen in the three graphs (northern, mid- and southern traverses) is the only parameter which does not show any obvious correlations or trends with a particular micro-environment, or distance from the proposed source terrane in the west. The dunes have a reasonably limited range of skewness values, which is similar to the range obtained for an individual dune. The Santab lineament has no effect on skewness for the sediments collected along the traverse.

The primary aim of this investigation was to determine the source terrane from which the sediments were derived, the reason for the generally coarse average particle size, and to attempt to relate average particle size to proximity of the source. Although Friedman (1961) classified several depositional environments according to these three parameters, the sediments in the Vaalputs area were noted (also by several other workers, e.g. McCarthy et al., 1985), not to conform to Friedmans proposed fields. From the traverse results it is, therefore, evident that the basement outcrops in the west are not the primary source of the surficial aeolian features, and rather that the underlying Vaalputs sediments are the major source of material. A more detailed account of the source of these sediments is given, after a comparative particle size analysis and chemical analysis is presented (Sections 7.7 and 7.8).

7.3 Deflation Pans

The most common closed basin in southern Africa is the pan, generally associated with temporary water bodies, and may vary in size from ephemeral puddles a few metres in diameter to structural basins such as the Etosha Pan in Namibia (Shaw, 1988). The unconsolidated Kalahari sands and friable sedimentary rocks of the Dwyka and Ecca shales are associated with the greatest number of deflation pans in southern Africa, due to, in part, their "lack of resistance" (Goudie and Thomas, 1985).

Occurrence of deflation pans in the study area

As deflation (the sorting, lifting, and removal of loose, dry, fine-grained clay/silt/sand particles by the turbulent eddy action of the wind) dominates certain parts of the Vaalputs land surface, deflated areas and deflation pans are sporadically developed in this region. As in the case of the aeolian deposits and dune forms, deflated areas are best developed on the eastern half of the Vaalputs property. Figure 7.14 shows a typical deflation pan on Vaalputs. Deflation pans are generally developed in inter-dune (trough) or low lying areas. They were also noted to occur on more stable and horizontal sub-outcrop such as basement or older sediments.



Figure 7.14 Typical occurrence of a deflation pan on the eastern side of Vaalputs.

Appearance

Deflation pans are typically 70 to 80 metres in diameter and usually fairly circular in plan view. Pebbles may be found scattered on the pan surfaces and include, in order of abundance, blue quartz pebbles, ferricrete nodules, fragments of basement, and sandstone/silcrete fragments. Calcrete nodules may also be found on the surface or close to the surface of the pan. Calcrete is commonly found at depths of about 30 centimetres below the pan floor. The calcrete layer, although usually fairly fragmented, nodular, or jointed, is impenetrable using conventional digging and auguring methods. A section through a pan floor is shown in Figure 7.15.

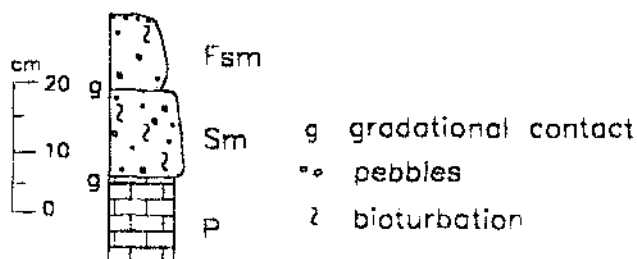


Figure 7.15 Section and simplified stratigraphic sketch through a deflation pan floor.

Approximately 15 to 25 centimetres of brown muddy sands typically overlie the calcrete horizon. These sands may be partly calcretized and show evidence of some bioturbation (Figure 7.15). They are in turn overlain by no more than 12 centimetres of brown muddy grits and sands which typically fine upwards (from coarse grits to coarse sands). Some pebbles, including calcrete nodules may be scattered throughout this upper muddy layer. Bioturbation may be present in the muddy sediment, depending on the degree of consolidation of the material: no bioturbation was found on well

developed muddy pan floors suggesting that this part of the pan is an inhospitable environment for any burrowing animals.

The deflation pans typically have a crescentic dune feature or lunette on the leeward side of the pan, which is composed of aeolian sands and clay, derived from the pan floors. Only the more developed and larger pans have well developed lunettes. Evidence of bioturbation was noted in the lunette deposits. The lunette surfaces may also be scattered with coarse blue quartz, ferricrete and calcrete fragments and appear to be stabilised to some extent by vegetation (shown in the foreground of Figure 7.14). The primary drainage into the pan is usually developed on the opposite side to the lunette. This drainage inlet is typically marked by a higher density of vegetation, which in turn acts a sediment trap, resulting in a slight progradation of coarser material toward the central part of the pan (also shown in the plan views of deflation pans: next section).

Deflation pans in plan view

Field observations together with other results of this study allowed for the determination of maturity of the deflation pans. A mature pan in this study simply refers to a large pan with a well developed consolidated muddy pan floor, whereas an immature pan is generally smaller, with obvious deflation on a less consolidated surface. One deflation pan identified as poorly developed or immature, and two well developed or mature deflation pans are described and shown in plan view in the following section. Figure 7.16a and 7.16b shows what is believed to be an immature and a mature deflation pan respectively.

Plane-tabled sketch maps of what is believed to be an immature deflation pan, and a mature deflation pan are shown in Figures 7.17 and 7.18 respectively. Both these deflated features were developed in interdunal areas. Figure 7.19 is a plane-tabled sketch map of a mature deflation pan developed on a solid or more resistant, and exposed substrate. In this case the substrate is an altered sandstone, but is more typically a calcrete or ferruginized sand (dorbank). A mature pan developed on such a substrate may expose an extensive area of the underlying resistant material upwind of the pan.

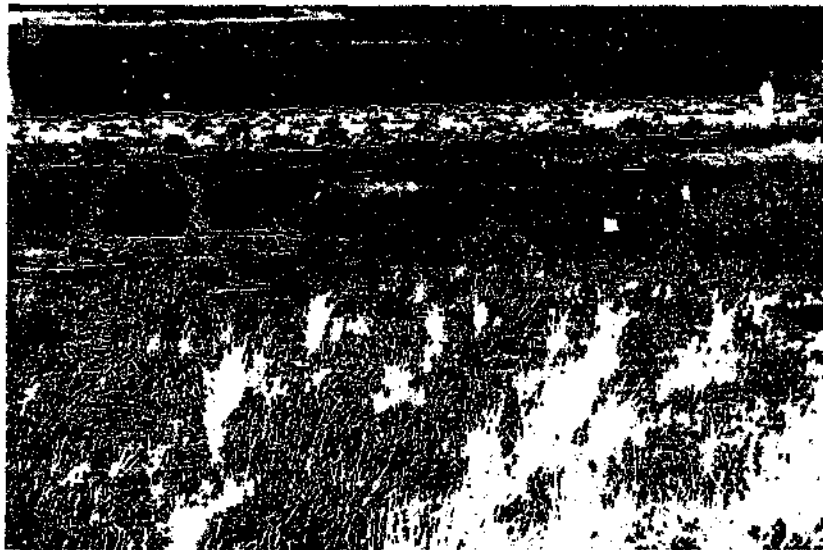
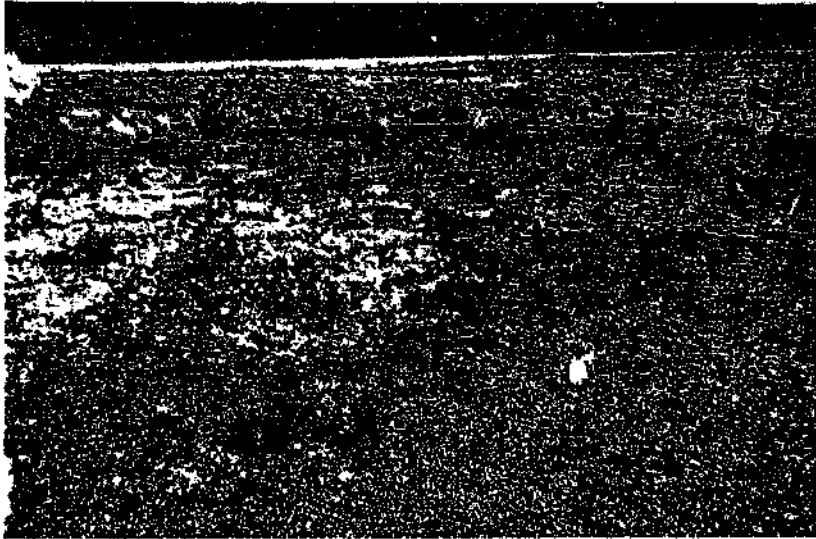


Figure 7.16 (a) Immature deflation pan. Note the highly bioturbated and pebble strewn pan floor. (b) Mature deflation pan with well developed lunette and muddy pan floor.

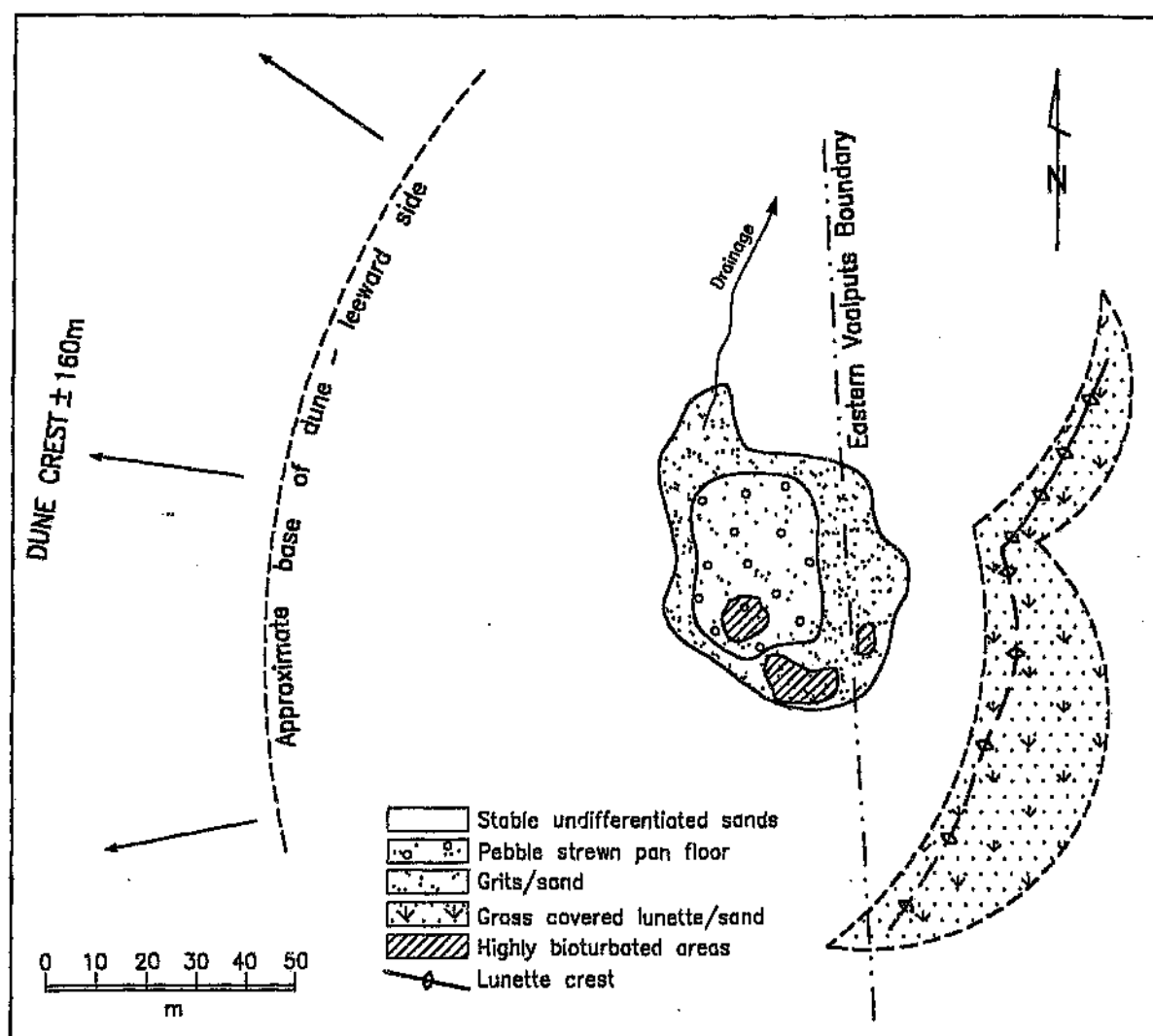


Figure 7.17 Plane-tabled sketch map of an immature pan, developing in an interdunal area, on the eastern boundary of Vaalputs.

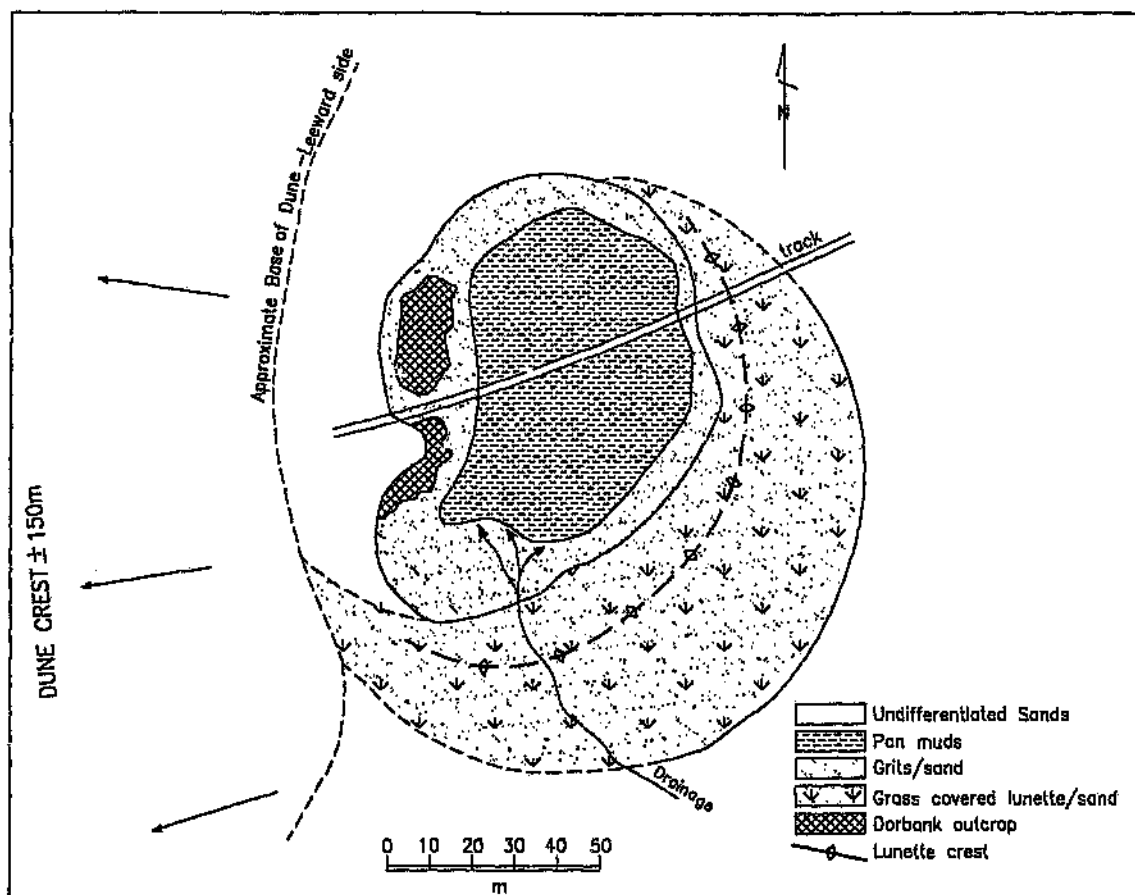


Figure 7.18 Plane-tabled sketch map a mature deflation pan, developed in an interdunal area, approximately two kilometres to the southeast of the disposal site.

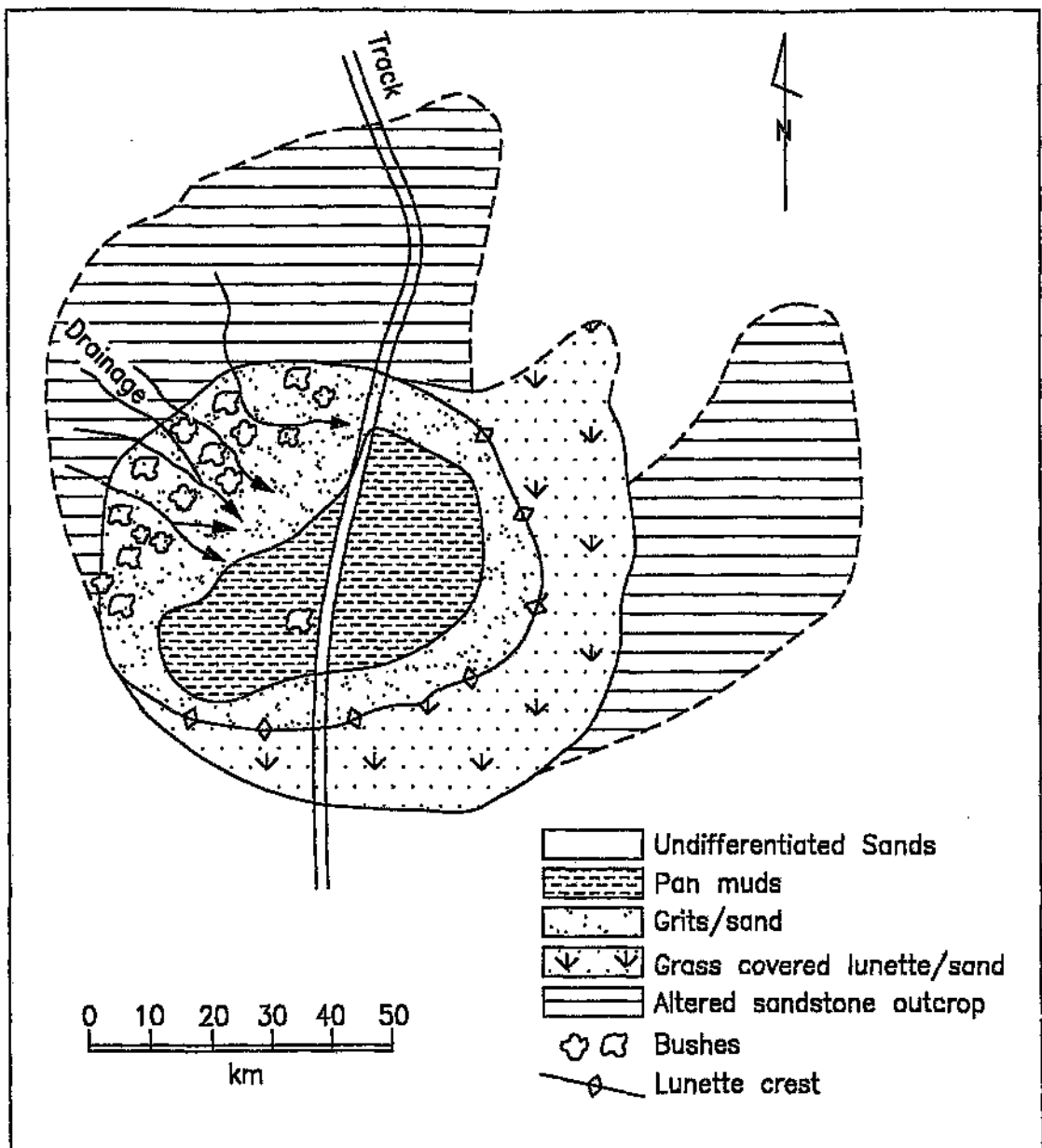


Figure 7.19 Plane-tabled sketch map of a mature deflation pan, developed on a resistant, horizontal substrate, approximately two kilometres to the south east of the Vaalputs airfield.

Deflation pan topographic profiles

Two topographic profiles (Figure 7.20) orthogonal to each other, in a north-south and an east-west direction respectively were obtained for a mature deflation pan of the area. This deflation pan has a maximum depth (lunette crest to floor) of 0.5 metres. The deflation pans are asymmetrical along both the east-west and north-south profiles. As

shown by Figure 7.20 there is a net accumulation of sediment on the southern and eastern sides of the deflation pan. This sediment accumulation relates to the prevailing wind directions and to the orientation of the dunes for this area. Lancaster (1978b) noticed a trend in pan shapes which parallel the dominant wind direction, and which, in part, he attributes to the product of adjacent dune alignments.

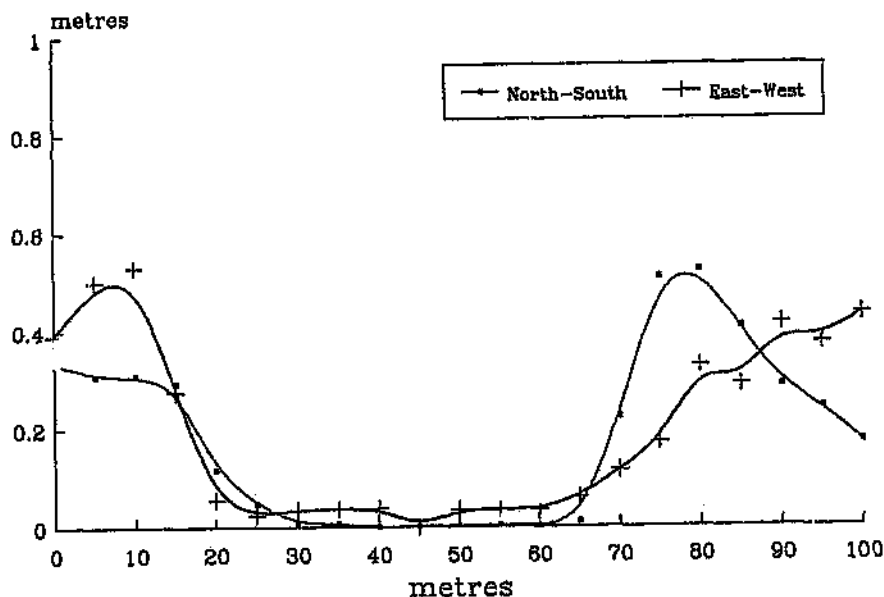


Figure 7.20 North-south and east-west profiles across a typical deflation pan in the study area.

Sand size analysis

Four deflation pans were investigated and the different sedimentary constituents were selected for a particle size analysis. The sedimentary constituents sampled included: the fine brown surface muds of the pan floor, the underlying brown muddy sands, and the surface and 30 centimetres depth material of a lunette dune deposit. The aim of this study was again to determine the grain size frequency distribution, characterising the different sediments which may be associated with the deflation pan environment, and which could be compared to the older sediments of the Vaalputs Formation. Average sedimentary parameters obtained for the constituents of the deflation pans studied are tabulated in Table 7.1.

Table 7.1 Average sedimentary parameters for the constituents of a deflation pan.

	Mean grain size (ϕ)	Standard deviation /Sorting (ϕ)	Skewness
Pan floor	2.14	1.64	0.07
Pan 30 cm depth	1.65	1.55	0.11
Lunette surface	1.06	1.46	0.10
Lunette 30 cm depth	0.75	1.47	0.09

Mean grain sizes for the pan sediments (surface muds and underlying pan sediments) are highly variable (3.13 to 1.15 ϕ / 0.1 to 0.45 mm) due to the highly variable nature of the pan floor sediments which may be dominated by silt and clay size particles or may be predominantly sandy. The latter case is usually found in less mature pans. Pan floor sediments from mature pans are the finest sediments within this environment. Lunette deposits are dominated by medium to coarse sands (1.32 to 0.75 ϕ / 0.40 to 0.59 mm), with typical values around 0.80 ϕ (0.57 mm). These sediments are generally coarser than other aeolian deposits such as those obtained for aeolian dunes (c.f. Figure 7.6a).

Standard deviation (sorting): sorting parameters for pan sediments (muds and underlying muddy sands) range from 1.11 (poorly sorted) to 2.17 (very poorly sorted). The pan floors consist predominantly of muds which appear to be comprised of similar particle sizes, however, within the smaller particle size range there is a large spread of sizes. That is, particles of all sizes, but generally smaller than approximately 2 ϕ (0.25 mm) accumulate in the pan muds. A much coarser, sometimes pebbly fraction may also be found on the pan floor surface, making the sorting even worse for these sediments. Lunette deposits show a range of sorting from 1.38 to 1.53 (poorly sorted). The poor sorting is presumably a direct function of the poorly sorted source material.

Skewness: all the deposits associated with deflation pans are near symmetrical to fine-skewed. This is due to the enrichment of fine sand and silt size particles which are

typically found on the pan floor and which form a significant proportion of the underlying, and often more sandy, deposits. These finer sediments form a "tail" of finer grains, resulting in the positive or fine-skewness. The lunette deposits are also comprised of both fines and coarse material, however, they tend to be slightly fine-skewed, due to the silt (rather than mud) size particle content in these sediments.

Petrology and mineralogy

Deflated deposits exhibit a wide range of compositions and grain sizes, ranging from almost 100 % silt and clays to coarse particles set in a clay to silt sized matrix. The coarser clasts and grains, when present also show a wide range of compositions (in order of abundance): quartz, various lithic fragments, feldspar (mostly altered), and small amounts of ilmenite and magnetite. The grains are typically subrounded to angular. The oxide grains are generally more rounded than the other types, and may be rounded to subangular. Sphericity of grains varies from low to high. Most quartz grains are coated in hematite or partially replaced by an iron oxide. The feldspar grains and rock fragments are typically replaced by iron oxide. A modal analysis of the grains of a coarse deflation deposit revealed a high iron oxide cemented (or rock fragment) percentage: 58%. Quartz and altered feldspar grains typically constitute 29% and 13 %, respectively.

Discussion

Enclosed depressions on the landsurface may be formed by a variety of processes, including tectonism, epeirogenesis and volcanic activity, meteorite impact, weathering, and geomorphological processes in both erosional and depositional contexts (Shaw, 1988). Shaw also noted the importance of animal and human activities and according to Flint and Bond (1968) deflation pans have diverse origins, including erosion by animals. In many parts of southern Africa deflation pans are distributed apparently at random, but as noted by Shaw (1988), may be associated with specific landforms, such as sand dunes, which may impede local drainage. The lack of integrated surface drainage in areas of pan development is commonly a result of the distribution of aeolian landforms and the highly permeable sand cover, which predispose such a landscape

to pan formation (Shaw, 1988).

Most pans in the study area seem to develop in the inter-dunal or trough areas, starting out as "open drainage" in which water may escape and flow along the trough (parallel to the dune crests). Hambleton-Jones (1986) found that interdune troughs have a gradient of approximately 1:500 and that drainage in these troughs is ephemeral, tending to evaporate or infiltrate rapidly. This would also allow for a possible mechanism for additional calcrete formation. In these early stages bioturbation by small burrowing animals appears to be a dominant process. A combination of bioturbation and deflation results in a concentration of coarse sediments and pebbles on the deflated floor (bioturbation loosens the finer material, making it easier to be removed by the wind). It is due to the dune field morphology and the strong prevailing winds of the region that certain trough areas are selectively deflated. The deflated material is deposited on the margin of the pan as a lunette. It should be noted that the orientation of the lunette is a function of the resultant winds of the region. The orientation of the lunette deposits is similar to the general trend of the longitudinal aeolian deposits in the region, that is, they are oriented approximately in a north-northeast direction with a transverse component to the east. With continued deflation the lunette increases in size and becomes more concentric.

During ephemeral rain storms water borne fines are deposited on the deflated floor. These impermeable muds dry to form a very hard layer finally causing bioturbation to cease, which in turn promotes the development of a well developed or mature deflation pan. The pebbles which are often noted on the pan floor have been suggested to have been "squeezed upwards" (Dr. I. Stengel, pers. comm. and Jessup, 1960; Cooke, 1970), from the pebble layer which accumulated in the immature stages of pan formation, by wetting and drying processes, causing expansion and contraction of the clay-rich, muddy sediments. Watson (1992) suggested other processes for the accumulation of coarse material in deflated settings: deflation of fine particles leaving a lag of coarse material on the surface and eluviation of fine-grained atmospheric deposits and their illuvial accretion beneath the gravelly surface (McFadden et al., 1987). Although these processes may play a role in the initial stages of deflation pan

formation (Figure 7.16a), the most likely process for the development of pebbles on a well developed muddy deflation pan floor (Figure 7.16b) appears to be a result of the upward movement of gravel-sized fragments through the mud as a result of volumetric changes in the host material caused by wetting and drying (Jessup, 1960; Cooke, 1970). No sedimentary structures left by this process, however, were noted in the muds of deflation pan floors. The suggested stages of deflation pan development are shown in Figure 7.21.

Duricrusts are a common manifestation of pans (Shaw, 1988). Calcrete types associated with pans (Goudie, 1973, 1983; Netterberg, 1980) range from calcic soils to massive hardpan calcretes and occur as both precipitates and alteration products. Calcrete has been noted (Shaw, 1988) to extend several hundred metres beyond the pan, usually on a subsurface drainage alignment. Ferruginized sands, referred to as "dorbank" in the study area, may well be associated with deflation pan development as it was commonly found at the margins of mature deflation pans of the region (shown in plan view - Figure 7.18). The exact subsurface extent of this ferruginized sediment was not determined and it is possible that it may also be associated with other stable areas. A more detailed account of this duricrust-type is given later in this chapter.

Other small, flat deflated areas (usually about 10 metres in width and fairly concentric) were noted on the slopes of dunes. The hardening of these areas is believed to be due to termite activity (termite "networks" were noted below these surfaces), caused by the binding of sediment in the construction of their tunnels. These areas are devoid of vegetation due to the presence of termites (and due to the hardness of the substrate). No additional sediment is likely to accumulate on these surfaces due to the lack of stabilising vegetation. These deflated areas do not appear to develop into mature deflation pans, but rather, bioturbation appears to encroach on these areas until they are completely reverted back to the original dune-type-surface. They are therefore not believed to play an important role in the development of the present landforms.

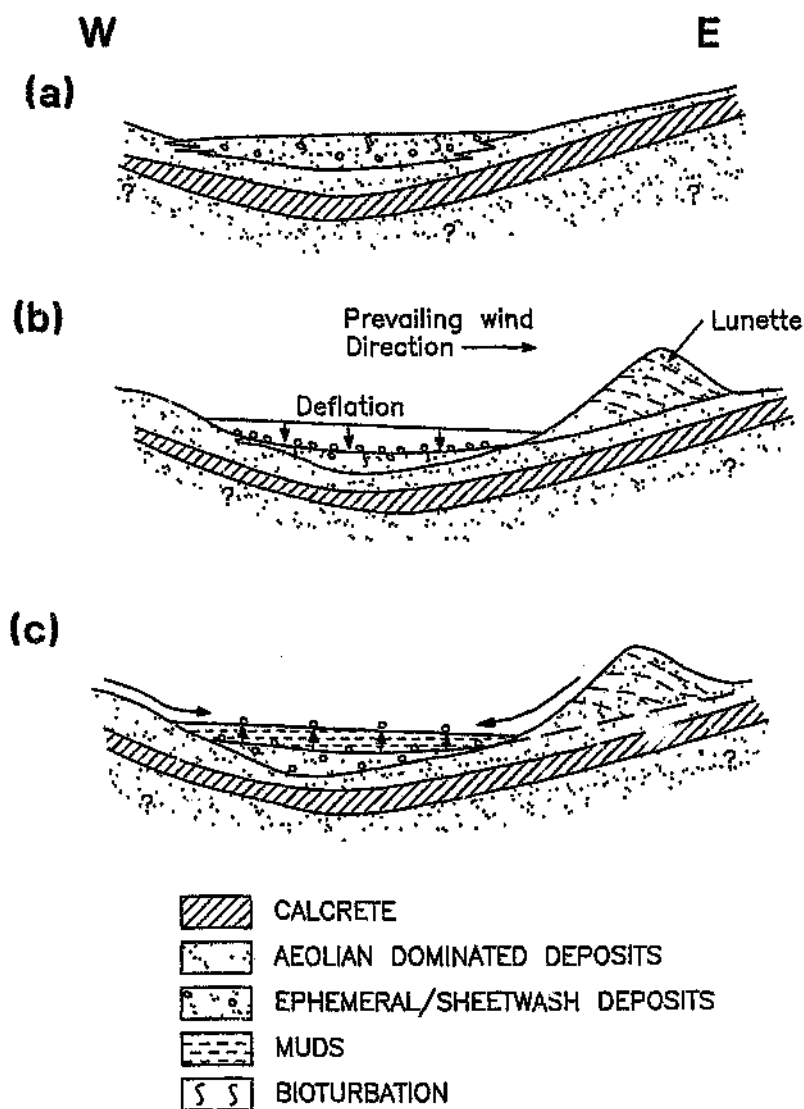


Figure 7.21 Proposed stages of interdunal deflation pan development. Sections are west-east, that is, most of the migration would be predominantly in a direction into the page.

Although not a common occurrence on the present landsurface the preservation potential of deflation pans is assumed to be fairly good, assuming burial at a mature stage. Preservation of these features is likely due to the fairly resistant calcrete horizon often found underlying the hardened muddy central pan deposits. Such deposits would be expected to be identified by a finning upward sequence overlying a calcrete (or an

iron rich) layer. Dispersed pebbles (predominantly blue quartz) may or may not be present on top of the muddy unit. The fine muds and silts at the top of such a sequence would be diagnostic, as no other micro-environment in this region was found to be comprised, in any way, of such sediments. Lunette features associated with these deflation pans would be preserved as homogeneous, poorly sorted sediments such as those described in the previous section for the deflated and bioturbated aeolian dune deposits. It should be noted that none of the features of pans described above were observed in the sections of the Vaalputs sediments suggesting that pans were not formed during the deposition of the Vaalputs Formation.

7.4 Lag Deposits

Several sites on the present land surface were noted to be almost entirely covered by pebbles. Although not a common occurrence in the study area, they are a constituent of the landsurface of the study area and are, therefore, briefly described below.

Occurrence of lag deposits

Pebbly lag deposits consist of fairly large areas (up to approximately 1 km²) of relatively flat or slightly inclined terrain (Figure 7.22a) which are strewn with pebbles of various lithologies (Figure 7.22b). An area approximately 15 kilometres to the south of Vaalputs, alongside the main Springbok - Platbakkies road, was identified to be dominated by lag deposits (Figure 7.22a). The dominance of sheetwash at this site is due to its location, on relatively high ground and fairly close to the marginal scarp or watershed.

Appearance of lag deposits

The sub-angular to rounded pebbles include: several forms of vein quartz, ferruginous nodules, calcrete nodules, and several types of basement lithologies (Figure 7.22b). At one particular site calcrete was found to outcrop slightly upslope of the deposit, resulting in a calcrete lag deposit (Figure 7.22c). Lag deposits, in general, are rarely thicker than a few centimetres and the underlying sediments appear to be predominantly aeolian in nature, containing scattered pebbles, most likely as a result of bioturbation.

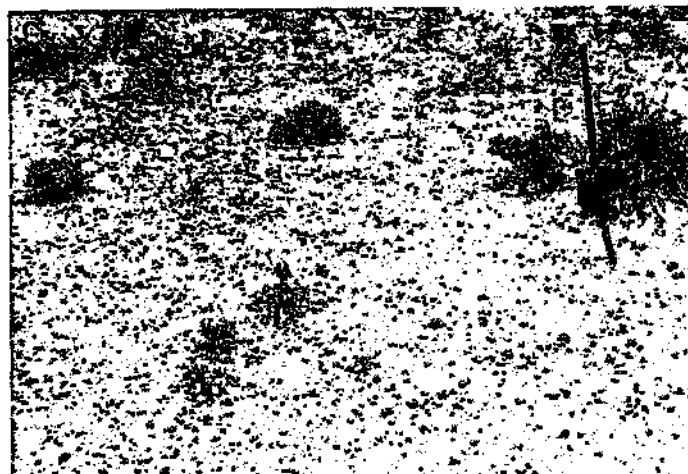
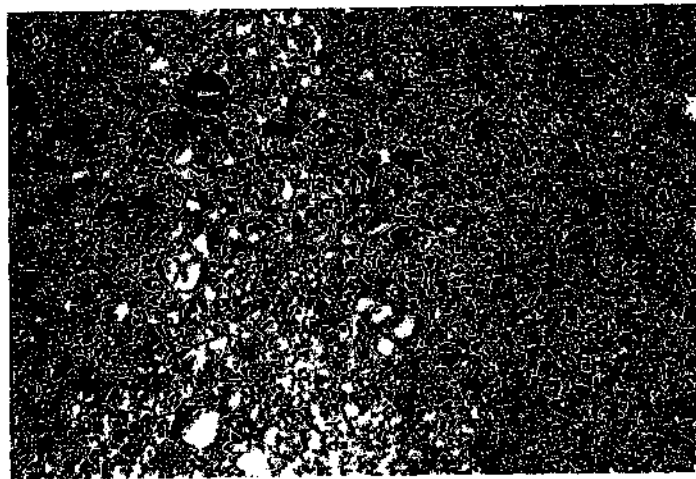
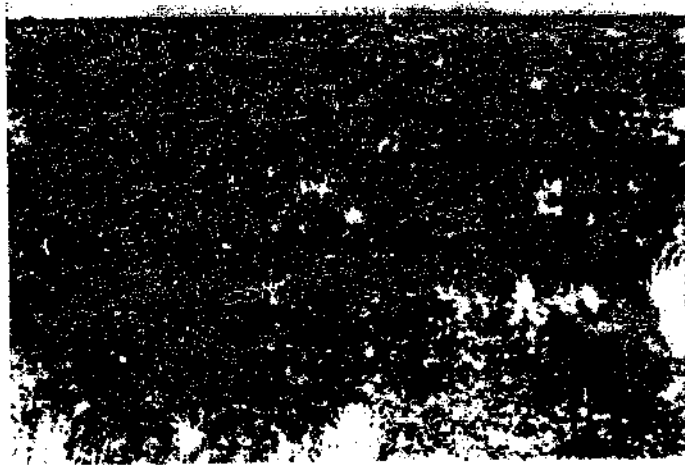


Figure 7.22 (a) Typical lag deposits on the present land surface. (b) Terrane covered by lag deposit showing typical subrounded pebbles of various compositions. (c) Calcrete lag deposit resulting from calcrete outcrop in the vicinity of the deposit.

Grain size analysis

Two surface deposits, and one from approximately 80 centimetres depth, identified as lag deposits were sampled for this analysis. Due to the pebbly nature of the samples, large (up to 1.35 kg) samples were required for a representative particle size analysis. As with previously described micro-environments, these coarse deposits were studied in an attempt to correlated with, and compare to, the older, underlying pebbly deposits which are clearly exposed in the trenches in the Vaalputs sediments. The finer sand and silt fractions of the samples were also sieved to allow for a complete particle size frequency distribution of the sample. The data (including ϕ values for the modes) for the three lag deposits are shown in Table 7.2. Due to the poly-modal size distribution for these pebbly deposits, the frequency histograms are also shown (Figure 7.23) in order to clarify the reason for the large range of values presented in Table 7.2.

Table 7.2 Sedimentary parameters for two surface (VP-53 and VP-54) and one 80-centimetre-depth (VP-62) lag deposit.

Sample	Mean Grain Size (ϕ)	Standard Deviation (Sorting)	Skewness	Modes (phi-values)
VP-53	1.13	1.98	-0.19	-4.5, -3.5, -2, 1.5
VP-54	-0.21	3.03	-0.42	-4, 2.5
VP-62	-1.43	2.15	0.54	-2, 0.5, 1.5

Mean grain sizes vary from 1.13 ϕ (0.46 mm) to -1.43 ϕ (2.69 mm). This range of mean grain sizes is suggestive of highly variable degrees of degradation or a variable "fines content" (Figure 7.23), which is largely due to difficulties in sampling of such a deposit, that is, sampling without mixing of the underlying material. The source material was also noted to be fairly variable.

Standard deviation (sorting) may be poor or very poor (1.98 to 3.03). Very poor sorting may well be expected for poly-modal deposits such as these, which contain a large range of grain sizes (Figure 7.23).

Skewness varies from -0.42 (strongly coarse-skewed) to 0.54 (strongly fine-skewed), again, due to the highly variable grain-size distribution of these deposits.

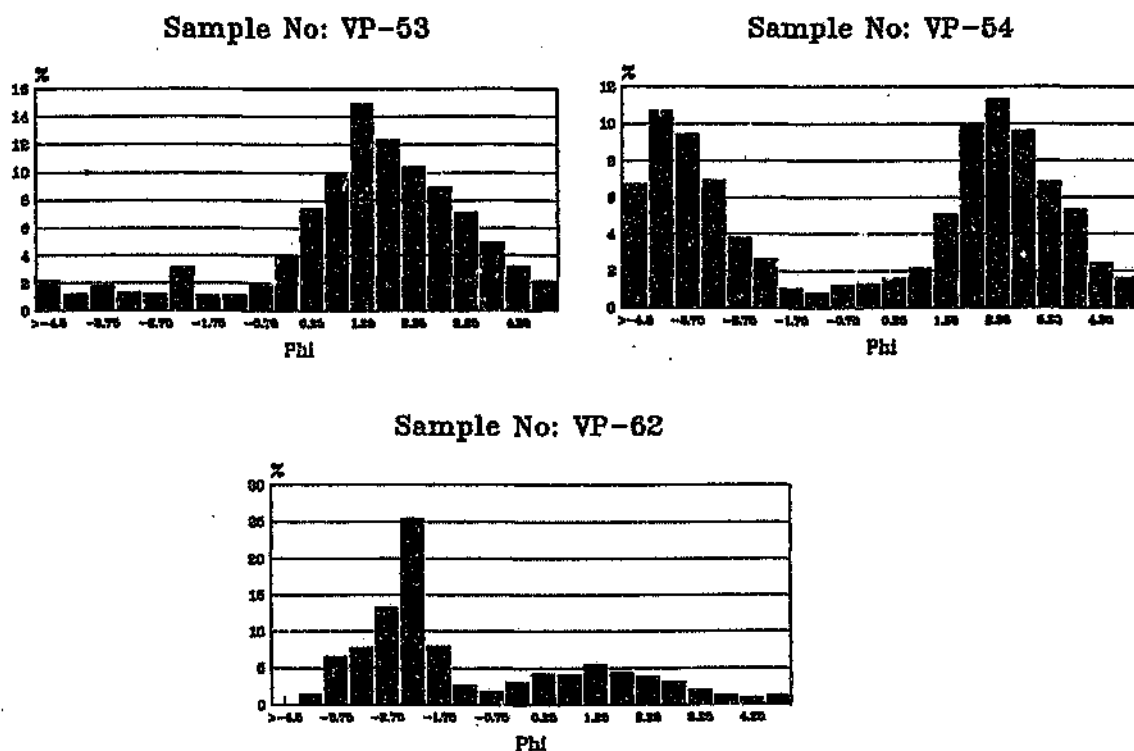


Figure 7.23 Size frequency histograms for pebble lag deposits: VP-53; VP-54; and VP-62.

Petrology and mineralogy

The clast types of the pebble fraction of these deposits, as mentioned above, consist of several forms of vein quartz, ferruginous nodules, calcrete nodules, and granite gneisses. The finer fraction of such a deposit typically shows poor sorting and sub-rounded to very angular, iron-oxide coated fragments set in a silt to clayey matrix, which usually constitutes about 3% of the sample. The grains consist predominantly of monocrystalline quartz. Both rounded to subrounded oxide grains and remobilized iron-oxide (which acts as a cement in iron-oxide concretions) are found throughout the sample, hence the reddish colour of these sands. Lithic fragments and minor amounts of altered feldspar are also present. A modal analysis of the finer fraction of such a deposit showed that quartz grains were the dominant fraction (67%), with less rock fragments and iron oxide cemented fragments (31%) and minor altered feldspar (2%).

Discussion

Although not a dominant process in the Vaalputs region, some areas are dominated by this pebble layer-forming process, which may have been a similar process, in part, responsible for the numerous pebbly lags or layers observed in the sections of the Vaalputs Formation. As shown by the sedimentary parameters these deposits show a wide range of particle characteristics due to the highly variable nature of these sediments and their source terrains. In addition the intermediate (sands) and finer fractions (muds) may be dominant, or entirely lacking. The slightly steeper slopes on which these sediments are found are believed to be a contributing factor to the removal of fines, i.e. that rain water run-off at this site probably exceeds groundwater infiltration.

Due to the coarse nature of these sediments, lag deposits would have a good chance of preservation. They would appear as isolated or laterally extensive pebble horizons in the sedimentary record. Modification by bioturbation could disperse the pebbles to some extent resulting in a mixed pebble, coarse sand, and clayey sediment.

7.5 Bioturbated Deposits

Bioturbation as defined by Richter (1936) is "all kinds of displacement within sediments and soils produced by the activity of organisms and plants". Bioturbation can take place pene-contemporaneously with deposition or after the sediment is partly or fully cemented. Bioturbation can physically alter the substrate by mixing, which results in homogenization, or may even produce new structures by compaction, dewatering, sorting, emplacement and removal (Taylor and Goldring, 1993). This variable process may destroy fine lamination or entire bedforms, depending on a number of biological factors, such as the type of organism present.

Bioturbation is extremely common in most parts of the study area and is believed to play an important role in the redistribution and mixing of the recent surficial deposits as well as in the underlying sediments of the Vaalputs Formation. Bioturbation may be found in any of the micro-environments described above and is a superimposed feature rather than constituting a specific environment as such. It has been noted on all parts

and forms of mobile and other aeolian deposits (older stable dunes and the lunette features associated with deflation pans), in areas dominated by lag deposits, as well as in other more stable areas. Bioturbation is rarely seen in the centres of mature deflation pans.

7.5.1 Types of Bioturbation

Bioturbation takes on many different forms, and may result from the activities of most of the life forms found in the arid environment of the Northern Cape. Wildlife species identified at Vaalputs are listed in Appendix C. Among these are burrowing mammals and fossorial arthropods (in particular ants and termites) which were reported by Hambleton-Jones (1986) to be capable of disturbing revegetation programmes. The following five forms of bioturbation are believed to be the primary types in the study area.

Bioturbation caused by ants and termites

Six abundant fossorial arthropods (Appendix C) are found at Vaalputs (Picker, 1987). Of these, the harvester termite (*Hodotermes mossambicus*) is by far the most widespread insect, and has the most extensive nest system. According to Picker (1987) the harvester termite constructs a varying number of nests, interconnected by horizontal and vertical tunnels. Two types of surface mounds are constructed: i) soil dumps where excavated material is deposited, and ii) openings which do not have an obvious mound structure and are only used during wet or cold weather for foraging activities. This termite brings large quantities of soil to the surface, which is not cemented in any way, and may, therefore, be rapidly degraded by wind and sheetwash processes. This material may then contribute to the biogenic horizon of the soil profile and to the sediment mixing process. In addition, studies of the common harvester ant (*Messor barbatus*) and the harvester ant (*Pheidole capensis*) have shown that the seed stores of these ants are extensive (Picker, 1987), and hence also require the removal and redistribution of large volumes of sediment.

Ant and termite mounds were noted in most areas at Vaalputs and are found on aeolian

deposits (old stable dune forms, and more recent aeolian sands), as well as in deflated areas. Picker (1987) reported termite and ant tunnels in all lithologies in the waste disposal trenches, and noted that they even find their way through harder strata such as calcrete. Different soil types do not appear to have a great effect on the tunnelling activities. Termite mounds may have two forms, both of which are low, rarely exceed 30 centimetres in height, and the nests are almost entirely below surface. Figure 7.24 shows the two common forms of the termite mounds. Termites are believed to be a major cause of bioturbation as the nests have been seen to extend to depths of 7.8 metres (where attempts to follow it were abandoned) and widths are commonly seen to exceed 0.5 metres. Depths exceeding 19.5 metres, in an attempt to reach the water table or very moist sand, were recorded by Marais (1938). Tunnelling to such depths to obtain water may well be necessary for these insects in the Vaalputs area. Picker (1987) suggests that in drier areas, such as at Vaalputs, the hives would be deeper, in an attempt to avoid heat stress, to minimize evaporative water loss, and to maintain the required 90 % humidity levels in the nest.

Picker recorded the excavation of considerable volumes of soil (associated with *Hodotermes mossambicus*), with a combined winter and summer average of 0.9 kg/m²/day and a mound density of 103 333 mounds/km². Also, the quality of the vegetation cover is an important factor in determining the intensity of soil excavation. In barren (arid) veld a far greater amount of soil is moved by the termites in attempts to cover greater foraging areas. Access to foraging areas is via subsurface tunnels, to avoid predators. In terms of biomass these termites play a considerable role in the energy flow of the region's food chain, and may be a "keystone" species in the energy pyramid of the area. In his investigations, Picker noticed that termite nests and tunnels which had been vacant for a few years soon filled with sand which suggests that bioturbation associated with termites is a highly efficient means of mixing sediment. Evidence of this type of bioturbation was noted in the Vaalputs sediments in the waste disposal trenches. Figure 6.7 shows a sand filled termite nest several metres below surface.

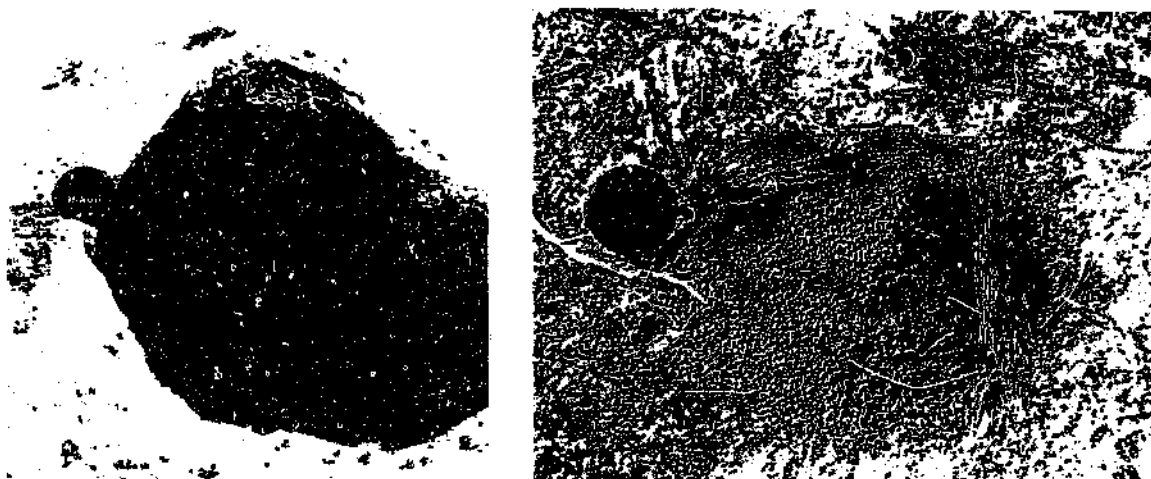


Figure 7.24 The two common forms of termite mounds observed in the study area.

Bioturbation caused by small burrowing animals

The bioturbation in dune or aeolian deposits is obvious, and consists typically of small burrows of species such as the Karoo rat (*Parotmys brantsii*), the spring hare (*Pedetes capensis*), the pygmy gerbil (*Gerbillurus paebsi*), the Namaqua gerbil (*Dermodillus auricularis*) and the suricate (*Suricata Suricata*) (Figure 7.25). Areas affected or dominated by small animal bioturbation may extend over several hundreds of square metres. Burrow widths are typically 8 to 15 centimetres in diameter. The burrow networks typically consist of a labyrinth of shallow tunnels parallel to the ground surface. The burrow network connects with the ground surface via riser tunnels which allows access for disposal of debris and also serves as feeding ports. These short tunnels are frequently backfilled with debris as burrowing continues (e.g. Vleck, 1981). Additional, deeper tunnels are primarily used for breeding and food storage.

These burrows are typically situated in poorly consolidated sediments which limits the size of the burrow. These burrows rarely exceed one metre depth (only a few species such as the suricate have been reported to burrow up to 1.5 metres - unpublished A.E.C. report of S.J. Posnick, 1989), but the colonial nature of these burrows does, however, result in a complex interwoven system, making the ground in these areas unstable. Furthermore, borrows of these smaller animals are generally restricted to the

sands overlying the calcrete horizon.

The slightly older material forming the roofs of the burrows is a light reddish-brown colour compared to the red more recent mobile sands often found surrounding the burrows. This lighter colour may be the product of a pedogenic calcite cementation. Figure 7.25 shows the mobile sands which are covered and hence mixed on surface with the underlying material which is brought to surface by the burrowing animals.

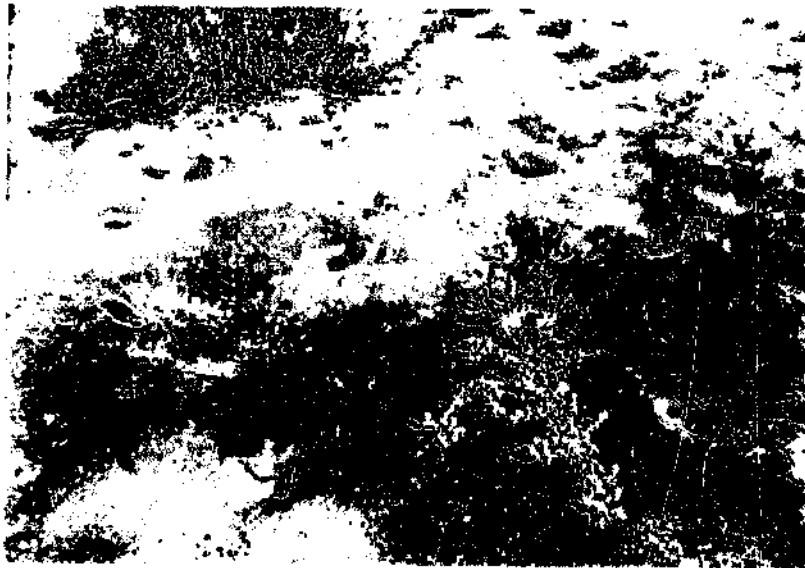


Figure 7.25 Bioturbation in dune deposits consists typically of burrows of small animals. The slightly older material forming the roofs of the burrows is a light brown colour; the red sands surrounding the burrows are more recent aeolian sands.

Bioturbation caused by large burrowing animals

The more common large burrowing animals of the region include: aardwolf (*Proteles cristatus*), honey badger (*Mellivora capensis*), caracal (*Felis caracal*), bat-eared fox (*Octocyon megalotis*) and the aardvark/antbear (*Orycteropus*). Larger animals tend to burrow in areas which are more stable as they require greater support for their larger domichina. This type of burrow is, therefore, mainly seen in older more stable dune areas where the soil is reasonably consolidated or cemented. The larger burrowing

animals tend to favour areas where calcrete is developed near surface, hence the lack of large burrows on the leeward side of dunes where the sand is unconsolidated and thicker. The aardvark and the aardwolf typically burrow deeper than one but less than two metres in depth. The aardvark appears to be the most important large mammal contributor to bioturbation in the study area (unpublished A.E.C report by Posnick, 1989). The burrows of the large mammals tend to be less complex than the small mammals, often forming simple or single burrows. Large areas (several tens of square metres) may be affected by these larger burrows.

Figure 7.26a shows a typical burrow in which large quantities of material (including several pebble types) are brought to the surface. In areas where calcrete has been penetrated, the calcrete forms a strong resistant roof to a burrows such as that seen in Figure 7.26b. This figure clearly illustrates the animal's ability to burrow through and overturn the hardest of lithologies. Large animal burrows play an important role in bringing larger pebbles, such as those seen in Figure 7.26c, to the surface and redistributing and mixing them.

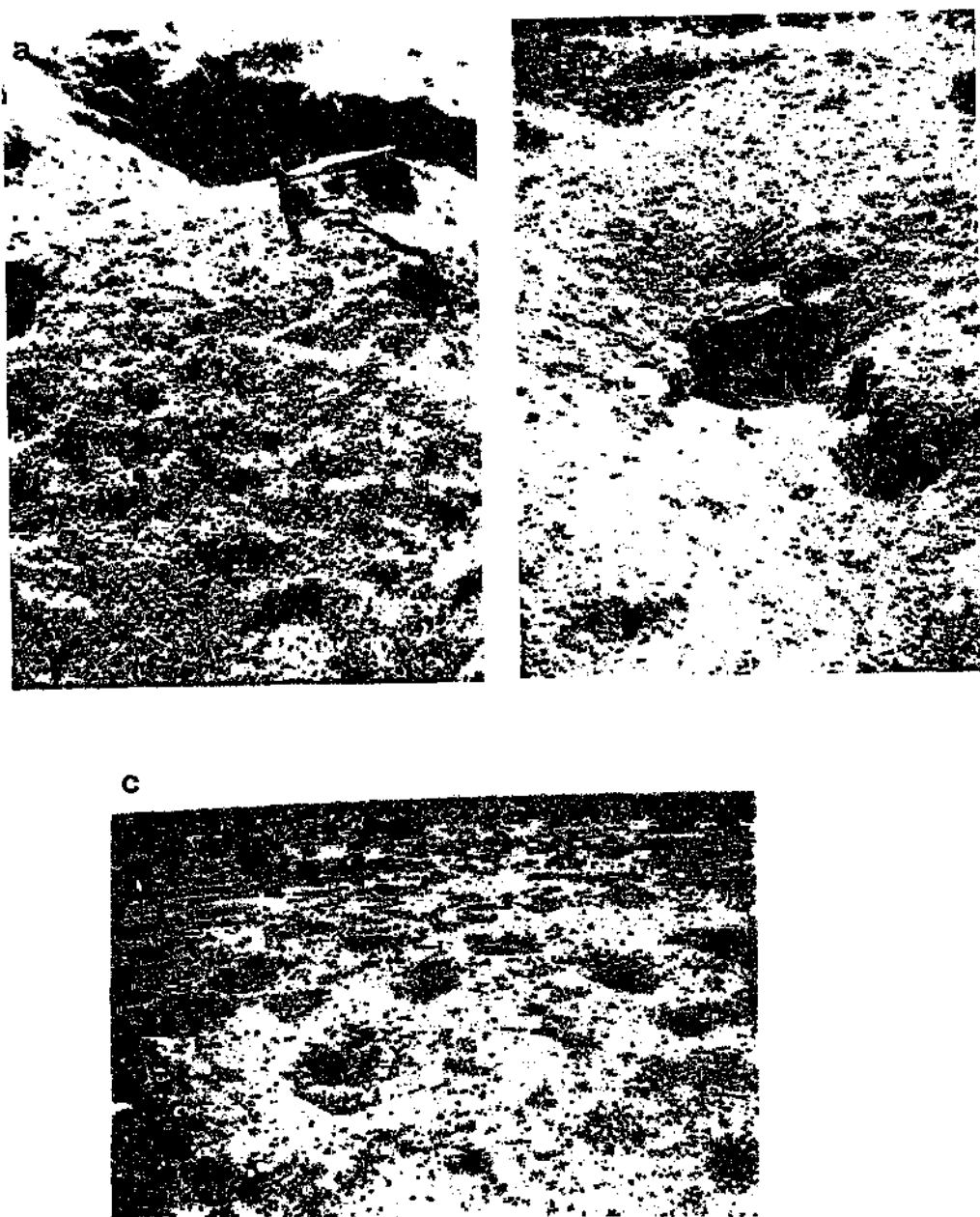


Figure 7.26 (a) Large animal burrows, in more stable areas, that is, where the soil is reasonably consolidated or cemented. (b) Calcrete may form the roof of large burrows. (c) Large areas of extensive bioturbation caused by large animals.

Secondary bioturbation

According to Black and Montgomery (1991) sediment transport due to burrowing activity can be subdivided into direct and indirect processes. Direct (or primary) transport or bioturbation involves the physical movement of debris by the animal. Indirect (or secondary) transport or bioturbation is due to the subsequent erosion and transport of the disturbed material. Secondary bioturbation in the study area is common in areas in which termite or ant nests are found. These mounds may be burrowed into by animals in search of food rather than burrowing to make nests or dwellings. The disturbed primary structures (Figure 7.27) will eventually erode, covering the surrounding area with material from below the surface. An additional component in assessing the destruction of primary burrows involves the collapse of old tunnels. It is inevitable that unmaintained tunnels will eventually collapse as burrows are abandoned, which results in further mixing of the sediments. There is also a component of debris that never appears at the surface, but is shuffled through the system, or is used to refill abandoned burrows. Consequently, surface debris volume should not be the only indicator of volume of material that is disturbed.

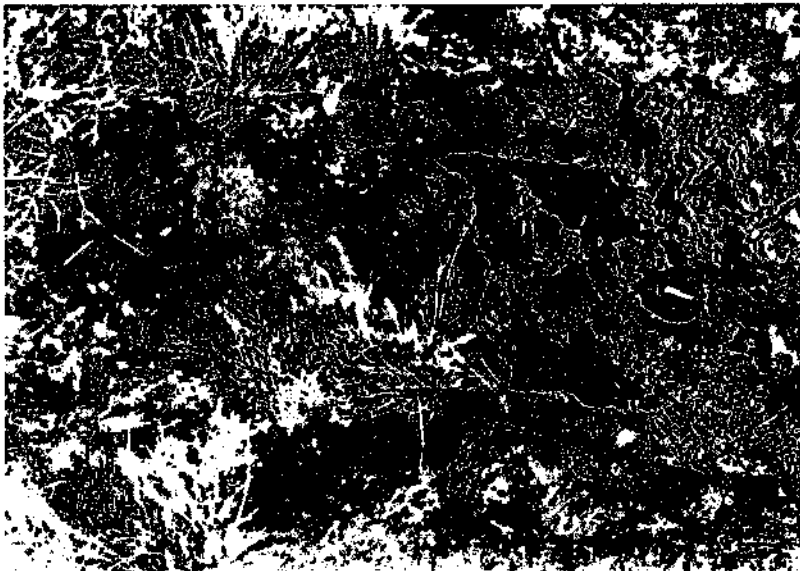


Figure 7.27 Mounds destroyed by animals burrowing in search of food.

Imeson and Kwaad (1976) suggested that 15 to 45 per cent of burrow mound degradation represents material transported down-slope or away from the mound, the remainder being attributable to mound deflation and compaction. Due to the sparse vegetation and lack of stabilizing ground cover in the study area, this figure may be slightly higher. Several mechanisms by which colluvial material is believed to be transported into the hollows from the surrounding area are: aeolian processes, entrainment by overland flow (sheetwash), rainsplash, soilcreep and other biologic agents.

Bioturbation caused by vegetation

Due to the sparse and slow growing vegetation typical of this area, it is not believed to be a significant contributor to the observed bioturbation. Casts of roots may be filled with alluvial soil after death of the plant. This form of bioturbation is best observed in the waste disposal trenches where a large number of red, vertical tubes may be observed, and which show no traces of organic material or biological substructure (Picker, 1987).

7.5.2 Characteristics of Bioturbated Sediments

It was found that particular types (or combination of types) of bioturbation occur in certain environments. For example dunes (and mobile deposits) are mostly inhabited by smaller animals, reflecting the greater ease of burrowing in these unconsolidated soils. Stable areas, deflated areas, or calcrete dominated areas are mostly inhabited by larger animals, which need the stability of the more consolidated ground for their larger burrows. Bioturbated deposits did not exhibit a particular size frequency distribution as their grain size data is dependant on the environment with which it is associated. As bioturbated samples are mixtures of the previously discussed deposits, they have similar characteristics to these samples. They are generally comprised of poorly sorted grains set in a fine grained matrix (constituting up to 71% of the sample). As in most of the sediments described above, the grains consist predominantly of

monocrystalline quartz, rock fragments, a subrounded fraction of oxides (ilmenite and magnetite) and minor amounts of altered feldspar. All grains, besides the oxide grains, are rounded to subangular, with low to high sphericity. All the quartz grains are coated in hematite. Pebbles scattered throughout these deposits were found to consist predominantly of blue quartz. Other pebble types include iron-oxide nodules, sandstone and jasper.

7.5.3 The Effect of Bioturbation on Sediment Dispersal

Techniques in mineral exploration have been reported (e.g., d'Orey, 1975) to make use of the fact that termites descend to the water-table to drink, and that they carry up mineral particles from more than 30 metre depths. Watson (1970) reported results of an investigation of the development of a zinc anomaly in Kalahari sand by analyzing the metal contents of termite sands. Due to the bioturbated nature of the sediments (Vaalputs Formation, Gordonia Formation, and other recent sedimentation) occupying the Vaalputs basin, a similar method to that used by other workers was used to investigate the significance of bioturbation at Vaalputs.

Geophysical work and drilling confirmed the presence of lamprophyric and kimberlitic bodies, which are intruded into the basement and underlie the younger Vaalputs sediments. Ilmenite concentrations were determined for selected unconsolidated surface sand samples collected from above these intrusions. This was done to determine whether ilmenite grains are concentrated at the surface, overlying ultramafic intrusions. This would allow for the recognition of the extent of vertical movement of material during bioturbation. The Cenozoic Vaalputs sediments may attain thicknesses of up to 30 metres in the "Vaalputs basin", and only bioturbation can account for a concentration of ilmenite grains in the surface sands above the mafic intrusive plugs.

Two sites above ultramafic intrusions (Figure 7.28) were chosen using the A.E.C geological map of the waste disposal site (compiled by Andreoli et al., 1986). These sites had been identified as areas of suboutcropping olivine-melilitite, kimberlite and

related diatremes, which had been confined by aeromagnetic and drilling data. Appendix D describes the sampling and preparation technique used to obtain the heavy mineral fractions.

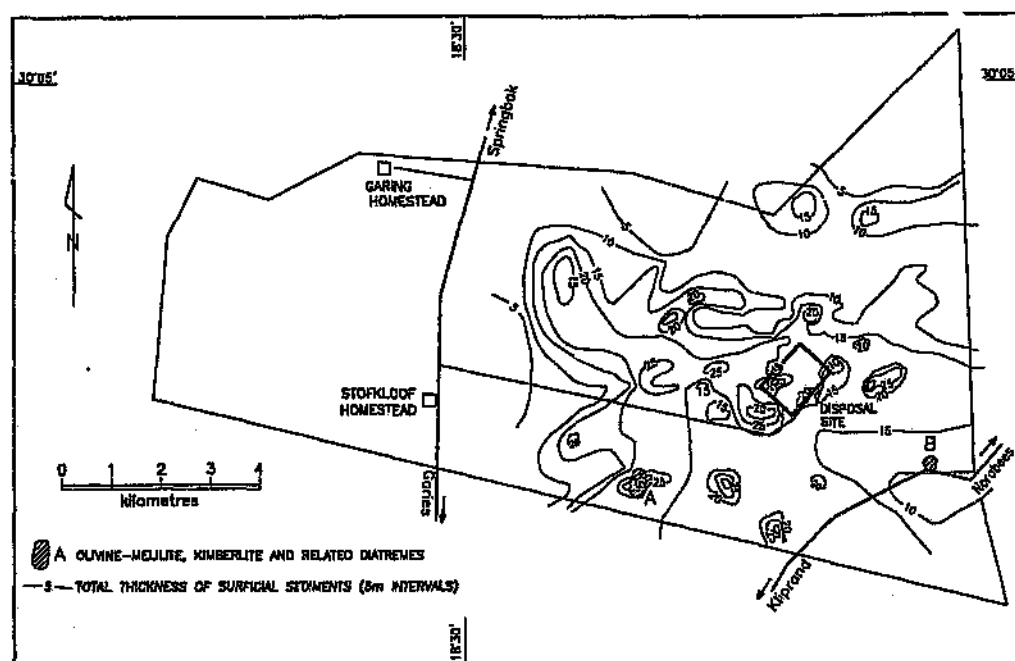
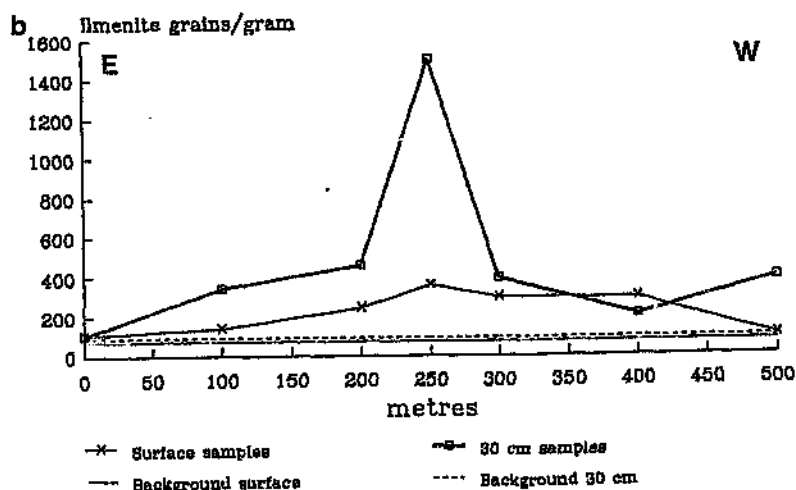
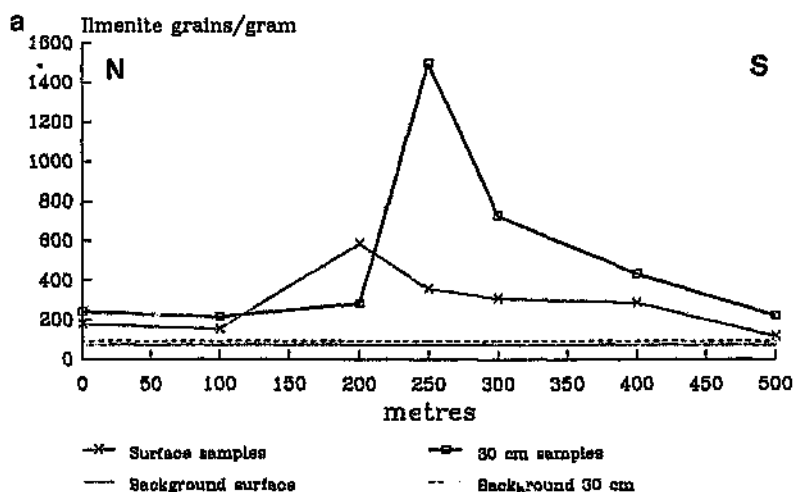


Figure 7.28 Positions of the sites (A and B) chosen for the heavy mineral study, using the A.E.C geological map of the waste disposal site (compiled by Andreoli et al., 1986).

Heavy mineral concentrations versus distance

Site A (Figure 7.28) is situated in an area where the surficial sediment thickness, as determined by the A.E.C. in a drilling programme, is approximately 20 metres. The heavy mineral concentrations obtained for this site showed no significant anomalies, that is, the values obtained fluctuated around the background values. The surficial sediment thickness at site B was determined to be approximately 12 metres thick. The heavy mineral concentrations obtained for site B are shown in Figures 7.29a, 7.29b, 7.29c and 7.29d.

Ilmenite concentrations (Figures 7.29a and 7.29b) exhibit anomalies with respect to background values. These anomalies, especially the 30 centimetre-depth samples, have well centred peaks which die out rapidly and almost attain background values at the limits of the sampled area. The surface anomalies are less pronounced than the 30 centimetre-depth anomalies, suggesting that the surface material is more diluted. Iron oxide concentrations (Figures 7.29c and 7.29d) also show anomalies, but are not as prominent as the ilmenite anomalies.



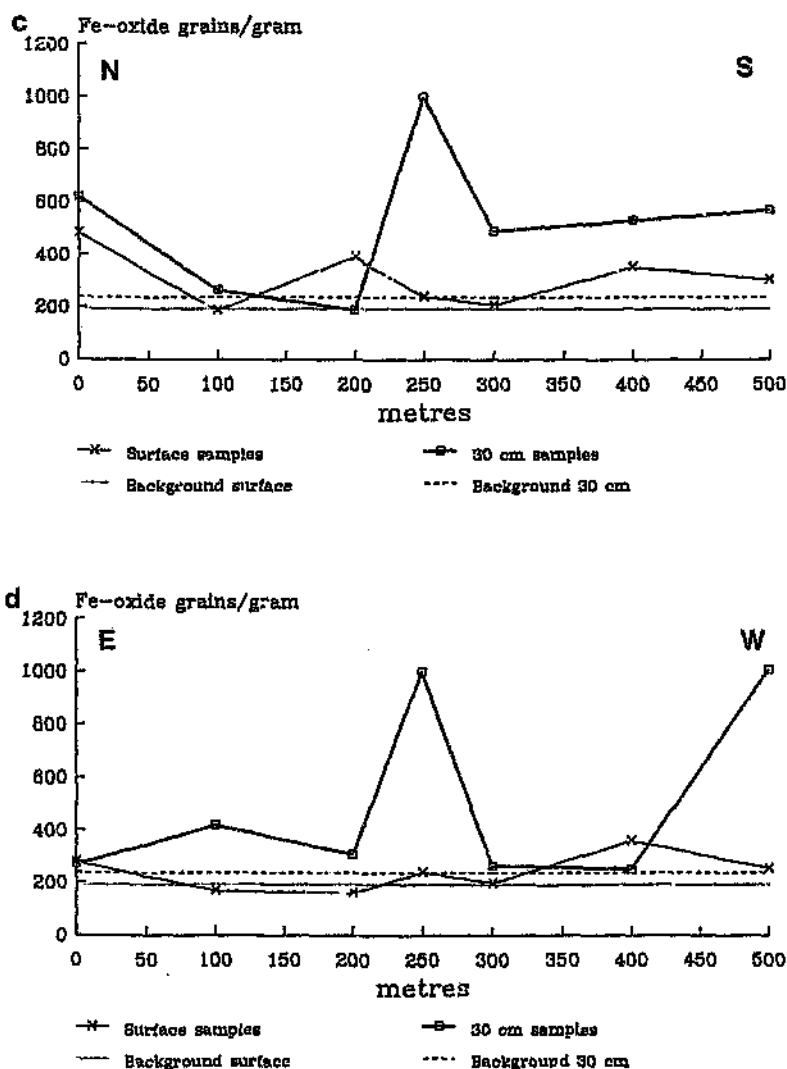


Figure 7.29 The heavy mineral concentrations versus distance for site B: (a) ilmenite, north-south profile; (b) ilmenite, east-west profile; (c) iron-oxide, north-south profile; and (d) iron-oxide, east-west profile.

S.E.M. Results

As other iron oxide grains were often indistinguishable from ilmenite grains the samples were analyzed using the S.E.M. In addition semi-quantitative analyses were obtained for the compositions of several ilmenite grains from Vaalputs, a kimberlitic ilmenite and an ilmenite grain from a mellilitite outcrop (Kalkdraai) in the Vaalputs region (Table 7.3). This was carried out for a comparative analysis of various ilmenite grains.

Table 7.3 Results of element-normalised, semi-quantitative S.E.M. results for ilmenite grains. All data are given in weight percent.

Oxide	Kimberlitic Ilmenite	Kalkdraai Ilmenite	Vaalputs (grain 1)	Vaalputs (grain 2)
MgO	8.8	4.1	-	-
Al ₂ O ₃	0.8	5.7	-	0.6
SiO ₂	2.0	12.5	-	0.5
CaO	0.5	0.6	-	0.2
TiO ₂	55.6	49.5	54.6	67.6
Cr ₂ O ₃	2.4	0.3	-	0.4
MnO	1.4	0.4	3.8	2.1
Fe ₂ O ₃	28.6	26.8	41.5	28.6

These results (Table 7.3) show a great variability and indicate that the ilmenite obtained from the Vaalputs region (Kalkdraai) and from the Vaalputs sediments have atypical, that is, low Mg and Cr contents for kimberlites. All the mafic intrusives in the area are, however, "kimberlite-related" rock types and not true kimberlites. It was, therefore, also not possible to separate ilmenites originating from the intrusions below the Vaalputs sediments and those of other origins. The S.E.M. results also indicated that the percentage of ilmenites in the heavy mineral separate (total ilmenite and iron oxide), varied from approximately 60% over the sub-outcrop to approximately 28% near the edges of the sub-outcrop. A value of approximately 28% was obtained for the background samples too. The remaining fraction consisted predominantly of iron-oxides.

Discussion of results of the heavy mineral study

The results obtained indicate that material from the sub-outcrop has been reworked by bioturbation processes and is found at surface in the form of heavy mineral concentrations. The ilmenite grains at this site are believed to be primary grains of the mafic plug situated beneath the Vaalputs sediments, whereas the iron oxide concentrations are most likely a secondary product of weathering, but nevertheless, associated with the mafic plug (due to its higher iron content).

The dilution of the surface ilmenite grains may be attributed to a combination of surface processes which include aeolian, sheetwash, and bioturbation processes. The overall resultant wind direction in this area is to the east, the results of which are reflected in Figure 7.29b, in which the subsurface (30 centimetre) anomaly, is slightly elevated on the east. There is also a slight southerly shift in the north-south traverses, perhaps indicating a local northerly wind effect. This result is in agreement with the morphology as depicted in the profiles of the deflation pans (Section 7.3). As in the case of the ilmenite anomalies, the iron oxide concentrations are also shifted to the east and the south.

From the above observations and results it is evident that bioturbation by animals and insect plays an extremely important role in the redistribution and mixing of the surficial deposits. Several generations of bioturbation caused by insects and small or large burrowing animals would be sufficient to mix the sediments and totally destroy any sedimentary structures which may have existed prior to bioturbation. Thus, vertical translocation of material in the surficial sediments of the region is a significant process.

7.6 Chemical Sediments

7.6.1 Iron Oxide Cemented Facies - Dorbank

Various iron oxides precipitate in different weathering environments, but only few iron

oxide relationships are so far understood on their basis of thermodynamic or kinetic considerations (Schwertmann, 1988). Although emphasis is generally placed on iron rich soils in tropical and sub-tropical climatic zones, they may also form extensive deposits in drier semi-arid regions (Fitzpatrick, 1988). Iron may be incorporated in layer silicates in the form of oxide finely dispersed in the soil matrix, in concentrations in glauabules and ferricretes, or as a cement. An iron oxide cemented facies (also referred to as dorbank) generally occurring as a sub-surface feature, was commonly found outcropping in the study area, particularly in deflated areas.

Appearance of dorbank

This deep red, iron-oxide rich facies (Figure 7.30) is typically 30 to 40 centimetres thick, but may be as thick as 1.5 metres. Both the upper contact, with the unconsolidated aeolian deposits, and the lower contact, usually with the upper calcrete horizon of the Vaalputs Formation, are sharp. The iron oxide cement which gives this sediment its hardness is more concentrated towards the top of the unit. The sediment consists of a coarse sand to grit, with a fairly high clay content (as much as 18%, but typically around 10 to 12%). Pebbles, up to 3 centimetres in diameter, and predominantly composed of blue quartz are scattered throughout. The surface texture of the grains comprising these sediments is frosted, such as that observed on wind blown fragments, and observed on the grains in the recent aeolian deposits. Calcrete may be developed along fractures in the upper parts of these sediments. Bioturbation is not as obvious in this unit as in the less consolidated sediments, but was noted in some areas. Sedimentary structures are lacking in this generally homogeneous unit, with the exception of thin muddy lenses which were noted in the sections provided by the waste disposal trenches. These lenses have a shiny appearance due to the fineness of the particles. They are usually several metres wide and a few centimetres thick.

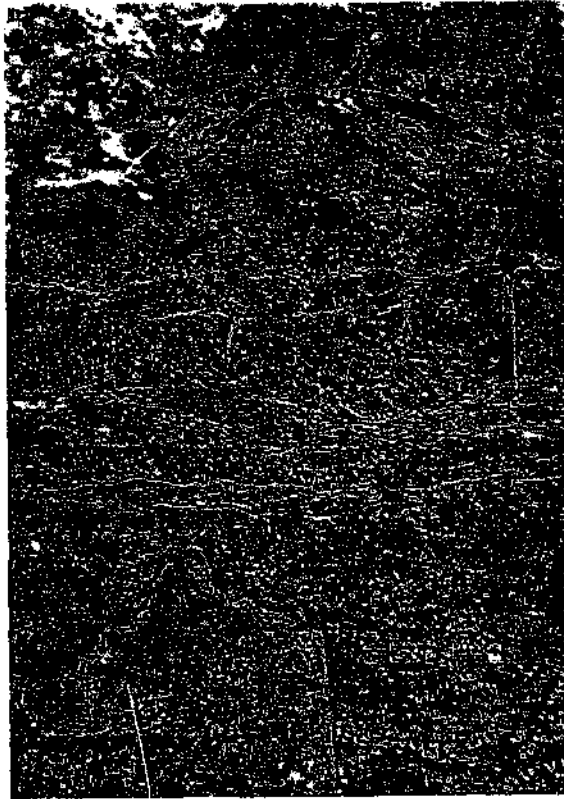


Figure 7.30 Iron oxide cemented facies, with the typical deep red colour and calcrete lined fractures.

Petrology and mineralogy

These sediments, which display a typical red colour consist predominantly of iron-oxide coated quartz grains, set in a fine-grained clay matrix (10 to 12%) and cement (iron oxide and silica). The quartz fragments may be rounded but are generally well angular, probably mainly due to resorption of the grain margins during the production of the cement. Some of the cement may be precipitated from surface or ground water. The quartz and iron oxide cement gives this sediment its hardness and red colour. The hardness of these sediments has been related (Ellis and Schlom, 1982; Klintworth, 1948) to the amount of free carbonates present. The more carbonates present the softer the sediment becomes. Few rock fragments and minor altered feldspar grains were also noted.

Sand size analysis

Ranges of grain size parameters for this sediment are summarized in Table 7.4 below. A range of values obtained for the aeolian Gordonia formation sediments is included in this table for a comparison. It should be noted that the ranges of dorbank sedimentary parameters (Table 7.4) all fall into the ranges obtained for the aeolian deposits of the Gordonia Formation, with the exception of one sample exhibiting poorer sorting.

Table 7.4 Range of sedimentary parameters for the iron oxide rich sandstone (dorbank), and the Gordonia Formation (aeolian sediments only).

	Mean Grain Size (ϕ)	Standard Deviation (Sorting)	Skewness
Dorbank (n=4)	1.30 - 1.36	1.34 - 1.75	0.11 - 0.17
Gordonia Formation (aeolian sands) (n=22)	0.85 - 1.55	0.93 - 1.44	0.11 - 0.36

Discussion

Dorbank occurs widely in the semi-arid to arid climates of the Little and Great Karoo, Namaqualand and Bushmanland (Ellis and Schloms, 1982), and is related to the duripan of soil classification systems (Soil Survey Staff, 1975). Massive types such as those observed in the study area (other types are referred to as platy or laminated) are mainly restricted to the northwestern part of the country and occur most commonly in transported materials and overly a variety of older geological formations (Ellis and Schloms, 1982).

Dorbanks, as referred to by Ellis and Schloms (1982) and MacVicar et al. (1977), were noted by Fitzpatrick (1988) to be restricted to the semi-arid and arid climatic zones where environmental conditions have been considered to favour the accumulation and formation of iron and silicified compounds in a weathering environment of a hot, dry climate. According to Ellis and Schloms (1982) soils with dorbank occur on level-terrain with slopes rarely exceeding 5%. Dorbank in Namaqualand and the Richtersveld were reported (Ellis, 1979) to always occur in the older parts or be associated with older

landscapes, which is in accordance with findings of Flach et al. (1969). Also, dorbanks occur in areas where, in every month of the year, evaporation exceeds precipitation, and in regions that favour neutral to alkali soil reactions, which in turn favours the solution of silica. The low rainfall causes the mobile silica to remain in the profile and to be deposited in the subsoil. Carbonate moves slightly further and tends to accumulate below the dorbank (gypsum moves the furthest) (Ellis and Schloms, 1982).

These observations suggest that the dorbank and the uppermost calcrete horizon in the study area may have been deposited contemporaneously. Iron is believed to play an important role in the cementation of dorbanks, although Ellis and Schloms (1982) noted that iron contents may be very low. One possible explanation for the cementation of dorbanks may be a result of iron closely bound to the silica in a Fe-O-Si bond. It has also been suggested that for cementation, the iron acts as a protective coating on the cementing silica, thereby protecting the silica from attack by strong alkaline solutions (Ellis and Schloms, 1982). The final hardening of the material is associated with exposure, due to the stripping of topsoil, as well as wetting and drying, particularly where rainfall is low (Thomas, 1974). Smale (1973) suggested a mechanism of formation by "replacement of carbonate by silica" or calcrete alteration to dorbank. No evidence, however, involving this sort of replacement was observed in the study area.

The dorbank of the study area conforms to the above observations and, therefore, may well be related to the present-day climate and micro-environments. The frosted surface texture of the grains in these sediments is similar to those of the aeolian sands of the region, suggesting an aeolian origin. In addition the thin muddy layers observed in these sediments appear to be the relics of what were once muddy deflation pans, such as those seen on the present land surface. No dorbanks were seen occurring directly on Karoo sediments (also noted by Ellis and Schloms, 1982). The exact distribution of these subsurface deposits was not possible in the study area. However, they appear to be related to flat stable areas and the marginal parts of deflation pans, where run-off is restricted and water infiltration is significant.

7.6.2 Calcrete

Surface calcrete exposures are not common in the study area, but, in deflated areas, where dorbank is absent, calcrete may be expected. Large bioturbation burrows often expose calcrete and result in a scatter of calcrete nodules on the surface. From the available exposures it appears that the calcrete exposed at surface can be planar laminar, massive or nodular, and follows the dune morphology (as described in the section on aeolian deposits). That is, the calcretes exposed at surface display a pedogenic profile (Netterberg, 1980), which is formed by the downward leaching of carbonate from soil horizons by infiltration of meteoric water. These waters transport the carbonate to the lower B horizon, where it precipitates. The carbonate may be derived from dust, precipitation, bio-activity (carbonate-rich water drawn from the phreatic zone) and shell material (Gould, 1973). Where calcrete is exposed some dissolution and erosion of the calcrete has been noted.

7.6.3 Silcrete

Surface silcretes are uncommon at Vaalputs, occurring predominantly as isolated ferruginous and silicified deflation pan sediments. Most silicified occurrences are related to the dorbank or the underlying Dasdap sediments (which were noted in the southern parts of Vaalputs). They consist of an opaline matrix (Brynard, 1988) with a variety of detrital grains, comprised of the typical grains constituting the dorbank and other sediments.

7.7 Grain Size Parameters: a Comparison with the Vaalputs Formation

According to Friedman (1961) the textural parameters of sands reflect the mode of transportation and the energy of the transporting medium. A comparison of the sedimentary parameters of the Vaalputs Formation, with sediments from the present day surficial micro-environments (Gordonia Formation) was undertaken in an attempt to determine to what extent the Vaalputs sediments may have contributed to the surface materials. In addition, an attempt was made to investigate whether size

characteristics can differentiate sedimentary environments. A number of representative samples were collected from the disposal site trenches and compared with a similar number of samples from the various micro-environments of the Gordonia sediments. For this comparative study the parameters for each of the facies constituting the two formations (Gordonia and Vaalputs respectively) were grouped together, and no distinction is drawn for the individual units or facies within these formations. Three separate plots were used for this comparative study and are described below.

Mean grain size versus standard deviation

The plot (Figure 7.31) allows for the classification of aeolian- and fluvial-type sediments (Friedman, 1961), the only likely processes for the Vaalputs and Gordonia sediments. Typical ranges for the two Formations are shown in the form of fields, and include 80% and 92% of data points for the Vaalputs and the Gordonia Formations respectively. Pebbly deposits have been excluded as they were found to be highly variable: their parameters depend strongly on sample localities and hence representative sampling of the material is difficult. The field of the Vaalputs sediments seems to coincide reasonably well with the field of the more recent Gordonia Formation (Figure 7.31). The Gordonia Formation is generally more variable, shown by a greater spread of points.

Also plotted on this figure are the approximate areas for dune and river sands (Friedman, 1961). All samples with the exception of one, plot in Friedman's wide "field of overlap". It should be noted that Friedman's fields plot in the upper left corner of Figure 7.31 and that the range of values depicted for this study is significantly larger than those identified by Friedman. Friedman (1961), and Thomas and Shaw (1990) emphasise that it is often difficult to distinguish between wind and water laid sediments. Also, all samples of this study, even those of obvious aeolian origin plot in the wide field of overlap with larger mean grain sizes and poorer sorting than was expected.

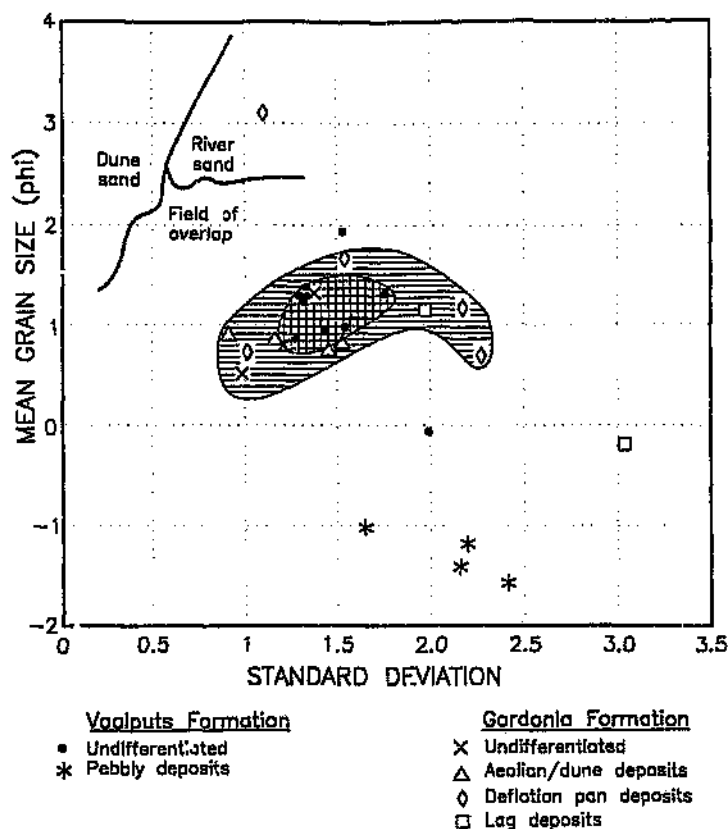


Figure 7.31 Plot of mean grain size versus standard deviation (sorting) for the Vaalputs and Gordonia sediments. Fields for the typical range of Vaalputs (vertically hatched) and the Gordonia (horizontally hashed) Formations are superimposed on the data. Dune and river sand fields are after Friedman (1961).

Skewness versus standard deviation

According to Friedman and Johnson (1982) the standard deviation and skewness are geologic process-sensitive parameters, and therefore a scatter plot of these two factors is likely to be significant. Figure 7.32 shows the similarities between samples of the Vaalputs sediments and those from the Gordonia Formation. The Vaalputs sediment field contains 100% of data points (excluding pebbly lenses) and the Gordonia sediment field 92% of data points (excluding lag deposits). Again the Gordonia Formation exhibits a larger field or spread of values than the Vaalputs sediments.

Friedman's fields for this plot were not included as they distinguish beach and river

sands, which are clearly not relevant to this study. In addition, the boundary between these fields would plot on the far left hand side of the diagram (Figure 7.32), classifying all the studied samples, including the aeolian Gordonia Formation as river sands.

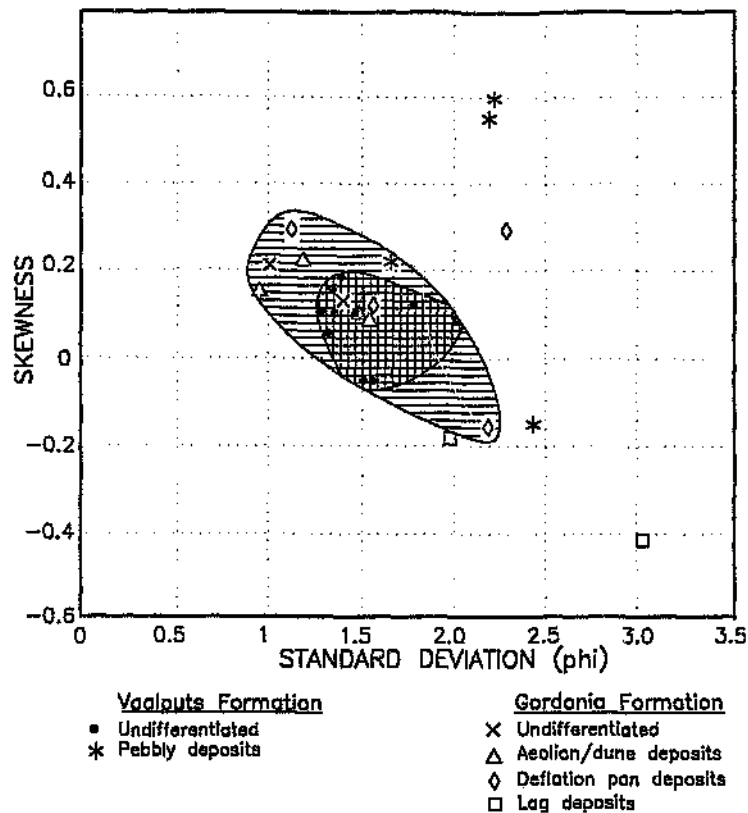


Figure 7.32 Plot of skewness versus standard deviation (sorting) for the Vaalputs and Gordonia sediments. Fields for the typical range of Vaalputs (vertically hatched) and the Gordonia (horizontally hashed) Formations are superimposed on the data. Fields exclude the highly variable pebbly deposits.

Mean grain size versus skewness

These two parameters (Figure 7.33) again show a reasonable cluster, and overlap of fields (Vaalputs and Gordonia Formation fields). In this case two data points of the Vaalputs Formation are not included in the field of overlap. The Gordonia field contains 92% of Gordonia data points and the Vaalputs field 100% of Vaalputs data points.

Pebbly deposits have been excluded in all accounts. Friedman's fields for this plot (Figure 7.33) are not shown as they are used to distinguish beach and dune sands, and which would obviously not aid in the identification of the sediments for this study.

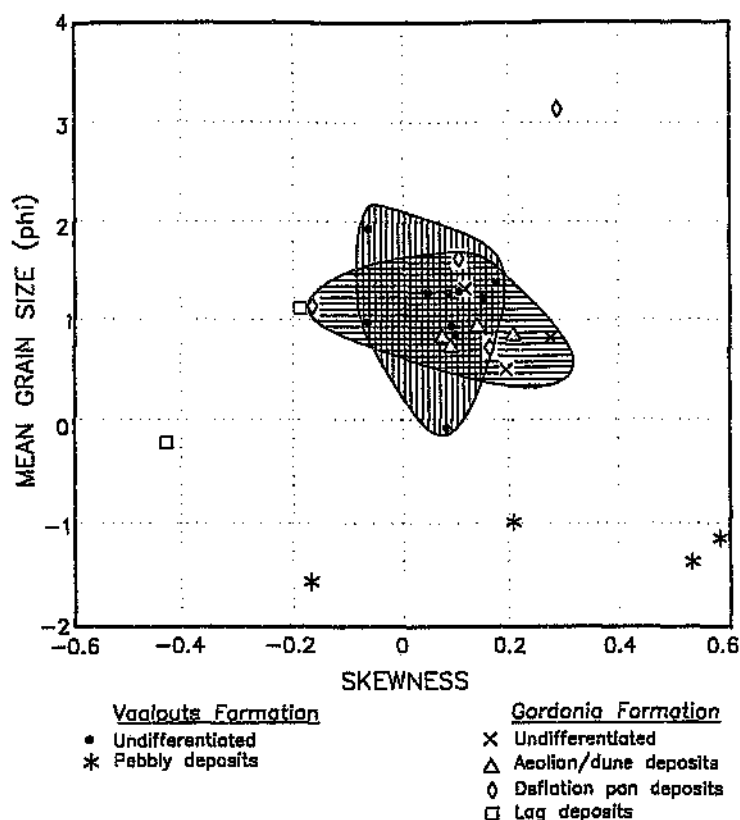


Figure 7.33 Plot of mean grain size versus skewness for the Vaalputs and Gordonia sediments. Fields for the typical range of Vaalputs (vertically hashed) and the Gordonia (horizontally hatched) Formations are superimposed on the data. Fields exclude pebbly deposits.

It should be noted that in all the plots, the points which are distinctly separate from the clustered data are coarse pebbly deposits. The surface (Gordonia Formation) lag deposits exhibit fairly different sedimentary parameters to the pebbly lenses of the Vaalputs Formation. This is mainly attributed to the sampling procedure for the surface deposits, which were difficult to sample without mixing the lag deposit with some of the underlying sediment. Furthermore, each pebbly deposit, both on surface and in the

Vaalputs sediments exhibits different sedimentary characteristics, such as maximum clast size, clay content and pebble types, making any correlation, between the present pebble deposits and older pebble lags (Vaalputs Formation) very difficult. However, all the other results are suggestive of a genetic relationship for the two formations, the implications of which are dealt with at the end of this chapter.

7.8 Chemical Results: a Comparison with the Vaalputs Formation

The chemical compositions of the Vaalputs, Gordonia and Dasdap sediments, and several other weathered, clayey samples from surface exposures, of the basement and the Dwyka are used in this study. The weathered, basement exposures on the western side of Vaalputs and the white clay facies at the base of the Vaalputs Formation are believed to be two possible source areas for the clay-rich surficial sediments. In addition to *in situ* clay formation, sediment from these two possible sources could presumably have been transported by primary processes (fluvial and aeolian) and mixed by secondary processes (bioturbation). A comparative study would also allow for the determination of a genetic association for the Vaalputs and Gordonia Formations. The major elements (Appendix E), rather than the trace elements were believed to be more useful for this study. These results are presented below.

SiO₂ versus TiO₂

Figure 7.34a exhibits a wide range of SiO₂ values, which can be attributed to the diverse suite of samples used for this analysis. Surface sediment (Gordonia) samples are fairly high in silica due to the dominance of quartz sand. The silica content of the weathered surface basement material show similar SiO₂ concentrations, suggesting a possible source for the Vaalputs and Gordonia Formation sediments. The wide range of SiO₂ values for the white clay can be attributed to the inhomogeneous nature of the underlying basement (samples were taken from the white clay overlying both granitic gneisses and norite). White clay samples taken from above noritic basement were found to have lower silica contents than those taken from over granitic gneisses.

The Vaalputs and four of the Gordonia sediment samples lie approximately in the centre of and coincide with a scatter of points for weathered samples taken from the Dwyka sediments (one Dwyka sample was noted to contain significant carbonate, suggesting possible calcretization and, therefore, is probably not representative), the white clay facies in the lower Vaalputs sediments and the weathered surface basement samples (Figure 7.34a). Thus, Figure 7.34a suggests that all the above mentioned possible sources may have contributed to a greater or lesser extent to the Vaalputs and Gordonia sediments.

The Gordonia Formation samples which are slightly enriched in titanium (Figure 7.34a), may be due to the concentration of detrital minerals, such as ilmenite, leucoxene, sphene, anatase, and as an exsolution phase in magnetite (Brynard, 1988) which are commonly found on the deflated, present land surface. In an attempt to explain the source of titanium in the surface sediments, several samples (medium to fine sand fraction) from the Gordonia Formation were magnetically separated to remove the heavy minerals, and acid washed to remove iron coatings. The results showed the expected range of SiO_2 values (94.43% - 96.88%), but TiO_2 (rutile) in the sand fraction ranged from 0.17% - 0.19%, showing that titanium is not associated with this fraction of the aeolian Gordonia Formation sands. A further possibility for the titanium was by TiO_2 (rutile) in the quartz pebbles (the quartz pebbles generally have a grey to blueish colour). Two pebbly deposits were analyzed, and again the titanium values were too low (0.16% for both samples) to account for the high surface values (approximately 0.5-1.2%). Two Dasdap samples have relatively high TiO_2 values (Figure 7.34a). It is known that ilmenite is concentrated in parts of the Dasdap sediments and, therefore, may be a contributing factor to the high TiO_2 values observed in the surface sediments (Dasdap sediments have been noted as far north as Vaalputs). However, it would appear that the main source and only plausible answer to the titanium concentration at surface is due to the concentration of detrital minerals, caused by deflation, as suggested by Brynard (1988).

SiO_2 versus Al_2O_3

Aluminium occurs primarily in feldspars in the less altered samples and forms a major component of the clay minerals in the weathered samples. A strong, inverse

relationship between silicon and aluminium is shown in Figure 7.34b. This mixing line shows a "high clay - low quartz" relationship (also noted in the petrology - see previous sections). Sediments of the Gordonia Formation may be fairly low in aluminium suggesting that the clay fraction has been decreased by aeolian processes. The white clay facies in the lower Vaalputs sediments show a range of Al_2O_3 values along the mixing line, which may be attributed to variability in these samples' source material. The Vaalputs and Gordonia sediments plot approximately mid-way on the mixing line. Dwyka material (generally lower aluminium and silica) may contribute to the scatter of points from a straight line relationship which generally exists between these two elements. The Dasdap samples plot on the lower end of this line, probably as a consequence of having a similar source terrain to the other sediments, and also suggesting a possible contribution to the Vaalputs and Gordonia sediments.

SiO₂ versus Fe₂O₃

The Gordonia sediments, and to a greater extent, the Vaalputs sediments have high iron concentrations (Figure 7.34c). Iron may be concentrated more in particular units, which gives rise to the spread observed in Figure 7.34c. The weathered basement (surface and white clay facies) and Dwyka material is also highly variable with respect to iron concentrations, and no obvious trends are evident in this plot. The variability of iron concentrations may also be attributed to the fact that Fe^{3+} may replace Al^{3+} in feldspars to a limited extent, and iron minerals are numerous and common (Day, 1963). The reasonably iron-rich Dwyka samples may be an important contributor to the iron observed in the younger sediments. The occurrence of iron in the Gordonia and Vaalputs Formation sediments is typically in the form of oxides and hydroxides. Sediment particles are typically coated in iron oxide. Iron oxide may also be disseminated in the finer clay fractions, or may occur as detrital grains of magnetite and ilmenite. Iron in biotite is essentially restricted to weathered basement material. All the Dasdap sediments, with the exception of one ferruginized sandstone, have low iron values.

SiO₂ versus MnO

As with iron, manganese in the Gordonia and Vaalputs sediments is generally more concentrated than in the weathered surface basement samples and white clay facies

(Figure 7.34d). The weathered basement is also highly variable with respect to manganese concentrations. Overall the manganese concentrations for all analyzed samples are low. Manganese may occur with iron oxides and hydroxides in the sediments, as well as dendritic layers on fracture planes in the clay rich sediments and in calcrete (Brynard, 1988), that is, manganese may be concentrated more in certain units than in others, which, as in the case of iron, gives rise to the spread of data. As with iron, the Dwyka may be a major contributor to the manganese observed in the younger sediments.

SiO₂ versus MgO

Magnesium-oxide generally shows an upward increase from the weathered surface basement and white clay facies into the Vaalputs sediments (Figure 7.34e). The Gordonia sediments show a large spread: in some cases approximating the values of the weathered surface basement material, and in other cases are similar to values obtained for the Vaalputs sediments. The higher values associated with the Vaalputs sediments have been attributed to disseminated calcrete and clay. Other occurrences of magnesium were detected by X-ray energy dispersive analysis, in iron-oxides and -hydroxide minerals (Brynard, 1988). The results of this study (Figure 7.34e) also suggest that the Dwyka is an important source of magnesium.

SiO₂ versus CaO

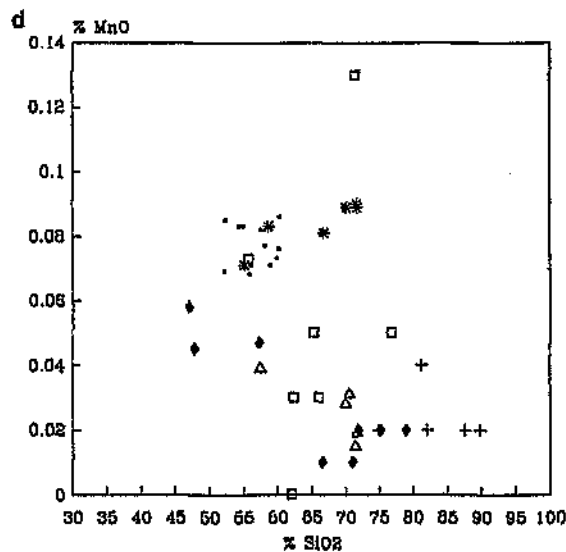
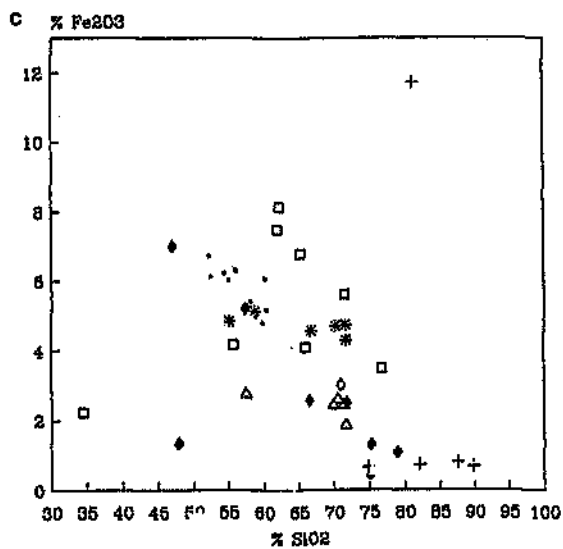
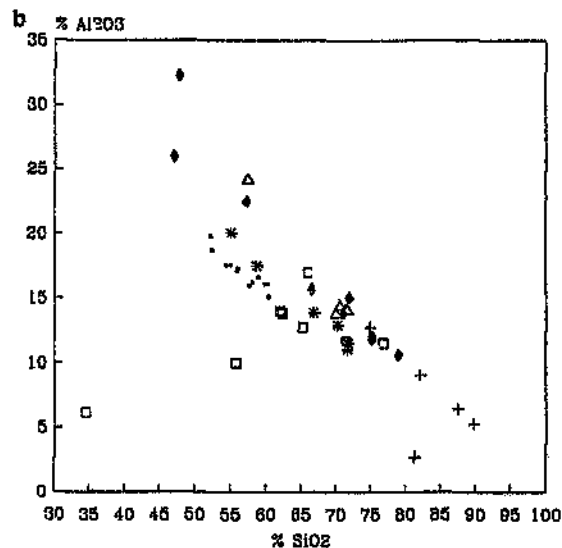
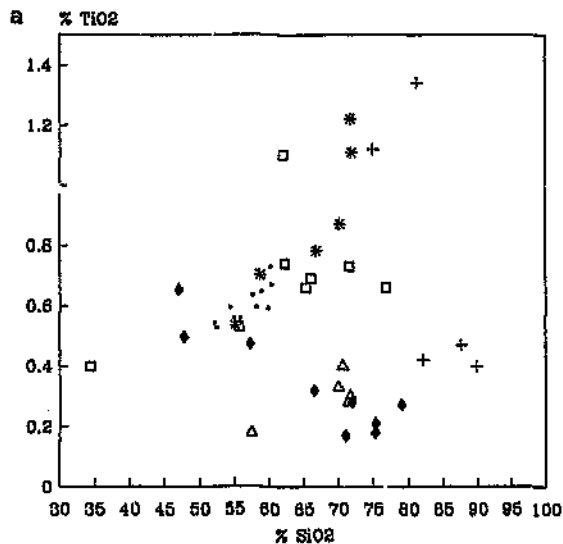
CaO is present in the sediments of the Vaalputs and Gordonia Formations, in addition to being the major constituent of the various calcrete layers. Most of the analyzed samples (Figure 7.34f) contain similar amounts of CaO, with the exception of a few, which have much higher concentrations. Two Dwyka samples exhibit the highest concentrations compared to all other samples (one Dwyka sample, which may have been replaced or enriched by calcium carbonate, contained 27.9% CaO: this sample has been omitted from Figure 7.34f). No particular trend was expected for this mobile element, but it is evident (Figure 7.34f) that sufficient CaO is present in all the possible sources, and can, therefore, easily account for the observed calcium in the sediments.

SiO₂ versus Na₂O

According to Day (1963) many sedimentary rocks contain minerals which are devoid of Na, as Na readily passes into solution during weathering processes. Brynard (1988) suggested that most of the sodium in the Vaalputs sediments may be in feldspars, in smectite clay and as halite in the surficial sediments. The surface sediment samples (Figure 7.34g) are relatively high in sodium and show similar silicon-sodium characteristics to several weathered surface basement and Dwyka samples. The white clay facies samples underlying the Vaalputs sediments are relatively sodium poor. The Vaalputs sediments lie approximately in a central position with respect to the underlying white clay facies, the majority of the overlying surface sediments of the Gordonia Formation, and several weathered surface basement samples.

SiO₂ versus K₂O

The characteristics of potassium are similar in some respects to those of sodium in that the surface sediments and in particular the weathered surface basement samples (with the exception of one) are generally relatively rich in potassium, possibly due to the presence of the smectite group minerals (Figure 7.34h). The Vaalputs sediments again lie approximately in the central position on Figure 7.34h. The overlying Gordonia Formation and surface sediments have similar concentrations of potassium to the Vaalputs sediments, and merely plot to the right (in the majority of cases) due to their slightly higher silica contents (more aeolian in nature). Figure 7.34h also reflects the amount of weathering of the analyzed samples. The most common occurrence of potassium is in the silicate minerals such as K-feldspars, micas and clays. During the weathering process, K passes into solution, with the decomposition of potassium bearing minerals and may be absorbed onto colloids (Day 1963), thus being retained in the clay minerals of the weathered products. The Dwyka sediments are relatively depleted in potassium, which may also contribute to the final pattern observed in Figure 7.34h.



- Vaalputs Formation
- ◆ White Clay Facies (lower Vaalputs Formation)
- * Gordonia Formation
- △ Weathered Surface Basement (N.M.C.)
- Dwyka
- + Dasedap sediments

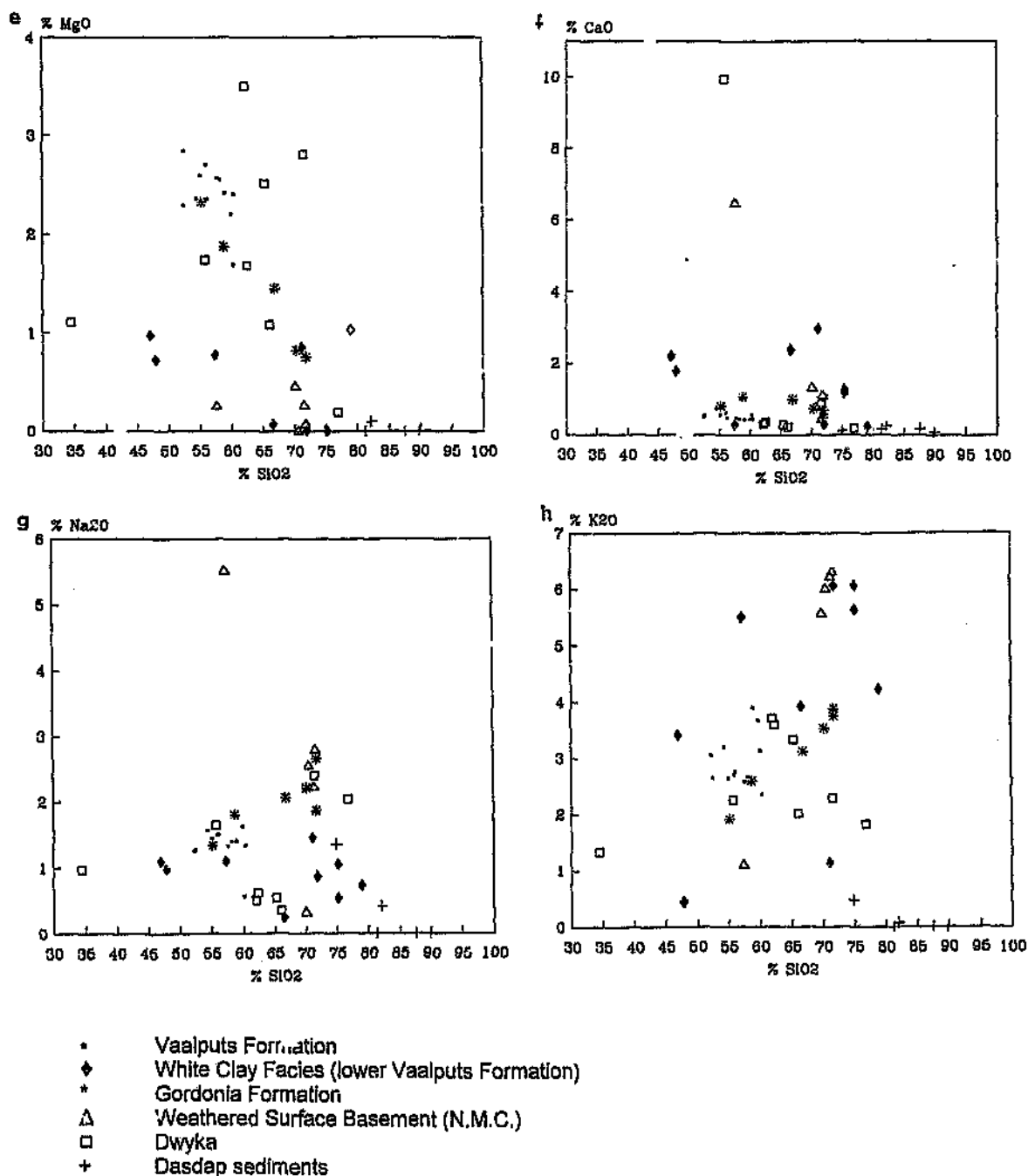


Figure 7.34 Plots of SiO₂ versus (a) TiO₂, (b) Al₂O₃, (c) Fe₂O₃, (d) MnO, (e) MgO, (f) CaO, (g) Na₂O, and (h) K₂O for the Gordonia and Vaalputs sediments, and selected sample suites from weathered surface basement deposits, Dwyka, and the Dasedap sediments.

Fe₂O₃-MgO-Al₂O₃ ternary plot

This ternary plot (Figure 7.35) shows the similarity and uniqueness of the characteristics for each sample suite. Although little or no overlap occurs, the Vaalputs and surficial (Gordonia) sediments have similar relative oxide abundances. The white clay facies and the weathered surface basement suites also show similar relative abundances. The fact that the sediments lie in the area between the weathered basement and Dwyka samples suggests that both these source materials could have contributed to the sediments of the Vaalputs and Gordonia Formations.

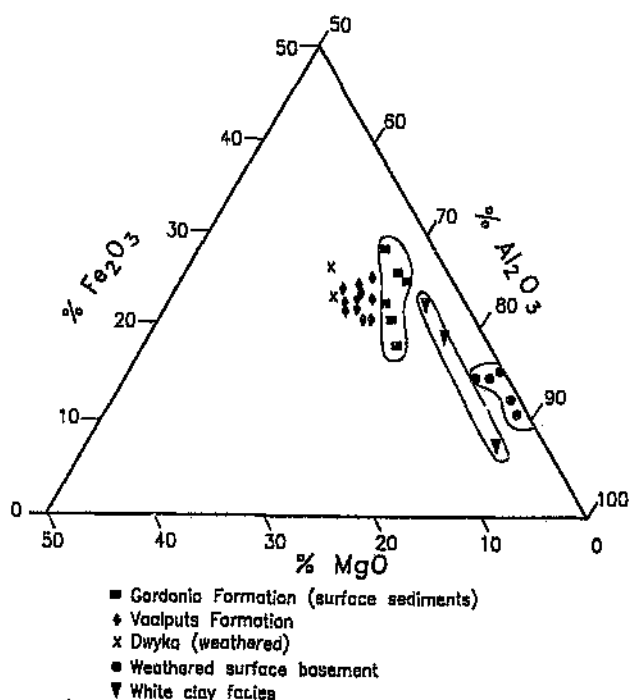


Figure 7.35 Fe₂O₃-MgO-Al₂O₃ ternary plot of the Vaalputs sediments and selected samples from the weathered surface basement, the white clay facies, surficial deposits of the Gordonia Formation, and Dwyka clay.

The comparative chemical study has shown that in most cases the Vaalputs and Gordonia Formations have similar chemical characteristics and relative oxide abundances. Also, from the data it appears as though the two formations are the product of various sources, which include the lower white clay facies and the basement (Namaqualand Metamorphic Complex, Dardap, and Dwyka).

7.9 Discussion

Some of the features of the Gordonia Formation and the surficial micro-environments are briefly discussed in the sections below after which a synthesis of these results is presented in a section dealing with their formation.

Atypical grain size parameters

Several factors are believed to influence the size frequency distribution of natural sediment populations. According to Solohub and Klován (1970) these are:

- i) distribution of the source material;
- ii) mineralogy and texture of the source material;
- iii) the type and amount of energy at a depositional site;
- iv) the rate of sediment supply;
- v) the possibility of sediment removal;
- vi) the mixing, sorting, and remixing of separate populations; and
- vii) diagenetic alterations.

All the above factors may influence the sedimentary parameters obtained for the Gordonia Formation samples, resulting in the scatter of data points (comparative sedimentary parameter plots). Most samples taken for the grain size analysis include many distinct depositional episodes, that is, the analyses may reflect several processes rather than depositional or transport sorting (Emery, 1978).

The mean grain sizes for the aeolian dune environments of this study (1-1.6 ϕ) are higher than those recorded for aeolian sands in the Kalahari basin and Namib Desert: for example, Namib sands 2.11 ϕ (0.23 mm) (Goudie, 1970), Namib dune crests 2.44 ϕ (0.18 mm), and Namib dune streets 1.99 ϕ (0.25 mm) (Lancaster, 1981); north-west and south-west Botswana, 2.3 ϕ (0.20 mm) (Grove, 1969); and central Kalahari, 2.4 ϕ (0.19 mm) (Lancaster, 1978a).

The coarser than expected mean grain sizes for the Gordonia Formation, especially

deposits which are obviously aeolian in nature, were at first believed to be due to the following factors:

- i) the Vaalputs sediments are fairly close to their source;
- ii) extremely strong winds are experienced in this area;
- iii) bioturbation has resulted in mixing of both coarse lags (sheetwash and deflated accumulations) and aeolian derived sediments;
- iv) deflation, and hence the removal of fines.

However, the three comparative grain size parameter plots (Figures 7.31, 7.32, and 7.33) show reasonable overlap of the Vaalputs and the Gordonia Formation fields. This correlation of sedimentary parameters may be partly attributed to the mixing associated with bioturbation. However, the results do suggest a common source for the two sediment suites. The results also suggest a genetic relationship or at least fairly similar sedimentary processes for the two sediment suites.

In addition, the long traverse results show that there is no regional change in grain size, particularly with distance from the basement in the west as was initially believed (McCarthy, 1985). Rather, the local or micro-environment seems to play a part in defining grain size characteristics.

The study of sedimentary parameters has shown that the Vaalputs and Gordonia sediments have very similar characteristics. The sedimentary parameters of the Vaalputs Formation generally fall within the larger field defined by those of the Gordonia Formation. The tighter clustering of the Vaalputs sediments is most likely due to the more homogeneous (due to mixing by bioturbation processes) nature of these sediments, whereas the Gordonia has a greater spread due to the reworking of what must have been predominantly Vaalputs sediments in different micro-environments, which combined, show a greater variability of sedimentary parameters. The sedimentary parameters of this study all indicate that the source of these sediments is primarily the Vaalputs Formation and that the present land surface must therefore be in a general state of degradation.

Petrology and chemical results

Petrographically the Gordonia sediments are similar to the Vaalputs sediments. The Vaalputs sediments tend to contain more iron cemented grains (iron cementation was noted to cause "clustering" of grains) and have a greater percentage of fine silt to clayey matrix. Reworking of the Vaalputs sediments on surface, by aeolian processes, could well account for the de-aggregation of iron clusters and the slight depletion of fine/clay fraction compared to the Vaalputs sediments. The fine fraction generally present throughout the surface sediment is also not typical of aeolian environments; the dominant surface forming process. The possibility that the fine fraction was derived from weathered basement to the west of the Gordonia deposits and deposited in a high energy aeolian environment also seems unlikely. Remnant feldspar grains in both the Gordonia and Vaalputs Formations suggests that the clay fraction is predominantly derived from *in situ* weathering of the Vaalputs sediments and reworked to some degree in the overlying Gordonia sediments.

The comparative chemical results show that the Gordonia (surface) samples are very closely related to the Vaalputs sediments and differ essentially only by being more quartz rich which may be accounted for by aeolian processes. Also, as previously mentioned, aeolian activity presumably reduces the clay fraction to some degree, and hence "cleans" these sediments with respect to the underlying, and more clay rich sediments. The higher CaO concentrations at surface may well be the result of the greater termite activity found in the near surface sediments. For many years petrologists have studied the factors which have led to the appreciable quantities of calcium carbonate in termite mounds on non-calcareous soils. Watson (1974) lists some of the proposed methods for the concentration of calcium carbonates, which all involve evaporation of water containing calcium carbonate from the termite mound, but differ in the source and mode of entry of water into the mound. Watson (1974) suggested another method in which the pH of the mound is elevated by termites bringing in vegetation and the precipitation of calcium carbonate as a result of contact between the termite mound of high pH and ground water of low pH. These processes may well contribute to the elevated CaO contents observed in the surficial sediments. Brynard (1988) observed similar magnesium-oxide trends to that of this study in most boreholes

on Vaalputs and related magnesium to calcrete, that is, he suggested that magnesium is co-precipitated with the calcium as dolomite along fractures in the calcrete. In addition, other concentrations of MgO, not associated with CaO he suggested, represents the presence of smectite clay, of which MgO is an important constituent.

The comparative chemical results also suggest that the Vaalputs sediments (the source of the Gordonia and surficial micro-environment sediments) are derived from: i) gneissic basement of the Namaqualand Metamorphic Complex; and ii) Dwyka rocks.

A number of conclusions may be drawn from the comparative chemical results: although all the analyzed sample suites exhibit individual chemical characteristics, weathering and soil forming processes played an important role in changing the characteristics of the source material, the Vaalputs Formation. In addition, mixing of the sediments by bioturbation processes and modern weathering has given rise to the chemical characteristics of the Gordonia (and Vaalputs) Formation.

Subsurface calcrete

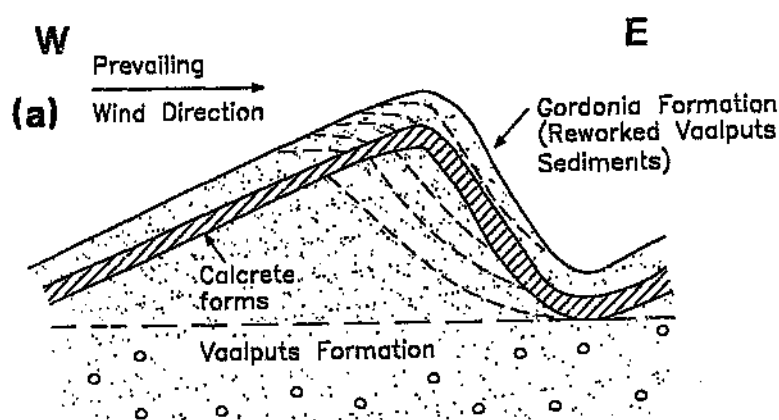
As all the observations and data indicate that the present landsurface is in a state of degradation it would, therefore, appear that the calcrete layer associated with the dune forms is continually being leached downwards by meteoric water. A similar scenario was described by McCarthy (1983) for calcretized river gravels in the Griqualand West region, where, as the layer migrates downwards the sediment is released at surface contributing to the derived deposits.

Formation of the Gordonia Formation and the surficial micro-environments

The surficial aeolian deposits of the region, resulting from aridification, are believed to be of late Tertiary to Quaternary age. The present day micro-environments (aeolian dunes, deflation pans and lag deposits) have been shown to be a product of the underlying Vaalputs Formation. This is exhibited in the correlation of grain size parameters and chemistry, the petrology, and presence of fines throughout these sediments.

The results of this study all indicate that the source of these sediments is primarily the underlying Vaalputs Formation which is in a state of degradation. At the onset of aridification reworking of the Vaalputs Formation gave rise to an aeolian dune dominated landsurface (Figure 7.36a). Surface processes (primarily aeolian) have reworked and modified the surface into longitudinal dunes with a transverse component. A subsurface calcrete layer in these dunes gave rise to a more stable dune morphology. With degradation of these forms the calcrete was exposed predominantly on the windward side of the dune, and allowed some aggradation of sands on the more protected leeward side of the dune (Figure 7.36b). This overall degradation "flattened" the aeolian dune morphology to some extent. Continued degradation exposed larger areas of calcrete and gave rise to a fairly flat landscape, with dunes of a fairly low amplitude (Figure 7.36c). The subsurface calcrete layer is continually being leached downwards by meteoric water and in doing so replaces the underlying Vaalputs Formation material. The exposed calcrete is processed and released at surface as degradation takes place.

It is on the lower lying areas of the stable hummocky landsurface that deflation pans may develop. Lag deposits occur in areas where the fines have been removed by aeolian and fluvial processes. The surficial deposits are continually undergoing modification and mixing with the underlying Vaalputs sediments by bioturbation.



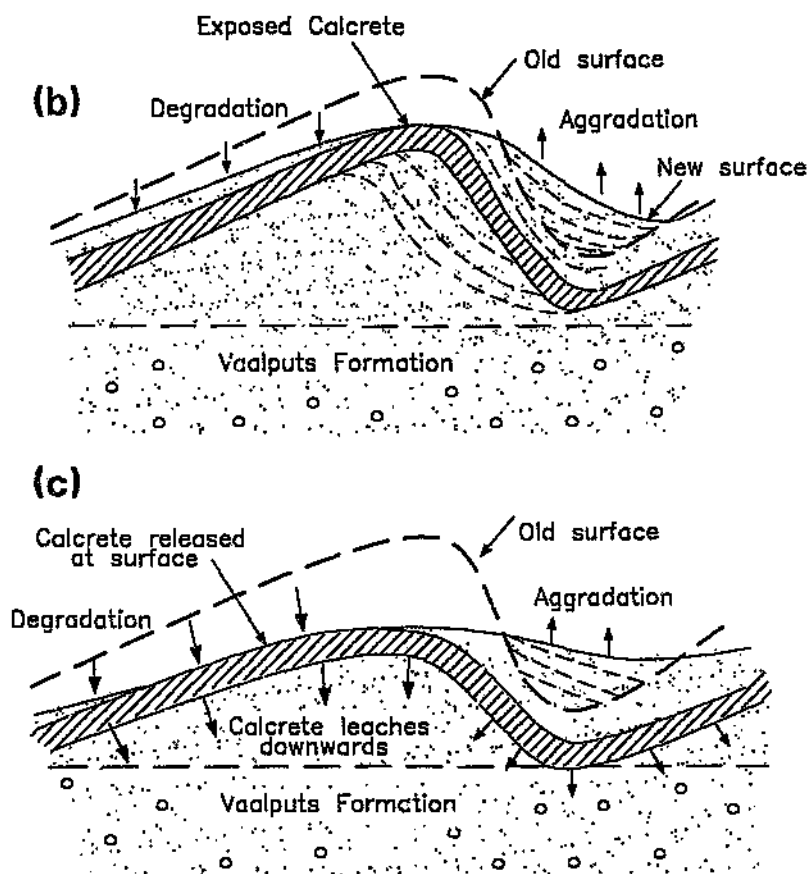


Figure 7.36 Stages in the development of the Gordonia Formation and surficial micro-environments.

CHAPTER 8: STRUCTURE

According to Partridge and Maud (1987) uplift of the subcontinent has occurred episodically, with extended periods of stasis since Mesozoic times. These uplifts are concentrated near the coastal margins and along discrete inland axes. Partridge and Maud (1987) also suggest that no major faulting has accompanied these movements. Some faulting, however, which may well be related to episodes of uplift can be observed on a local scale. Faults, fractures, joints and other manifestations of stress in the lithosphere are commonly selectively weathered and eroded. Fault scarps, offset drainage channels, lineaments and other structural features are indicative of tectonic events.

In this chapter, macroscale approaches were used to establish broader and more generalized causal links between tectonics and landform development in the Vaalputs region. In many cases, macroscale tectonic controls are reflected in small-scale morphological features. In the study area the tectonic interpretations of such morphological features was crucial in unravelling the nature of past and recent tectonic activity. TM-5 LANDSAT imagery was processed and interpreted for lineaments, allowing for the compilation of a lineament map for Vaalputs and its environs. More detailed studies were carried out on specific lineaments and field work included slickenside measurements and joint analyses. Seismic data were analyzed, and finally, all the data was synthesised and interpreted to produce a model for the tectonic history of the area which gave rise to the accumulation and preservation of the surficial sediments in the Vaalputs region.

8.1 Lineament Analyses

The approximate area, and the image used for the lineament analysis is shown in Figure 7.1. The image and a lineament map was produced at a scale of 1:100,000. Figure 8.1 shows the results of this analysis. All structural lineaments shown are either faults or master joints. Lineaments which were attributed to foliation and lithological fabric were excluded. A rose diagram (Figure 8.2) shows the orientation of all mapped lineaments, as determined from data presented in Figure 8.1.

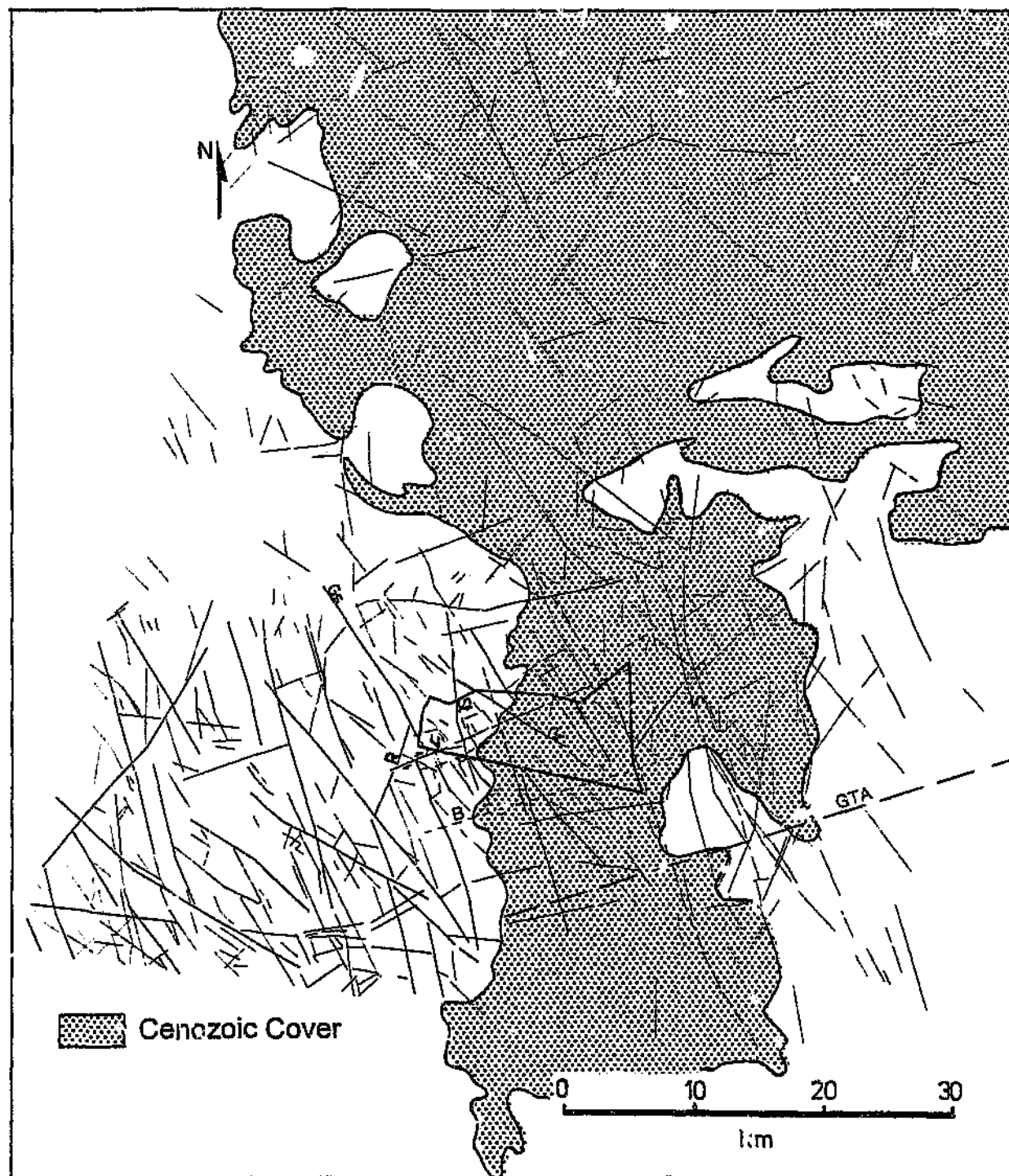


Figure 8.1 Structural lineaments in the Vaalputs area derived from TM-5 Landsat data (various combinations). Gr=Garing fault; Gs=Gasab fault; R=Riembreek fault; S=Santab fault; St=Stofkloof fault; V=Vaalputs fault; B=Bok-puts fault and GTA=Griqualand-Transvaal Axis of uplift.

The lineament orientations (Figure 8.2) for all lineaments, expressed as a percentage of the total length, exhibit strikingly similar orientations to those obtained by Andersen (1992) and Corner (1993). The primary lineament orientation, that is, approximately 160° as mapped by Andersen (1992) and Corner (1993) is similar to the primary orientations obtained in this study. Other lineament trends (Figure 8.2), which are less prominent, but nevertheless, may have a significant role in recent tectonism are: a north-northeast trend, a north-east trend and a east-northeast trend. These other three orientations were observed by both Andersen (1992) and Corner (1993) using geophysical methods.



Figure 8.2 Rose diagram showing strike of all lineaments, as determined from data presented in Figure 8.1. All data are expressed as percentages of total lineament length.

Several faults which have previously been identified by other methods such as geological mapping and air-photo interpretation (e.g. Andersen, 1992) and aeromagnetic methods (Andersen, 1992; Corner, 1993) were recognised in this study using TM-5 Landsat Imagery (Figure 8.1). These include:

i) **the Garing fault**,

ii) **the Vaalputs fault**,

iii) **the Gasab fault**, which correlates with the position of the Gasab river and has clearly been displaced (right-laterally) by the Vaalputs fault. This displacement was also noted by Corner (1993), and suggests an older age for the Gasab fault;

iv) **the Stofkloof fault**, also associated with present drainage, appears to be slightly displaced by the Vaalputs fault, which implies a younger age for the latter fault. Corner suggested that the Stofkloof fault was displaced right-laterally by the Vaalputs fault - the sense of displacement, however, is not well defined by the LANDSAT data of this study (evidence for reactivation of the Stofkloof fault has been observed and is described in Section 8.3.2);

v) **the Riemtrek fault**, and

vi) **the Santab fault**, which is a prominent feature, identifiable on the LANDSAT image and on airphoto, and also observed by Corner (1993) to correlate with a strong thermal infra-red lineament. The reader is referred to Section 8.3.2 for further observations related to the reactivation of some of the above mentioned structures.

The **Bok-puts fault** which parallels the Vaalputs fault (Corner, 1993) was not visible on any of the studied LANDSAT images (the position of this fault is shown on Figure 8.1). According to Andersen (1992) this fault represents a zone of higher magnetisation, and the depth to the highly magnetised rocks was interpreted as 1500 metres. Corner (1993) suggests a much shallower depth due to sharp changes in magnetic field as one crosses the fault. Nevertheless, as the Bok-puts fault has not been observed by Landsat imagery, it has most probably been inactive since the deposition of the overlying sediments (the Vaalputs and Gordonia Formations).

Figure 8.3 shows the lineaments over the Vaalputs area as determined from LANDSAT imagery, superimposed on elevation contours of the base of the "Vaalputs basin" (contours were determined by Jamieson, 1986, from borehole logging). Figure 8.3 shows a definite association between the observed lineaments and the Vaalputs basin shape, and elevation contours of the basement. The association exists predominantly with a set of north-northwest trending lineaments (some of which were newly recognised in this study), and which represents the primary lineament direction of the area as seen in Figure 8.2. The Garing and Vaalputs faults may have some influence on the basin shape, but the borehole spacing is too great to state this with any certainty. The lows depicted by the contours appear to be mainly bounded by the north-northwest trending lineaments.

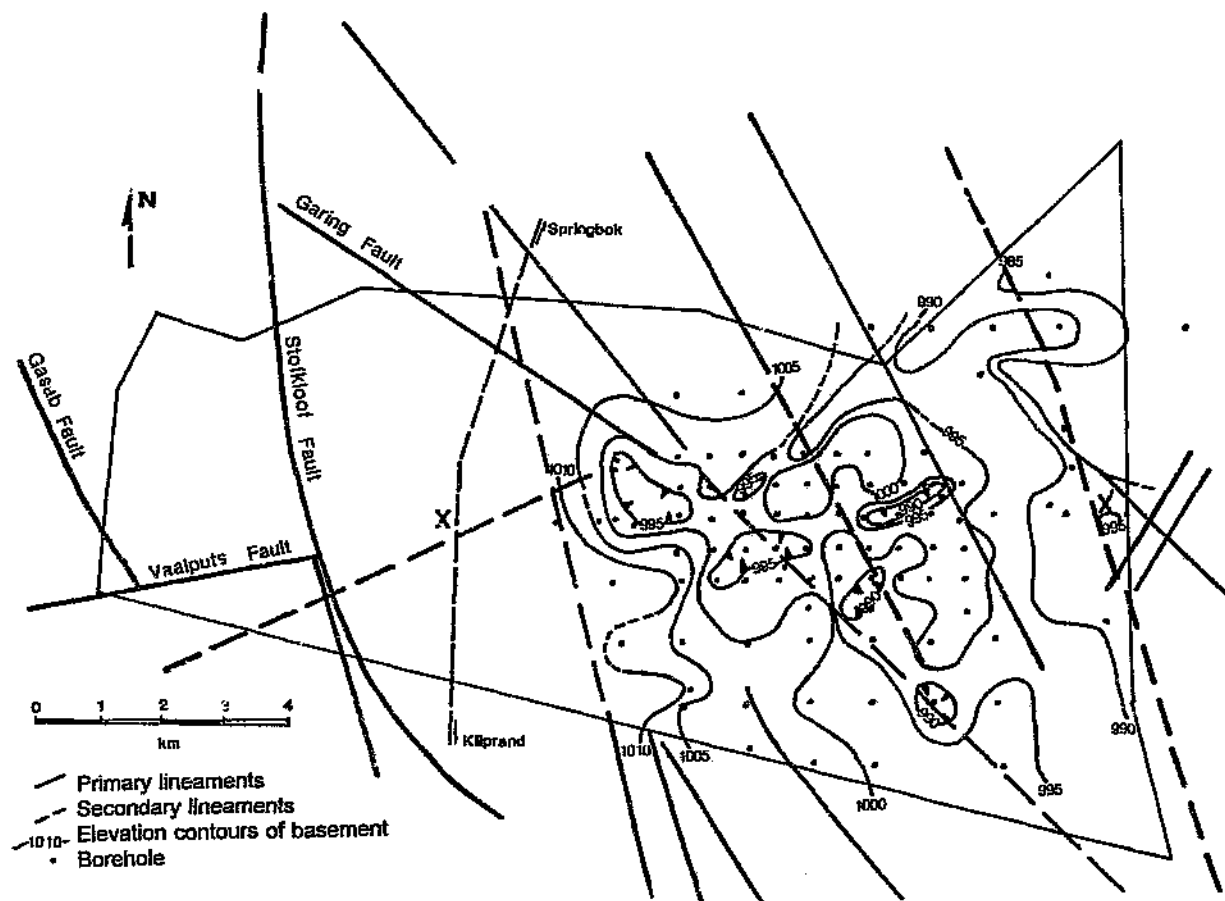


Figure 8.3 Lineaments of Vaalputs superimposed on elevation contours of the base of the Vaalputs Formation. Basement rock contours were determined by Jamieson (1986). Section X-X' is described below (see Figure 8.5).

Figure 8.4 shows an east-west cross section across Vaalputs. The subsurface data for the eastern part of the section were taken from contours as determined by Jamieson (1986). The figure clearly shows changes in the height of the palaeo-weathered and silicified basement surfaces along the section. The silicified surfaces on the western side of Vaalputs are characteristically horizontal, suggesting that the observed height differences, at least in this area, are not due to palaeo-topography, but rather indicate tectonism. As no silicified basement is present on the eastern side of Vaalputs and since the weathered white clay facies of the Vaalputs Formation is generally fairly thick, relative elevation differences could not be reliably established.

Figure 8.5 shows a west-east cross section across the eastern part of Vaalputs (position of the cross section is indicated in Figure 8.3), approximately half a kilometre to the north of the disposal site along a line of closely spaced drillholes. In Jamieson's (1986) interpretation of the borehole information he proposed an undulating basement-sediment contact. This appears to be incorrect as it is now known that there are north-northwest trending lineaments, which are more than likely faults, and which appear to cross-cut the Vaalputs and Gordonia sediments. Figure 8.5 is therefore a reinterpretation combining the measured depths to the unaltered basement and the newly recognized lineaments.

Figure 8.5 shows that the Vaalputs sediments may occupy a series of graben-type structures, defined by a set of north-northwest trending faults. Sediment covered faults makes determination of the exact vertical and lateral limits of the "grabens" difficult, but from this interpretation they seem to extend from approximately 2 kilometres east of the main Springbok road to the Santab lineament in the east. The east-west section using Jamieson's (1986) borehole data alone (Figure 8.4) suggests that faulting preceded the onset of sedimentation, as the basement lows are filled with "white clay".

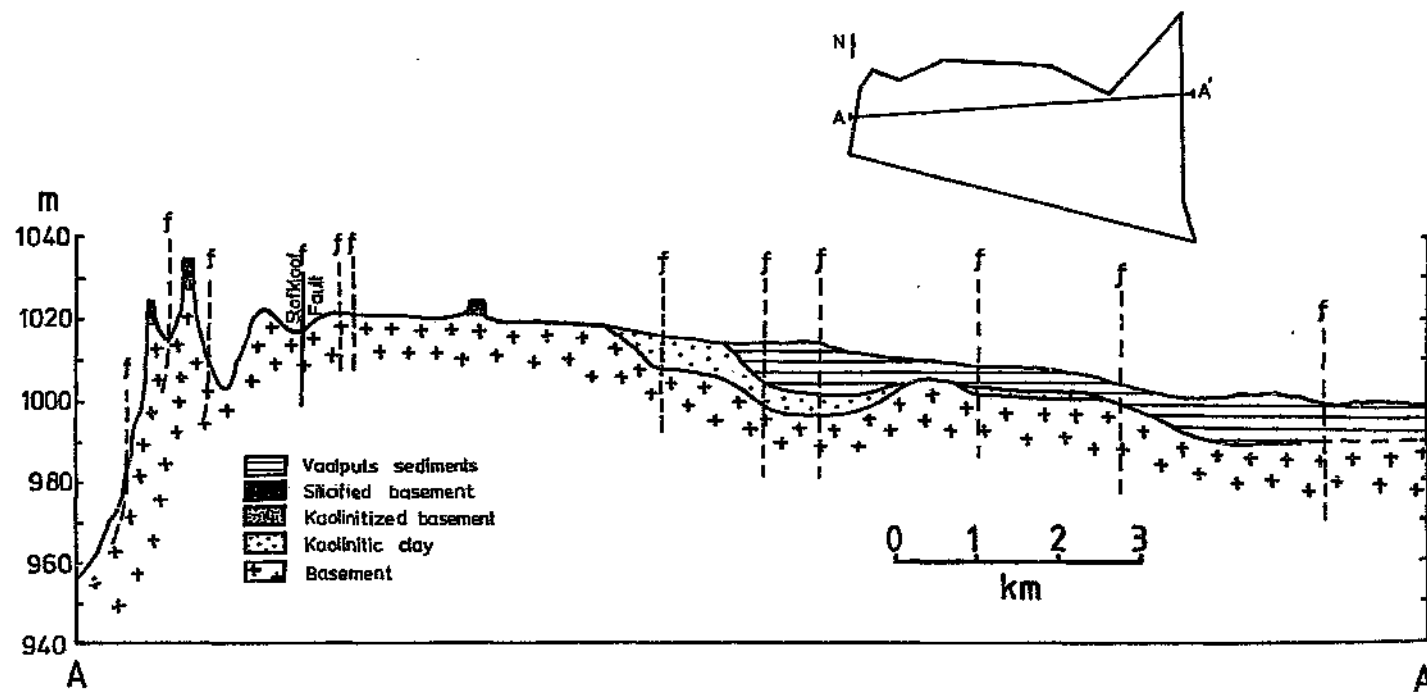


Figure 8.4 Topographic west-east cross section of Vaalputs, indicating the vertical displacements of palaeo-weathered and silicified basement occurrences.

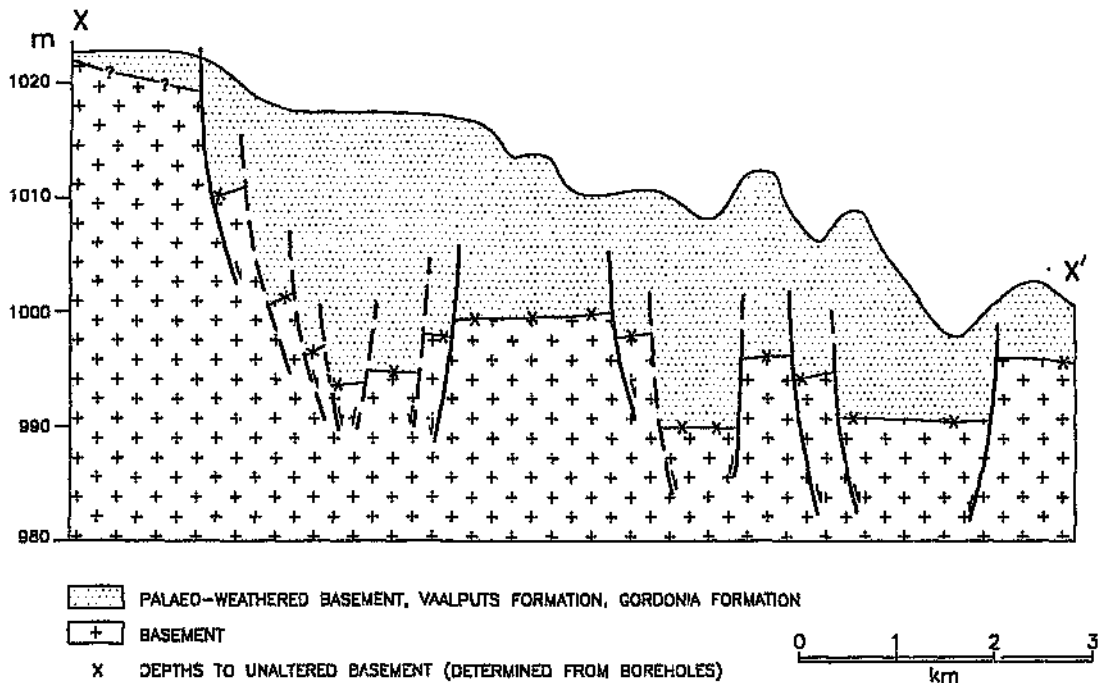


Figure 8.5 West-east cross section of the eastern part of Vaalputs. The section is approximately 500 metres to the north of the disposal site, the position of which is shown in Figure 8.3. Solid lines represent primary (prominent) lineaments, whereas dashed lines are secondary lineaments.

Andersen et al. (1996), in an independent aeromagnetic investigation, also recognised vertical displacement patterns of small magnitude on total field aeromagnetic images of the areas referred to above as, and defined by, "grabens". They noticed that the overall magnetic intensities are homogeneous within clearly defined blocks that terminate abruptly against north-northwest trending Pan-African aged faults. Areas of higher magnetic intensities were used to indicate horsts and the lower values grabens.

The fact that faulting is seen in the sediments, indicates a post Vaalputs and Gordonia Formation age for the faulting. It is therefore suggested that faulting and reactivation of pre-existing faults has been ongoing since at least the time when the palaeo surface was formed, that is, since the Cretaceous (Partridge and Maud, 1987; Andreoli et al., 1987).

SPOT panchromatic imagery techniques were used in an analysis of the surficial cover of the Dasdap sediments to identify lineaments in the southern portion of the study area. Figure 8.6 shows the lineament map for the Dasdap area as determined using SPOT satellite imagery. Figure 8.7 shows the orientations for all lineaments in the Dasdap area, expressed as a percentage of the total length.

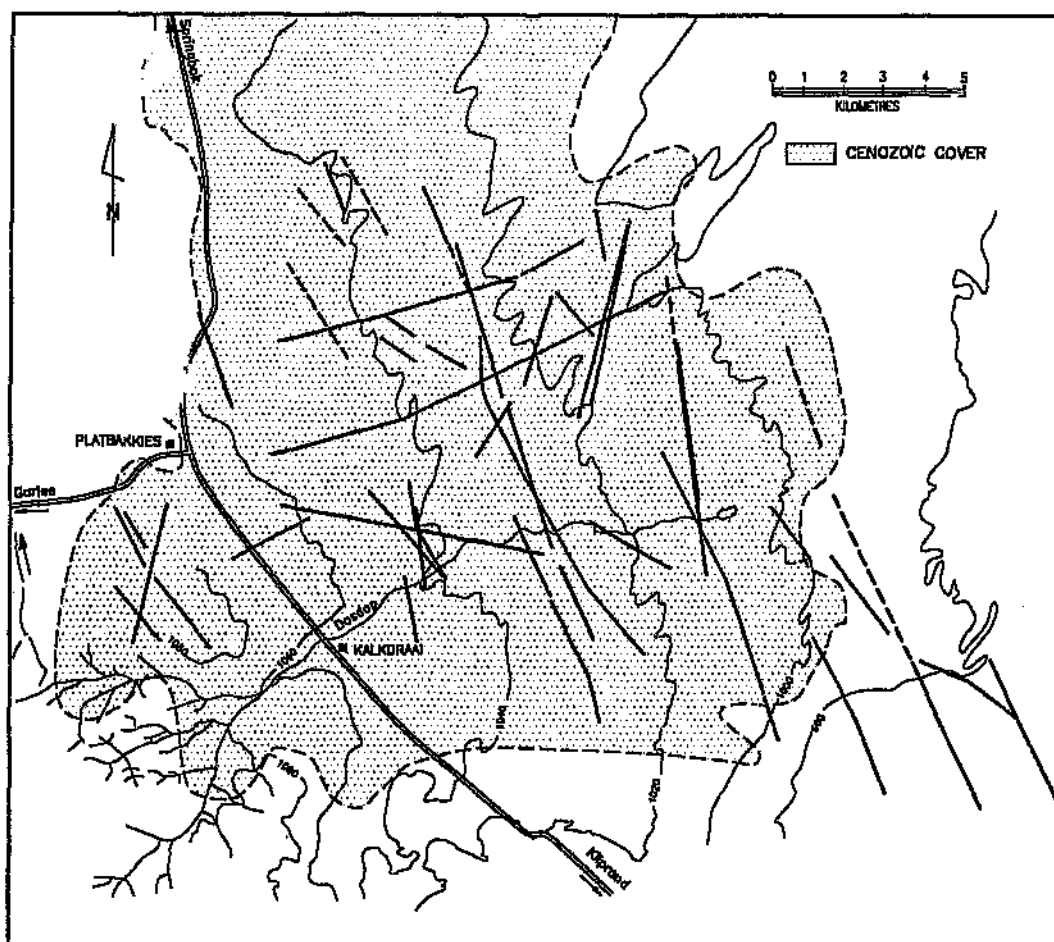


Figure 8.6 Lineament map for the Dasdap area, obtained using SPOT panchromatic imagery. Also shown are the present land surface contours and the Dasdap drainage.

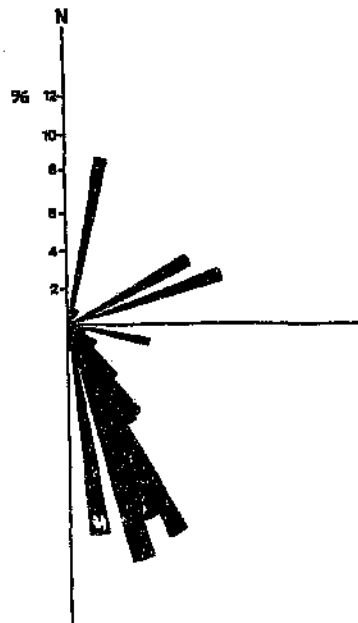


Figure 8.7 Rose diagram showing strike of all lineaments for the Dasdap area, as determined from data presented in Figure 8.6. All data are expressed as a percentage of total lineament length.

From Figure 8.7 it is evident that the orientations of this slightly more southerly area, which is predominantly covered in Cenozoic deposits are similar to those of the Vaalputs area (Figure 8.2). That is, a dominant north-northwest orientation, and less prominent northeasterly orientations are present in the Dasdap area. The lineaments obtained using SPOT imagery, were investigated in the field but field observations revealed no noticeable displacement or surface expressions. This was attributed to the fact that the terrane is extremely flat and that mobile aeolian sands would not allow the development of a well defined fault scarp, but would rather tend to smooth out such an expression, allowing subtle features such as these to be viewed, using remote sensing techniques only.

In an attempt to reveal the lineaments and possible faults, which are generally orthogonal to the drainage path (Figure 8.6), a down-stream profile along the Dasdap drainage was carried out. The results of this study are presented in Section 7.3 in which the disturbance of recent drainage patterns, by tectonism, is dealt with.

8.2 Structure of the Palaeo-weathered Cretaceous Land Surface

A structural analysis was carried out on the prominent palaeo-weathered mesas that are preserved on the western part of the Vaalputs property. A structural analysis of these features would contribute to the overall understanding of the structure of the basement in the region. The analysis included documenting orientation and sense of movement, where possible, of any tectonic related features: fault and shear zones, lineaments, master joints, and surfaces containing slickensides. Figure 8.8 is a map of the western side of Vaalputs showing these palaeo-weathered occurrences. Both older structures and those which post-date the Cretaceous weathering event are preserved in these features, thus allowing for the recognition and identification of older and Cenozoic structures.

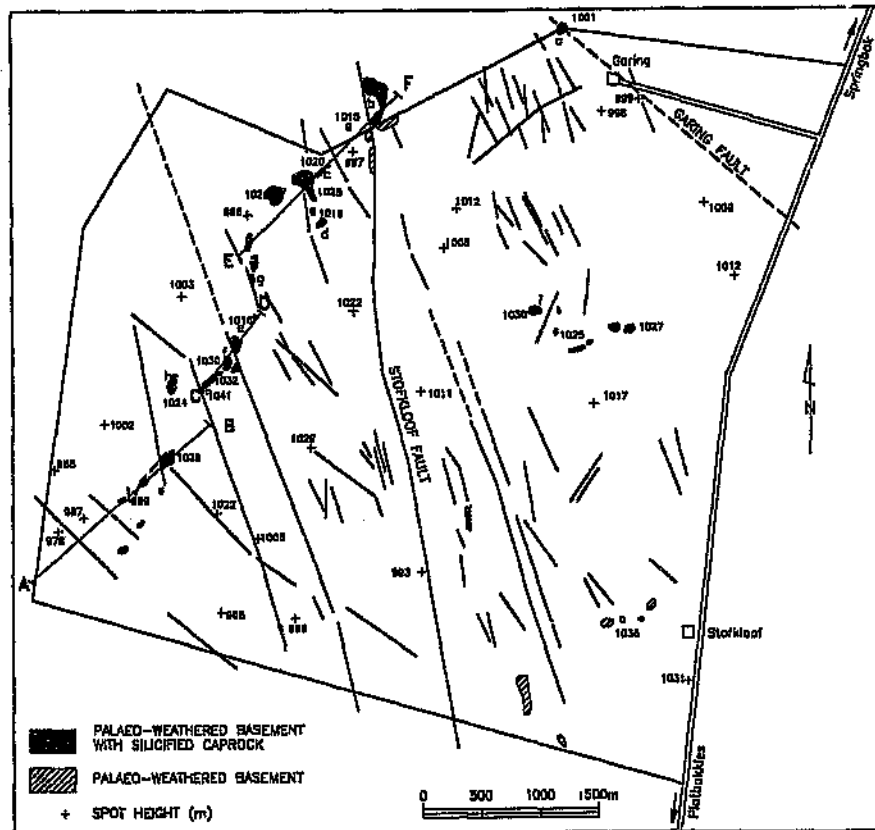


Figure 8.8 Map of the western portion of Vaalputs, that is, to the west of the Springbok road, showing the occurrences of altered basement and the observed lineaments (for section A-F see Figure 8.10). Lower case letters represent areas where detailed slickenside analyses were carried out, and are referred to in Section 3.2.2.

8.2.1 Faulting

Evidence for faulting, some of which may be contemporaneous to that on the eastern portion of Vaalputs is shown in Figure 8.9. This staggered northeast trending cross section (the position is shown in Figure 8.8) displays vertical displacement of up to 40 metres in the palaeo-weathered and silicified basement on the western side of Vaalputs. The section (Figure 8.9) confirms displacement resulting from the numerous northwesterly trending faults which are known to exist in the basement and which are also seen to affect the sediments occupying the Vaalputs basin (Figure 8.5). Several other workers (e.g., Stephens, 1971; Senior, 1978; Wopfner, 1978; Milnes and Twidale, 1983) who have observed the relationships of silicified materials with weathered profiles, have also recognised the effects of tectonics on the disposition of silcrete horizons.

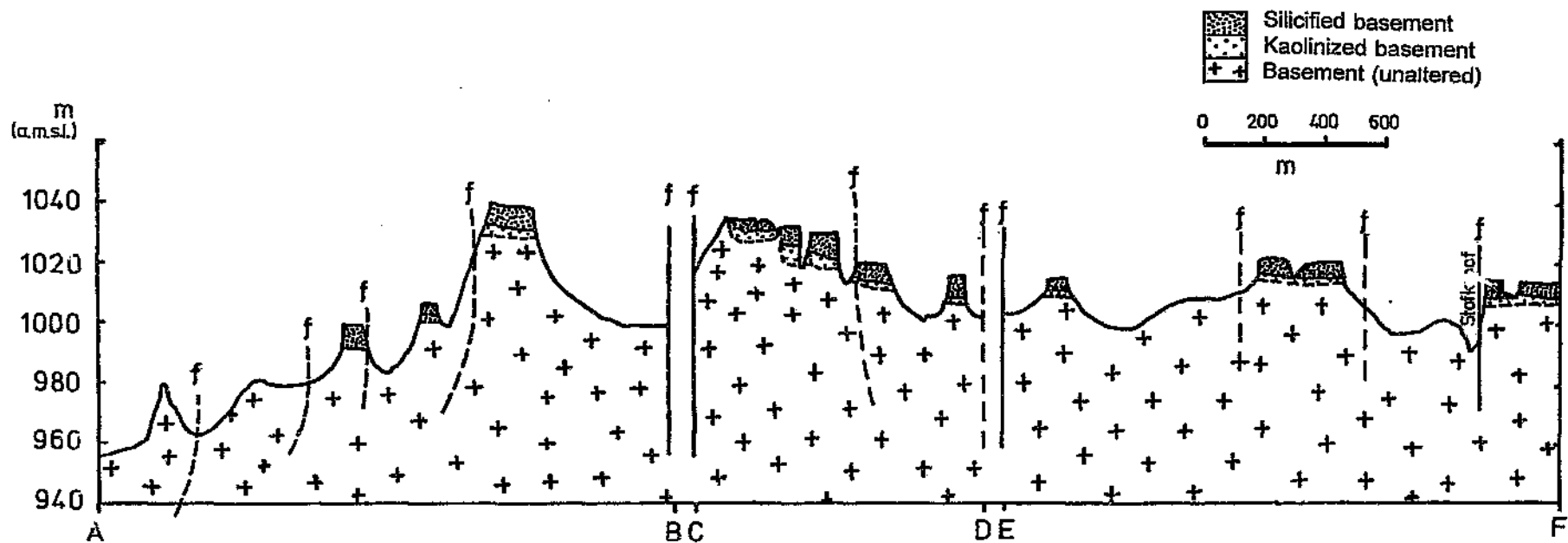


Figure 8.9 Staggered northeast trending cross section (the position of which is shown in Figure 8.9). Solid lines = primary faults; dashed lines = probable/secondary faults.

8.2.2 Slickensides

The results presented above indicate post weathering displacement: Figure 8.9 shows offsets in the silicified cap rock. In addition numerous slickensided surfaces were noted in these palaeo-weathered occurrences. Slickensides occur on silicified or clayey surfaces which are typically polished. The clayey and silicified lithologies appear to be ideal for the formation and preservation of slickensides and their associated planes. A typical, well preserved slickensided surface is shown in Figure 8.10.



Figure 8.10 Typical well preserved slickensided surface in the prominent palaeo-weathered basement occurrences.

Characteristics and possible origins of slickensides

Field observations indicated two distinct slickenside types which have different physical characteristics (Table 8.1). The characteristics of the slickensides are suggestive of different origins, namely those resulting from tectonism and those related to the expansion of clays, and are, therefore, referred to as such in Table 8

Table 8.1 Characteristics of two slickenside types (based on proposed origins) present on fracture surfaces in the palaeo-weathered and silicified basement occurrences.

Origin:	Slickensides associated with the expansion/swelling of clay	Slickensides associated with tectonism
1)	Occur on conchoidal or curvi-planar surfaces	Occur on flat surfaces
2)	Two or more slickenside directions may be present on a surface	Generally only a single slickenside direction on any particular surface
3)	Occur on small, non-continuous, non-penetrative, fracture surfaces	Occur on large, continuous, penetrative, fracture surfaces.
4)	Slickenside striations often poorly developed	Slickenside striations usually well developed
5)	Sense of movement often difficult to determine	Sense of movement sometimes definable
6)	Large variations of slickenside orientations observed at an outcrop.	Similar orientations of slickensides (often exhibiting conjugate pairs) observed at any particular outcrop

Slickenside orientations

All surfaces observed containing slickensides were measured and documented. The orientations of the planes and slickensides are tabulated in Appendix F. As the palaeo-weathered basement occurrences are bound or defined, in most cases, by faults, all slickensided surfaces could have been influenced by tectonism to a greater or lesser degree. Thus, the analysis of slickensided surfaces in the palaeo-weathered and silicified units formed a major part of the tectonic analysis as they are abundant and suggestive of Late- or Post-Cretaceous tectonism.

The orientations of all surfaces containing slickensides (Appendix F) were plotted on an equal area stereo-net projection using the program "S-plot". The poles to all planes (Figure 8.11) show random orientations. The distribution of these poles was determined statistically to be 95% uniform.

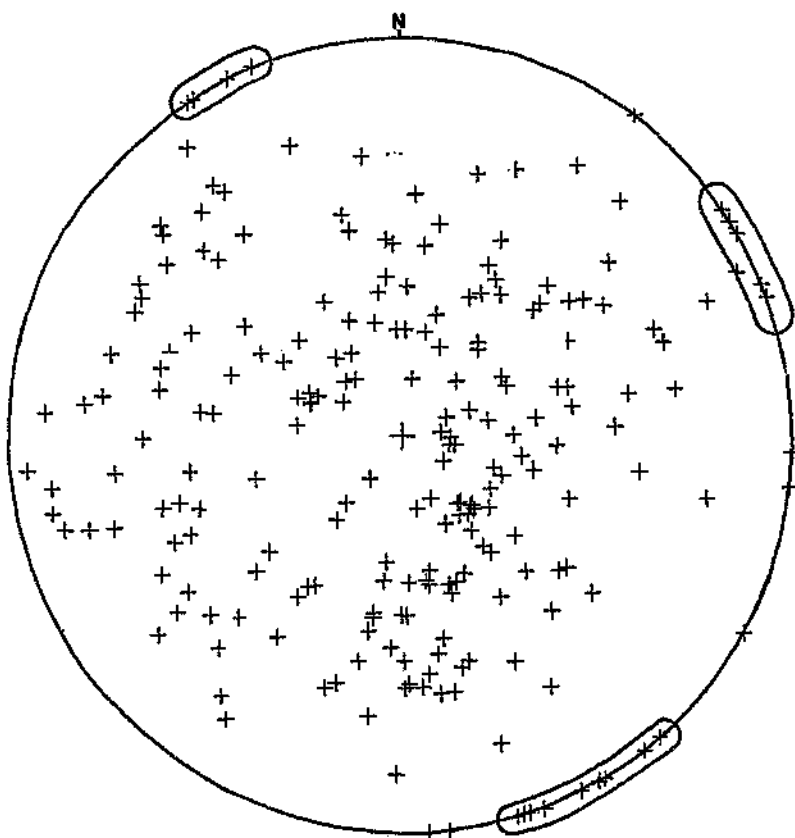


Figure 8.11 Stereo-net plot of all poles to the measured planes containing slickensides in the palaeo-weathered basement.

The strikes of all planes containing slickensides were plotted on a rose diagram in an attempt to further enhance and extract any preferred orientation. This was attempted to determine whether any planes of possible tectonic origin would be revealed, which were being "hidden" by the scatter of other planes of possible swelling origin in Figure 8.11. The results of this rose diagram plot are shown in Figure 8.12.

Besides the expected "noisy background" (Figure 8.12), two prominent orientations are evident: a north-northwest orientation (which coincides with the regional lineament trend - Figure 8.2) and a northeast orientation. The stereo-net plot (Figure 8.11) shows three clusters of poles to planes containing slickensides which are most probably associated with the two trends evident in Figure 8.12. These two orientations trend approximately 70° and 142° .

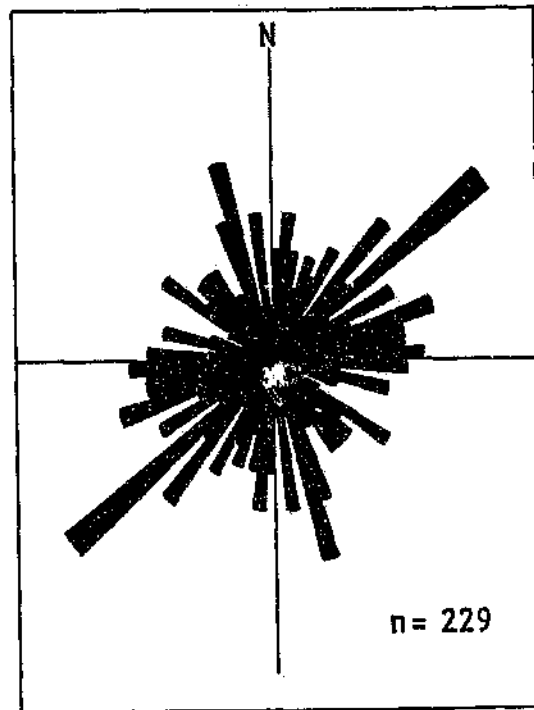


Figure 8.12 Rose diagram of all strike orientations of planes containing slickensides in the palaeo-weathered basement.

As most clays expand when wet and according to Nettleton and Brasher (1983) kaolinite expands by $12 \pm 2\%$ when wet, the orientations believed to be associated with tectonism only, were extracted from the rose diagram (Figure 8.12) and plotted on a separate rose diagram: Figure 8.13. This figure again shows the prominent orientations obtained previously, that is, a northeast and a north-northwest trend. Two other trends are also present: a northwest trend (possibly associated with the north-northwest trend), and a less prominent north-northeast trend. These results support the interpretation, initially based on field observations, of two origins for the slickensides.

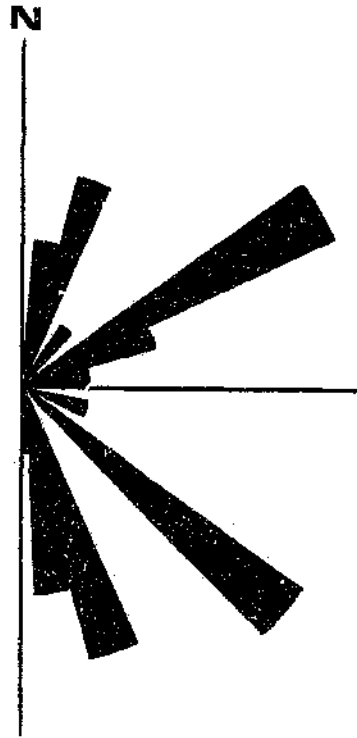
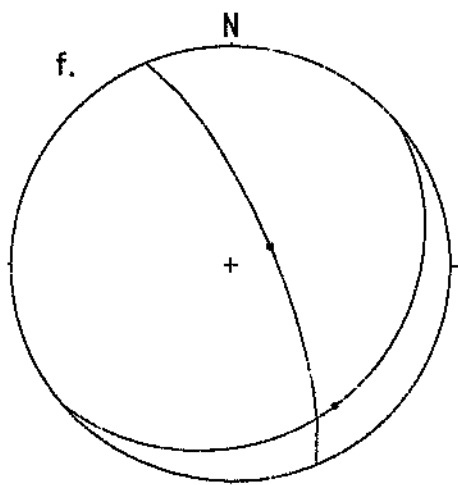
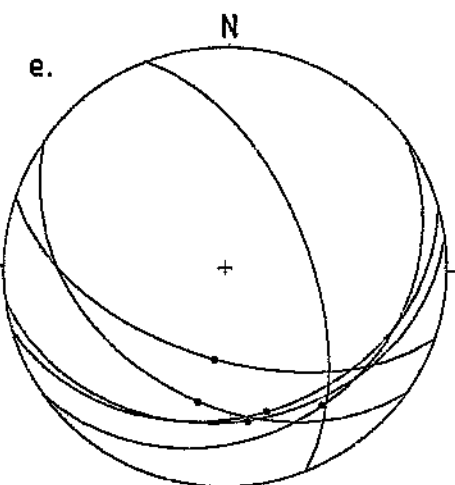
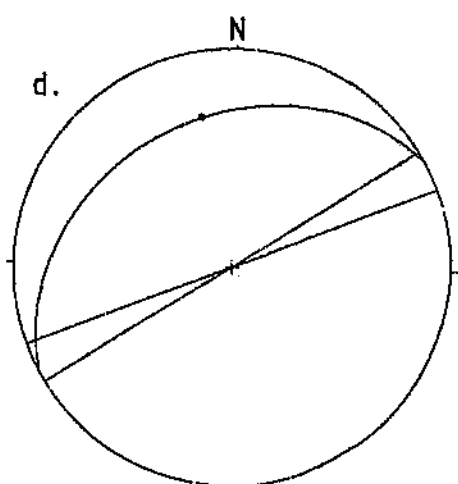
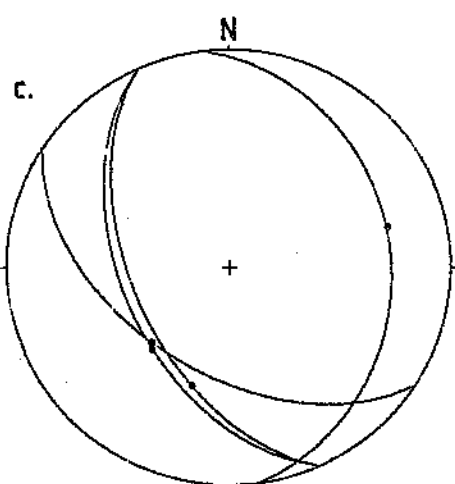
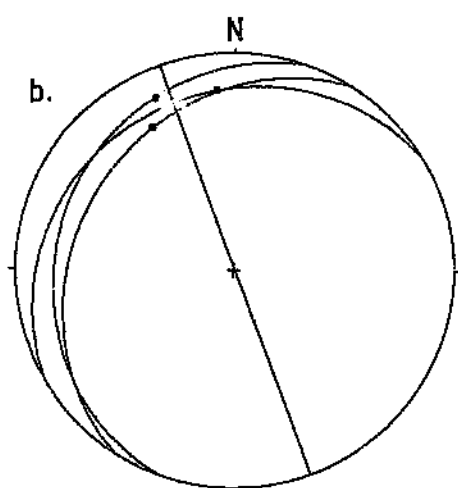
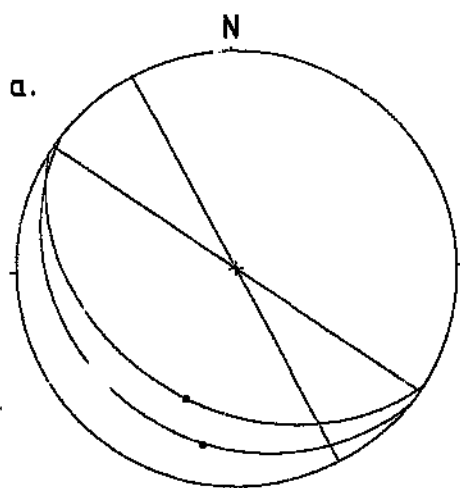


Figure 8.13 Rose diagram of all strike orientations of planes in the palaeo-weathered basement occurrences which are believed to be associated with tectonism (n=29).

8.2.3 Slickenside Analysis

The better preserved and developed, continuous and penetrative surfaces for selected localities were plotted on stereo-nets (Figure 8.14). The localities for these plots are shown in Figure 8.8. These plots, with the exception of two (Figures 8.14h and 8.14i), show similar preferred strike orientations of planes, to those of Figure 8.12 and 8.13. That is, two prominent trends are present: a north-northwest and a northeast trend.



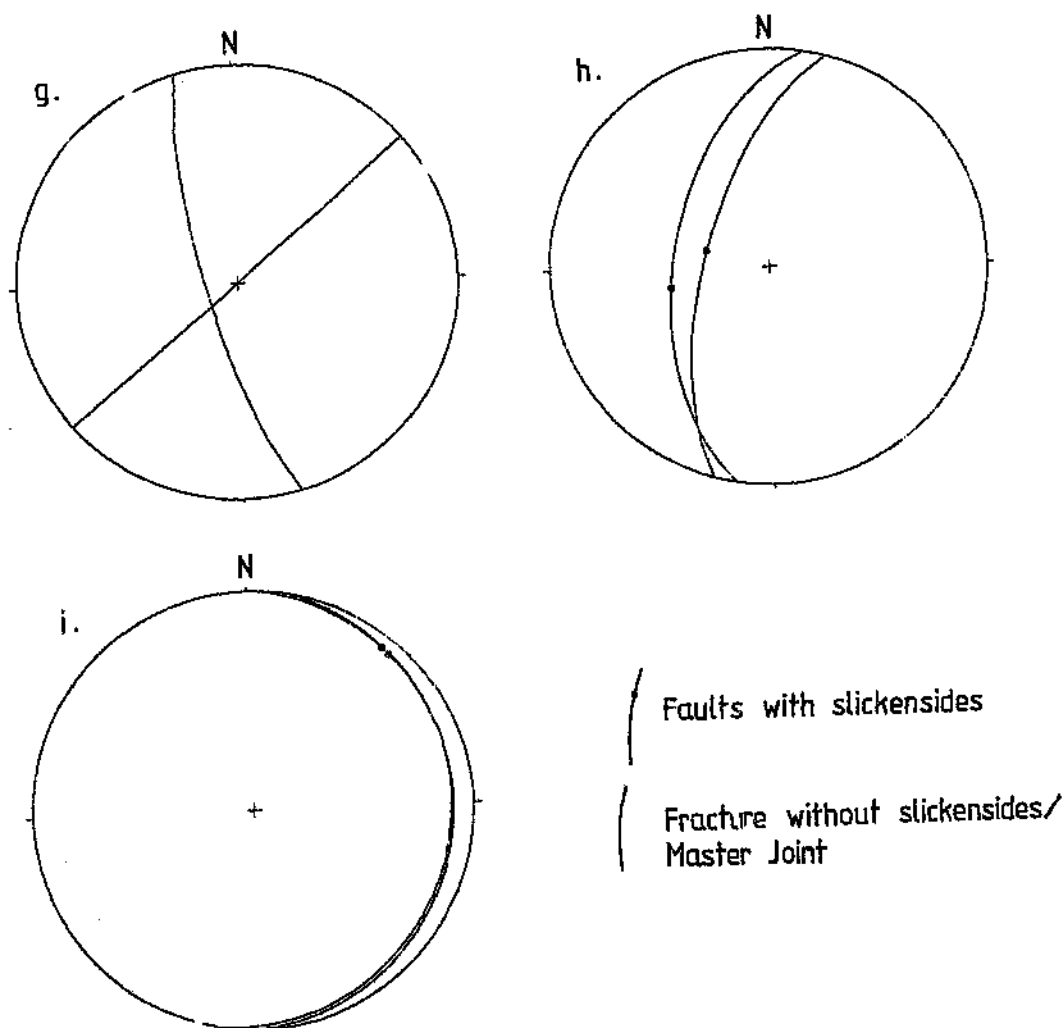


Figure 8.14 Orientations of selected surfaces of proposed tectonic origin. For localities see Figure 8.8.

Using the method described by Jaroszewski (1984), principal stress directions for five of the stereo-net plots of Figure 8.14 could be obtained:

- b. 48° on 240°
- c. 9° on 251°
- e. 18° on 043°
- f. 34° on 046°
- g. 10° on 020°

These results indicate two principal stress directions: a west-southwest (b and c above), and a northeast to north-northeast (e, f and g above) oriented principal stress direction. In most of these cases the principal stress is sub-horizontal.

The method employed above (Jaroszewski, 1984) to determine principal stress directions for selected stereo-net plots (Figure 8.15) is generally unsatisfactory, as only individual sites could be analyzed. As the majority of slickenside lineations are formed in an anisotropic medium which contains numerous surfaces of discontinuity (Van der Merwe et al., 1988), for example, joints and faults, a method was required to determine principal stress directions using slickenside orientations from the entire study area. This would give the prevailing regional stress directions responsible for the observed slickensides, rather than the stress directions for individual sites in what may well be an anisotropic medium. According to Aleksandrowski (1985) the relationship between the orientations and magnitude of principal stresses, and the directions of slip on variably orientated pre-existing planes in such a medium is highly complex. The orientations of slip directions which are developed on a multitude of differently oriented planes can be used to determine the orientation of the prevailing stress field (Aleksandrowski, 1985). Aleksandrowski modified an earlier approach to this problem by Arthaud (1969). This method for the analyzed data is, however, based on the assumption that all planes and slickensides (of proposed tectonic origin) in the paraeo-weathered basement occurrences were formed by the same stress field.

Arthaud's (1969) method is based on the concept of movement planes (M-planes) which are planes perpendicular to the slip plane and also contain the direction of the slickenside lineation. Applying Arthaud's (or Aleksandrowski's) method to a fault population active in a single tectonic episode, it is necessary to:

- i) plot the poles to fault planes and the penetration points of the striae on a stereo-net;
- ii) join each fault pole and the corresponding striae penetration point with a great circle, thus tracing individual movement planes (M-planes) and
- iii) plot the poles (π M-points) to the movement planes. All the M-planes should intersect at none, two, or three points, that are the axes of the same number of mutually

perpendicular great circles of π M-points.

The points of intersection of the movement planes correspond to an orthogonal system of deformation axes.

A movement plane was constructed for every locality where slickensides were observed and which appeared to be related to tectonism only. Slip movement planes (M-planes) were constructed (Figure 8.15a). In many cases it was not possible to determine sense of movement and, therefore, specific directions are not indicated. The resultant pattern of slip movements, excluding 16 points (35 % of data) which did not conform to any one of Aleksandrowski's patterns, may be seen in Figure 8.15b. The resultant pattern (Figure 8.15b) is similar to the case $C=1$ (also similar to $C=1.1$) of Aleksandrowski (1985). Aleksandrowski's pattern for the case of $C=1$ is shown in Figure 8.15c. The C -value defines a certain stress condition and is defined as $C=(\sigma_1-\sigma_3)(\sigma_2-\sigma_3)^{-1}$ where $1 < C < \infty$. The slip-movement directions which do not conform to the pattern (Figure 8.15a) may be the result of expansion-related slickensides of the palaeo-weathered zone which have been incorrectly interpreted as tectonic-related slickensides, or may represent an addition or superimposed pattern belonging to another stress field, for which insufficient data are available.

The data in Figure 8.15b corresponds to a stress field where $\sigma_1=\sigma_2$, one of which is vertical and the other oriented NNW-SSE (σ_3 is oriented ENE-WSW). This stress field is characteristic of normal or strike slip faulting (Anderson, 1951). Due to the amount of data available ($n=46$), it was not possible to determine whether C was in fact 1.1 rather than 1 (these two cases - Aleksandrowski, 1985, are very similar). For $C=1.1$ the stress field would be defined by a vertical σ_1 , a NNW-SSE σ_2 and an ENE-WSW σ_3 , that is, a stress field characteristic of a normal fault.

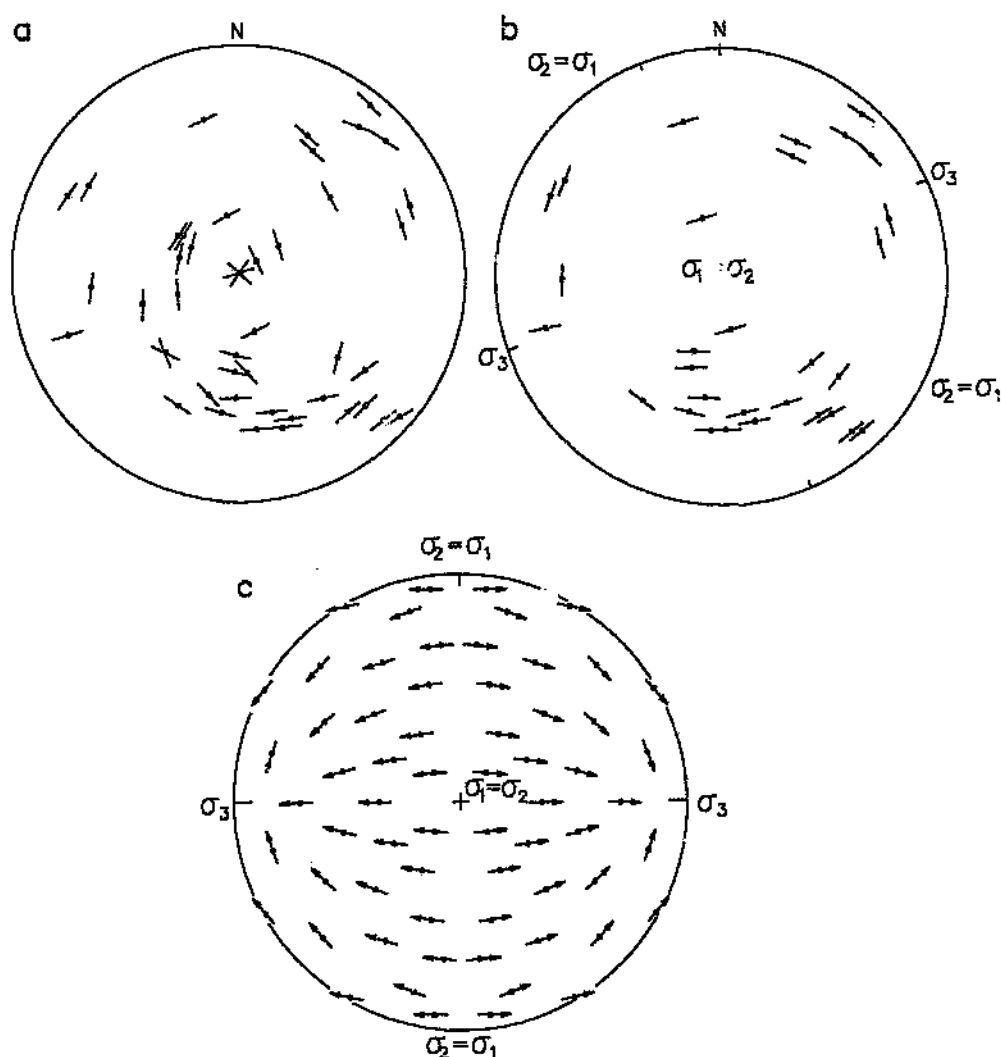


Figure 8.15 (a) Slip movement directions on movement planes for all proposed tectonically derived fractures in the palaeo-weathered basement occurrences on the western part of Vaalputs; (b) selected data of (a), which conforms to the case $C=1/1.1$ of Aleksandrowski (1985) [shown in (c)].

According to Aleksandrowski (1985) there are two disadvantages to the method of movement planes: the procedure is time consuming and needs many measurements (only 46 measurements were available for this study); and secondly, even a large number of readings does not guarantee a successful result. Nevertheless, the use of

Aleksandrowski's (1985) technique on the available data has suggested that perhaps two stress fields have functioned in this area to produce the observed slickenside orientations.

8.2.4 Comparative Joint Analysis

8.2.4.1 Jointing in the Basement Rocks

Statistical analysis of the orientations and physical properties of joints in the study area was carried out. This was aimed primarily at comparing the joint density and orientations in the unaltered basement with those in the overlying and younger Cretaceous weathered and silicified basement. Such a study would allow for the determination of more recently formed joint sets in the Cretaceous rocks and the possible effect that the palaeo-weathering may have had on sealing of older joints.

Method

No attempt was made to show the physical traces of joints on a map as they were generally far too numerous and much too short to portray at reasonable map scales. Instead, the orientations of the dominant sets of joints are portrayed through a series of rose diagrams, which was possible as most of the joints were found to be vertical. This was achieved by carrying out a detailed structural analysis of several exposures of rock assemblages which were subdivided into domains, designated on the basis of host lithologies, namely, silicified basement, weathered basement and the unaltered basement. The study was based on the structural analysis of joints at 15 selected stations, five stations within each of the lithologic domains. Five sites at which all three domains could be studied was believed to cover a large enough area with sufficient measurements to give representative statistics for the study. The five sites, all of which are on the western portion of Vaalputs, and in the vicinity of localities c, d, e, f and i (Figure 8.8), were chosen primarily due to good exposure. As faulting is pervasive throughout this area it was felt that proximity to faults was not important, however, in all

cases the sites were placed several tens of metres away from primary faults. Stations were positioned at various sites to determine if joint trends changed over the study area. The nature of the overall joint system could be determined through the systematic examination of representative subareas within the domains. Stations were designated as circular inventory areas with diameters of two metres. This inventory method, as described by Davis (1984), requires measuring and classifying every single joint at a station site. As outcrops are generally smooth and flat at sites of good exposure, only trends could be measured (this posed no problem as all joint sets were vertical to sub-vertical).

Characteristics of the analyzed joints

Joints in the study area exhibit diverse characteristics. Joints may be sealed (typically in the palaeo-weathered and silicified units) or may be open, exhibiting fractures of up to a few millimetres. Dilation may be exaggerated due to weathering and erosional effects. Joints are typically vertical to sub-vertical, a few metres in length, but range from 0.5 metres (commonly in the silicified unit as partly sealed joints) to tens of metres in length. In certain areas it was found that master joints run for very long distances. Some of the prominent lineaments seen on aerial photographs of the area are probably master joints rather than faults, particularly at sites where there is no obvious displacement. The spacing distance between adjacent joints at one locality may vary from centimetres to a few metres. This characteristic gives rise to a fairly large range of joint densities. Joint surfaces are typically stained by secondary iron-oxide.

Joint density

Joint density can be measured and described in a number of ways: total cumulative length in a specified area was used for this study, that is, the summed length of all joints within an inventory circle, divided by the area of the circle:

$$\text{Joint density} = L/\pi r^2$$

where L = cumulative length of all joints, and
 r = radius of inventory circle.

Joint density is expressed in units of length/area, that is, m^{-1} .

The average joint densities and the range of joint densities for each domain (basement, palaeo-weathered basement and silicified basement) are listed in Table 8.2.

Table 8.2 Average, and range of joint densities obtained for the unaltered basement, and the palaeo-weathered and silicified basement.

	Average Joint Density (m^{-1})	Range (m^{-1})
Silicified Basement	3.67	1.91-5.41
Weathered Basement	3.98	2.45-5.77
Basement	5.66	3.33-11.05

From these results (Table 8.2) it is evident that the joint density varies according to the lithological unit in which they were measured. The joint density is markedly higher in the basement than in the weathered and silicified basement.

Joint orientations

Orientation data collected during the course of the joint analysis is summarized in rose diagrams: Figures 8.16a, 8.16b and 8.16c. Rose diagrams with class intervals of five degrees were effectively used in presenting the orientations of the steeply dipping joint sets. Two preferred orientations of joint sets are obvious in all three figures, that is, a northeast and a northwest to north-northwest trend. The basement (Figure 8.16a) exhibits a third less developed set trending east-southeast. This trend is not present in the overlying altered (particularly the silicified) basement, indicating that this joint may have been dormant (or not reactivated) since at least the Cretaceous. The silicified basement shows an increased intensity in the northeast trending joint set (Figure 8.16c), when compared to the other two lithologies (Figures 8.16a and 8.16b).

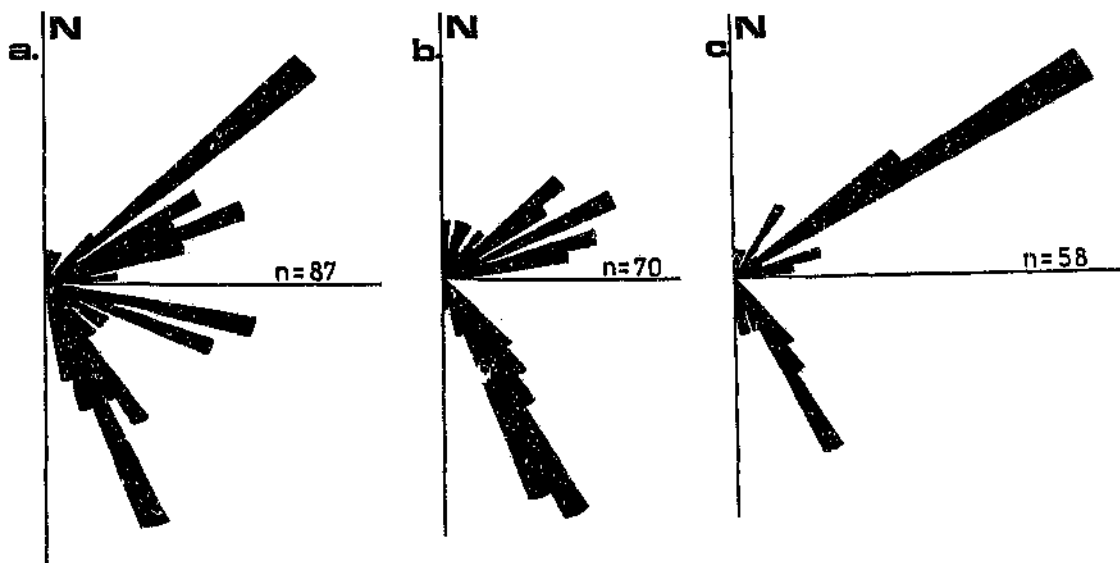


Figure 8.16 Orientation data summarized in rose diagrams for joints in the: (a) unaltered basement; (b) palaeo-weathered basement; and (c) silicified basement. All rose diagrams have class intervals of five degrees.

Interpretation of the joint analysis

Joints exist because the rocks in which they are found were forced to undergo dilation, distortion, or both (Davis, 1984). Within a rock mass, individual joint bounded blocks are free to move imperceptibly in relation to one another when forced to do so. The joints encountered in the study area, however, were ordinary featureless joints that are devoid of vein fillings, striations, and stylolitic solution surfaces which would usually reveal their kinematic functions.

No effects of the positioning of the section sites can be observed in the results, that is, joint densities and joint orientations are not noticeably affected by proximity to large scale lineaments. Also, orientations throughout the entire study area, and in the three lithological units used for this comparative joint analysis, are fairly consistent. This may be attributed to sealing of joints in the palaeo-weathered and silicified zones, many joints having been sealed by clay and silica (silicification), and the joint densities for

these two lithologies (Table 8.2) are probably a result of reactivation of pre-existing (or sealed) joints due to either tectonic activity or natural stress release processes. That is, the jointing in the palaeo-weathered and silicified occurrences are simply inherited from the basement, and the fact that certain orientations are absent in these zones implies that joints in these overlying lithologies formed after alteration.

Classical interpretation states that conjugate joints intersect in the axis of intermediate stress (σ_2), with the axis of greatest stress (σ_1) splitting the acute angle between the conjugate fractures. Tension fractures or joints may also form during brittle failure, breaking at right angles to the direction of least principal stress (σ_3) (Davis, 1984). A general direction of the principal stress can be obtained from the rose diagram trends according to the classical stress interpretation. By observation, the principal stress (σ_1) is approximately north-south for the older joint set and possibly (assuming brittle fracturing perpendicular to the least principal stress direction) northeast for the prominent joint set in the palaeo-weathered and silicified zones.

It is very difficult to establish the exact time of formation of specific joints or joint sets. Joints are also surfaces of negligible discernable movement. As joints are cohesionless surfaces, the joints may have been activated and reactivated in numerous deformational events. As joints can form in so many ways, it is impossible to determine their exact origin. However, the joint sets encountered in the study area coincide with the principal lineament directions observed on satellite images, as well as with some of the principal directions obtained from the slickensided-fault-surface analysis.

8.2.4.2 Jointing in the Surficial Sediments

Jointing was observed in the Vaalputs sediments in the walls of the two waste disposal trenches. These vertical to sub-vertical joints (Figure 8.17) are usually filled with calcrete, but may be slightly open (few millimetres), in which case the calcrete coated joint surfaces allow for accurate orientation measurements. These features have been interpreted as joints as they do not appear to be laterally continuous such as that expected for large scale faulting, and are typically non-penetrative. The joints rarely

extend more than 2.5 metres below the surface, which may be attributed to the good sealing properties of the clays in these sediments.



Figure 8.17 Typical calcrete-filled joint in the upper section of the surficial sediments (southwest wall of the low level waste disposal trench).

The joints in the trenches exhibit a north-south trend which may consist of two separate trends: north-northwest and north-northeast (Figure 8.18). Most orientations are only accurate to within a few degrees, which may account for the observed spread of orientations (Figure 8.18). Also, the orientation of the waste disposal trenches are such that measurements of the north-northwest trend were favoured and it is possible that the other conjugate orientation (an east-northeast orientation) may be poorly exposed or is at very low angles to the trench wall making identification and measurement of this orientation very difficult.

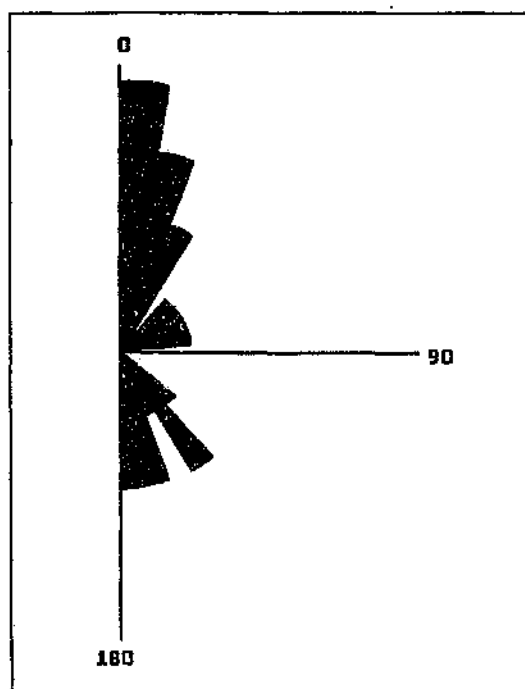


Figure 8.18 Orientation of joints present in the low and medium level waste disposal trenches (n=21).

As the joints show two preferred orientations (Figure 8.18) they are probably not related to swelling processes. Rather, they appear to be influenced by the north-northwest trending orientation or possibly as a consequence of the conjugate orientations of a northeast oriented principal stress. The fact that there is a preferred orientation for these joints, excludes the possibility of displacive growth of calcrete, as described by Watts (1978). These joints, rather, appear to be the result of crystallization into a void as a result of "passive" filling, whether the void was created as a result of drying out (drying cracks) or tectonism.

8.3 Evidence of Neotectonic Activity

The term "neotectonics" originates from Russian nomenclature (Mercherikov, 1968; Fairbridge, 1981) where it was used to denote crustal movements from the Miocene onwards. Most workers use this term to denote the upper Cenozoic and younger on-going tectonics (e.g. Mörrner, 1989; Vita-Finzi, 1986). Although the temporal span of many neotectonic investigations is based on a relatively short time scale of a few

thousand years, many regard it as encompassing the whole of the Late Cenozoic (Summerfield, 1987). The relationship between neotectonics and geomorphology, according to Summerfield (1987), involves the assessment of the role of recent or continuing crustal deformation in landform genesis. Such tectonic controls and the use of morphological evidence, in conjunction with other geological data was used to identify possible locations and styles of tectonic activity in the study area. The study also aimed at determining the main active or potentially active faults in the area and the possible orientation of stresses responsible for this neotectonism. In the following section several examples of neotectonic activity, identified in the study area are presented.

8.3.1 Deformation in the Karoo Rocks

Although the Karoo pre-dates the breakup of Gondwanaland and no ages of deformation could reliably be obtained, numerous sites in the Karoo are suggestive of more recent tectonism and are therefore briefly described. Numerous lineaments were observed in the Karoo rocks using satellite images and airphotos (Section 8.1). Deformation in the Karoo rocks was rarely seen in the study area due to the nature of the outcrop as the rocks are generally horizontal in a fairly flat terrane, making section studies particularly difficult. The following descriptions are mainly from the greater region where these rocks are better exposed.

Approximately 35 kilometres to the east of Vaalputs, on the Kliprand-Pofadder road, a well exposed section of the Karoo Supergroup rocks was observed in a borrow pit. The planar bedded and originally horizontal sediments (predominantly clays and siltstones), have been deformed by what appears to be a horizontal, east-west oriented, maximum principal stress. Figure 8.19a shows this deformation which has occurred in proximity to a vertical, 0.5 metre wide, dyke. Similar deformation, with the same fold axis orientation, is found more than 20 metres away from the dyke (Figure 8.19b), that is, a dyke of this size is not likely to have caused such intense deformation over such a large area. In addition the dyke thickness does not equal the total amount of shortening observed in this area, which appears to be of the order of several metres. Small scale folding is suggestive of vergence to the west. The nodular calcrete overlying the deformed sediments have not been affected by this deformational event. At this locality (Figure 8.19b) the presence of tight upright folds in calcrete implies the possibility of

"tepee structures" rather than tectonically controlled deformation. Antiform structures, referred to as "tepee structures" occur in many calcretes (Kendall and Warren, 1987), and owe their origins to displacive growth of carbonate within another substrate (Watts, 1977). Evidence of post-Karoo deformation at this site, therefore, should be treated with care, as some, if not all, of the deformation may be related to calcrete growth in the underlying sediments.

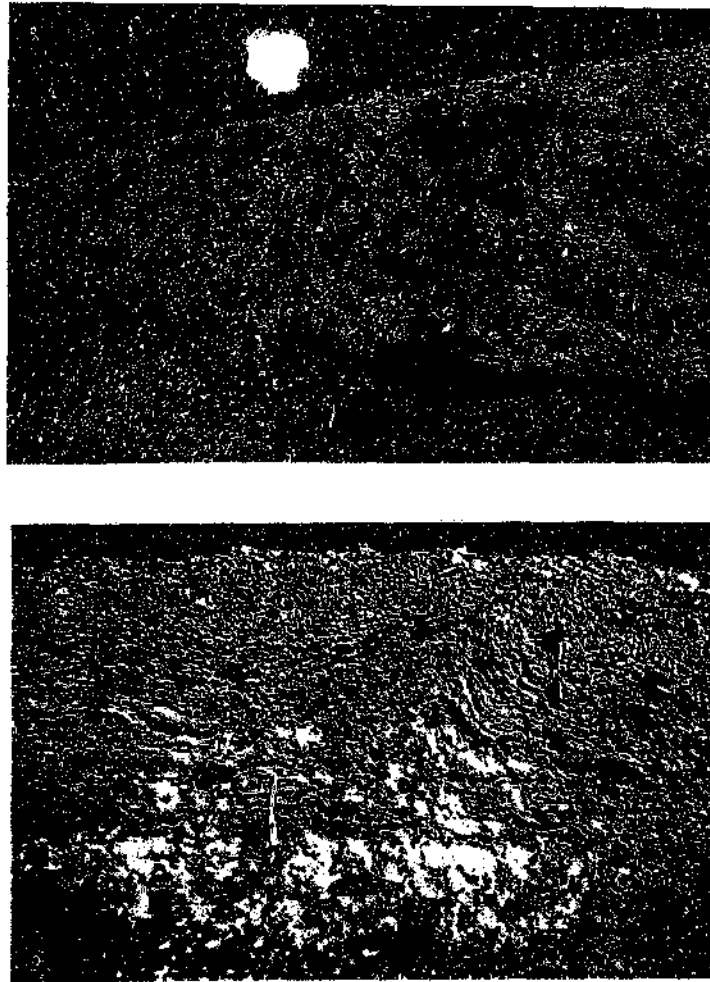


Figure 8.19 (a) East-west section showing folding in the Karoo sediments in proximity to a vertical dolerite dyke (mostly replaced by calcrete). The hammer is positioned in the centre of the dyke. (b) East-west section, 20 metres to the east of (a).

A second site exhibiting post-Karoo tectonism was noted 80 kilometres southeast of Vaalputs (40 kilometres northwest of Loeriesfontein; Figure 8.29; site K) along the Krom River. This site was investigated due to the anomalous seismic activity in the area (the results of which are dealt with in Section 8.3.4: Seismic Data). Although this site is a fair distance from the disposal site or central part of the study area, lineaments of similar orientations to those noted in the Vaalputs area were observed on aerial photographs of this region (photo numbers: 2807 and 2808, job number 381, line number 10), suggesting that the entire area has experienced a similar tectonic history. In particular a strong northeast oriented fabric, and lineaments, were noted in the Karoo cover rocks in the Krom River area.

Small scale faulting is present on the basement (granitic gneiss)/ Dwyka contact (Figure 8.20). Slickensides on the basement side suggest approximately vertical movement, with downthrow to the southeast. The orientation of the fault plane in Figure 8.20 is $042^{\circ}/80^{\circ}\text{SE}$. Also, in this area the road is situated in a northeast trending valley which appears to be structurally controlled. This was further supported by the observation that on the eastern side of the road Dwyka outcrop is at a much lower elevation (approximately 20 to 30 metres) to that on the western side suggesting that the Dwyka at this locality has been downfaulted to the east. Intense jointing with a northeast orientation was also noted in this area.

The Karoo (Dwyka) dominated Santab-se-Vloer is also an obvious structurally controlled deflation pan, with the two prominent Santab faults (Figure 7.1) defining the margins of this north-northwest oriented feature. The very flat deflation pan area is bound in the east and the west by prominent higher ground of Karoo sediments. Figure 8.21 shows this raised flank in the west, which defines the fault scarp. The pan sediments occupy a shallow graben feature, which is a result of the north-northwest trending faults. The eastern fault of Santab-se-Vloer is well exposed on surface and is shown in Figure 8.22. Several boreholes have been placed along this fault. According to Mr Gerrit Schreuder (pers. comm.), the Santab faults have resulted in downthrown, normal displacement to the west (dip to the west). This correlates well with other structure observed to the west of this site in the proposed Vaalputs basin and these faults may well be part of the eastern margins of the Vaalputs graben, at which normal, stepped, or downthrown faulting would be expected. Widespread slickensides in Dwyka diamictite were also noted on the southerly extension of the Santab fault, where the

Bitterfontein-Pofadder road intersects this fault (Figure 8.29), and to the north-northeast of Santab-se-Vloer (pers. comm. to Dr. M.A.G. Andreoli).

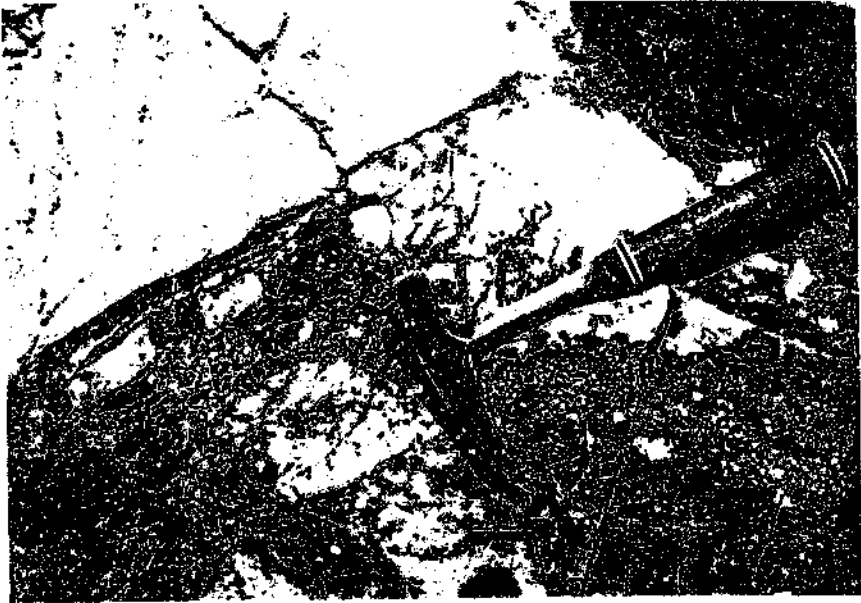


Figure 8.20 Northeast oriented faulting in the Dwyka rocks in the area of the Krom River, approximately 80 kilometres southeast of Vaalputs.

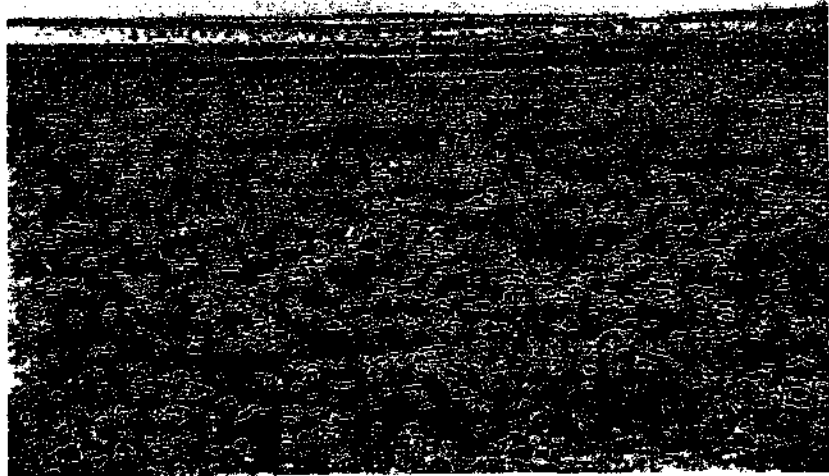


Figure 8.21 Santab-se-Vloer with the higher western margin in the distance which defines the western Santab fault.

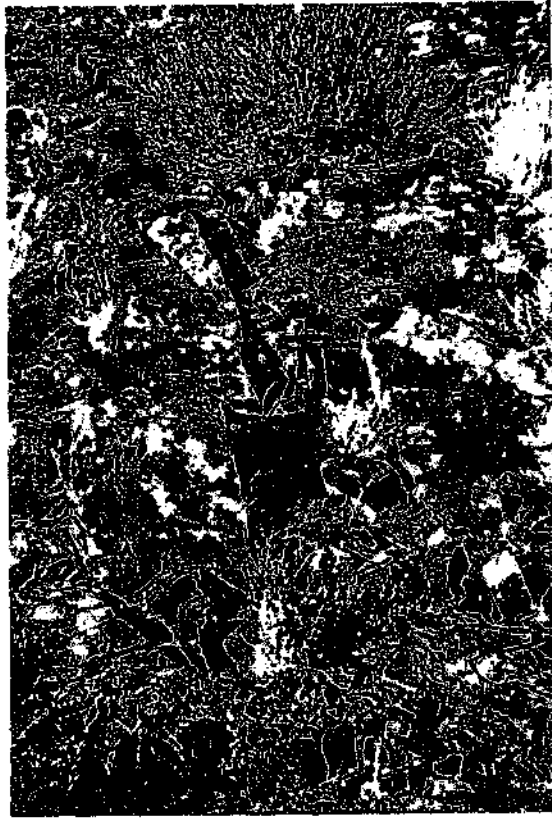


Figure 8.22 Surface expression of the eastern Santab fault, trending 160°.

8.3.2 Reactivation of Older Structures

A description of the prominent structures, identified using satellite imagery of the area, is given in Section 8.1. This section only deals with the possible reactivation of older structures and faulting in Post-Cretaceous (and possibly Plio-Pleistocene) times. For the localities of these structures the reader is referred to Figure 8.1.

The Stofkloof Fault

At the northern boundary of Vaalputs (locality b - Figure 8.8) the valley-defining Stofkloof fault truncates the palaeo-weathered and silicified basement. This fault appears to have been reactivated during the main slickenside forming event (which presumably post dates the palaeo-weathering and silicification). It is known (e.g. Ranalli, 1975) that young faults may use planes of, or take place in the vicinity of, earlier

displacement. A shear zone, parallel to the main fault (oriented approximately 160°) on the eastern flank of the Stofkloof fault (northern Vaalputs boundary: Figure 8.8) was noted in the silicified basement. This zone, several metres in length, exhibits an older grey quartz (in the form of extension gashes and which may be related to an earlier phase of deformation) which is truncated by a younger amorphous silica containing slickensided surfaces. This amorphous silica is common to most other slickensided surfaces in the palaeo-weathered and silicified basement. Figure 8.23 shows the fault breccia found in this shear zone.

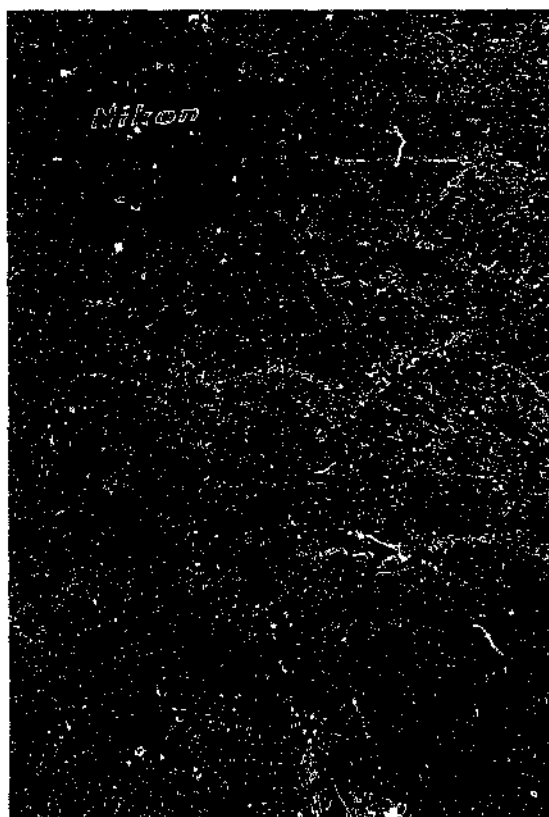


Figure 8.23 Fault breccia in a shear zone adjacent to the Stofkloof fault.

The Santab Fault

The main Santab fault is clearly defined by a distinct soil change from red aeolian sands on the western side, to browner, thinner sandy soils overlying a broad ridge of shallow basement on the eastern side (pers. comm. to Dr. M.A.G. Andreoli). This ridge coincides with the western end of the Pliocene Griqualand-Transvaal axis of uplift (Partridge, 1994). If these structures are associated with one another, the main period

of movement of the Santab fault may have been as recent as the Plio-Pleistocene. Also, as described in the previous section the Dwyka rocks along this fault have been sheared or intensely fractured.

The Garing Fault

Slickensides occurring in fractured silicified rocks on the Garing fault can be traced as straight, horizontal lines over a strike length of several metres. The Garing fault is also one of the largest water-bearing structure on Vaalputs: potentially active faults appear to be important *in situ* hydraulic conduits.

8.3.3 Disturbance of Recent Drainage Patterns

According to Summerfield (1987), distinguishing tectonic from other controls is most clearly illustrated in the relationship between drainage and neotectonic activity. The most obvious consequences of neotectonic activity on drainage systems are stream channel offsets resulting from strike-slip faulting. Although neotectonic deformation rates are typically slow in comparison to changes in other variables affecting channel morphology, the persistence of such deformation for only a few decades is sufficient to upset the equilibrium between hydrological and sedimentological variables and channel slope (Summerfield, 1987).

8.3.3.1 The Buffels River

Approximately 20 kilometres west-northwest of Vaalputs at the settlement of Rooifontein, where the Buffels River crosses the Springbok-Kamieskroon road, the recent fluvial sediments of the Buffels River have been disturbed by what appears to be recent reactivation of a north-northeast trending lineament. This lineament (Figure 8.24) is well defined in the basement gneisses and coincides with a steep-sided valley. This valley presumably formed along an older fault or fault zone. The non-perennial Buffels River flows from east to west and is perpendicular to the fault at this site (Rooifontein). This north-northeast trending fault appears to be solely responsible for the abrupt change in the characteristics of the fluvial deposits of the river and channel shape. To the west of the fault, the valley narrows abruptly. On the eastern side the channel exhibits large accumulations of fluvial deposits, which are absent on the western side (see Figure 8.25). Field observations suggest that the eastern side of the

lineament has been down faulted, resulting in the accumulation of fluvial deposits on this side. These fluvial deposits are sharply truncated by the fault and to the west of the fault the channel characteristics and channel shape are once again typical for drainage in this terrane, that is, the valley/channel has a typical narrower V-shape. Some older flood plain deposits may be seen on the southern bank (west of the fault), but do not appear to be related to the more recent accumulation of river gravels and sands on the eastern side of the fault. It should be noted that the settlement of Rooifontein obtains its water from the "sump" formed on the eastern side of this fault, where the ground water collects in the aquifer formed by the coarse deposits which have accumulated on the eastern (down-thrown) side of the fault.

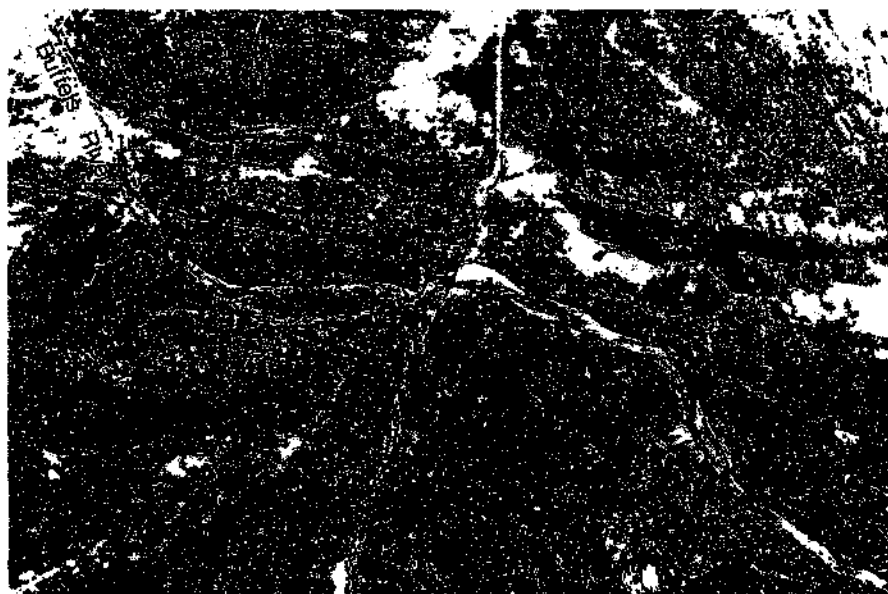


Figure 8.24 Part of aerial photograph (number 1652, job number 588) showing the effects of possible fault reactivation along the Buffels River in the area around Rooifontein. Scale of photograph is 1:35 000, N to the top, and flow direction is from the east to the west. Fault f-f coincides with the road.

The above observations are suggestive of reactivation, which appears to have occurred as recently as the Quaternary and suggest that recent tectonism is present in the region around Vaalputs. These results are in keeping with the reactivation of the approximate north-south trending set of lineaments, a major component of the lineament orientations obtained for the Vaalputs region.

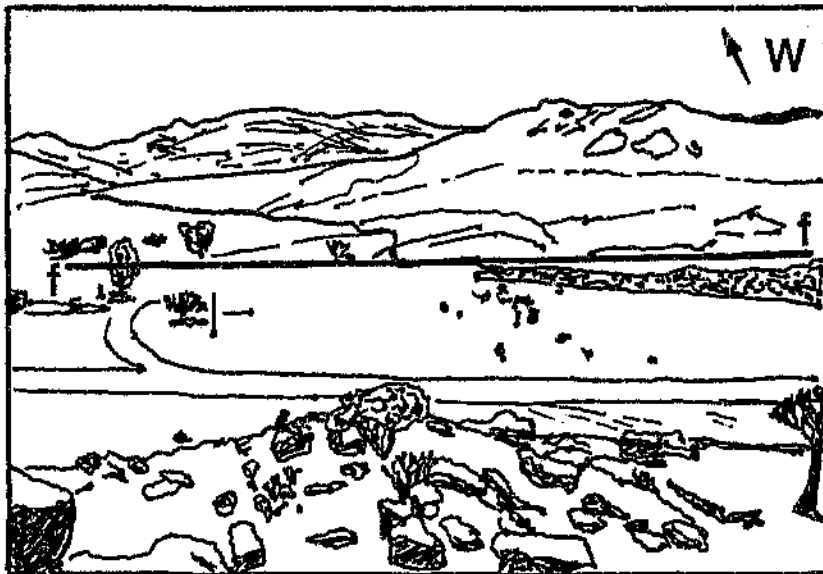


Figure 8.25 Photograph taken from the eastern side of the north-northeast trending lineament at Rooifontein, showing the accumulation of sediments in the foreground, that is, on the eastern side of the lineament (f-f).

8.3.3.2 The Dasdap Drainage

The present-day Dasdap, non-perennial drainage system, incises alluvial fan sediments of the Dasdap Formation and more recent sediments of the Gordonia Formation. In places the drainage has truncated dorbank and calcrete (usually of a nodular form), although these occurrences are only found sporadically along the course of the river. Red aeolian sands may be up to 3 metres in thickness, and were always seen to overlie the dorbank and calcrete occurrences. The present-day Dasdap drainage is from west to east and the sinuosity is fairly low with a value of 1.19 (13.96 km/11.7 km), or in other words the river path is reasonably straight, with a few meanders developed in places. The gradient of the river is very low: it falls 44.86 metres over 14 kilometres, i.e. the gradient is 1 in 312.

In an attempt to investigate offsets of the channel and possible faults which were observed on the SPOT panchromatic satellite image (dealt with in Section 8.1), and which are generally orthogonal to the drainage path of the Dasdap, a down-stream profile was carried out using a self-levelling (Kern) level. The profile (Figure 8.26) starts 1.2 kilometres WSW of the Platbakkies-Kliprand road, in the river bed (see Figure 8.6). Levelling was conducted in the thalweg at 20 metre intervals over a channel distance of 14 kilometres. Superimposed on this profile are the positions of the lineaments identified using remote sensing techniques (Section 8.1). It should be noted that only the prominent lineaments are shown. The profile shows a very constant gradient with no obvious variations in slope at, or near the positions of the lineaments.

As this scale (Figure 8.26) is too large to identify any small changes in slope, sections of this profile were plotted for selected reaches where lineaments are more frequent. Figures 8.27a, 8.27b, 8.27c and 8.27d show these plots. From these figures it is evident that some of the lineaments coincide with offsets or changes in gradient. It is also evident that most offsets show a down-throw to the west, which may be related to displacement associated with the faulting observed further to the north in the Vaalputs basin.

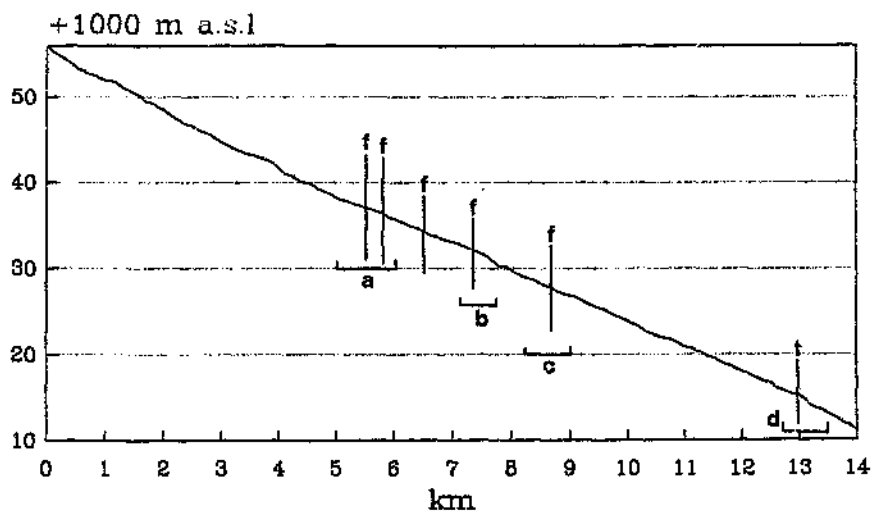
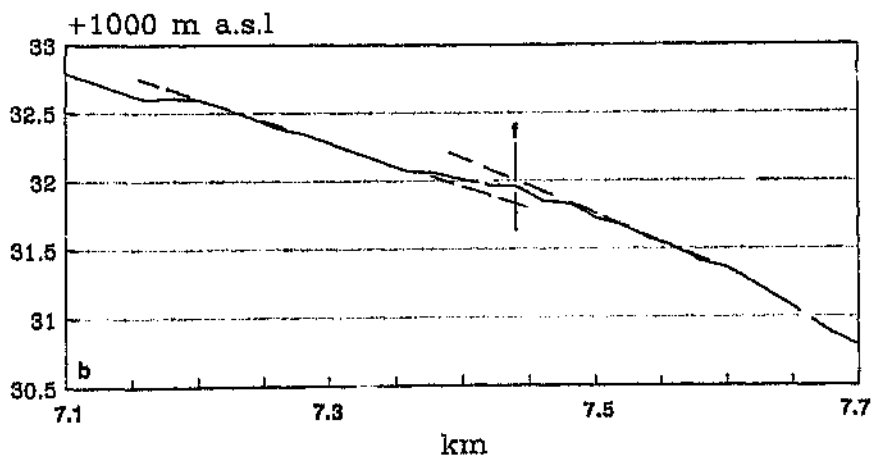
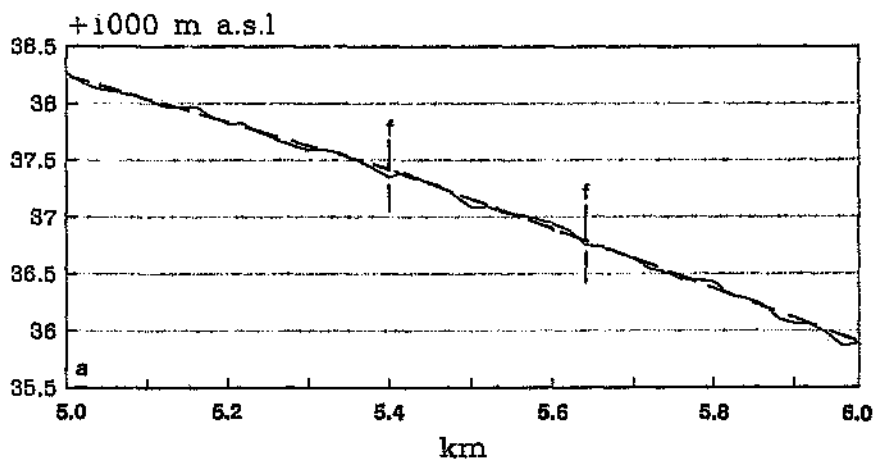


Figure 8.26 Southwest-northeast profile of the present Dasdap drainage. Letters refer to detailed sections in the following figure.



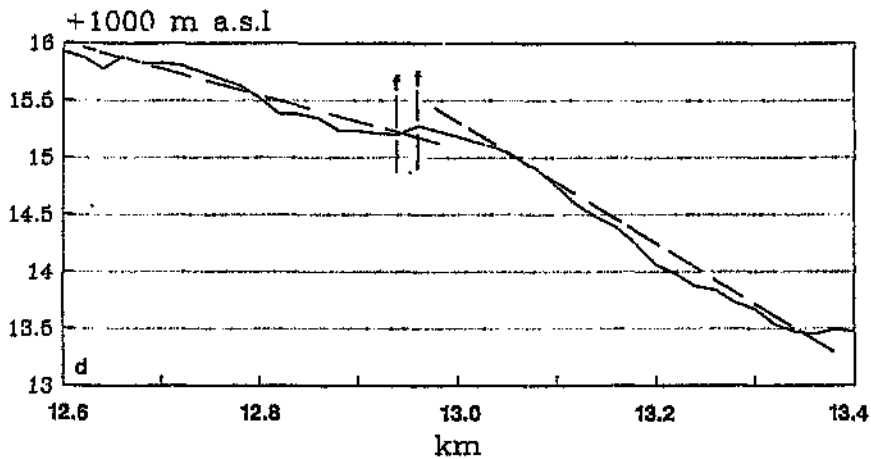
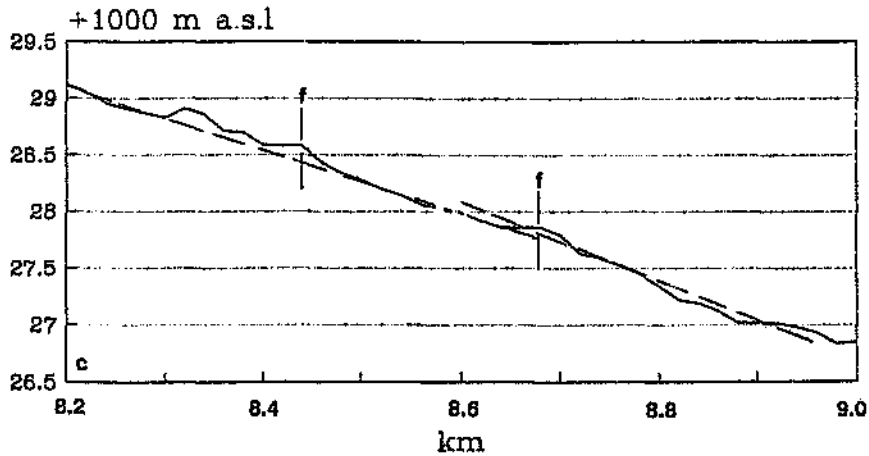


Figure 8.27 Detailed sections of the Dasdap drainage (see previous figure for positions): (a) 5-6 km section; (b) 7.1-7.7 km section; (c) 8.2-9.0 km section; (d) 12.6-13.4 km section. Dashed lines indicate approximate average slopes for various sections of the profiles.

The lineaments (features originally identified using SPOT panchromatic satellite imagery) may well be active faults and fractures, as the recent Dasdap drainage appears to have been affected by them. The effects are, however, subtle due to low gradients and mobile aeolian sand cover. The lineaments observed have a similar orientation to those in the Vaalputs sediments implying that this fracture orientation (NNW) is pervasive throughout the Vaalputs region.

8.3.4 Seismicity

South Africa experiences seismicity which is mainly low-level, with sporadic occurrences of larger earthquakes. Seismological data obtained by the A.E.C. from the Seismological Data Bank of the Geological Survey of South Africa revealed that a number of relatively large earthquakes have been recorded in the northwestern Cape region (Figure 8.28). Numerous earthquakes of lower intensity were reported, but went undetected due to the lack of seismic recording stations in the area.

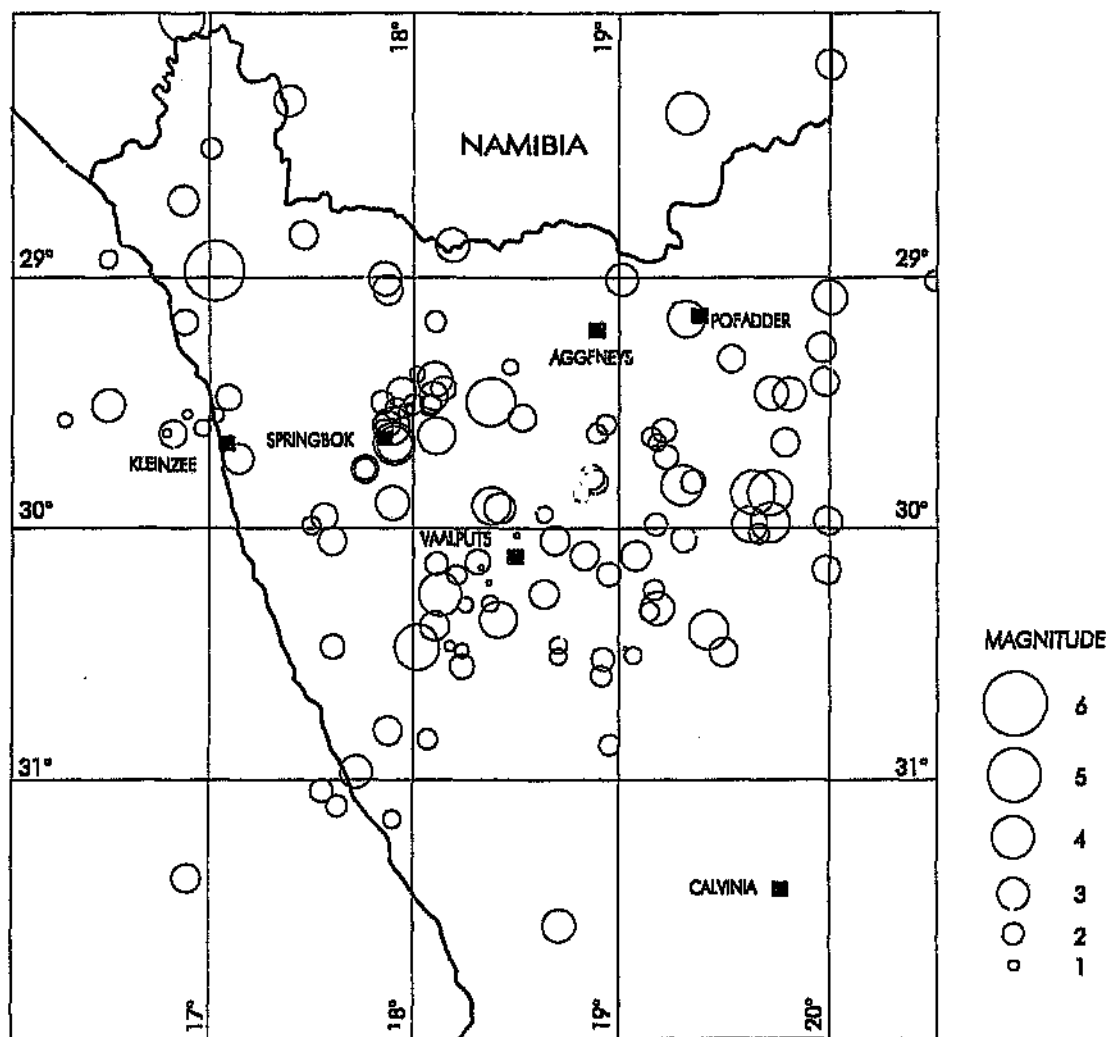


Figure 8.28 Epicentres of seismic events recorded by the A.E.C. in the northwestern Cape.

Two seismic stations, installed at Stofkloof and the waste disposal site at Vaalputs allowed for the monitoring and recording of small, local seismic events. In particular, the seismic station at Stofkloof, located on basement, allowed for the accurate identification of earthquake foci within a radius of about 100 kilometres. The most recent, available seismic data for this study are the seismic events recorded between January and September 1996 at Vaalputs. A continuous record of processed seismic events is unfortunately not available. Two stations were operative during this period: the Stofkloof station (located on basement), and one at the radioactive waste disposal site (located on the clay rich sediments of the Vaalputs and Gordonia Formations). The data of the Stofkloof station were primarily used for this study as several events were undetected by the other station. All the recorded events (56 in total) for this period were found to range in magnitude between 0.6 and 4.4, and were plotted on a map centred on Stofkloof (Figure 8.29). Also shown in Figure 8.29 are all lineaments obtained for this study, using predominantly remote sensing techniques.

Intraplate seismic activity tends to concentrate along pre-existing lines of weakness (Sykes, 1978). Figure 8.29 shows that several of the lineaments appear to be associated with centres of seismic activity, as indicated by the distribution of epicentres. The Platbakkies fault, or shear zone some 15 kilometres south of Vaalputs (with an east-northeast trend) has been classified as an "active fault" by Andersen (1992). Seismic activity was also more recently recorded in the vicinity of this fault, as evidenced by the cluster of events in the vicinity of the Bitterfontein-Pofadder road (Figure 8.29).

The recorded seismic events in the southwestern portion of Figure 8.29 appear to be related to the north-northwest trending set of faults and which are apparently related to the marginal escarpment. The Garies Shear Zone (Figure 8.29) also seems to be associated to some extent with some earthquake foci. The anomalous area in the northeast is difficult to associate with any primary lineaments, possibly due to lack of information available for this area. The southeast anomalies appear to be associated with both the north-northwest and the northeast trending set of lineaments.

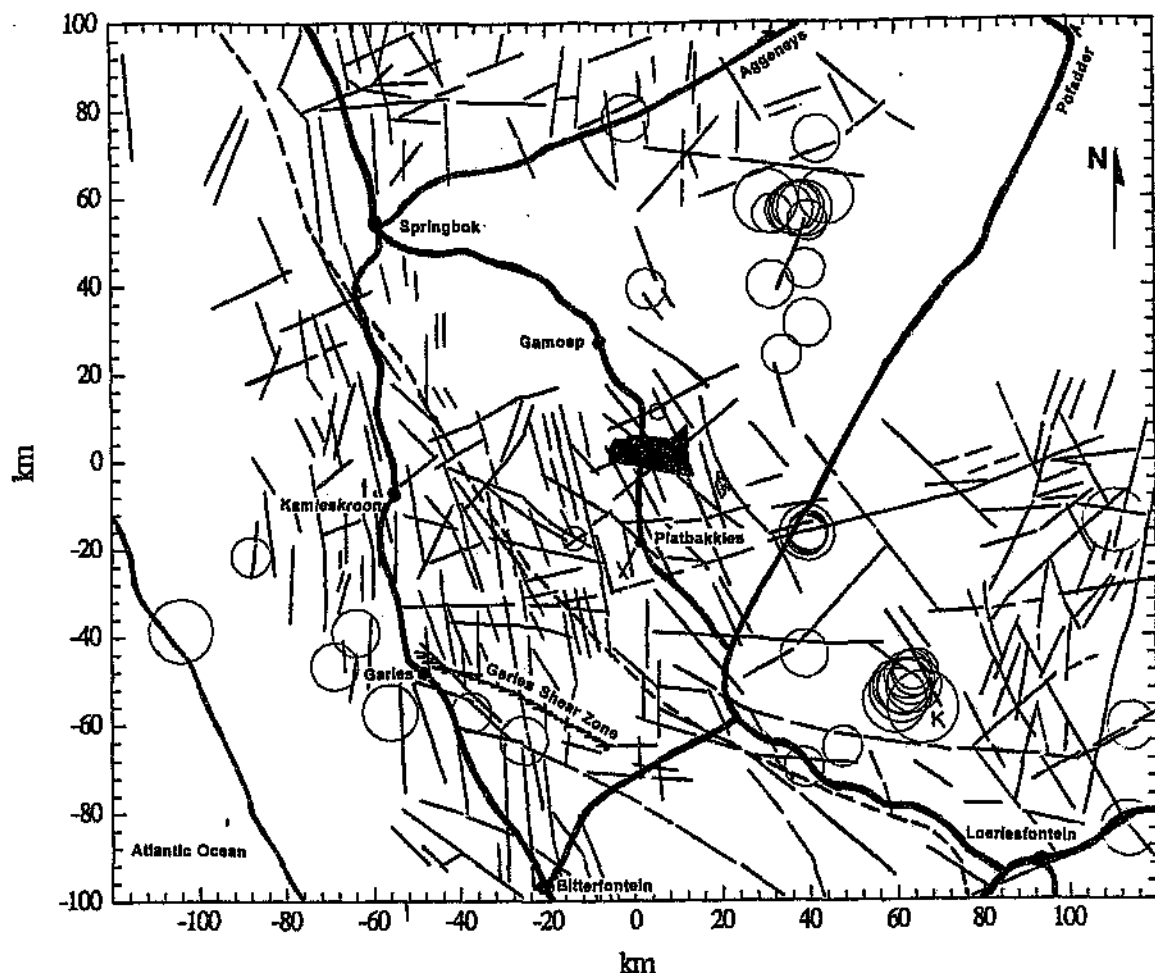


Figure 8.29 Recorded events (56 in total) for the period January to September 1996. Circles are directly proportional to the magnitude (ranging between 0.6 and 4.4). Also plotted are the primary lineaments of the region. Dashed line indicates the approximate position of the Great Escarpment and K refers to the area investigated in the vicinity of the Krom River.

Faurie and Hennop (1993) noted what appeared to be seismicity related to the Platbakkies and Stofkloof shear zones, and the Garing lineament. At the time of their investigations, however, they had insufficient recorded historic information to conclusively prove the direct association between seismic events and these structural features in the area. More recent processed data from these two seismic stations have not, as yet, been made available, however, the data presented above for 1996 are strong proof of ongoing tectonism in the Vaalputs region.

In an attempt to determine the present stress field associated with the seismicity, borehole breakouts (the measurable deformation of a drill hole, measured at various depths after extraction of the core) were analyzed. Borehole breakouts have been used (e.g. Zobak et al., 1989) to determine the strain, a result of recent stresses and may, therefore, substantiate the findings of recent seismic activity in the region. Borehole breakout measurements were taken in two boreholes drilled at Vaalputs to depths of ca. 1000 m and 520 m (Brandt et al., 1995). The data show that the azimuth of the breakouts, e.g. the long axis of the caved/deformed borehole, ranges between 160 and 120 degrees, with a maximum in the N130-N150 direction. The mean of 41 measurements of the azimuths of the breakouts in the HLD-1 borehole (situated on Vaalputs), between the depths of 185 and 440 m, are N128 degrees with a standard deviation of 11.6 degrees. These data suggest that in the Vaalputs area the direction of minimum principal horizontal stress has a broad NW-SE orientation.

8.4 Discussion

Stresses of different origins are presumed to have given rise to the numerous tectonic effects (inherent and new structure orientations) which have developed in the study area since the Cretaceous. The ridge-push force (a plate boundary force), which originates at oceanic ridges, and which helps to force plates apart, causes lateral compression in adjacent plates (Park, 1988). Loading stresses result when the lithosphere is loaded by surface topography such as mountain building or sedimentation. According to Park (*op. cit.*) the most significant stresses of this sort are produced when a large topographic load is isostatically compensated for, causing horizontal deviatoric tension in the region between the load and the compensatory mass. These stresses in turn cause tension in the adjoining areas. Non-renewable stresses, such as membrane stresses (Park, 1988), result from changes in the radius of curvature of a plate as it moves across the Earth's surface. On a more local scale induced stress may result from topography, such as an escarpment, and from the anisotropy of the strength of material.

The study area and surrounding region is affected by two important uplift axes: the Griqualand-Transvaal and the Kamiesberge axes, which were active between the Miocene and the Plio-Pleistocene. The rise of the Griqualand-Transvaal axis, according to Partridge (1994) may be linked to the neotectonic reactivation of older fractures in

the Bushmanland plateau northeast of Vaalputs. Vaalputs is situated on the western end of the Griqualand-Transvaal axis. Several ideas have been proposed for the source of the uplift, such as isostatic compensation of the rifted continental margin in response to denudational unloading (Gilchrist and Summerfield, 1990) for the Kamiesberge axis, and lithosphere deformation as a result of events originating deep in the mantle (e.g. Hartnady and Partridge, 1995). According to Hartnady (1990), and based on work in the Lesotho highlands (eastern continental margin), and a variety of tectonothermal phenomena in this part of south-eastern Africa, the regional pattern of natural seismicity in southern Africa does not support the conventional explanations which uses isostatically generated differential stresses.

The study area has been subjected to a prolonged history of tectonic activity during which time faults and major shear zones have been reactivated and others formed. On a regional scale the larger and older faults, which dictate the drainage courses in the area are predominantly north-northwesterly trending. This faulting was suggested by Joubert (1986a) to be of Pan African age (700 Ma.). Both dextral and sinistral movement of these faults may be observed (Andersen, 1992), but the dominant movement is believed to be vertical. These faults have presumably been reactivated as evidenced from the elevations of the palaeo-weathered basement occurrences, and other structures on Vaalputs.

A westerly dip of these faults, in the sand covered central and eastern portion of the study area, has been determined by Andersen (1992), using orthophotos and aeromagnetics. This interpretation has been based on the fact that the magnetic (deeper) locations of the faults is to the west of the surface expression shown on the orthophotos (Andreoli et al., 1986). These faults are considered to have controlled the deposition of the Dwyka Tillite (Andersen, 1992) as well as the shape of Santab-se-Vloer. Andersen attributes the apparent sinistral and dextral movement of these faults to vertical block, rather than strike slip, movement.

A tectonic analysis of the study area, using visible structures (ground studies and remote sensing techniques) and kinematic patterns has allowed for the interpretation of stress orientations. Two phases of deformation are believed to have been primarily responsible for the structures observed in the Vaalputs region. The regional strain ellipses for these phases is shown in Figure 8.30, and are discussed below.

At about 60 Ma ago the minimum principal stress was most probably oriented to the northwest (Figure 8.30a) as it caused extensive dip-slip faulting with a northeasterly strike (Brandt et al., 1995). This stress field most probably also gave rise to the inherent joint pattern observed in the basement, as the orientations obtained for the joints (Figure 8.16) are similar to those depicted in Figure 8.30a. Deformation of the Karoo (Section 8.3.1) with northeast oriented normal faulting (downthrown to the south-west) is most probably related to this phase.

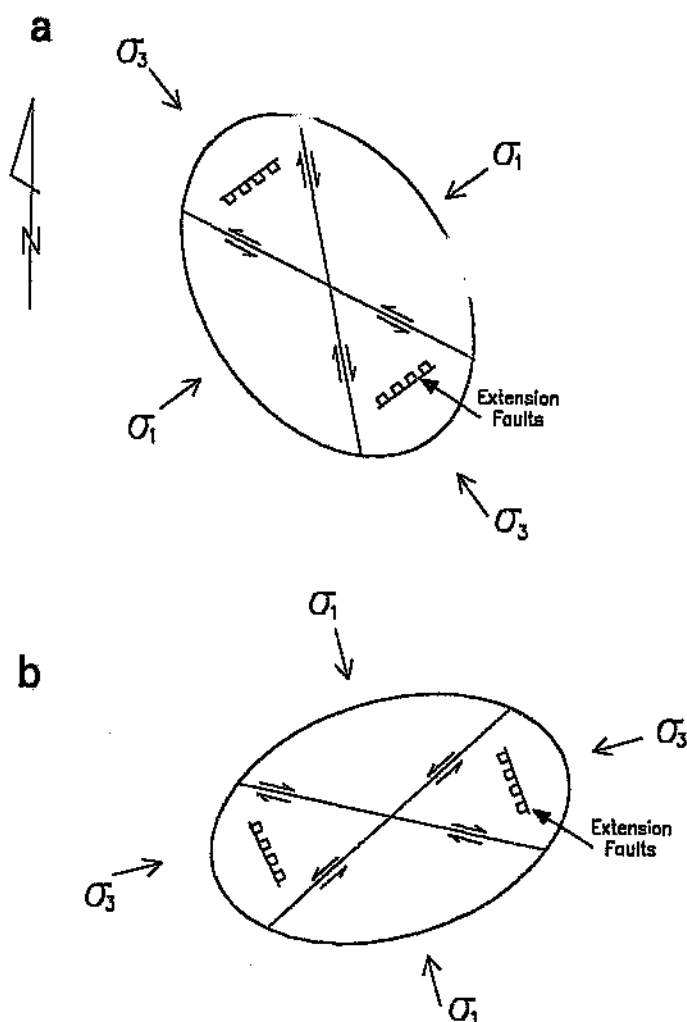


Figure 8.30 Regional strain ellipses associated with the deformational phases responsible for the observed structures in the Vaalputs region at about 60 Ma (a), and during most of the Cenozoic (b).

The stress field believed to be active during most of the Cenozoic is an east-northeast oriented minimum principal horizontal stress (Figure 8.30b), which probably accompanied the development of a fault-bound sedimentary basin which was filled by the surficial sediments. In the investigated area the Great Escarpment is mainly a monoclinical scarp, altered by erosion. Local differences in uplift have caused distinct manifestations in the escarpment (c.f. Gilchrist and Summerfield, 1990; Spönemann, 1995). According to models proposed by Watts (1982) (c.f. Summerfield, 1991a) and Keen (1987), the continental margin was uplifted in response to rifting. Due to regional isostatic compensation in response to denudation a monoclinical flexure developed, creating the Great Escarpment. A roughly rift-parallel upwarp (as postulated by Prins, 1981) has deformed the surface producing incised valleys to the west of the marginal scarp. Accompanying downwarping on the inland side of the marginal scarp may well be a contributing factor to basin development in these parts. This was also noted by Spönemann (1995) further to the north in Namibia, where combined faults and monoclinical flexures caused a series of north-south trending (approximately parallel to the escarpment) grabens and half-grabens. A similar orientation for a principal horizontal compressive stress is suggested by north-northwesterly oriented post-Miocene faulting in the Algoa Basin (McMillan, 1990). The Vaalputs basin may well be a southerly extension of the graben and half graben features, developed on the inland side of the marginal scarp, and which extends along most of the length (Windhoek to around the Orange River) of Namibia (Spönemann, 1995).

The stress field associated with tectonism, as indicated by Aleksandrowski's (1985) method using the available slickenside data, indicates extensional (normal), and perhaps some strike-slip movements. The results of this analysis indicated predominantly normal faulting trending NNW-SSE which is an acceptable mechanism as the Vaalputs Basin is defined by faults of such orientation. This suggests that the stress field responsible for some of the observed slickensides was most probably responsible for the development, or reactivation of the Vaalputs basin as well. Deformation in the form of east-northeast trending faults and two northeast oriented axes of upwarp of the pre-Cenozoic basement, east of Vaalputs was reported by Andreoli et al. (1996). This deformation was interpreted to be of Pliocene age and

appears to be the result of this more recent stress field. Faults such as the Stofkloof and Santab faults, for which evidence of reactivation was observed, could also have been reactivated during this deformational phase.

The present day stress field in the Vaalputs area as determined from borehole breakout data suggests a compression oriented northeast-southwest. Such orientation is approximately perpendicular to that of the minimum horizontal stress direction in the mines of the Okiep area ca. 100 km to the north (Andersen, 1992). A northeast oriented present principal stress is also in disagreement with the northwest oriented water-bearing Garing fault. The principal stress obtained from the borehole breakout data may be due to local effects due to heterogeneity of rocks, which may redistribute and reorientate the regional stress field. It should also be noted that the borehole breakout data may not be meaningful as measurements at Vaalputs were taken in a poly-orogenic granulite complex and not in a Mesozoic sedimentary basin in which the theory of borehole breakouts (Zobak et al., 1989) was developed.

The recent disturbance of the Buffels River drainage, jointing in the surficial sediments and reactivation of faults such as the north-northwest oriented Stofkloof fault are better explained by a north-northwest oriented principal stress. Small deviations from this orientation may well be related to synthetic and antithetic faulting associated with such a stress system.

Although an attempt to relate all the observed orientations to stress fields was made, this is not always possible, as pre-existing structures may be reactivated, which complicates the observed patterns. The Platbakkies shear zone (Figure 8.3), according to Andersen (1992), is on strike with the landward extension of an oceanic transform fault. Andersen believes that the east-northeast trend of the shear zone is a fundamental element in the crustal architecture of the Vaalputs sub-terrane that was reactivated during the breakup of Gondwana. The deformation along this shear zone is obviously long lived, as indicated by the recent seismic activity along the structure.

The Garing and Vaalputs faults (Figure 8.1) were suggested (Andersen, 1992) to have

formed as a conjugate pair during the third deformational episode (D3) of the Precambrian structural events of the Namaqualand Metamorphic Complex. They have since been rejuvenated with the Vaalputs fault being intruded by noritoids of the Koperberg Suite (Andersen, 1992). Present stress fields may well have exploited these faults. Andersen (1992) also suggested that the Garing fault has remained active well into Tertiary times. This fault can be traced on aerial photographs and satellite images, through the Vaalputs sediments, reinforcing the interpretation that post-Tertiary rejuvenation has also occurred along a northeast orientation.

The data provided by the study of the Vaalputs site indicate that the area has experienced distinct changes in stress orientation since the Late Mesozoic. The post-Gondwana evolution of the Vaalputs area is difficult to interpret according to the neotectonic model proposed for the southwestern Cape by Ransome and de Wit (1992). The ENE-WSW oriented Griqualand-Transvaal upwarp axis (Partridge and Maud, 1987; Partridge, 1994) and the NNW trending faults of the Vaalputs basin (Brandt et al., 1995) are all inconsistent with their ridge-push model. Also, the absence of any significant transform faults in the Cape basin (Cande et al., 1988) on the offshore extension of the Platbakkies Shear Zone and the orientations of the maximum principal stresses all disagree with a ridge push model for the dominant (NNW-oriented) structures of the Vaalputs region. Similarly, flexural isostatic uplift models (Kooi and Beaumont, 1994; Gilchrist and Summerfield, 1990; Gilchrist et al., 1994) cannot account for the northeast-southwest trending features, but may account for the north-northwest trending faults recognised in the sediments of the Vaalputs basin. Burke (1995) has proposed that the African Plate came to rest over the underlying circulating mantle about 30 million years ago with consequences which include:

- 1) the development of the present basin and swell structure of the African Plate;
- 2) a general elevation and reactivation of older fault systems in many parts of the continent, and;
- 3) a regressive episode at the African continental margin as a result of the new continental elevation.

The Quathlambe hotspot (Lesotho highlands) hypothesis of Hartnady (1990), which

attempts to show the interaction with the southwards propagating East African Rift regime may be important for the eastern seaboard, but does not appear to have an effect on the western (and more passive) continental margin, and hence the region around Vaalputs. Finally, these results suggest that current models on the post-Gondwana geomorphic evolution of rifted continental margins, of southwestern Africa, based on isostatic thresholds to landscape cycles (Partridge and Maud, 1987, 1988), or on differential denudation with flexural isostatic uplift (Kooi and Beaumont, 1994; Gilchrist and Summerfield, 1990; Gilchrist et al., 1994) do not adequately explain all the phases of deformation. It is suggested that stresses proposed in these models may have influenced the various phases of deformation to a greater or lesser extent: the earlier phase being dominated by ridge push during the late-Cretaceous and the latter phase by isostatic readjustment. Further theoretical formulation, as noted by Hartnady (1990), is needed to explain the seismological, gravimetric, geological and geomorphological observations in terms of asthenospheric and lithospheric heat flux, temperatures, thermal properties, thicknesses, densities, viscoelastic properties, stresses, lateral motions and vertical uplift rates.

CHAPTER 9 : DISCUSSION

As prevailing climate and tectonic settings change, so do types and rates of geomorphological and geological processes. This chapter deals with the reconstruction of the sequence of events that is believed to have shaped the landscape, and given rise to the sequence of sediments preserved in the study area.

The Cretaceous and Pre-Cretaceous

Before rifting, the topography of the Gondwanaland supercontinent was probably of predominantly low local relief. This Gilchrist and Summerfield (1990) attribute to prolonged denudation. Regional elevation may be relatively high in areas remote from pre-rifting coastlines, where local channel gradients, and hence rates of gradation, are low. The separation of Africa from South America around 150 Ma resulted in the generation of a high marginal scarp (already at a high elevation due its central position within Gondwanaland), which was accentuated by upwarping of the rift shoulders prior to the separation (Partridge and Maud, 1987). The extensive elevated area immediately inland of the Great Escarpment on which Vaalputs is situated coincides with the inner margin of the zone affected by upwarping of the continental hinterland prior to rifting. It has been suggested (e.g. Dixey, 1955a) that the Kalahari basin was formed by the uprising of the rims and by the sinking of the central parts, and that the interior Kalahari basin was initiated during the Late Jurassic and Early Cretaceous, resulting from the rift-faulting stage of the break-up of the south Atlantic.

Rifting initiated erosion in the Cretaceous, leading to recession of the marginal scarp. This period of erosion was aided by the humid, tropical conditions of the Cretaceous (Partridge and Maud, 1987). The surface produced by the erosion cycle, initiated by the break-up of Gondwanaland is referred to by Partridge and Maud (1987) as the African surface. This erosion cycle, they believe lasted until the early Miocene and caused extensive planation.

The high local relief along the marginal scarp is associated with high slope and channel gradients, which presumably promoted relatively high denudation rates, whereas, inland

of the Great Escarpment denudation rates were presumably lower due to the lower local relief (the regional elevation was relatively high, generally > 1000 metres). The preservation of Karoo rocks and Cretaceous weathering profiles suggests that denudation rates were generally lower in the interior. The study area at this time was underlain by predominantly gneisses and tillite and the base level was most probably that offered by the proto-Koa valley. It is proposed that the Dasedap sediments were deposited during this period, on the inland side of the marginal scarp, as a direct consequence of uplift and removal of considerable thicknesses of material from the scarp. Partridge and Maud (1987) noted that most of the recession of the Great Escarpment occurred during the Cretaceous, and back-wearing in later cycles (Post-African I) was, by comparison, very limited, involving no more than a few tens of kilometres. Igneous activity appears to have been associated with the deposition of the Dasedap sediments due to the apparent overlap of the sediments with the intrusions. The ultramafic igneous activity was presumably associated with tectonic instability, which most probably also contributed to the accumulation of the Dasedap sediments. Fossil vegetation recovered from the Arnot Pipe, and believed to be of a similar age to the Dasedap sediments suggests that the vegetation in this region was forest (Scholtz, 1985), which agrees with the interpretation of the humid environment proposed for this time.

Although evidence for only one extensive alluvial fan system is preserved in the study area in the vicinity of the present Dasedap drainage, it is envisaged that several fans accumulated sediments off the uplifted western marginal escarpment, which is believed to have been positioned further to the north and to the west at the time of deposition. The position of the proposed palaeo-watershed is in agreement with palaeo-current directions of these sediments. This irregular watershed pattern (which is still observed in the present watershed - Figure 5.8) is believed to be due to heterogeneity in the basement and different weathering, denudational and river capture rates. The proposed depositional environment for the Dasedap Formation is shown in Figure 9.1.

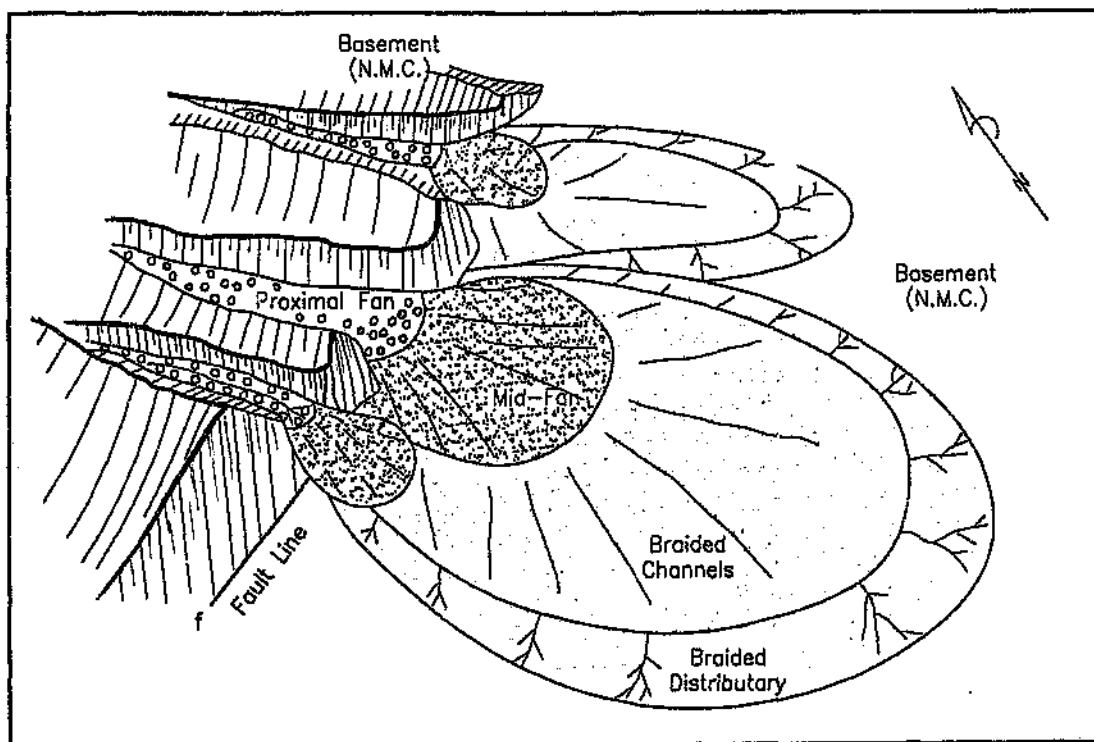


Figure 9.1 Proposed depositional environment for the Dasdap Formation.

According to Andersen (1992) and Levin et al. (1986) the onset of the Dasdap alluvial fan began in late-Cretaceous to early-Tertiary times with the uplift of the Kamiesberg highlands to the southwest of the Bushmanland Plateau. However, palaeocurrent directions (Figure 5.8) indicate that uplift was most probably affecting the entire north-south length of the marginal scarp in this region, at the time of the Dasdap sedimentation. This rejuvenation is believed to have taken place along the prominent north-northwest trending Pan-African faults of the region. In addition extensive dip-slip faulting caused by a northwest oriented minimum principal stress (earlier phase in the Late-Cretaceous) may have resulted in the scarps required for the onset of the deposition associated with alluvial fan deposits. The uplift which gave rise to the fan accumulation may well have had the effect of initiating the events which ultimately led to the capture of the Gamoep-Buffels system by the Koa River in the Miocene.

Cretaceous Palaeo-weathering and silicification

Where visible evidence of environmental conditions is lacking, palaeoclimatic interpretation of the diagenetic products of subaerial processes occurring in the stratigraphic record is particularly valuable (Summerfield, 1983a). Silcretes have been increasingly cited, in which their occurrence has almost invariably been associated with an arid to semi-arid environment (e.g. James et al., 1968; Waugh, 1970; Collison, 1978; Rubin and Friedman, 1981). Summerfield (1983a), however, suggests that although supporting evidence is provided for this palaeoclimatic interpretation, the notion that all silcretes can be interpreted in this way is incompatible with ideas developed from recent studies of Cenozoic silcretes in northwest Europe, Australia and southern Africa.

Warm, humid conditions favour the release of silica within weathering profiles, and with sufficiently sluggish drainage, the silica could become precipitated elsewhere in the profile (Summerfield, 1978, 1979; Wopfner, 1978). Summerfield (1983a) re-evaluated the basis for the palaeoclimatic interpretation of silcrete with respect to southern African examples and demonstrated that although some silcretes can be confidently linked to an arid to semi-arid environment, numerous other occurrences strongly suggest development under a humid climatic regime. Summerfield (1983a) also noted that climate is not the only factor controlling silcrete development: poor drainage, water-table control and topography are other important factors in silcrete genesis.

Geochemical and petrographic evidence for the silicified rocks of the study area strongly suggests a genetic association between silicification and intense bedrock weathering. Although externally derived silica may have been introduced into the weathering mantle, the weathered basement indicates that sufficient silica could have been mobilised by decomposition of the thickness of bedrock represented by the existing profile depths.

From an analysis of the sedimentologic, geomorphic and spatial context, and probable geochemical conditions of silcrete formation in the study area, the following climatic regime is proposed: the weathering profile silcretes exhibit geochemical and petrographic characteristics indicative of silicification under a much more humid climate in highly acidic, poorly drained weathering environments. Figure 9.2a is a hypothetical simplified cross-section of the area during the period of Cretaceous weathering. Figure 9.2b shows the start of the modification of this land surface during a period of increased

tectonism, which contributed to the preservation of the Dasdap sediments and most probably caused the onset of the deposition of the Vaalputs sediments. It should be noted that the Dasdap sediments form part of the basement material which was affected by the palaeo-weathering. Erosion and deposition, at the time of weathering and silicification, must have been minimal suggesting a period of sufficient surface stability. Local depressions in this palaeo-surface may be a result of preferential erosion due to a number of possible factors: the presence of softer rock; slight tectonic subsidence; mylonitization of the rock; jointing or fracturing; or a combination of any of these. In these areas the more resistant silicified basement has been removed, leaving only the palaeo-weathered or unaltered basement (Figure 9.2b).

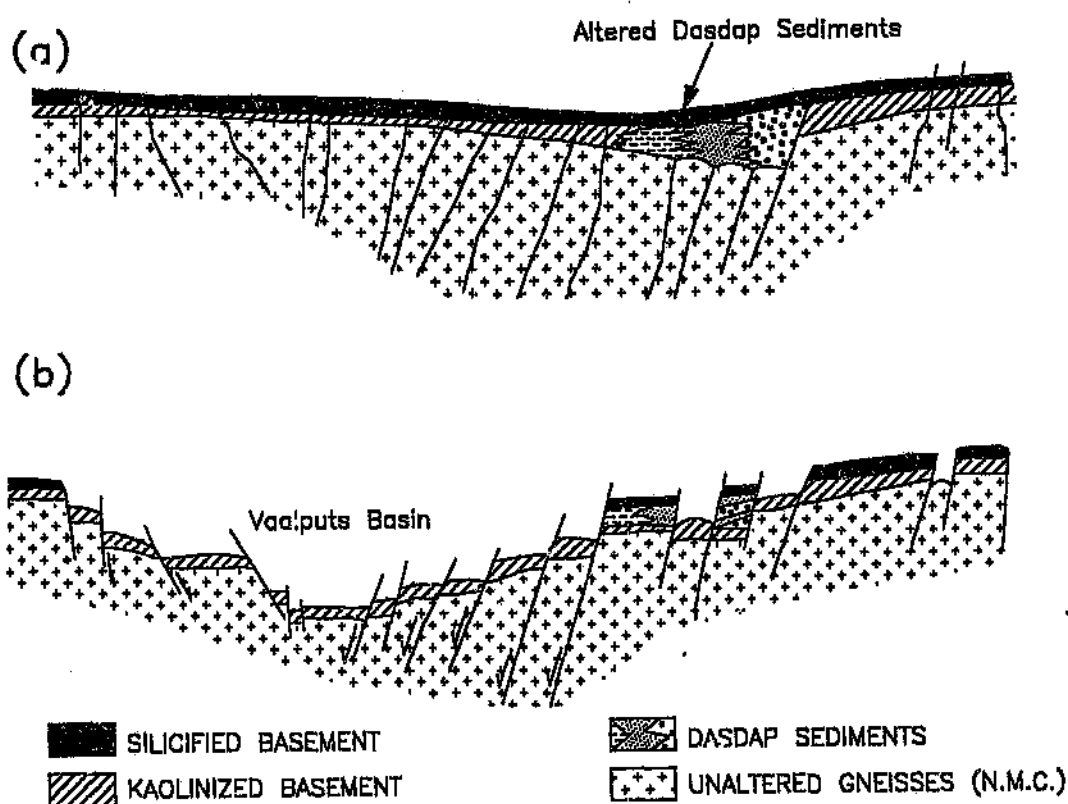


Figure 9.2 Simplified cross-section of the Vaalputs region during: (a) the Cretaceous weathering phase; and (b) the initial modification of the Cretaceous surface.

The tropical climates of the late Cretaceous would have favoured deep weathering, with the silicified duricrusts protecting the weathered basement from further denudation in places (including some of the Dasdap sediments). Only a few mountain massifs, such as the Namaqua Highlands remained above the otherwise low relief of the pediplain Cretaceous surface. Partridge and Maud (1987) refer to this surface as the African surface and interpret the Dasdap sediments as overlying this surface, but, evidence presented above suggests that the Dasdap sediments have been affected by the same weathering and alteration episodes as that which affected the basement rocks on the Vaalputs property.

The Vaalputs Formation

Partridge and Maud's (1987) interpretation that the Great Escarpment is primarily a product of the high pre-rifting elevation of Africa, which occupied a central position within the Gondwanaland mosaic, does not fully account for the observed lineaments, and higher elevation with respect to the adjacent hinterland, which are clearly associated with this margin. As monoclinial folding during the Pan-African deformation resulted in a set of north-northwest trending faults (Joubert, 1986a) so has continued uplift in the Cenozoic caused reactivation of these older structures, as well as new features with similar orientations.

There is a correlation between lineaments and basin shape and sediment thickness of the Vaalputs basin. The correlation exists predominantly with a newly recognised set of north-northwest trending lineaments, which corresponds to the primary lineament direction of the area. As the basin lows contain "white clay", the faults defining the basin may either: i) pre-date the weathered (and silicified) Cretaceous surfaces, that is, the weathered surfaces formed in the depressions or lows which resulted from faulting; or ii) post-date the weathered surfaces, preserving the altered basement in lows formed by the faulting. A third and more likely possibility is that the faulting both pre- and post-dates the alteration and the accumulation of the Vaalputs sediments, that is, faulting has been taking place either as primary or as reactivated faulting since the formation of the palaeo-weathered and silicified basement.

The stress field believed to be primarily responsible for the Vaalputs basin is an east-northeast oriented minimum principal horizontal stress, which probably accompanied the development of the fault-bound sedimentary basin. Various stress determination methods, such as that of Aleksandrowski (1985) indicate that the stress field at this time would have produced predominantly normal faults striking NNW-SSE, which is an acceptable mechanism as the Vaalputs Basin is defined by faults of such orientations. It is proposed that during the Oligocene the Vaalputs Graben was in its juvenile state, and may have represented a palaeochannel. However, a depressional form comprised of weathered basement must have been formed, which could later be buried and preserved by the Vaalputs sediments.

Sedimentological analyses of the Vaalputs sediments are suggestive of sedimentary processes which are slightly different to those proposed by previous workers. The source area had a high clay content: the source area was presumably weathered such as that on the western part of Vaalputs (which is preserved, in places, in the form of the flat mesas and buttes). The sediment was most probably derived from the elevated margins of the basin and deposited predominantly in the form of ephemeral fluvial deposits.

The lower white clay facies is predominantly the result of *in situ* weathering, with minor reworking and mixing. The chemical and morphological features of the Dasdap Formation and the white clay unit are too different to conciliate and no other hypothesis can be offered to explain the petrogenesis of this unit. Pebbly lenses scattered throughout the overlying pebbly and gritty clay facies are indicative of high energy fluvial events and the roundness and sphericity of the pebbles indicate that these sediments have been transported over a reasonable distance, presumably from as far as the western marginal scarp. The high clay content and relic feldspar grains in these sediments are suggestive of intense *in situ* weathering, which would further contribute to the extremely poorly sorted nature of these sediments. The reasons for the colour differences in these sediments is primarily due to variations in iron content.

It is proposed that the pebbly and gritty clay facies were predominantly deposited in "floodouts", where channelised flow and bedload transport of sands and gravels largely cease, and where large floods continue across typical broad, low-gradient surfaces. Declining gradients, aeolian, structural or hydrologic obstructions to flow, may have contributed to decreased channelized flow causing the flow to spill across adjacent alluvial surfaces and ultimately dissipate (Tooth, 1998). Such deposits are known for semi-arid environments in which ephemeral streams which generally remain dry for much of the year dominate the surface. These occurrences can be largely related to increased desiccation in the Cenozoic. It is likely that several floodouts, particular in the distal reaches (floodplains), converged giving rise to the deposition silts and sands, whereas coarser pebbly deposits represent channel bedload deposits. The geomorphic setting in low-gradient plains, the large aerial extent and the relatively fine-grained deposits typical of floodouts differentiates these deposits from alluvial fans.

Fluvial-aeolian interactions in the distal reaches of what was an arid environment gave rise to thin layers of alluvial silts and clays deposited over aeolian sands following flood events. Changes in the vertical section of the Vaalputs sediments, where subtle changes in grain sizes and colour were noted, may be due to fluvial-aeolian interactions. Sediments typically found in sections of animal burrows or nests suggest an origin from the overlying aeolian surface deposits.

The calcrete horizons in the Vaalputs sediments are suggestive of drier interludes and most probably define previous land surfaces. That is, some, if not all of these calcrete horizons probably represent surface stabilization stages during less tectonically active periods or during periods of lower sediment supply.

Thus, the Vaalputs sediments were deposited in semi-arid conditions by predominantly floodout deposition. Post depositional alteration and bioturbation, has given rise to the generally structureless and massive sediments of the Vaalputs Formation. Finally, desiccation gave rise to the aeolian sediments and the well developed calcrete horizon which cap the Vaalputs sequence of sediments.

Most of the Cenozoic deposits contain no macro- or micro-fossils and are not suited for any other dating technique (De Wit, 1993). Most ages quoted in previous work have, therefore, been obtained geomorphologically. The Miocene age for the Vaalputs sediments, as suggested by McCarthy et al. (1985), is in agreement with observations from this study. The accumulation of these sediments may well have been initiated by the end of the early Miocene (18 Ma) episode of uplift as recognised by Partridge and Maud (1987).

As previously mentioned epeirogenic uplift during the early Miocene resulted in rejuvenation of the regional drainage causing erosion of up to 40 to 130 metres below the crests of the African residuals (Partridge and Maud, 1987). Various portions of the Koa Valley channel (to which this surface is clearly graded to) contains deposits of early mid-Miocene age (Dingle and Hendy, 1984; Partridge and Maud, 1987, de Wit, 1993). It is during this period of rejuvenation that the lowermost (pebbly clay facies) is believed to have been deposited. The driving forces for this period of uplift may well have been partly or wholly responsible for the opening of the Vaalputs basin.

A second phase of rejuvenation in the Pliocene (Partridge and Maud, 1987) may well have been the driving mechanism for the final cycle (gritty clay facies) of deposition in the Vaalputs sediments. Drainages in the study area are incised between 50 and 150 metres below the Post-African I surface, especially in the Karoo rocks (Partridge and Maud, 1987). Fossil material from terraces and gravel fills, associated with the more important of these drainage lines such as the Sak River and Carnarvon Leegte, indicates downcutting and increased fluvial activity during this period (de Wit, 1993). With deepening of the Vaalputs Basin and the increased fluvial activity associated with greater rainfall (and coupled with uplift) the lower erosional surface and subsequent deposition of sediments of the uppermost Vaalputs cycle seems quite plausible.

Uplift has persisted to recent times and is most probably still active, hence the reactivation of the older faults. Evidence of other stress fields such as that generated by the mid-oceanic ridge appears to be a contributing and superimposed stress, giving rise to the lineaments of the Vaalputs graben.

The Gordonia Formation and present day micro-environments

Aridification was probably initiated by the onset of cold water upwelling along the coast in the late Miocene (ca 10 Ma) (Siesser, 1980). During this period the Koa River is believed to have ceased flowing (McCarthy et al., 1985) due to the choking of the valley with sand and possible tectonic warping (Du Toit, 1933).

The aeolian deposits, resulting from aridification and dune sand transgression, of the Gordonia Formation are believed to be of late Tertiary to Quaternary age. The source of the predominantly aeolian deposits of the Gordonia Formation in this region was originally believed to be the western highlands of gneissic country rock. Degradation of the dune field was attributed to a diminished sediment supply due to the breakthrough of the Buffels and Olifants Rivers into the inland plateau (McCarthy et al., 1985). Andersen (1992) also attributed the cut off of sediment supply from the Kamiesberg highlands to the Bushmanland Plateau, to the headward erosion of tributaries of the major rivers in the area.

The present day micro-environments are dominated by aeolian, deflation pan and lag deposits which have all been and are presently being modified by bioturbation. The mean grain sizes for the aeolian dune environments of this study (1-1.6 ϕ) are significantly larger than those recorded for aeolian sands in the Kalahari basin and Namib Desert (for example, 2.44 ϕ - Lancaster, 1981). Comparative grain size parameter analyses, however, have shown reasonable similarities of the Vaalputs and Gordonia Formation sediments. This correlation of sedimentary parameters may be partly attributed to the mixing associated with bioturbation, but the results do suggest a common source and genetic relationship for the two sediment suites. In addition no regional change in grain size with distance from the basement in the west (a possible source terrain) was noticed. Rather, the local or micro-environment seems to play an important part in determining grain size parameters.

Petrographically the Gordonia sediments are similar to the Vaalputs sediments. The fine fraction of the surface sediments are also not typical of aeolian environments; the dominant surface forming process. The possibility that the fine fraction was derived

from weathered basement to the west of the Gordonia deposits and deposited in a high energy aeolian environment also seems unlikely. Remnant feldspar grains in both the Gordonia and Vaalputs Formations suggests that the clay fraction is predominantly derived from *in situ* weathering of the Vaalputs sediments and reworked to some degree in the overlying Gordonia sediments.

The comparative chemical analysis indicates that the Gordonia (surface) samples are very closely related to the Vaalputs sediments and differ essentially only by being more quartz rich which may be accounted for by aeolian or weathering processes; aeolian activity also reduces the clay fraction to some degree.

The results of this study all indicate that the source of these sediments is primarily the underlying Vaalputs Formation which is in a state of degradation. The calcrete layer associated with the dune forms is continually being leached downwards by meteoric water. Surface processes (primarily aeolian) have reworked and modified the surface into longitudinal dunes with a transverse component and which in turn affects and results in the sinuous subsurface calcrete morphology. Other modifying processes include bioturbation or mixing and the removal of fines as a result of high wind velocities.

The sequence of the Late-Mesozoic and Cenozoic sediments preserved on the Namaqualand Metamorphic Complex, in the Vaalputs Region, is therefore, a consequence of both climatic and tectonic changes that took place during the geological history of the area. The climate was pluvial during the deposition of the Dasedap sediments. The Late-Cretaceous weathering profiles were formed during the late stages of this more humid period and affected the Dasedap sediments too. The Tertiary saw the onset of more arid conditions as suggested by the increased desiccation of the Vaalputs Formation and finally the arid conditions for the formation of Gordonia Formation.

CHAPTER 10: CONCLUSIONS

The objectives of this study were to obtain a better understanding of the post Karoo, recent, and present tectonic history of the northwestern Cape, particularly in the Vaalputs area. Geomorphological, sedimentological and geological episodes needed to be placed in a well constrained, relative time frame. These episodes could then be directly correlated to major events in the area, providing valuable tectonic information. That is, the response of landscape development (processes and products), to tectonic processes was the key objective of this study.

The sequence of sediments preserved on the Bushmanland Plateau, in the area around Vaalputs, reflect changes in climate and tectonism since the onset of the deposition of these sediments. During the Cretaceous the alluvial Dasdap sediments were deposited as a result of uplift along the marginal scarp. These sediments were deposited rapidly in an alluvial fan setting. Crater sediments overlying olivine melilitites and kimberlites were also deposited during the middle and latter part of the Cretaceous. The late Cretaceous saw tropical conditions which caused extensive deep weathering and silicification of the Namaqualand Metamorphic Complex and the Dasdap Formation. This wet period terminated around the end of the Cretaceous when the climate changed to semi-arid and arid. Erosion has subsequently exposed the palaeo-weathered and silicified basement, and tectonism, throughout most of the Cenozoic, largely in the form of reactivated older structures has caused differences in the elevation of these surfaces and resulted in the accumulation of the Vaalputs sediments.

North-northwest oriented graben formation during the Tertiary resulted in the accumulation of the fluvial and aeolian Vaalputs sediments. The extremely altered white clay at the base of the Vaalputs Formation is suggestive of a wetter period during which intense *in situ* weathering of the basement could take place. Subsidence or deepening of the graben gave rise to the preservation of this weathered facies and to the deposition of the Vaalputs sediments. The sediment was eroded from the elevated basin margins and deposited as floodouts, with some aeolian deposits, in the Vaalputs basin. Weathering and mixing of these sediments ultimately gave rise to the observed

sequence of clay-rich Vaalputs sediments.

The calcrete horizons preserved in the Vaalputs Formation indicates drier interludes with an overall desiccation trend through time. The calcrete horizons generally define previous land surfaces, that is, the calcrete horizons probably represent surface stabilization stages during less tectonically active periods or during periods of lower sediment supply. The overall desiccation throughout the Cenozoic finally gave rise to the aeolian dominated Gordonia Formation and present day micro-environments. The present day micro-environments are dominated by aeolian, deflation pan and lag deposits the source of which is primarily the underlying Vaalputs Formation which is in a state of degradation. Sub-surface calcrete associated with the dunes is continually being leached downwards by meteoric water. Aeolian processes have reworked and modified the surface into low amplitude longitudinal dunes with a transverse component.

Evidence of two stress fields believed to have given rise to the numerous tectonic products (inherent and new structures) in the study area since the Cretaceous were observed. The study area is affected by two important uplift axes: the Griqualand-Transvaal and the Kamiesberge axes, which were active between the Miocene and the Plio-Pleistocene. The study area has also been subjected to a prolonged history of tectonic activity during which time faults and major shear zones have been reactivated and others formed. On a regional scale the larger and older faults, which dictate the drainage courses in the area are predominantly north-northwesterly trending. This faulting is most probably of a Pan African age (700 Ma.), and has been reactivated as evidenced from the elevations of the palaeo-weathered and silicified basement and the resultant Vaalputs basin.

During the Late-Cretaceous and Palaeocene, the minimum principle stress was most probably oriented to the northwest causing extensive dip-slip faulting with a northeasterly strike. This stress field most probably also gave rise to the joint pattern observed in the basement. The stress field believed to be responsible for most of the Cenozoic, with an east-northeast oriented minimum principle horizontal stress probably

accompanied the development of a fault-bound sedimentary basin which was filled by the sediments of the Vaalputs Formation. It is suggested that the earlier phase was dominated by ridge push during the Late-Cretaceous and Palaeocene and the later phase by isostatic readjustment.

REFERENCES

- Adamson, D., Williams, M.A.J. and Baxter, J.T. (1987). Complex Late Quaternary alluvial history in the Nile, Murray-Darling, and Ganges basins: three river systems presently linked to the Southern Oscillation. In Gardiner, V. (Ed.), *International Geomorphology 1986: Part II*, John Wiley and Sons Ltd, 875-887.
- Albat, H.M. (1984). The Proterozoic granulite facies terrane around Kliprand, Namaqualand Metamorphic Complex. *Bull. Precamb. Res. Unit*, Univ. Cape Town, **33**, 382 pp.
- Aleksandrowski, P. (1985). Graphical determination of principal stress directions for slickenside lineation populations: an attempt to modify Arthaud's method. *J. Struct. Geol.*, **7**, 73-82.
- Allsopp, H.L., Kostlin, E.O., Welke, H.J., Burger, A.J., Kröner, A. and Blignault, H.J. (1979). Rb-Sr and U-Pb geochronology of late Precambrian-early Palaeozoic igneous activity in the Richtersveld (South Africa) and southern South West Africa. *Trans. Soc. S. Afr.*, **82**, 185-204.
- Andersen, N.J.B. (1992). *A structural analysis of the Vaalputs waste disposal site and environs, Bushmanland, South Africa*. M.Sc. dissertation, University of Pretoria, 197 pp.
- Andersen, N.J.B. and Muller, J.A. (1984). *A geophysical study of the Vaalputs melnoite pipe*. Unpublished AEC Report, (GEA-552).
- Andersen, N.J.B., Raubenheimer, E. and Levin, M. (1983). *The Geology of the Vaalputs Radioactive Waste Disposal Site and Environs*. Unpublished AEC report, PER-107, (GEA-403).
- Andersen, N.J.B., Andersen, L.M., Watkeys, M. and Raubenheimer, E. (1996). *Regional Structural Development of the Vaalputs Sub-terrane*. Unpublished AEC Report, (GEA-1178).
- Andreoli, M.A.G., Andersen, N.J.B. and Faurie, J.N. (1986). Anorthosite-related pliometallic thorium-uranium deposits in the Namaqualand Metamorphic Complex, South Africa. Technical Committee Meeting on Geological Data Integration. Vienna, Austria, October 1986.
- Andreoli, M.A.G., Andersen, N.J.B., Levin, M. and Niemand, N. (1987). *Geology of the Vaalputs Radioactive Waste Disposal Site in the Republic of South Africa. Explanatory notes for the geological map of the site on the scale 1:25,000*. Unpublished AEC report, PER-151, (GEA-720).

Andreoli, M.A.G., Smith, C.B., Watkeys, M., Moore, J.M., Ashwal, L.D. and Hart, R.J. (1994). The geology of the Steenkampskraal monazite deposit, South Africa: implications for REE-Th-Cu mineralization in charnockite granulite terranes. *Econ. Geol.*, **89**, 994-1016.

Andreoli, M.A.G., Doucoure, M., Van Bever Donker, J., Brandt, D. and Andersen, N.J.B. (1996). Neotectonics of southern Africa - a review. *African Geosciences Review*, **3** (1), 1-16.

Arthaud, F. (1969). Methode de determination graphique des directions de raccourcissement, d'allongement et intermediaire d'une population de failles. *Bull. Soc. geol. Fr.*, **7** Ser. 11, 729-737.

Ash, J.E. and Wasson, R.J. (1983). Vegetation and sand mobility in the Australian desert dunefield. *Zeitschrift für Geomorphologie*, **45**, Supplementband, 7-25.

Ashwal, L.D., Andreoli, M.A.G., Page, M., Armstrong, R.A. and Tucker, R.D. (1997). Geology and geochronology of high temperature granulites, Vaalputs area, central Namaqualand, South Africa. *Tect. Div. of the Geol. Soc. of S. Afr.*, XIIIth Anniversary Conference, 2pp.

Axelrod, D.I. and Raven, P.H. (1978). Late Cretaceous and Tertiary history of Africa. In J. Werger (ed.), *Biogeography and Ecology of Southern Africa*, W. Junk, The Hague, 77-130.

Baes Jr., C.F. and Mesmer, R.E. (1976). *The hydrolysis of cations*. Wiley, New York, N.Y.

Barron, E.J., Thompson, S.L. and Schneider, S.H. (1981). An ice-free Cretaceous? Results from climate model simulations. *Science*, **212**, 501-508.

Beaumont, P.B. (1986). Where did all the young men go during O-18 stage 2? *Palaeoecology of Africa*, **17**, 79-86.

Beetz, P.F.W. (1933). The geology of south-west Angola between Cunene and Lunda axis. *Trans. geol. Soc. S. Afr.*, **36**, 137-176.

Berner, R.A. (1994). 3GEOCARB II: A revised model of the atmosphere CO₂ over Phanerozoic time. *Journal of Geology*, **294**, 56-91.

Besler, H. (1983). The response diagram: distinction between aeolian mobility and stability of sands and eolian residuals by grain size parameters. *Zeitschrift für Geomorphologie*, **45**, Supplement Band, 287-301.

Black, T.A. and Montgomery, D.R. (1991). Sediment transport by burrowing mammals, Marin County, California, *Earth Surface Processes and Landforms*, **16**, 163-172.

Blair, T.C. and McPherson, J.G. (1994). Alluvial fans and their natural distinction from rivers based on morphology, hydraulic processes, sedimentary processes, and facies assemblages. *J. Sed. Res.*, **64**, 470-489.

Blair, T.C., Baker, F. and Turner, J. (1991). Cenozoic fluvial-facies architecture and aquifer heterogeneity, Oroville, California, Superfund Site and vicinity. In N. Tyler and A.D. Miall (eds.), *Three Dimensional Facies Architecture of Terrigenous Clastic Sediments and Its Implications for Hydrocarbon Discovery and Recovery: SEPM Concepts in Sedimentology and Paleontology*, v. 3, 147-159.

Blissenbach, E. (1954). Geology of alluvial fans in semi-arid regions. *Geol. Soc. Am. Bull.*, **65**, 175-190.

Botha, B.J.V., Grobler, N.J., Strom, W. and Smit, C.A. (1977). Major structural features of the area between Langeberg range and Kenhardt, Northern Cape Province. *Trans. geol. Soc. S. Afr.*, **80**, 101-109.

Brandt, D., McCarthy, T.S., Andreoli, M.A.G. and Andersen, N.J.B. (1995). Tectonic and lineament investigations of the Vaalputs area, Namaqualand, South Africa: implications for the geomorphic evolution of rifted continental margins. *Extended Abstracts Volume Geocongress 95*, Johannesburg, 3-7 April 1995. *Geol. Soc. S. Afr.*, 445-448.

Bremer, H. (1967). Zur Morphologie von Zentralaustralien. *Heidelberger Geographische Arbeiten*, **17**, 244 pp.

Briner, G.P. and Jackson, M.L. (1970). Mineralogical analysis of clays developed from basalt in Australia. *Isr. J. Chem.*, **8**, 487-500.

Brock, R.W. (1943). Weathering of igneous rocks near Hong Kong. *Geol. Soc. America Bull.*, **54**, 717-738.

Brown, R.W., Rust, D.J., Summerfield, M.A., Gleadow, A.J.W. and De Wit, M.C.J. (1990). An Early Cretaceous phase of accelerated erosion on the south-western margin of Africa: evidence from apatite fission track analysis and the offshore sedimentary record. *Nuclear Tracks and Radiation Measurement*, **17**, 339-350.

Brynard, H.J. (1988). *A petrological and geochemical study regarding the suitability of the Vaalputs radioactive waste disposal facility*. Ph.D. thesis, University of Pretoria, 230 pp.

Büdel, J. (1982). *Climatic Geomorphology*. Princeton University Press, New Jersey, 443 pp.

Bull, W.B. (1964). Alluvial fans and near surface subsidence in Western Fresno County, California. *U.S. Geol. Surv. Profess. Papers*, 437 A, 1-71.

Burke, K. (1995). Developments on the African Plate over the past 30 million years. *Centennial Geocongress Abstracts*, 2-4.

Callen, R.A. (1983). Late Tertiary "grey billy" and the age and origin of surficial silicifications (silcrete) in South Australia. *Jour. Geol. Soc. Aust.*, 30, 393-410.

Calvet, F., Pomar, L. and Esteban, M. (1975). Las rizocretiones del Pleistoceno de Mallorca. *Inst. Invest. Geol. Univ. Barcelona*, 30, 35-60.

Cande, S.C., LaBreque, J.L. and Haxby, W.F. (1988). Plate kinematics of the south Atlantic: chron C34 to present. *J. Geophys. Res.*, 93, B11, 13479-13492.

Carrington, A.J. and Kensley, B.F. (1969). Pleistocene molluscs from the Namaqualand coast. *Ann. S. Afr. Mus.*, 52, 189-223.

Cerling, T.E. (1984). The stable isotopic composition of modern soil carbonate and its relationship to climate. *Earth Plan. Sci. Lett.*, 71, 229-240.

Clifford, T.N. Gronow, J., Rex, D.C. and Burger, A.J. (1975). Geochronological and petrogenic studies of high-grade metamorphic rocks and intrusives in Namaqualand, South Africa. *J. Petrology*, 16, 154-188.

Cloetingh, S. and Kooi, H. (1992). Tectonics and global change: inferences from Late Cenozoic subsidence and uplift patterns in the Atlantic/Mediterranean region. *Ter. Nova*, 4, 340-350.

Coetzee, J.A., Scholtz, A. and Deacon, H.J. (1983). Palynological studies and vegetation history of the fynbos. In H.J. Deacon, Q.B. Hendey and J.J.N. Lambrechts (eds.), *Fynbos Palaeoecology: a Preliminary Synthesis*, South African National Scientific Programmes, Report No. 75, C.S.I.R. Pretoria, 156-173.

Collison, J.D. (1978). Deserts. In H.G. Reading (editor), *Sedimentary environments and facies*. Blackwell, Oxford, 15-60.

Colliston, W.P., Praekelt, H.E. and Schoch, A.E. (1989). A broad perspective (Haramoep) of geological relations established by sequence mapping in the Proterozoic Aggeneys terrane, Bushmanland, South Africa. *S. Afr. J. Geol.*, 92, 42-48.

Cooke, R.U. (1970). Stone pavements in deserts. *Ann. Assoc. Am. Geogr.*, **60**, 560-577.

Cornelissen, A.K. and Verwoerd, W.J. (1975). The Bushmanland kimberlites and related rocks. In L. M. Ahrens, J.B. Dawson, A.R. Duncan and A. Erlank (eds.), *Physics and Chemistry of the Earth*, **9**, Pergamon Press, Oxford, 71-80.

Corner, B. (1993). *A reinterpretation of the magnetic data covering the Vaalputs national radioactive waste disposal facility and environs*. Unpublished AEC report.

Costa, J.E. (1984). Physical geomorphology of debris flows. In J.E. Costa and P.J. Fleisher (eds.), *Developments and Applications of Geomorphology*, Springer-Verlag, Berlin, 268-317.

Costa, J.E. (1988). Rheologic, geomorphic, and sedimentologic differentiation of water floods, hyperconcentrated flows, and debris flows. In V.R. Baker, R.C. Kochel and P.C. Patton (eds.), *Flood Geomorphology*, Wiley, New York, 113-122.

Coward, M.P. (1986). Heterogeneous stretching, simple shear and basin development. *Earth and Planetary Science Letters*, **80**, 325-336.

Crowley, T. (1983). The geologic record of climatic change. *Rev. Geophys. Space phys.*, **21**, 828-877.

Davis, G.H. (1984). *Structural Geology of Rocks and regions*. John Wiley and Sons, U.S.A.

Davis, W.M. (1899). The geographical cycle. *Geogr. J.*, **14**, 482-504.

Day, F.H. (1963). *The Chemical Elements in Nature*. Reinhold, New York, 372 pp.

Deacon, J. and Lancaster, N. (1988). *Late Quaternary Palaeoenvironments of Southern Africa*. Oxford University Press, Oxford, 225 pp.

De Swardt, A.M.J. and Bennet, G. (1974). Structural and physiographic development of Natal since the late Jurassic. *Trans. geol. Soc. S. Afr.*, **77**, 309-322.

De Wit, M.C.J. (1988). Aspects of the geomorphology of the north-western Cape, South Africa. In: Dardis, G.F. and Moon, B.P. (Eds), *Geomorphological studies in southern Africa*, 57-69.

De Wit, M.C.J. (1993). *Cainozoic Evolution of Drainage Systems in the North-Western Cape*. Ph.D. thesis, Dept. of Geol., Univ. of Cape Town, 371 pp.

Dingle, R.V. and Hendey, Q.B. (1984). Late Mesozoic and Tertiary sediment supply to the eastern Cape Basin (S.E. Atlantic) and palaeo-drainage systems in southwestern Africa. *Mar. Geol.*, **56**, 13-26.

Dingle, R.V., Siesser, W.G. and Newton, A.R. (1983). *Mesozoic and Tertiary geology of southern Africa*. A A Balkema, Rotterdam, 375 pp.

Dixey, F. (1942). Erosion cycles in central and southern Africa. *Trans. geol. Soc. S. Afr.*, **45**, 151-181.

Dixey, F. (1955a). Erosion surfaces in Africa: some consideration of age and origin. *Trans. geol. Soc. S. Afr.*, **58**, 265-280.

Dixey, F. (1955b). Some aspects of the geomorphology of central and southern Africa. *Trans. geol. Soc. S. Afr.*, **58**, 1-58.

D'Orey, F.L.C. (1975). Contribution of termite mounds to locating hidden copper deposits. *Trans. Instn. Min. Metall. (Sect. B: Appl. earth sci.)*, **84**, B150-151.

Dunbar, J.A. and Sawyer, D.S. (1988). Continental rifting at pre-existing lithospheric weakness. *Nature*, **333**, 450-452.

Du Toit, A.L. (1909). Kimberlite and allied pipes and fissures in Prieska, Britstown, Victoria West and Carnarvon. *Ann. Rep. Geol. Comm. C.G.H.*, **13**, 111-127.

Du Toit, A.L. (1933). Crustal movements as a factor in the geological evolution of South Africa, *South African Geographical Journal*, **16**, 3-20.

Ellis, F. (1979). The genesis, morphological and chemical properties of soils from the arid Annis Plain in the Richtersveld, Namaqualand. *9th Congr. Soil Sci. Soc. S. Afr. Proc.*

Ellis, F. and Schloms, B.H.A. (1978). Observations on the properties and genesis of dorbank soils in the Western Cape Province. *8th Congr. Soil Sci. Soc. S. Afr. Proc.*, Technical Communication No. 165, Dept. Agric. Tech Services, 178-181.

Ellis, F. and Schloms, B.H.A. (1982). A note on the dorbanks (duripans) of South Africa. In J.A. Coetzee and E.M. Van Zinderen Bakker SR (eds.), *Palaeoecology of Africa and the Surrounding Islands*, *Proc. of VIth Conference of the S. Afr. Soc. for Quarternary Res.*, **15**, A.A. Balkema, Rotterdam, 149-157.

Emery, K.O. (1978). Grain size in laminae of beach sand. *J. Sed. Petrol.*, **48**, 1203-

Engelbreton, D.C., Kelley, K.P., Cahsman, H.J. and Richards, M.A. (1992). 180 million years of subduction. *Geological Society of America Today*, **2**, 93-95, 100.

Estes, R. (1977). Relationships of the South African fossil frog *Eoxonopoides reunini* (Anura, Pipidae). *Annals. S. Afr. Museum*, **73**, 49-80.

Fairbridge, R.W. (1981). *Z. Geomorphology*, **40**, p. VII.

Faurie, J.N. and Hennop, F. (1993). *Vaalputs seismic monitoring programme*, Status Report 1 (unpublished), (GEA 1077).

Fitzpatrick, R.W. (1988). *Iron compounds as indicators of pedogenic processes: examples from the Southern Hemisphere*. In J.W. Stucki, B.A. Goodman and U. Schwertmann (eds.), *Iron in Soils and Clay Minerals*, NATO ASI Series C: Mathematical and Physical Sciences, Vol **217**, 351-396.

Flach, K.W., Nettleton, W.D., Gile, L.H. and Cady, J.G. (1969). Pedocementation: induration by silica, carbonates and sesquioxides in the Quarternary. *Soil Sci.*, **107**, 442-453.

Flint, R.F. and Bond, G. (1968). Pleistocene sand ridges and pans in western Rhodesia. *Bulletin of the Geological Society of America*, **79**, 299-314.

Folk, R.L. (1974). *Petrology of sedimentary rocks*. Hemphills, Austin, Texas.

Frakes, L.A. (1979). *Climates throughout Geological Time*, Elsevier, Amsterdam, 310 pp.

Frakes, L.A. (1986). Mesozoic- Cenozoic climatic history and causes of the glaciation. In: Hsu, K.J. (Ed.), *Mesozoic and Cenozoic Oceans*, *Geol. Soc. Am., Geodynamics series*, **15**, 33-48.

Frankel, J.J. and Kent, L.E. (1938). Grahamstown surface quartzites (silcretes). *Trans. Geol. Soc. S. Afr.*, **40**, 1-42.

Friedman, G.M. (1961). Distinction between dune, beach, and river sands from their textural characteristics. *J. sedim. Petrol.*, **31**, 514-529.

Friedman, G.M. and Johnson, K.G. (1982). *Exercises in Sedimentology*. John Wiley and Sons, New York, 208 pp. *Journal of Sedimentary Petrology*, **48**, 1193-1202.

Galehouse, J.S. (1971). Point counting, 385-407. In: R.E. Carver (Ed.), *Procedures in Sedimentary Petrology*, Wiley Interscience, New York, 653 pp.

Garrels, R.M. and MacKenzie, F.T. (1967). Origin of the chemical compositions of some springs and lakes. In R.F. Gould, (editor), *Equilibrium Concepts in Natural Water Systems: Amer. Chem. Soc. Adv. Chem. Series*, 67, 222-242.

Gilchrist, A.R. and Summerfield, M.A. (1990). Differential denudation and flexural isostasy in formation of rifted-margin upwarps. *Nature*, 346, 739-742.

Gilchrist, A.R., Kooi, H. and Beaumont, C. (1994). Post-Gondwana geomorphic evolution of southwestern Africa: implications for the controls on landscape development from observations and numerical experiments. *Journal of Geophysical Research*, 99 (B6), 12,211-12,288.

Gohain, K. and Parkash, G. (1990). Morphology of the Kosi Megafan. In Rachocki, A.H and Church, M. (Eds.), *Alluvial Fans: A Field Approach*, John Wiley and Sons, Chichester, 151-178.

Goudie, A.S. (1970). Notes on some of the major dune types in southern Africa. *South African Geographical Journal*, 52, 93-101.

Goudie, A.S. (1973). *Duricrusts in Tropical and Subtropical Landscapes*. Clarendon Press, Oxford.

Goudie, A.S. (1983). Calcrete. In Goudie, A.S. and Pye, K., (editors): *Chemical sediments and geomorphology: precipitates and residua in the near-surface environment*. Academic Press Inc., London, 59-91.

Goudie, A.S. and Thomas, D.S.G. (1985). Pans in southern Africa with particular reference to South Africa and Zimbabwe. *Zeitschrift für Geomorphologie*, 29, 1-19.

Grandin, G. and Thiry, M. (1983). Les grande surfaces continentales Tertiaires des regions chaudes succession des types d'alteration. *Cah. ORSTOM, Ser. Geol.*, 13, 3-18.

Grant, K. and Aitchison, G.D. (1970). The engineering significance of silcretes and ferricretes in Australia. *Eng. Geol.*, 4, 93-120.

Grant, W.H. (1963). Weathering of Stone Mountain Granite. In E. Ingersoll, (editor), *Clays and Clay Minerals*, Oxford, Pergamon, 65-73.

Grove, A.T. (1951). Land use and soil conservation in parts of Onitsha and Owerri

Provinces. *Bulletin, Geological Survey, Nigeria, No. 21.*

Grove, A.T. (1969). Landforms and climatic change in the Kalahari and Namaqualand, *Geographical Journal*, **135**, 191-212.

Gunn, R. (1949). Isostasy - extended. *Journal of Geology*, **57**, 263-279.

Haibich, I.W. (1962). On the morphology of the Dwyka Series in the vicinity of Loeriesfontein, Cape Province. *Ann. Univ. Stellenbosch*, **37**, 43-162.

Hallam, A. (1985). A review of Mesozoic climates. *J. Geol. Soc.*, **142**, 433-445.

Hambleton-Jones, B.B. (1986). *A summary of the geotechnical and environmental investigations pertaining to the Vaalputs National Radioactive Waste Disposal Facility.* PER 143. AEC.

Hartnady, C.J.H. (1990). Seismicity and plate boundary evolution in southeastern Africa. *S. Afr. J. Geol.*, **93**, 473-484.

Hartnady, C.J.H. and Partridge, T.C. (1995). Neotectonic uplift in southern Africa: a brief review and geodynamic conjecture. *Extended Abstracts Volume Gecongress 95*, Johannesburg, 3-7 April 1995. *Geol. Soc. S. Afr.*, 456-459.

Haughton, S.H. (1915). On some dinosaur remains from Bushmanland. *Transactions, Royal Society of South Africa*, **5**, 259-264.

Haughton, S.H. (1930). On a collection of fossil frogs from the clays at Banke. *Trans. Royal. Soc. S. Afr.*, **19**, 233-249.

Haughton, S.H. (1932). The fossil *equidae* of South Africa. *Annals, South African Museum*, **28**, 407-427.

Haughton, S.H. (1969). Geological history of Southern Africa. *Geol. Soc. S. Afr.*, Cape and Transvaal printers. 535 pp.

Hendey, Q.B. (1978). Preliminary report on the Miocene vertebrates from Arrisdrift, South West Africa. *Ann. S. Afr. Mus.*, **76**, 1-41.

Hendey, Q.B. (1981). Palaeoecology of the late Tertiary fossil occurrences in 'E' quarry, Langebaanweg, South Africa, and a reinterpretation of their geological context. *Ann. S. Afr. Mus.*, **84**, 1-104.

Hendey, Q.B. (1983). Cenozoic geology and palaeogeography of the fynbos region. In: Deacon, H.J. et al., Eds., *Fynbos Palaeoecology: a Preliminary Synthesis*. S. Afr. Natn. Prog. Rep. **75**, 35-60, CSIR, Pretoria.

Hillel, D. (1971). *Soil and Water: Physical Principles and Processes*. Academic Press, New York. 288 pp.

Hooke, R. Leeb. (1967). Processes on arid-region alluvial fans. *J. Geol.*, **75**, 438-460.

Imeson, A.C. and Kwaad, F.J.P.M. (1976). Some effects of burrowing animals on slope processes in the Luxembourg Ardennes Part 2: The erosion of animal mounds by splash under forest, *Geografiska Annaler*, **58A**, 317-328.

James, H.L., Dutton, C.E., Pettijohn, F.H. and Wier, K.L. (1968). Geology and ore deposits of the Iron River - Crystal Falls District, Iron County, Michigan. *U.S. Geol. Surv. Prof. Pap.*, 570.

Jamieson, B. (1986). *Isopach maps of the Vaalputs basin*. Unpublished AEC report, PIN 977 (B/R), (GEA 718).

Jaroszewski, W. (1984). *Fault and fold tectonics*. John Wiley and Sons, New York-Chichester-Brisbane-Toronto, 565 pp.

Jessup, R.W. (1960). An introduction to the soils of the south-eastern portion of the Australian arid zone, *J. Soil Sci.*, **11**, 92-105.

Johnson, A.M. (1984). Debris flow. In D. Brunnsden and D.B. Prior (eds.), *Slope Instability*, Wiley, New York, 257-361.

Johnson, D.L. (1967). Caliche on the Channel Island. *Miner. Inf. Calif. Div. Mines Geol.*, **20**, 151-158.

Joubert, P. (1971). The regional tectonism of the gneisses of part of Namaqualand. *Bull. Precamb. Res. Unit*, Univ. Cape Town, **10**, 220 pp.

Joubert, P. (1974). Wrench fault tectonics in the Namaqualand Metamorphic Complex. *Bull. Precamb. Res. Unit*, **15**, Cape Town, 213 pp.

Joubert, P. (1986a). The Namaqualand Metamorphic Complex - A summary. In: Anhaeusser, C.R. and Maske, S. (Eds.), *Mineral Deposits of Southern Africa, Vols. I and II*, *Geol. Soc. S. Afr.*, 1395-1420.

Joubert, P. (1986b). Namaqualand - a model of Proterozoic accretion. *Trans. geol. Soc.*

S. Afr., 89, 79-96.

Keen, C.E. (1985). The dynamics of rifting: deformation of the lithosphere by active and passive driving forces. *Geophysical Journal of the Royal Astronomical Society*, 80, 95-120.

Keen, C.E. (1987). Some important consequences of lithospheric extension. In M.P. Coward, J.F. Dewey and P.L. Hancock (eds), *Continental Extensional Tectonics*. Geol. Soc. Spec. Publ., 28, 67-73.

Kendall, C.G. St C. and Warren, J. (1987). A review of the origin and setting of tepees and their associated fabrics. *Sedimentology*, 34, 1007-1027.

Kindle, E.M. (1925). A note on rhizocretions. *J. Geol.*, 33, 744-746.

King, L.C. (1949). On the ages of African land-surfaces. *Q. J. geol. Soc. Lond.*, 104(4), 439-453.

King, L.C. (1951). *South African Scenery*. Oliver and Boyd, Edinburgh, 379 pp.

King, L.C. (1955). Pediplanation and isostasy: an example from South Africa. *Q.J. geol. Soc. Lond.*, 111, 353-359.

King, L.C. (1962). *The Morphology of the Earth*. Oliver and Boyd, Edinburgh, 699 pp.

King, L.C. (1972). The coastal plain of southeast Africa: its form, deposits and development. *Z. Geomorph. N.F.*, 16, 239-251.

King, L.C. and King, L.A. (1959). A reappraisal of the Natal monocline. *South African Geographic Journal*, 41, 15-30.

Kirchheimer, F. (1934). On pollen from the upper Cretaceous dysodil of Banke, Namaqualand (South Africa). *Trans. R. Soc. S. Afr.*, 21, 41-50.

Klappa, C.F. (1991). Rhizoliths in terrestrial carbonates: classification, recognition, genesis and significance. In V.P. Wright and M.E. Tucker (eds.), *Calcretes*, Blackwell Scientific Publications, Oxford, 352 pp.

Klintworth, H. (1948). *The Karoo soils of the Klaver irrigation scheme*. SIRI Report No. 273. Dept. Agric. Tech. Services, Pretoria.

Kooi, H. and Beaumont, C. (1994). Escarpment evolution on high-elevation rifted

margins: insights derived from a surface processes model that combines diffusion, advection and reaction. *Journal of Geophysical Research*, **99 (B6)**, 12,191-12,209.

Krauskopf, K.B. (1967). *Introduction to Geochemistry*. McGraw Hill, New York, 721 pp.

Kröner, A. (1973). Comments on "is the African plate stationary?" *Nature*, **243**, 29-30.

Kröner, A. and Blignault, H.J. (1976). Towards a definition of some tectonic and igneous provinces in the western South Africa and southern South West Africa. *Trans. geol. Soc. S. Afr.*, **79 (2)**, 232-230.

Lamb, H.H. (1972). *Climate, Present, Past and Future. Vol. 1*, Methuen, London, 613 pp.

Lambeck, K. and Stephenson, R. (1985). Post-orogenic evolution of a mountain range: southeastern Australian Highlands. *Geophysical Research Letters*, **12**, 801-804.

Lamplugh, G.W. (1902). Calcrete. *Geol. Mag.*, **9**, 75.

Lamplugh, G.W. (1907). The geology of the Zambezi Basin around the Batoka Gorge (Rhodesia). *Q. J. Geol. Soc. Lond.*, **63**, 162-216.

Lancaster, I.N. (1978a). Composition and formation of southern Kalahari pan margin dunes. *Zeitschrift für Geomorphologie*, **22(2)**, 148-169.

Lancaster, I.N. (1978b). The pans of the southern Kalahari, Botswana. *Geographical Journal*, **144**, 80-98.

Lancaster, I.N. (1981). Grain size characteristics of Namib linear dunes. *Sedimentology*, **28**, 115-122.

Langford, R.P. (1989). Fluvial-aeolian interactions: Part 1, modern systems, *Sedimentology*, **36**, 1023-1035.

Law, J.D.M., Bailey, A.C., Cadle, A.B., Phillips, G.N. and Stanistroet, I.G. (1990). Reconstructive approach to the classification of Witwatersrand 'quartzites'. *S. Afr. J. Geol.*, **93**, 83-92.

Leeder, M.R. (1982). *Sedimentology: process and product*. Unwin Hyman Ltd, London, 344 pp.

Le Roux, J.P. (1986). Sedimentological investigations of the Dasdap Formation in the

area southeast of Sringbok. In *Reports on the Dasdap Formation*. Unpublished AEC report, PIN-950 (B/R), (GEA-686).

Levin, M. (1988). *A geohydrological appraisal of the Vaalputs waste disposal facility in Namaqualand, South Africa*. PhD thesis. (unpubl.) Univ. Orange Free State, Bloemfontein, 216.

Levin, M. and Raubenheimer, E. (1983). Report on the site-selection program for the disposal/storage of radioactive waste in the Republic of South Africa, site suitability phase, *Progress report No. 10, Results of the percussion drilling program on the Vaalputs radioactive waste disposal site*. Unpublished NUCOR report, PIN-680 (B/R).

Levin, M., Niemand, N. and Le Roux, J.P. (1986). The development of the Tertiary formations of the Bushmanland Plateau. *Extended Abstracts Volume Geocongress 86*, Johannesburg, 7-11 July 1986. Geol. Soc. S. Afr., 1035-1039.

Lindesay, J.A. (1990). Mechanisms of climatic change: a review. *S. Afr. J. Sci.*, **86**(6, 7, 8), 340-349.

Loeppert, R.H. (1988). *Chemistry of iron in calcareous systems*. In J.W. Stucki, B.A. Goodman and U. Schwertmann (eds.), *Iron in Soils and Clay Minerals*, NATO ASI Series C: Mathematical and Physical Sciences, Vol 217, 689-714.

Lovering, T.S. (1959). Significance of accumulator plants in rock weathering. *Geol. Soc. America Bull.*, **70**, 781-800.

Mabbutt, J.A. (1955). Erosion surfaces in Namaqualand and the ages of surface deposits in the south western Kalahari. *Transactions, Geological Society of South Africa*, **58**, 13-30.

MacVicar, C.N., de Villiers, J.M., Loxton, R.F., Verster, E., Lamprechts, J.J.N., Merryweather, F.R., le Roux, J., van Rooyen, T.H. and von M. Harmse, H.J. (1977). Soil classification. A binomial system for South Africa. *Sci. Bull.*, **390**, Soil and Irrigation Research Institute, Dept. Agric. Serv., Pretoria, 1-150.

Marais, E.N. (1938). *The soul of the white ant*. Methuen and Co., London.

Marion, G.M., Schlesinger, W.H. and Fonteyn, P.J. (1985). Caldep: a regional model for soil CaCO₃ (caliche) deposition in south western deserts. *Soil Sci.*, **139**, 468-481.

Markovics, G. (1977). *Chemistry of weathering of the Toorongro Granodiorite, Mt. Baw Baw Vic*. Honours thesis, La Trobe Univ. (unpubl.), 36 p.

Martin, H. (1953). Notes on the Dwyka succession and some pre-Dwyka valleys in the South West Africa. *Trans. geol. Soc. S. Afr.*, **56**, 37-43.

Maud, R.R. (1961). A preliminary review of the structure of coastal Natal. *Trans. geol. Soc. S. Afr.*, **64**, 247-256.

Mayer, J.J. (1973). Morphotectonic development of the Harts River Valley in relation to the Griqualand-Transvaal Axis and the Vaal and Molopo Rivers. *Transactions, Geological Society of South Africa*, **76**, 183-194.

McCarthy, T.S. (1983). Evidence for the former existence of a major southerly flowing river in Griqualand West. *Transactions, Geological Society of South Africa*, **86**, 37-49.

McCarthy, T.S., Levin, M. and Moon, B.P. (1984). *Geomorphology of the Vaalputs low-level Radioactive Waste Disposal Site and Environs*. Site Selection Program for the disposal/storage of Radioactive waste in S.A. Site suitability phase. Progress report no. 23. NUCOR Rep. PER-121, 32 pp.

McCarthy, T.S., Moon, B.P. and Levin, M. (1985). Geomorphology of the western Bushmanland plateau, Namaqualand, South Africa. *South African Geographical Journal*, **67**, 160-178.

McFadden, L.D., Wells, S.G. and Jercinovich, M.J. (1987). Influences of eolian and pedogenic processes on the origin and evolution of desert pavements. *Geology*, **15**, 504-508.

McKenzie, D.P. (1978). Some remarks on the development of sedimentary basins. *Earth and Planetary Science Letters*, **40**, 25-32.

McMillan, I.K. (1990). A foraminiferal biostratigraphy and chronostratigraphy for the Pliocene to Pleistocene Upper Algoa Group, eastern Cape, South Africa. *S. Afr. J. Geol.*, **93** (4), 622-644.

Mercherikov, Y.A. (1968). In *Encyclopedia of Gemorphology*, ed. R.W. Fairbridge, Reinhold, 768 pp.

Meunier, A. and Velde, B. (1976). Mineral reactions at grain contacts in early stages of granite weathering. *Clay Minerals*, **11**, 235-240.

Miall, A.D. (1977). A review of the braided river depositional environment. *Earth Sci. Rev.*, **13**, 1-62.

Miall, A.D. (1978). Fluvial sedimentology: an historical review. In A.D. Miall (ed.), *Fluvial sedimentology*. Canadian Society of Petroleum Geologist, Memoir 5, 1-47.

Middleton, G.V. and Hampton, M.A. (1976). Subaqueous sediment transport and deposition by sediment gravity flows. In D.J. Stanley and D.J.P. Swift (eds.), *Marine Sediment Transport and Environmental Management*, Wiley, New York, 197-218.

Milnes, A.R. and Thiry, M. (1972). Silcretes. In I.P. Martini and W. Chesworth (Eds.), *Weathering, Soils and Paleosols*, Developments in Earth Surface Processes 2, Elsevier, Amsterdam, 349-377.

Milnes, A.R. and Twidale, C.R. (1983). An overview of silicification in Cenozoic landscapes of arid central and southern Australia. *Aust. J. Soil Res.*, **21**, 387-410.

Moore, A.E. (1979). *The Geochemistry of the Olivine Melilitites and Related Rocks of Namaqualand-Bushmanland, South Africa*. Ph.D. thesis, University of Cape Town, 199 pp.

Moore, A.C. (1981). The Tantalite Valley Shear Zone - a major locus for igneous activity in southern Namibia (SWA)? *J. Volc. Geotherm. Res.*, **10**, 383-393.

Moore, J.M. and Reid, A.D. (1989). A Pan-African staurolite imprint on Namaqua quartz-gahnite-sillimanite assemblages. *Mineralog. Mag.*, **53**, 63-70.

Moore, A.E. and Verwoerd, W.J. (1985). The olivine-melilitite kimberlite - carbonatite suite of Namaqualand and Bushmanland, South Africa. *Trans. Geol. Soc. S. Afr.*, **88**, 281-294.

Mörner, N.A. (1989). *Tectonophysics*, **163**, p. 181.

Muller, M.J., Posnik, S.J. and Levin, M. (1990). *A Palaeoclimatology of Bushmanland, with Particular Reference to the Last 25 000 Years*. Unpublished AEC report, PIN-1201, (GEA-955), 76 pp.

Nanson, G.C., Chen, X.Y. and Price, D.M. (1995). Aeolian and fluvial evidence of changing climate and wind patterns during the past 100 ka in the western Simpson Desert, Australia. *Palaeogeography, Palaeoclimatology, Palaeoecology*, **113**, 87-102.

Nash, D.J., Shaw, P.A. and Thomas, D.S.G. (1994). Duricrust development and valley evolution: process-landform links in the Kalahari. *Earth Surface Processes and Landforms*, **19**, 299-317.

Nesbitt, H.W. (1979). Mobility and fractionation of rare earth elements during

weathering of a granodiorite. *Nature*, **279**, 206-210.

Nesbitt, H.W., Markovics, G. and Price, R.C. (1980). Chemical processes affecting alkalis and alkaline earths during continental weathering. *Geochim. Cosmochim. Acta*, **44**, 1659-1666.

Nesbitt, H.W. and Young, G.M. (1982). Early Proterozoic climates and plate motions inferred from major element chemistry of lutites. *Nature*, **299**, 715-717.

Nesbitt, H.W. and Young, G.M. (1984). Prediction of some weathering trends of plutonic and volcanic rocks based on thermodynamic and kinetic considerations. *Geochim. Cosmochim. Acta*, **48**, 1523-1534.

Nesbitt, H.W. and Young, G.M. (1989). Formation and diagenesis of weathering profiles. *J. Geol.*, **97** (2), 129-147.

Netterberg, F. (1969). *The geology and engineering properties of South African calcretes: Vol. 1, Summary, classification, distribution, composition and origin*. Ph.D. thesis, Univ. of the Witwatersrand, Johannesburg, 312 pp.

Netterberg, F. (1980). Geology of southern African calcretes 1: Terminology, description and classification. *Trans. Geol. Soc. S. Afr.*, **83** (2), 255-283.

Nettleton, W.D. and Brasher, B.R. (1983). Correlation of clay minerals and properties of soils in the Western United States. *Soil Science Society of American Journal*, **67**, 1032-1036.

Niemand, N. (1986). The Dasdap Formation. In *Reports on the Dasdap Formation*. Unpublished AEC report, PIN-950 (B/R), (GEA-686).

Norish, K. and Hutton, J.T. (1969). An accurate X-ray spectrographic method for the analysis of a wide range of geological samples. *Geochim. Cosmochim. Acta*, **33**, 431-453.

Nyblade, A.A. and Robinson, S.W. (1994). The African Superswell. *Geophysical Research Letters*, **21**, 765-768.

Ollier, C.D. (1985a). Morphotectonics of passive continental margins: introduction. *Z. Geomorph. N.F., Suppl.-Bd.* **54**, 1-9.

Ollier, C.D. (1985b). Morphotectonics of continental margins with great escarpments. In: M. Morisawa and J.T. Hack (Eds.), *Tectonic Geomorphology*. Allen and Unwin,

Boston, 390 pp.

Ollier, C.D. (1991). Aspects of silcrete formation in Australia. *Zeitschrift für Geomorphologie*, **35**, 151-163.

Ollier, C.D. and Marker, M.E. (1985). The great escarpment of Southern Africa. *Z. Geomorph. N.F., Suppl-Bd.*, **54**, 37-56.

Ori, G.G. (1989). Terminal fluvial systems under different climatic conditions. *Program and Abstracts, 4th International Conference on Fluvial Sedimentology*, Barcelona, Stiges, p.97.

Park, R.G. (1988). *Geological structures and moving plates*. Blackie, 337 pp.

Partridge, T.C. (1985). The palaeoclimatic significance of Cainozoic terrestrial stratigraphic and tectonic evidence from South Africa: a review. *S. Afr. J. of Sci.*, **81**, 245-247.

Partridge, T.C. (1994). *Report on a reconnaissance geomorphological survey of an area in the north-western Cape Province to assist the selection of a site for the disposal of high level radioactive waste*. Unpublished AEC report 1-7/93.

Partridge, T.C. and Maud, R.R. (1987). Geomorphic evolution of southern Africa since the Mesozoic. *S. Afr. J. Geol.*, **90** (2), 179-208.

Partridge, T.C. and Maud, R.R. (1988). *Geomorphological Studies in Southern Africa*. Balkema, Rotterdam, 5-15.

Partridge, T.C. and Dalbey, T.S. (1986). Geoarchaeology of the Haaskraal Pan: a preliminary palaeoenvironmental model. *Palaeoecology of Africa*, **17**, 69-78.

Partridge, T.C., Bond, G.C., Hartnady, C.J.H., deMenocal, P.B. and Ruddiman, W.F. (1995a). Climatic effects of late Neogene tectonism and volcanism. In E.S. Vrba, G.H. Denton, T.C. Partridge and L.H. Burckle (eds.), *Paleoclimate and Evolution with an Emphasis on Human Origins*, Yale University Press, 8-23.

Partridge, T.C., Wood, B.A., and deMenocal, P.B. (1995b). The influence of global climatic change and regional uplift on large-mammalian evolution in east and southern Africa. In E.S. Vrba, G.H. Denton, T.C. Partridge and L.H. Burckle (eds.), *Paleoclimate and Evolution with an Emphasis on Human Origins*, Yale University Press, 331-355.

Penck, A. (1908). Der Drakensberg und der Quatlambaburch. *Z.d.K. Preuss. Akad. Wiss.*, **11**, 15-30.

Picker, M.D. (1987). *Burrow and nest characteristics of the harvester termite (Hodotermes mossambicus), and the seed storing activities of the common harvester ant (Messor Barbatulus)*. Unpublished AEC report, PER-154, (GEA-735).

Praekelt, H.E. and Colliston, W.P. (1988). The flaw in the floor rocks of Bushmanland. *Abstr. Geocongress*, 22, Durban, 469-472.

Pretorius, D.A. (1974). The structural boundary between the Kaapvaal and Sonama crustal province. *Econ. geol. Res. Unit, Univ. of the Witwatersrand, Circ.*, 88, 1-27.

Prins, P. (1981). The geochemical evolution of the alkaline and carbonatite complexes of the Damaraland igneous province, South West Africa. *Ann. Univ. Stellenbosch, Ser. A1 (Geol.)*, 3, 145-278.

Pye, K. (1987). *Eolian Dust and Dust Deposits*. Academic Press, London, 334 pp.

Ranalli, G. (1975). Geotectonic relevance of rock-stress determinations, *Tectonophysics*, 29, 1-4.

Ransome, I.G.D. and de Wit, M.J. (1992). Preliminary investigations into a microplate model for the South Western Cape. In M.J. de Wit and I.G.D. Ransome (eds.), *Inversion Tectonics of the Cape Fold Belt, Karoo and Cretaceous Basins of Southern Africa*, Balkema, Rotterdam, 257-266.

Redding, S.J. and Hudson, J.L. (1983). *Part I: The general climate of Bushmanland. Part II: Estimates of percolation at the buried waste facility, Bushmanland*. Site Selection Program for the Disposal/Storage of Radioactive Waste in South Africa. Site Suitability phase. Progress report no. 16. NUCOR Rep., Per-114, 33.

Reeves, C.C. (1976). *Caliche: Origin, Classification, Morphology and Uses*. Estacado Books, Lubbock.

Reineck, H.E. (1963). Sedimentgefüge im Bereich der südlichen Nordsee. *Abhandlungen der senckenbergische naturforschende Gesellschaft*, 505, 1-138.

Reinfelds, I. and Nanson, G. (1993). Formation of braided river floodplains, Waimakariri River, New Zealand, *Sedimentology*, 40, 1113-1127.

Reuning, E. (1930). Erosion surfaces in Namaqualand and the ages of surface deposits in the south western Kalahari. *Trans. Roy. Soc. S. Afr.*, 58, 13-30.

Reuning, E. (19... contribution to the geology and palaeontology of the western edge of the Bushmanland plateau. *Transactions, Royal Society of South Africa*, 19,

Reuning, E. (1932). The composition of the deeper sediments of the pipe at Banke, Namaqualand, and their relation to kimberlite. *Transactions, Royal Society of South Africa*, **21**, 33-39.

Richter, R. (1936). Marken und Spuren im Hunsrück-Schiefer. II. Schichtung and Grund-Leben. *Senckenbergiana*, **18**, 215-244.

Rodier, J.A. (1985). Aspect of arid zone hydrology. In Rodda, J.C. (Ed.), *Facets of Hydrology, Volume II*, John Wiley and Sons, Chichester, 205-247.

Rogers, A.W. (1911). Reports on the geological survey of parts of the divisions of Van Rhyn's Dorp and Namaqualand. *Sixteenth Annual Report*, Geological Commission, Cape of Good Hope, 9-84.

Rogers, A.W. (1915). The occurrence of dinosaurs in Bushmanland. *Trans. Roy. Soc. S. Afr.*, **5**, 265-272.

Rowley, D.B. and Sahagian, D. (1986). Depth-dependent stretching: a different approach. *Geology*, **14**, 32-35.

Rubin, D.M. and Friedman, G.M. (1981). Origin of chert grains and a halite-silcrete bed in the Cambrian and Ordovician Whitehall Formation of eastern New York State. *J. Sediment. Petrol.*, **51**, 69-72.

Ruddiman, W.F., and Kutzbach, J.E. (1989). Forcing of Late Cenozoic northern hemisphere climate by plateau uplift in southern Asia and the American West. *Journal of Geophysical Research*, **94**, 18409-18427.

Rust, D.J. and Summerfield, M.A. (1990). Isopach and borehole data indicators of rifted margin evolution in southwestern Africa. *Marine and Petroleum Geology*, **7**, 277-287.

Salomons, W. and Mook, W.G. (1986). Isotope geochemistry of carbonates in the weathering zone. In P. Fritz and J. Ch. Fontes (eds.), *Handbook of Environmental Isotope Geochemistry, Vol 2*, Elsevier, Amsterdam, New York, 239-269.

Sand, L.B. and Bates, T.L. (1953). Mineralogy of the residual kaolins of the southern Appalachians. *Am. Mineral.*, **38**, 358-372.

Savin, S.M. (1977). The history of the Earth's surface temperature during the past 100 million years. *Ann. Rev. Earth Plan. Sci.*, **5**, 319-355.

Schlegel, G.C.J., Harmse, H.J. von M. and Brunke, O. (1989). Granulometric and mineralogical characteristics of the Kalahari sands of southern Africa. *South African Journal of Geology*, **92** (3), 207-222.

Scholtz, A. (1985). The palynology of the upper lacustrine sediments of the Arnot pipe, Banke, Namaqualand. *Ann. S. Afr. Mus.*, **95** (1), 1-109.

Schumm, S.A. (1977). *The Fluvial System*, Wiley-Interscience, New York.

Schwertmann, U. (1988). Occurrence and formation of iron oxides in various pedoenvironments. In J.W. Stucki, B.A. Goodman and U. Schwertmann (eds.), *Iron in Soils and Clay Minerals*, NATO ASI Series C: Mathematical and Physical Sciences, Vol 217, 267-308.

Senior, B.R. (1978). Silcrete and chemically weathered sediments in southwest Queensland. In T. Langford-Smith (ed.), *Silcrete in Australia*, University of New England, Armidale, N.S.W., 41-50.

Shaw, P.A. (1988). Lakes and pans. In *The Geomorphology of Southern Africa*, B.P. Moon and G.F. Dardis, Southern Book Publishers, Johannesburg, 320 pp.

Shaw, P.A. and Nash, D.J. (1997). Silica accumulation in the distal reaches of the Okavango delta fan, Botswana: some implications for the formation of fluvial silcretes. (in prep.).

Sieffermann, G. and Millot, G. (1969). Equatorial and tropical weathering of recent basalts from Cameroon: allophanes, halloysite, metahalloysite, kaolinite and gibbsite. *Int. Clay Conf.*, Tokyo, 417-430.

Siesser, W.G. (1980). Late Miocene origin of the Benguela upwelling system off northern Namibia. *Science*, **208**, 283-285.

Siesser, W.G. and Dingle, R.V. (1981). Tertiary sea-level movements around southern Africa. *J. Geol.*, **89**, 523-536.

Singer, A. (1966). The mineralogy of the clay fraction from basaltic soils in the Galilee, Israel. *J. Soil Sci.*, **17**, 136-147.

Singer, A. (1980). The paleoclimatic interpretation of clay minerals in soils and weathering profiles. *Earth Sci. Rev.*, **15**, 303-326.

Singer, A. (1989). Illite in the hot-aridic soil environment. *Soil Sci.*, **116**, 146-155.

Smale, D. (1973). Silcretes and associated silica diagenesis in southern Africa. *J. Sediment. Petrol.*, **43**, 1077-1089.

Smith, R.M.H. (1986). Sedimentation and palaeoenvironments of late Cretaceous crater-lake deposits in Bushmanland, South Africa. *Sedimentology*, **33**, 369-386.

Soil Survey Staff. (1975). *Soil Taxonomy*. Soil Conservation Service, US Dept. Agric. Handbook, No. 436.

South African Committee for Stratigraphy (SACS). (1980). Stratigraphy of South Africa. Part I (comp. L.E. Kent). Lithostratigraphy of the Republic of South Africa, South West Africa/Namibia, and the Republics of Bophuthatswana, Transkei and Venda. *Handbk. Geol. Surv. S. Afr.*, **8**, 690 pp.

Solohub, J.T. and Klován, J.E. (1970). Evaluation of grain-size parameters in lacustrine environments. *Journal of Sedimentary Petrology*, **40**, 81-101.

Spoeremann, J. (1995). Some results of recent morphotectonic studies in southwestern Africa. *Centennial Geocongress Extended Abstracts*, Johannesburg, 3-7 April, 1995, 479-482.

Stanistreet, I.G. and McCarthy, T.S. (1993). The Okavango Fan and the classification of subaerial fan systems, *Sedimentary Geology*, **85**, 115-133.

Stephens, C.G. (1971). Laterite and silcrete in Australia: a study of the genetic relationships of laterite and silcrete and their companion materials, and their collective significance in the formation of the weathered mantle, soils, relief and drainage of the Australian continent. *Geoderma*, **5**, 5-52.

Stratten, T. (1968). *The Dwyka glaciation and its relationship to the pre-karoo surface*. Ph.D. thesis. University of the Witwatersrand, 196 pp.

Stratten, T. (1979). The origin of the diamondiferous alluvial gravels in the north western Transvaal. In: Anderson, A.M. and Van Biljon, W.J. (eds.), *Some Sedimentary Basins and Associated Ore Deposits in South Africa*, special publication No. 6, Geological Society of South Africa, 219-228.

Strydom, D. (1979). *The geology of an area north of Carnarvon with special reference to the Precambrian rocks*. Unpubl. M.Sc. thesis, University of the Orange Free State, 145 pp.

Suess, E. (1904). *The Face of the Earth*. Vol. 1. Clarendon Press, Oxford, 604 pp.

Summerfield, M.A. (1978). *The Nature and Origin of Silcrete with Particular Reference to Southern Africa*. D. Phil. Thesis, University of Oxford.

Summerfield, M.A. (1979). Origin and palaeoenvironmental significance of sarsens. *Nature*, **281**, 137-139.

Summerfield, M.A. (1981). Nature and occurrence of silcrete, southern Cape Province, South Africa. *Sch. Geogr., Univ. Oxford, Res. Pap.*, 28.

Summerfield, M.A. (1983a). Silcrete as a palaeoclimatic indicator: evidence from southern Africa. *Palaeogeography, Palaeoclimatology, Palaeoecology*, **41**, 65-79.

Summerfield, M.A. (1983b). Geochemistry of weathering profile silcretes, southern Cape Province, South Africa. In R.C.L. Wilson (editor), *Residual deposits: surface related weathering products and materials*. *Geol. Soc. Lond., Spec. Publ.*, **11**, 167-178.

Summerfield, M.A. (1983c). Silcrete. In Goudie, A.S. and Pye, K., (editors), *Chemical sediments and geomorphology: precipitates and residua in the near-surface environment*. Academic Press Inc., London, 59-91.

Summerfield M.A. (1984). Isovolumetric weathering and silcrete formation, southern Cape Province, South Africa. *Earth Surf. Processes Landforms*, **9**, 135-141.

Summerfield, M.A. (1985). Plate tectonics and landscape development on the African continent. In Morisawa, M. and Hack, J.T., (editors), *Tectonic Geomorphology*, Allen and Unwin, Boston, 27-51.

Summerfield, M.A. (1986). Reply to discussion of silcrete as a palaeoclimatic indicator: evidence from southern Africa. *Palaeogeography, Palaeoclimatology, Palaeoecology*, **52**, 356-360.

Summerfield, M.A. (1987). Neotectonic and landform genesis. *Progress in Physical Geography*, **11**, 384-397.

Summerfield, M.A. (1988). Global tectonics and landform development. *Progress in Physical Geography*, **12**, 389-404.

Summerfield, M.A. (1991a). *Global Geomorphology: An introduction to the study of landforms*. Longman, London; John Wiley and Sons, New York.

Summerfield, M.A. (1991b). Tectonic Geomorphology. *Progress in Physical Geography*, **15** (2), 193-205.

Summerfield, M.A. and Whalley, W.B. (1980). Petrographic investigation of sarsens (Cenozoic silcretes) from southern England. *Geol. Mij.*, **59**, 145-153.

Swindale, L.D. (1966). A mineralogical study of soils derived from basalt and ultrabasic rocks in New Zealand, *N. Z. J. Sci.*, **9**, 484-506.

Sykes, L.R. (1978). Intraplate seismicity, reactivation of pre-existing zones of weakness, alkaline magmatism and other tectonism postdating continental fragmentation. *Reviews of Geophysics and Space Physics*, **16** (4), 621-687.

Tankard, A.J. (1976). Pleistocene history and coastal morphology of the Ysterfontein-Elands Bay area, Cape Province. *Ann. S. Afr. Mus.*, **69**, 73-119.

Tankard, A.J. and Rogers, J. (1978). Late Cenozoic palaeo-environments on the west coast of southern Africa. *J. Biogeogr.*, **5**, 319-337.

Tankard, A.J., Jackson, M.P.A., Eriksson, K.A., Hobday, D.K., Hunter, D.R., Minter, W.E.L. (1982). *Crustal Evolution of Southern Africa*. Springer-Verlag, New York, 523 pp.

Taylor, A.M. and Goldring, R. (1993). Description and analysis of bioturbation and ichnofabric. *J. Geol. Soc., London*, **150**, 141-148.

Ten Brink, U. and Stern, T. (1992). Rift flank uplifts and hinterland basins: comparison of the Transantarctic mountains with the Great Escarpment of southern Africa. *Journal of Geophysical Research*, **97**, 569-585.

Thomas, D.S.G. (1988). The geomorphological role of vegetation in the dune systems of the Kalahari. In G.F. Dardis and B.P. Moon (eds.), *Geomorphological studies in Southern Africa*, Balkema, Rotterdam, 509 pp.

Thomas, D.S.G. and Shaw, P.A. (1990). The deposition and development of the Kalahari Group sediments, central southern Africa. *Journal of African Earth Sciences*, **10**, (1/2), 187-197.

Thomas M.F. (1974). *Tropical Geomorphology - A Study of Weathering and Landform Development in Warm Climates*. Halsted Press, John Wiley and Sons, Inc., New York, 332 pp.

Thomas, M.F. and Summerfield, M.A. (1987). Long-term landform development: key themes and research problems. In Gardiner, V. et al., (editors), *International geomorphology*, Part II, John Wiley, Chichester, 935-956.

- Tooth, S. (1998). Floodouts in Central Australia. In Miller, A. and Gupta, A. (Eds), *Varieties of Fluvial Form*, John Wiley and Sons, New York (in press).
- Toth, J. (1962). A theoretical analysis of groundwater flow in small drainage basins. *Third Canad. Hydrology Symposium*, Calgary, 75-96.
- Trendall, A.F. (1962). The formation of "Apparent Peneplains" by a process of combined laterisation and surface wash. *Z. Geomorph.*, N.F., 6, 183-197.
- Tucker, G.E. and Slingerland, R.L. (1994). Erosional dynamics, flexural isostasy, and long-lived escarpments: a numerical modeling study. *Journal of Geophysical Research*, 99 (B6), 12,229-12,243.
- Twidale, C.R. and Milnes, A.R. (1983). Aspects of the distribution and disintegration of siliceous duricrusts in arid Australia. *Geol. Mijnbouw*, 62, 373-382.
- Twidale, C.R., Shepard, J.A. and Thompson, R.M. (1970). Geomorphology of the southern part of the Arcoona Plateau and the Tent Hill region, west and north of Fort Augusta, South Australia. *Trans. R. Soc. S. Aust.*, 94, 55-69.
- Vail, P.R. and Hardebol, J. (1979). Sea-level changes during the Tertiary. *Oceanus*, 22, 71-79.
- Vail, P.R., Mitchum, R.M. and Thompson, S. (1977). Seismic stratigraphy and global changes in sea level. Part 4: Global cycles of relative changes of sea level. *Mem. Amer. Assoc. Petrol. Geol.*, 26, 83-97.
- Van der Merwe, C.R. (1940). *Soil Groups and Subgroups of South Africa*. Sci. Bull. Dept. Agric. No. 231.
- Van der Merwe, C.R. and Heystek, H. (1955). Clay minerals of South African soil groups: III. Soils of the desert and adjoining semiarid regions. *Soil Sci.*, 80, 479-494.
- Van der Merwe, R., Roering, C. and Smit, C.A. (1988). Slickenside analysis of the Potchefstroom Fault. *S. Afr. J. Geol.*, 91(2), 264-274.
- Van Zinderen Bakker, E.M. (1982). Pollen analytical studies of the Wonderwerk cave, South Africa. *Pollen et Spores*, 24, 235-250.
- Varnes, D.J. (1978). Slope movement types and processes. In R.L. Schuster and R.J. Krizek (eds.), *Landslides, Analysis and Control: Washington D.C.*, Transportation Research Board, National Academy of Sciences, Special Report 176, 11-33.

Versfelt, J. and Rosendahl, B.R. (1989). Relationships between prerift structure and rift architecture in Lakes Tanganyika and Malawi, East Africa. *Nature*, **337**, 354-357.

Vine, H. (1987). Wind-blown materials and W African soils: an explanation of the 'ferrallitic soil over loose sandy sediments' profile. In L. Frostick and I Reid (eds), *Desert Sediments: Ancient and Modern, Geological Society Special Publication, No. 35*, Blackwell Scientific Publications, London, 171-183.

Visser, J.N.J. (1981). Carboniferous topography and glaciation in the north-western part of the Karoo-basin, South Africa. *S. Afr. Geol. Surv., Ann.*, **15(1)**, 13-24.

Visser, J.N.J. (1985). The Dwyka Formation along the north-western margin of the Karoo basin in the Cape Province, South Africa. *Trans. geol. Soc. S. Afr.*, **88**, 37-48.

Visser, J.N.J. (1988). Bespreking van 'Die afsetting en verspreiding van spoel diamante in Suid-Afrika'. *S. Afr. J. Geol.*, **91 (3)**, 420-421.

Vita-Finzi, C. (1986). *Recent Earth Movements - An introduction to Neotectonics*, Acad. Press.

Vleck, D. (1981). Burrowing structure and foraging costs in the fossorial rodent, *Thomomys bottae*. *Oecologia*, **49**, 391-396.

Vogel, J.C. (1982). The age of the Kuiseb River silt terrace at Homeb. *Palaeoecol. Afr.*, **15**, 201-209.

Wahlstrom, E.E. (1948). Pre-Fountain and recent weathering on Flagstaff Mountain near Boulder, Colorado. *Geol. Soc. America Bull.*, **59**, 1173-1190.

Walker, F. and Poldervaart, A. (1949). Karoo dolerites of the Union of South Africa. *Geol. Soc. Am. Bull.*, **60**, 591-706.

Watkeys, M.K. (1986). The Achab Gneiss: a "floor" in Bushmanland or a flaw in Namaqualand. *Trans. Geol. Soc. S. Afr.*, **89**, 103-116.

Watson, A. (1992). Desert soils. In I.P. Martini and W. Chesworth (Eds.), *Weathering, Soils and Paleosols*, Developments in Earth Surface Processes 2, Elsevier, Amsterdam, 225-260.

Watson, J.P. (1970). Contribution of termites to development of a zinc anomaly in Kalahari sand. *Trans. Instn. Min. Metall. (Sect. B: Appl. earth sci.)*, **79**, B53-59.

- Watson, J.P. (1974). Calcium carbonate in termite mounds. *Nature*, **247**, 74.
- Watts, A.B. (1982). Tectonic subsidence, flexure and global changes of sea level. *Nature*, **297**, 469-474.
- Watts, N.L. (1977). Pseudo-anticlines and other structures in some calcretes of Botswana and South Africa. *Earth Surf. Process.*, **2**, 63-74.
- Watts, N.L. (1978). Displacive calcrete: evidence from recent and ancient calcretes. *Geology*, **6**, 699-703.
- Watts, S.H. (1977). Major element geochemistry of silcrete of a portion of inland Australia. *Geochim. Cosmochim. Acta*, **41**, 1164-1167.
- Watts, S.H. (1978). A petrographic study of silcrete from inland Australia. *J. Sed. Petrol.*, **48**, 987-994.
- Waugh, B. (1970). Petrology, provenance and silica diagenesis of the Penrith sandstone (Lower Permian) of northwest England. *J. Sediment. Petrol.*, **40**, 1226-1240.
- Wayland, E.J. (1947). The study of past climates in tropical Africa. *Proc. Pan African Congr. Prehistory*, 59-66.
- Wellington, J.H. (1955). *Southern Africa: A Geographical Study, Vol I: Physical Geography*. The University Press, Cambridge, 528 pp.
- Wernicke, B. (1981). Low-angle normal faults in the Basin and Range Province - nappe tectonics in an extending orogen. *Nature*, **291**, 645-648.
- Wernicke, B. (1985). Uniform-sense normal simple shear of the continental lithosphere. *Canadian Journal of Earth Sciences*, **22**, 108-125.
- Whalley, W.B. (1978). Earth surface diagenesis of an orthoquartzite: scanning electron microscope examination of sarsen stones from southern England and silcretes from Australia. In Whalley, W.B. (editor). *Scanning Electron Microscopy in the Study of Sediments*, Geoabstracts, Norwich, 383-398.
- Wopfner, H. (1978). Silcretes in Northern South Australia and adjacent regions. In T. Langford-Smith, (editor), *Silcrete in Australia*. Dept. Geography, Univ. N.S.W., Armidale, N.S.W., 93-141.
- Wright and M.E. Tucker (1991). Calcretes: an introduction. In V.P. Wright and M.E. Tucker (eds.), *Calcretes*, Blackwell Scientific Publications, Oxford, 352 pp.

Zoback, M.L., Zoback, M.D., Adams, J., Assumpcao, M., Bell, S., Bergman, E.A., Blumling, P., Brereton, N.R., Denham, D., Ding, J., Fuchs, K., Klein, R., Knoll, P., Magee, M., Mercier, J.L., Muller, B.C., Paquin, C., Rajendran, K., Stephansson, O., Suarez, G., Suter, M., Udias, A., Xu, Z.H. and Zhizhin, M. (1989). Global patterns of tectonic stress. *Nature*, **341**, 291-298.

APPENDIX A: MAJOR ELEMENT RESULTS - THE DASDAP FORMATION

Sample No.	SiO ₂	TiO ₂	Al ₂ O ₃	Fe ₂ O ₃	MnO	MgO	CaO	Na ₂ O	K ₂ O	P ₂ O ₅	LOI	TOTAL
VP-K1A*	74.85	1.12	12.76	0.66	0.02	0.00	0.12	1.35	0.47	0.12	7.40	98.85
VP-K2*	32.52	1.20	4.19	4.26	0.39	0.80	28.80	0.21	1.70	0.36	24.63	99.06
VP-K3*	89.82	0.40	5.26	0.68	0.02	0.00	0.07	0.00	0.00	0.05	2.94	99.22
VP-K6*	87.55	0.47	6.43	0.80	0.02	0.00	0.17	0.00	0.01	0.06	3.97	99.47
VP-K7*	81.27	1.34	2.72	11.71	0.04	0.00	0.16	0.00	0.00	0.24	3.02	100.48
RGT 4#	64.06	0.94	19.25	0.60	0.02	0.19	0.50	0.89	0.07	0.40	12.61	99.65
RGT 5#	82.05	0.42	9.03	0.72	0.02	0.10	0.24	0.41	0.08	0.20	3.30	96.55

All data are expressed in weight % Total Fe as Fe₂O₃

- ♦ Basal sediments (Kookoppe)
- * Upper sandstone (Kookoppe)
- + Sandstones (Burtons Puts)
- # Sandstones (Rondegat - Brynard, 1988)

APPENDIX B: MAJOR ELEMENT RESULTS - PALAEO-WEATHERED BASEMENT

Sample No.	SiO ₂	TiO ₂	Al ₂ O ₃	Fe ₂ O ₃	MnO	MgO	CaO	Na ₂ O	K ₂ O	P ₂ O ₅	LOI	TOTAL
Profile 1:												
VP-32 [‡]	72.73	0.29	14.71	0.90	0.06	0.43	0.56	3.32	6.02	0.11	1.03	100.14
VP-31 [‡]	73.91	0.28	14.00	0.91	0.06	0.46	0.04	1.25	5.56	0.12	3.87	100.45
VP-30 [‡]	72.22	0.27	13.89	2.56	0.06	0.54	0.04	1.35	5.57	0.12	3.61	100.22
VP-29 [‡]	72.38	0.27	13.71	1.96	0.06	0.73	0.15	1.30	6.04	0.10	3.68	100.36
VP-28 [‡]	72.84	0.28	14.27	0.76	0.05	0.51	0.22	1.98	6.67	0.14	2.44	100.16
VP-27 [‡]	70.29	0.27	12.90	4.78	0.06	0.54	0.10	1.63	5.79	0.13	3.67	100.16
VP-26 [‡]	71.76	0.30	14.25	1.80	0.06	0.40	0.09	2.21	6.72	0.11	2.52	100.21
VP-25 [‡]	72.77	0.31	14.60	0.95	0.06	0.42	0.39	3.37	6.20	0.12	1.18	100.36
VP-24 [‡]	74.45	0.28	13.50	1.06	0.06	0.36	0.00	1.27	5.19	0.16	3.90	100.22
Profile 2:												
VP-41 [‡]	72.98	0.26	13.96	0.77	0.05	0.30	0.00	1.21	5.64	0.11	3.35	98.63
VP-40 [‡]	74.33	0.26	13.49	0.91	0.05	0.40	0.05	1.64	5.46	0.13	3.85	100.54
VP-39 [‡]	73.45	0.26	13.59	1.12	0.05	0.53	0.03	1.65	5.81	0.11	3.55	100.16
VP-38 [‡]	73.31	0.26	13.28	1.08	0.06	0.51	0.12	2.33	5.52	0.13	3.54	100.14
VP-37 [‡]	72.62	0.35	14.06	1.20	0.06	0.46	0.11	1.61	5.67	0.13	3.72	99.98
VP-36 [‡]	73.90	0.26	13.43	1.62	0.07	0.42	0.38	2.91	6.31	0.10	0.84	100.24
VP-35 [‡]	72.13	0.28	13.73	2.68	0.06	0.60	0.91	3.31	5.70	0.16	0.85	100.41
VP-34 [‡]	73.35	0.27	13.85	1.60	0.07	0.48	0.79	3.12	6.08	0.14	0.51	100.26
VP-33 [‡]	73.85	0.30	13.65	1.35	0.06	0.38	0.88	3.10	5.66	0.17	0.74	100.13
VP-Base 1 [#]	72.20	0.54	15.13	1.26	0.06	0.67	1.54	0.66	0.22	0.11	7.84	100.22
VP-Base 2 [#]	60.63	0.54	17.13	5.25	0.06	0.82	2.51	0.48	4.00	0.12	7.98	99.50
VP-Base 3 [#]	68.41	0.39	15.40	3.76	0.06	0.74	0.18	0.52	5.23	0.14	4.59	99.41

All data are expressed in weight % Total Fe as Fe₂O₃

- ♦ Silicified Basement
- * Kaolinized Basement
- + Basement
- # Weathered basement (white clay) - lower Vaalputs Formation

APPENDIX C: Animal Species Identified at Vaalputs

Order	Family	Species: Latin Name	Common Name	Habitat/Burrow Depth (m)
Insectivora	Macroscelididae	<i>Elephantulus rupestris</i>	Rock elephant shrew	
		<i>Macroscelides proboscideus</i>	Round-eared elephant shrew	
Lagomorpha	Leporidae	<i>Lepus capensis</i>	Vlakhaas	
Rodentia	Cricetidae	<i>Parotomys brantsii</i>	Karoo rat	soft sand, 0.75
		<i>Aethomys namaquensis</i>	Rock rat	
		<i>Gerrbilurus paeba</i>	Pygmy gerbil	sand, 0.2-0.3
		<i>Dermodillus auriculalis</i>	Namaqua gerbil	sand; calcareous soils, 0.3-0.6
		<i>Malacothrix typica</i>	Large-eared mouse	
	Petromuridae	<i>Petromus typicus</i>	Dassie rat	
	Pedetidae	<i>Pedetes capensis</i>	Spring hare	consolidated sand, 0.7-1
	Hyaenidae	<i>Proteles cristatus</i>	Aardwolf	sand, up to 1m and deeper
		<i>Mellivora capensis</i>	Honey badger	
	Felidae	<i>Felis caracal</i>	Caracal	
Carnivora	Canidae	<i>Otocyon magalotis</i>	Bat-eared fox	sand, up to 0.5
		<i>Vulpes chama</i>	Silver fox	sand
	Viverridae	<i>Suricata</i>	Suricate	consolidated sand and calcareous, up to 1.5
Tubulidentata	Orycteropodidae	<i>Orycteropus</i>	Aardvark	sand, up to 1m and deeper
Arthropoda	Formicidae	<i>Messor barbatus</i>	Common harvesting ant	
		<i>Pheidole capensis</i>	Harvesting ant	
		<i>Anoplolepis stelnegroveri</i>	Black pugnacious ant	
	Scorpiones	<i>Scorpiones opisthothelms</i>	Scorpion	
	Isopterae	<i>Trinervus trinervoides</i>	Snouted harvester termite	
		<i>Hodotermes mossambicus</i>	Common harvester termite	

Summarized from AEC report PER-143 (1986) [20].

APPENDIX D: SAMPLE PREPARATION OF HEAVY MINERAL CONCENTRATES

Two sites, identified as areas of suboutcropping olivine-melilitite, kimberlite and related diatremes, which had been confined by aeromagnetic and drilling data, were used for the heavy mineral study. Prior to detailed sampling for this investigation, two samples (one surface sample and one from 30 centimetres depth) from each of the sites, as well as from three other random sites were collected. The random sites would allow for the determination of background concentrations. The samples from the two sites initially showed concentrations up to 10 times the background concentrations.

A total of 30 and 26 samples (surface and 30 cm depth samples) were collected at sites A and B respectively, along east-west and north-south traverses at 50 or 100 metre spacings, depending on the length of the section line over the sub-outcrop. Samples were sieved to obtain the 0.5mm-1mm size fraction, as this fraction is larger than that expected to be of aeolian origin. 100 grams of this size fraction was "jigged", using a portable mechanical jig, for three minutes to ensure reproducibility. These heavy mineral concentrates were further concentrated in the laboratory using bromoform.

All the grains in the final concentrate were identified and counted using a binocular microscope. S.E.M. results were used to aid in the recognition of, and confirm the obtained percentages of ilmenite grains in the heavy mineral separate. These percentages were found to vary from approximately 60% (of the total ilmenite and iron oxide concentrate) over the sub-outcrop to approximately 28% near the edges of the sub-outcrop. A value of approximately 28% was obtained for the background samples too. The remaining fraction consisted predominantly of iron-oxides.

APPENDIX E: MAJOR ELEMENT RESULTS - SURFICIAL SEDIMENTS AND RECENTLY WEATHERED BASEMENT

Sample No.	SiO ₂	TiO ₂	Al ₂ O ₃	Fe ₂ O ₃	MnO	MgO	CaO	Na ₂ O	K ₂ O	P ₂ O ₅	LOI	TOTAL
VP-T1/1*	55.88	0.56	17.12	6.32	0.07	2.70	0.63	1.50	2.70	0.14	12.76	100.36
VP-T1/4*	58.11	0.59	16.21	5.40	0.08	2.55	0.44	1.39	2.66	0.13	12.59	100.15
VP-T1/5*	60.17	0.73	16.11	6.08	0.08	1.68	0.56	1.67	3.13	0.13	9.12	99.45
VP-T1/6*	60.30	0.67	15.11	5.17	0.09	2.40	0.43	1.33	2.35	0.12	11.95	99.91
VP-T1/9*	52.14	0.53	18.68	6.11	0.09	2.84	0.54	1.27	2.64	0.13	14.70	99.96
VP-T1/10*	57.60	0.63	15.97	5.27	0.08	2.56	0.47	1.32	2.57	0.12	12.85	98.25
VP-T1/11*	58.87	0.65	16.57	4.98	0.07	2.41	0.42	1.40	3.89	0.13	10.95	100.34
VP-T2/1*	54.98	0.56	17.53	6.01	0.08	2.59	0.56	1.44	2.53	0.12	13.85	100.35
VP-T2/2*	54.36	0.59	17.52	6.21	0.08	2.36	0.74	1.56	3.19	0.12	13.47	100.20
VP-T2/3*	52.34	0.54	18.77	6.71	0.07	2.29	0.48	1.25	3.04	0.14	13.39	99.92
VP-T2/4*	59.66	0.59	16.05	6.79	0.07	2.20	0.44	1.62	3.66	0.12	10.83	100.23
VP-T2/6*	56.05	0.54	17.28	6.28	0.07	2.35	0.48	1.50	2.74	0.13	12.84	100.27
VP-S/1*	58.69	0.70	17.47	5.14	0.08	1.87	1.06	1.81	2.60	0.23	10.67	100.31
VP-S/4*	70.21	0.87	12.94	4.71	0.09	0.82	0.73	2.21	3.53	0.15	3.79	100.06
VP-S/5*	55.13	0.53	20.01	4.84	0.07	2.32	0.81	1.33	1.91	0.23	13.27	100.46
VP-S/7*	71.67	1.22	11.05	4.74	0.09	0.75	0.48	1.88	3.88	0.16	3.40	99.29
VP-S/8*	66.79	0.78	13.88	4.57	0.08	1.45	1.00	2.06	3.12	0.17	6.45	100.35
VP-S/9*	71.78	1.11	11.52	4.31	0.09	0.76	0.69	2.66	3.75	0.16	3.32	100.14
VP-Base 1*	72.20	0.54	15.13	1.26	0.06	0.67	1.54	0.66	0.22	0.11	-	100.22
VP-Base 2*	60.63	0.54	17.13	5.25	0.06	0.82	2.51	0.48	4.00	0.12	7.11	99.50
VP-Base 3*	68.41	0.39	15.40	3.76	0.06	0.74	0.18	0.52	5.23	0.14	4.59	99.41
W20N0(18)*†	71.00	0.17	13.81	3.01	0.01	0.85	2.96	1.45	1.13	0.03	4.13	98.62
W30S10(12)*†	66.49	0.32	15.72	2.57	0.01	0.07	2.39	0.23	3.92	0.08	6.58	98.94
W60N0(20)*†	75.17	0.18	11.84	0.45	0.02	0.00	1.26	0.53	6.00	0.06	3.32	98.92
W70N0(7)*†	75.19	0.21	12.10	1.29	0.02	0.00	1.16	1.05	5.63	0.07	2.45	99.75
W70S10(7)*†	78.96	0.27	10.61	1.08	0.02	1.03	0.23	0.73	4.23	0.11	2.36	101.44
W80N0(9)*†	71.85	0.28	15.06	2.50	0.02	0.01	0.29	0.86	6.07	0.10	2.84	100.31
VP-55*	57.46	0.18	24.17	2.76	0.04	0.25	6.46	5.52	1.10	0.09	1.24	99.26
VP-56*	69.95	0.33	13.33	2.43	0.03	0.46	1.13	0.31	5.57	0.16	4.99	99.39
VP-57*	71.66	0.30	14.06	1.86	0.02	0.07	1.10	2.79	6.31	0.10	1.00	99.27
VP-58*	71.39	0.28	14.14	2.44	0.02	0.26	0.43	2.22	6.22	0.09	3.14	100.62
VP-60*	70.59	0.40	14.39	2.61	0.03	0.00	0.78	2.55	6.02	0.12	1.69	99.17
VP-51*	34.45	0.40	6.15	2.22	1.01	1.11	27.94	0.97	1.33	0.14	23.73	98.44
VP-52*	55.72	0.53	9.99	4.16	0.07	1.74	9.94	1.85	2.25	0.13	13.34	98.50
HLD2-17.5m*	62.0	1.1	14.0	7.5	0.0	3.5	0.3	0.5	3.7	0.1	-	-
HLD3-9m*	65.99	0.69	16.96	4.08	0.03	1.08	0.21	0.34	2.01	0.13	8.07	99.59
HLD3-15m*	65.27	0.66	12.77	6.78	0.05	2.51	0.28	0.53	3.33	0.04	8.40	100.63
HLD3-18m*	62.30	0.74	13.81	8.14	0.03	1.68	0.37	0.62	3.59	0.06	8.93	100.28
VP-74*	76.80	0.66	11.50	3.48	0.05	0.19	0.17	2.04	1.82	0.15	3.29	100.17
VP-75*	71.50	0.73	11.67	5.61	0.13	2.81	0.85	2.40	2.28	0.14	2.75	100.88

All data are expressed in weight %

Total Fe as Fe₂O₃

- ♦ Vaalputs Formation
- * Surface sediments/ Gordonia Formation
- # Weathered basement (white clay) - lower Vaalputs Formation (#1): analyses from Brynard (1988)
- + Weathered surface basement
- x C. ka/Weathered Dwyka (HLD samples are from drillcores from Vaalputs, with depths in metres)

APPENDIX F: STRUCTURAL DATA OF PLANES CONTAINING SLICKENSIDES IN THE PALAEO-WEATHERED BASEMENT

PLANE		SLICKENSIDE	
Dip Direction (°)	Dip (°)	Azimuth (°)	Plunge (°)
083	28	074	26
213	50	223	48
140	90	157	90
028	46	028	46
300	34	293	33
246	50	226	48
246	54	196	44
254	72	152	18
323	80	-	-
196	54	161	44
162	90	253	70
154	90	154	90
164	90	164	90
032	38	060	42
274	80	170	36
040	25	029	30
017	58	017	58
081	60	028	51
030	34	030	34
188	60	192	60
320	21	344	20
160	32	160	32
265	85	353	0
090	23	070	22
054	48	054	48
024	20	050	14
003	31	003	31
169	43	169	43
358	22	-	-
093	90	116	90
163	34	163	34
347	24	351	22
024	62	037	60
014	22	023	21
003	22	023	19
065	24	065	24
338	90	-	-
330	32	345	28
011	12	339	08
334	90	334	90
073	34	066	32
238	90	330	76
327	90	-	-
328	90	328	90
130	52	130	52
221	18	217	12
100	25	126	23
359	60	023	54

PLANE		SLICKENSIDE	
Dip Direction (°)	Dip (°)	Azimuth (°)	Plunge (°)
352	60	352	60
228	58	228	56
261	46	190	19
313	58	337	58
295	64	303	62
253	66	-	-
263	63	265	62
190	37	185	37
191	41	210	35
179	52	210	47
219	22	199	22
213	37	212	35
180	47	153	46
166	50	200	46
170	31	163	34
105	28	065	28
144	28	144	28
129	44	129	44
150	62	150	62
-	-	208	44
060	24	060	24
154	53	154	53
179	37	190	35
355	33	030	32
171	46	191	44
172	55	194	54
180	53	185	53
181	37	147	30
164	49	172	49
323	68	014	28
339	67	340	72
300	14	254	05
295	21	015	10
254	54	254	54
277	43	277	43
289	20	334	11
277	40	291	35
302	29	327	25
329	20	354	19
290	38	303	35
290	53	297	52
313	29	313	29
314	54	015	25

PLANE		SLICKENSIDE	
Dip Direction (°)	Dip (°)	Azimuth (°)	Plunge (°)
163	32	163	32
144	24	144	24
230	37	207	36
171	30	171	30
214	40	190	37
182	74	188	66
174	50	187	30
192	48	151	30
068	59	-	-
065	85	065	85
163	70	163	70
314	16	314	16
151	90	090	10
198	56	185	55
216	69	169	68
169	55	153	50
358	40	350	40
080	49	053	46
131	43	131	43
109	20	109	20
150	90	060	00
160	90	070	00
160	90	070	19
160	90	070	38
135	20	135	20
067	74	067	74
290	20	290	20
305	40	266	36
098	90	002	60
345	48	295	21
099	51	134	40
143	30	143	30
132	31	132	31
296	50	296	50
141	18	158	17
311	70	311	70
101	10	136	10
121	21	121	21
058	51	064	49
136	21	136	21
140	21	140	21
144	20	159	18
051	58	089	58
061	40	074	35
011	45	021	45
160	90	160	90

PLANE		SLICKENSIDE	
Dip Direction (°)	Dip (°)	Azimuth (°)	Plunge (°)
130	23	130	23
154	20	142	24
174	90	084	90
060	90	150	90
177	90	087	90
139	18	139	18
068	90	158	70
140	90	-	-
255	78	-	-
163	90	-	-
346	44	346	44
318	65	050	60
258	80	211	53
233	62	232	62
281	53	281	53
217	90	217	90
213	73	190	7
027	32	017	32
046	16	046	16
232	69	-	-
156	14	177	14
098	90	008	70
241	60	241	60
211	36	148	19
176	53	166	51
222	60	196	59
074	36	074	36
251	46	251	46
169	15	278	10
228	42	220	42
143	90	-	-
102	68	102	68
270	56	230	41
280	54	256	48
120	90	120	90
306	63	336	60
276	70	276	70
286	66	286	66
298	64	298	64
136	20	161	13
278	66	250	64
300	66	300	66
262	79	262	79
008	40	008	40
047	40	034	40
149	39	170	37
094	32	094	32

PLANE		SLICKENSIDE	
Dip Direction (°)	Dip (°)	Azimuth (°)	Plunge (°)
188	30	138	30
036	36	036	36
071	60	071	60
140	48	113	44
004	51	004	51
045	44	035	43
052	45	052	45
081	36	086	35
112	22	192	18
184	44	184	44
324	66	352	64
310	68	-	-
223	52	181	45
254	50	254	50
088	45	088	45
322	54	322	54
044	70	044	70
034	70	034	70
235	57	235	57
070	90	160	56
056	90	146	85
190	38	230	32
068	10	042	10
017	26	031	19
156	31	156	31
047	38	047	38
042	24	042	24
336	26	336	26
295	19	295	19
356	41	356	41
028	40	028	40
321	15	321	15
169	28	169	28
254	32	254	32
219	11	250	09
351	30	043	19
138	38	096	27
080	18	080	18
100	11	140	10
092	10	136	10
085	08	118	04
121	10	121	10
290	23	310	20
111	37	111	37
276	22	276	22
188	26	179	26
178	30	178	30
070	15	098	12

Author: Brandt, Dion.

Name of thesis: The recent morpho-tectonic history of the Vaalputs radioactive waste repository and environs - Dion Brandt.

PUBLISHER:

University of the Witwatersrand, Johannesburg

©2015

LEGALNOTICES:

Copyright Notice: All materials on the University of the Witwatersrand, Johannesburg Library website are protected by South African copyright law and may not be distributed, transmitted, displayed or otherwise published in any format, without the prior written permission of the copyright owner.

Disclaimer and Terms of Use: Provided that you maintain all copyright and other notices contained therein, you may download material (one machine readable copy and one print copy per page) for your personal and/or educational non-commercial use only.

The University of the Witwatersrand, Johannesburg, is not responsible for any errors or omissions and excludes any and all liability for any errors in or omissions from the information on the Library website.